Etching and Chemomechanical Polishing of Compound Semiconductors using Halogen-Based Reagents

Irene Nicol

Submitted for the degree of Doctor of Philosophy
to the Department of Chemistry
at the University of Glasgow

August 1996

To Robert

Summary

This thesis presents research into the operation of halogen based reagents in the etching and chemomechanical polishing of compound semiconductors.

The chemical reactions of sodium hypochlorite, dichlorine, dibromine and hydrogen peroxide on gallium arsenide and cadmium telluride are investigated and presented in a form relevant to their use in chemomechanical polishing. Their dependence on pH, concentration and polishing conditions is also discussed. The results of these experiments are then brought together in the formulation of a General Model for Chemomechanical Polishing which consolidates the chemistry of the polishing process with the mechanical aspects of passivation and product removal. The general predictions made in the formulation of this model are then applied in the design of novel, bromine-based reagents, to illustrate how etch rate and surface quality may be controlled by changing the physical and chemical environment of the etchant.

The reactions of dichlorine and dibromine on compound semiconductors follow a pattern of halogenation of the substrate surface, followed by solvation of the halogenated products and removal of the secondary products in the etchant solutions. The reactions of hypochlorite and hydrogen peroxide follow a similar pattern, beginning with oxidation of the substrate surface, followed by subsequent hydration in the etchant solution and final product removal. The solubility of the products and the action of the polishing pad and abrasive are all critical to the passivation of the surface and the production of a polished substrate.

The pH dependence of sodium hypochlorite is explained in terms of its composition. At low pH (< 8) the main component of the etchant solution is dichlorine. At high pH (> 8) the main component of the etchant solution is hypochlorite anion. Thus hypochlorite solution may be considered as a parallel to dibromine at low pH, but is more consistent with the behaviour of hydrogen peroxide at high pH. Thus, aqueous sodium hypochlorite solution may be formulated as part of the series

O-O, O-X, X-X,

where X represents a halogen. The General Model for Chemomechanical Polishing is formulated on the basis of the three stages of reaction observed for all the reagents examined: Oxidation of the substrate; solvation/hydration of the oxidation products; removal of the products from the substrate surface.

Novel bromine-based organic reagents have been designed, synthesised and used to etch and polish gallium arsenide and cadmium telluride substrates. These compounds have shown that properties such as stock removal rate, pH dependence and selectivity may be predicted and even designed into etchants to produce the optimum conditions for polishing a given substrate.

Acknowledgements

I would like to thank the staff and students at the Chemistry Department, University of Glasgow, for helping to make my research an enjoyable experience and this thesis possible. Special thanks are due to my supervisor Professor John M. Winfield for advice on everything from gravimetrics to grammar, and for patience while I composed my thesis. Many thanks to all at Logitech Ltd., my industrial sponsors, for their technical and financial support, and to Max Robertson, my industrial supervisor. I would like to specifically thank the technicians Larry, Vicky and Rose for their high standard of technical support, including help with equipment and electron microscopy (and always knowing where things were!). Thanks to Bob for photography, micrographs and help with graphics on many and various poster presentations.

Finally I would like to thank my husband Robert and my parents for their continuing love and support throughout my first degree and Ph.D.

Contents

CHAPTER ONE

INTRODUCTION

1.1 COMPOUND SEMICONDUCTORS AND THEIR APPLICATIONS.

There can be little doubt that recent advances in electronics owe much to the development of silicon (Si) as the material for device fabrication. However, compound semiconductors such as gallium arsenide (GaAs) and cadmium telluride (CdTe) have properties that can be applied in areas such as microwave technology and optoelectronics[1], where silicon has not proved as useful.

GaAs, because of the nature of its band gap (Figure 1.1.1a), has the ability to convert directly between light and electric current, whereas the band gap in silicon (Figure 1.1.1b) only permits an indirect conversion[2]. In GaAs, a direct transition between the valence band and the conduction band can occur. In Si, an allowed transition occurs to an exciton state, where an exciton is a bound electron-hole pair with energy levels within the band gap. This exciton unit has the ability to move through the crystal lattice. The final transition to the conduction band in Si is then accompanied by a loss of energy, dissipated in the lattice, and is therefore less efficient. Thus, GaAs is particularly attractive for use in laser technology and, for example, in solar panels. CdTe and mercury cadmium telluride (HgCdTe) have found most recent application as laser materials, with a feasible wavelength range of 0.9 - 20 microns (μm), as opposed to the more restrictive GaAs system with aluminium gallium arsenide (AlGaAs) which has a range of only 0.7 - 1.0 microns[1].

In addition to these well-established industrial applications, research into the development of compound semiconductors as alternatives to silicon is widespread. Ongoing work includes the formation of metal contacts to 13-15 semiconductors like GaAs for use in very large scale integration (VLSI) circuits[3] and the use of GaAs in the formation of field effect transistors (FETs)[4]; both of these are traditionally silicon-based applications.

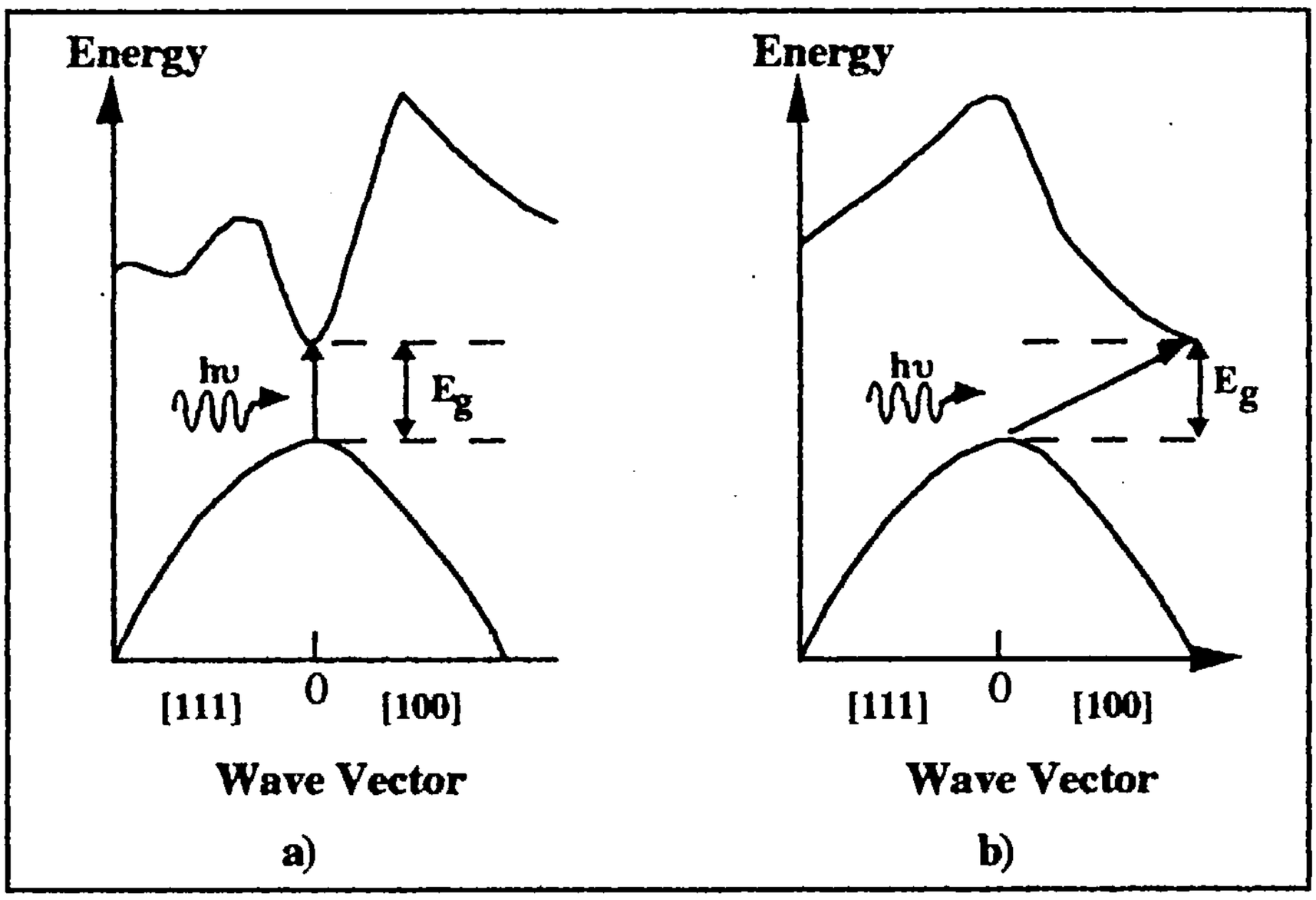

Figure 1.1.1: Energy Band Structures of a) GaAs and b) Si, where Eg is the energy gap between valence and conduction bands.

1.2 Structure and Bonding in Gallium Arsenide and Cadmium Telluride.

Reactions on crystalline materials can be affected by the particular orientation of atoms that is in contact with the reagent. This is defined by the direction across which the crystal has been cut, i.e. the cleavage plane which is revealed. Such planes are described using a system of notation known as Miller indices[5]. The Miller indices (hkl) for a plane or set of planes are defined by the intersection points of that plane with the three axes of the unit cell, taking one corner of the unit cell as the origin, as in Figure 1.2.1. For the plane shown, the intersections would be a/2, b/3 and c/1, i.e. 1/2, 1/3 and 1. The reciprocals of these fractions are taken, to allow the plane to be defined using integers.

Thus, the plane shown would be defined by the notation (231). This notation would also apply to other planes which are parallel to this one. In many crystals there are planes that, due to symmetry, are equivalent in terms of the atoms they contain. In such cases the notation {hkl} is used to describe a group of equivalent planes.

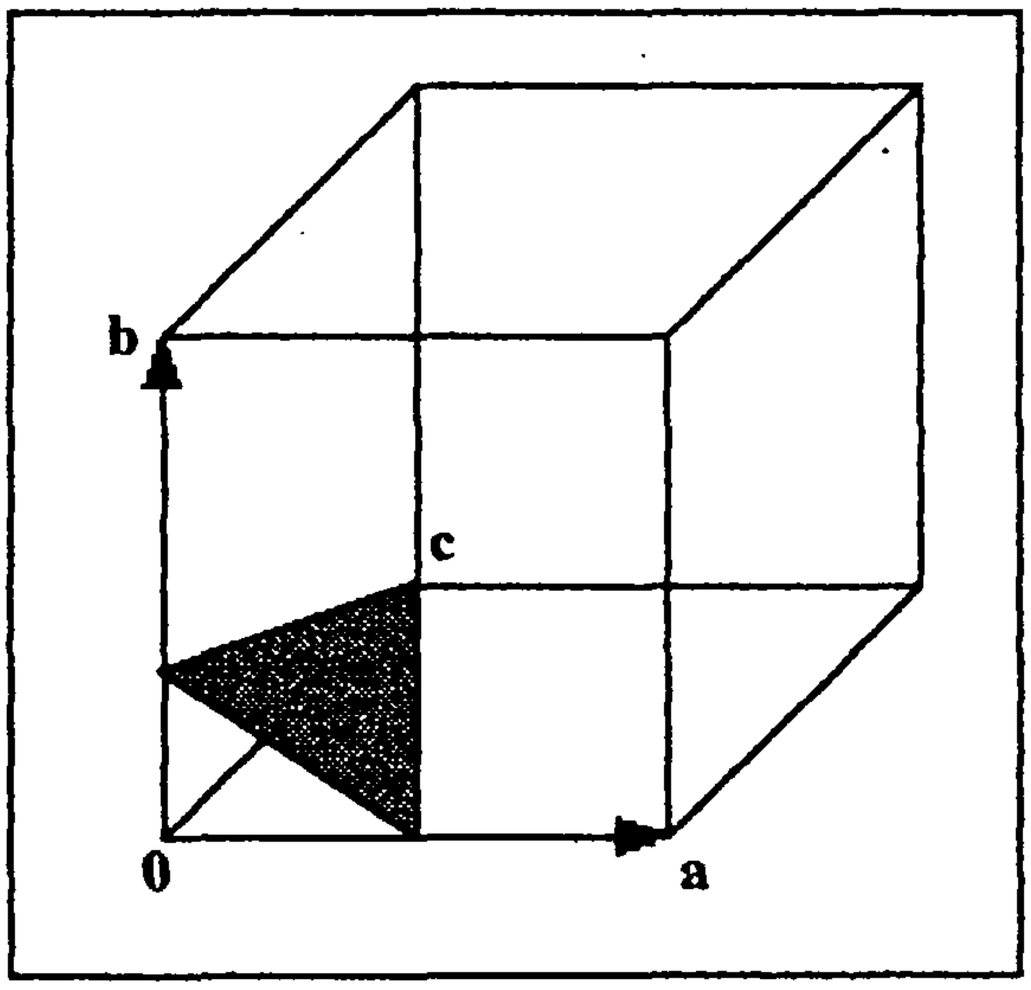

Figure 1.2.1: How to Define Miller Indices.

Directions in crystals are defined in a similar way, by taking the fractional co-ordinates at which a line, passing through the origin in the desired direction, intersects the a, b and c axes of the unit cell. Co ordinates are divided or multiplied through to give the smallest possible integers, e.g. [440], [110] and [1/4 1/4 0] all describe the [110] direction. In cubic systems like zinc blende, the [hkl] direction is always normal to the (hkl) plane. Directions that are equivalent by symmetry are notated <hkl>.

There are three main cleavage planes in cubic systems and these are illustrated in Figure 1.2.2. For clarity, a simple cubic unit cell is shown but the directions of the planes apply equally well to the zinc blende unit cell shown in Figure 1.2.5.

In GaAs, all the planes in the <100> direction are equivalent, containing equal numbers of Ga and As atoms. This is also true of the <110> direction. However, the planes in the <111> direction in GaAs and many other compound semiconductors contain atoms of one type only, with alternating planes of type A (As) and type B (Ga) atoms. Thus, a crystal cut across the <111> direction in GaAs will have either a (111)A (all As) or a (111)B (all Ga) face. The reactivity on this crystal will obviously depend on whether the A or B face is exposed[6].

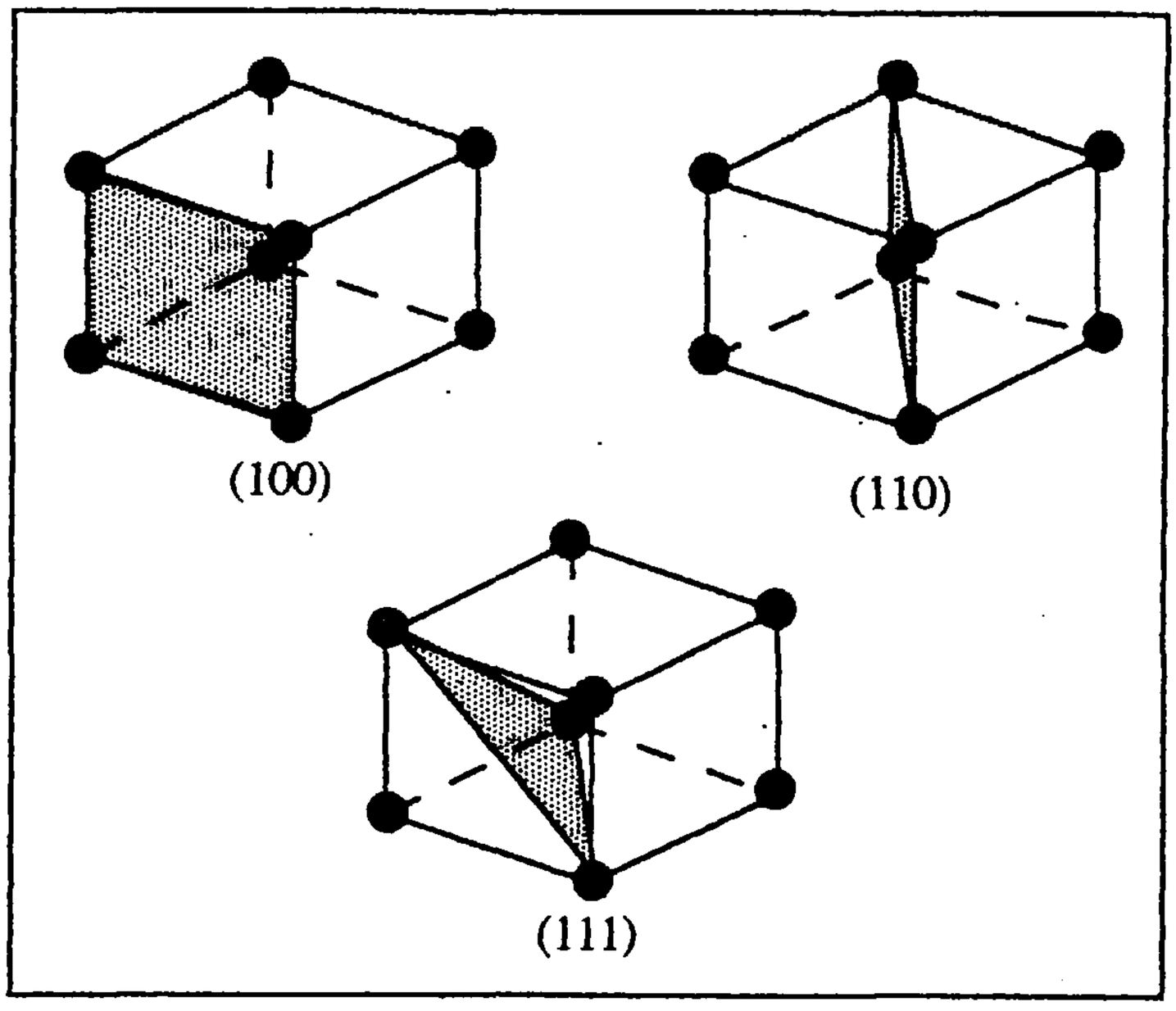

Figure 1.2.2: The Three Cleavage Planes in a Cubic System.

1.2.1 GALLIUM ARSENIDE.

Semiconducting materials are generally prepared by crystal growth from the pure elements, to ensure maximum purity[7]. For 13-15 semiconductors, there are three important methods of crystal growth, all involving crystallisation from a stoichiometric melt[8]. These are the liquid encapsulated Czochralski technique, the horizontal Bridgman technique and the magnetic Czochralski technique. These specialised methods are necessary to overcome problems with the evaporation of volatile components from the melt.

The simple apparatus used in the basic Czochralski method of crystal growth is shown in Figure 1.2.3.

In the liquid encapsulated Czochralski (LEC) technique, the melt surface is covered with a liquid encapsulant. Combined with the introduction of a pressure of gas which exceeds the dissociation pressure of the compound, this suppresses the evaporation of volatile components from the melt. The liquid encapsulant must be immiscible with the melt and have a low melting point, vapour pressure and density. Boron (III) oxide is a commonly used example of such a compound.

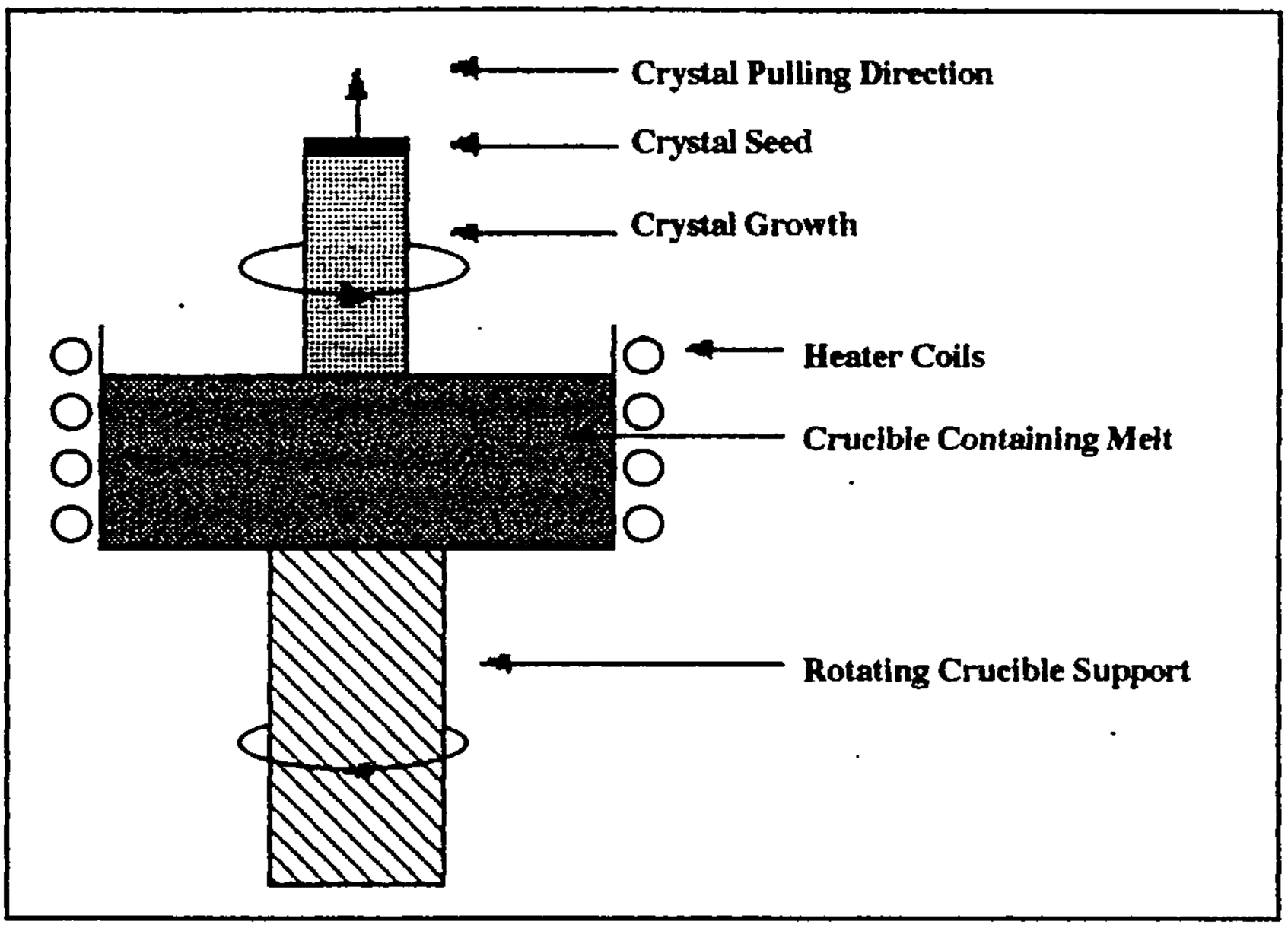

Figure 1.2.3: The Czochralski Method of Crystal Growth.

In the horizontal Bridgman technique, the melt will generally contain a seed crystal to initiate growth and will be contained within a sealed tube rather than an open crucible. To maintain the stoichiometry of the melt, an excess of the volatile constituent (arsenic in the case of GaAs) is added. The crystal is grown by applying a temperature gradient across the melt, encouraging crystallisation at the cooler end.

The magnetic Czochralski technique also employs a sealed tube rather than an open crucible. A radio frequency heated graphite crucible contains the melt but is itself contained within a special sealed silica ampoule. The seed crystal is mounted on a graphite holder and can be moved using external electromagnets, allowing it to be pulled from the melt as in the standard Czochralski method.

In the case of GaAs, because of the impurities incurred by purifying liquid GaAs in quartz[7], it is essential to ensure that the elements are pre-purified before crystal growth of the semiconductor.

Gallium (Ga, Latin Gallus, a translation of Lecoq, a cock) is a silvery-blue solid. Melting at only 303K, it is one of the few metals that can be liquid near room temperature and has one of the longest liquid ranges of any metal, boiling at 2478K[9]. Although present in small amounts in many natural ores, Ga is now obtained by extraction from the by-products of the aluminium, germanium and zinc industries. The extracted metal is

purified by treatment with acid and oxygen at high temperature before crystallisation and zone refinement. This level of treatment is essential to produce ultra-pure Ga for the semiconductor industry, where impurities are present only in parts per million (ppm)[7].

Arsenic (As, Greek arsenikon, male, from the belief that metals were different sexes) in its most stable form is a grey solid, melting at 1090K at elevated pressures (21280 Torr) and subliming at 886K[9]. The isolated element occurs occasionally in nature, but arsenic appears predominantly as sulphide ores (As_4S_4, As_2S_3) and as the oxide (As_2O_3). The element is commonly prepared by smelting and sublimation followed by reduction over charcoal. There are three allotropes of As, the most common being the grey α-form (rhombohedral). Sublimed As retains its vapour phase molecular unit of As_4 and is observed as a cubic crystalline yellow solid. The third form, ε-As is commonly known as the mineral arsenolamprite.

Purification methods for As range from vacuum sublimation to zone refining and are too many to detail individually here[8]. Zone refining, however, is one of the most common techniques used to purify metals and semiconductors and is worthy of a brief description. The method is based on the principle that impurities will concentrate in the liquid phase in preference to the solid phase. The basic apparatus used is illustrated in Figure 1.2.4.

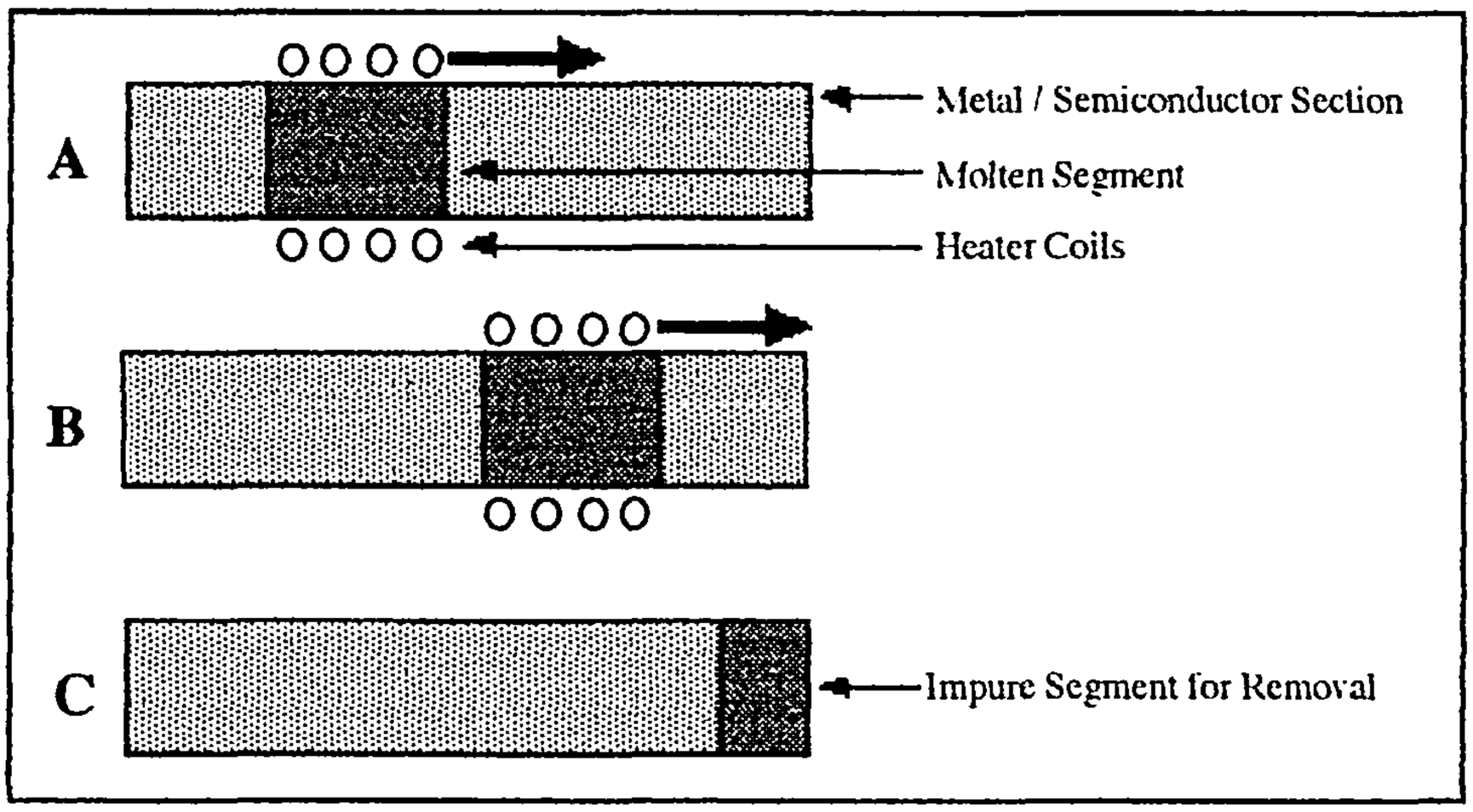

Figure 1.2.4: The Zone Refining Purification Method.

The impurities are concentrated in the molten zone, which is moved along to the end of the segment using a mobile heating coil. The section remaining at the end of the material is removed after cooling.

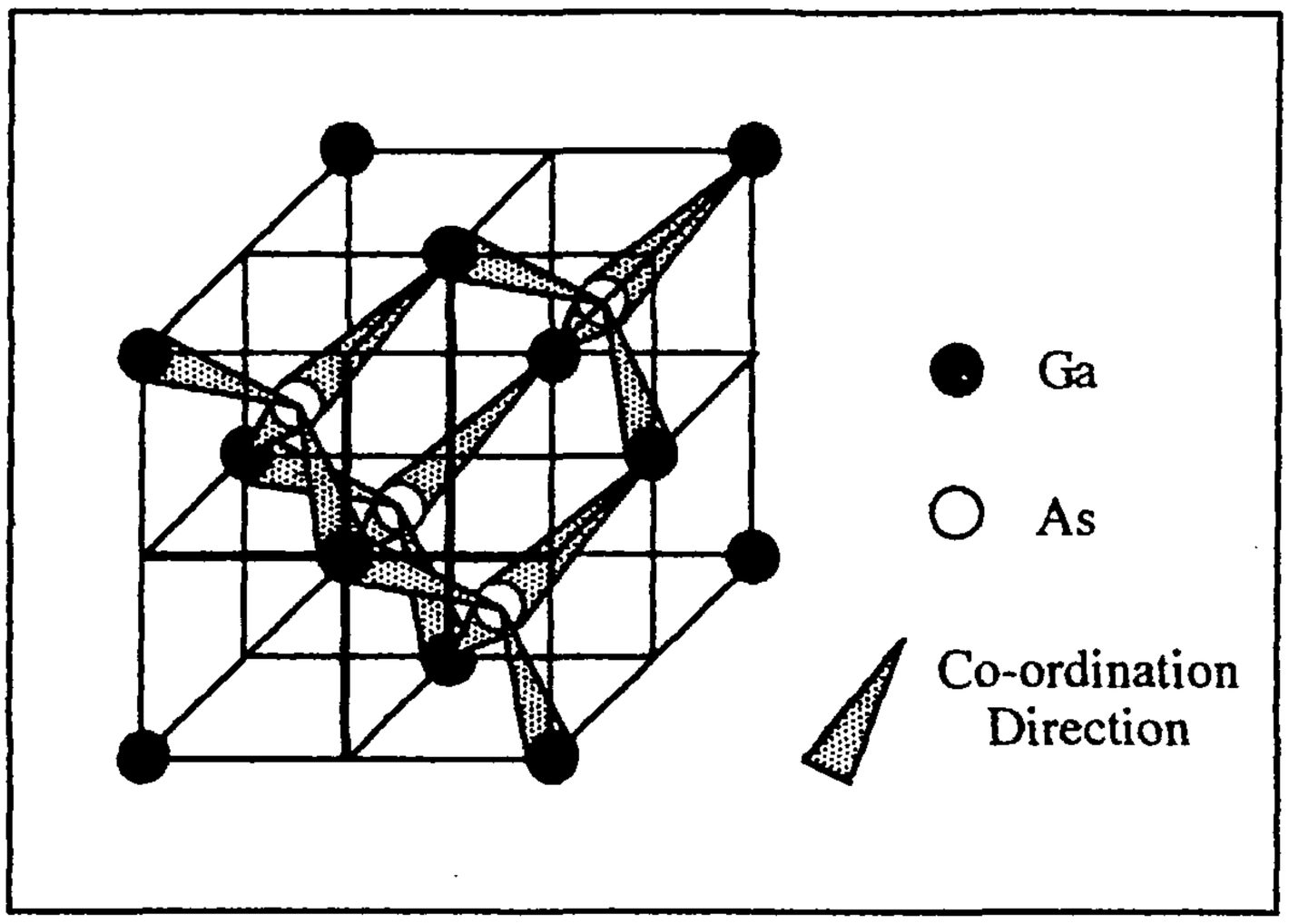

Figure 1.2.5: The Zinc Blende Structure of GaAs.

Gallium arsenide itself, in common with all known 13-15 semiconductors, shares the zinc blende crystal structure (Figure 1.2.5) with diamond and many other covalent solids, yielding a co ordination number of four.

The chemical bond in compounds of this type cannot be described as completely covalent. There is a polarity introduced by the difference in electronegativity between Ga and As. Pauling[10] described this type of bonding as mixed covalent-ionic. In 1959, Mooser and Pearson[11] defined the term 'ionicity' to describe the degree to which crystal structures were affected by such polarity. The concept was later developed into a mathematical description of bonding which is intermediate between covalent and ionic[12]. The ionicity of a bond (Equation 1.2.1) is governed by electronegativity and the valence shell size of the elements involved and is hence related to the band gap in the crystal.

$$\text{Ionicity} = \frac{C^2}{E_g^2} \qquad \text{.....(1.2.1)}$$

where $C =$ charge transfer between atom A and atom B (i.e. the degree of electron sharing between the two atoms) and

$E_g =$ the size of the band gap in the crystal.

1.2.2 CADMIUM TELLURIDE.

Cadmium (Latin cadmia, the ancient name for calamine) was discovered in 1817 as an impurity in calamine (zinc carbonate)[9]. Cadmium is a soft, bluish-white metal and is found predominantly in the form of the mineral Greenockite (CdS). Industrially, it is obtained as a by-product from the treatment of the ores of zinc, copper and lead.

Tellurium (Latin tellus, meaning earth)[9] has a silvery-white metallic appearance in its crystalline form. An amorphous solid can be obtained by precipitation from telluric (H_6TeO_6) or tellurous (H_2TeO_3) acid solutions. Although occasionally found in its native form, it is usually found combined with other metals, including gold. Industrially, tellurium is obtained as a by-product of the copper refining industry.

High-pressure techniques are often used for bulk crystal growth of 12-16 compounds, due to rapid dissociation of the melt under normal conditions. Sublimation[8] from bulk CdTe through a temperature gradient to form crystalline material can be used, but this method takes several days to form reasonably sized crystals. Single crystal samples of CdTe are rare and expensive because of the techniques used to prepare them. For this reason, most CdTe sections used in this project were polycrystalline. The presence of grain boundaries in such a sample limits the quality of surface finish achievable and leads to preferential etching at certain points on the surface. In device fabrication, films deposited in vacuum are often used because of the difficulties in growing a perfect crystal.

Cadmium telluride, like GaAs, requires very pure elemental starting materials for crystal growth, although this is not as critical in the case of CdTe because zone refining of the single crystal product is less problematic. CdTe shares the zinc blende structure (Figure 1.2.5) with its 13-15 counterparts but the difference in atomic size yields a much larger unit cell than in GaAs. The cubic lattice parameter, a, measuring the size of the unit cell, is 6.48Å for CdTe and only 5.65Å for GaAs[13].

1.3 THE POLISHING PROCESS.

The surfaces required on semiconductors for device fabrication must meet stringent chemical and physical specifications. Chemically, the surface must retain the defect-free, single crystal nature of the bulk in order to retain the electrical properties required.

Physically, the surface must be flat and smooth to allow good electrical contacts to be made to it on a sub-micron scale. The ultimate aim with respect to surface roughness is to produce a surface which can be described as 'sub-nanometre' smooth i.e. with no peaks or troughs in the topography of more than one nanometre. The chemical reactions which are employed to reach these levels of surface smoothness are therefore required to be selective down to an atomic level. From a chemist's perspective, the term 'sub-nanometre' is unrealistic, although it is justified by its use in the industry. Since the Ga-As interatomic distance in crystalline GaAs is 0.4nm, the production of a real sub-nanometre surface would mean selective removal of 1 or 2 atoms at a time. Also, this hypothesis does not account for single atom variances in the surface topography which are brought about by the crystal orientation. Current polishing techniques have developed largely as a result of trial and error[14] and for many systems there is little known about the mechanism or specificity of the chemical reagents involved.

Chemomechanical polishing, as the name suggests, operates via two components: The chemical component etches the material by chemical reaction and the mechanical component aids the process by incorporation of a "wipe-away" action on the substrate surface. The mechanical aspect of such a process is traditionally thought to operate via a mechanism known as the passivating layer model. This model was postulated by Beilby (the redeposition of substrate material during metal polishing is often referred to as a Beilby layer) and is mentioned in the literature during discussions between Lord Rayleigh and another polishing researcher (Rosenhain) at the Optical Convention of 1905[15]: "He (Mr Rosenhain) did not know whether it would ever be possible to show analytically the presence of a chemically different layer upon a polished surface....". The model is illustrated schematically in Figure 1.3.1.

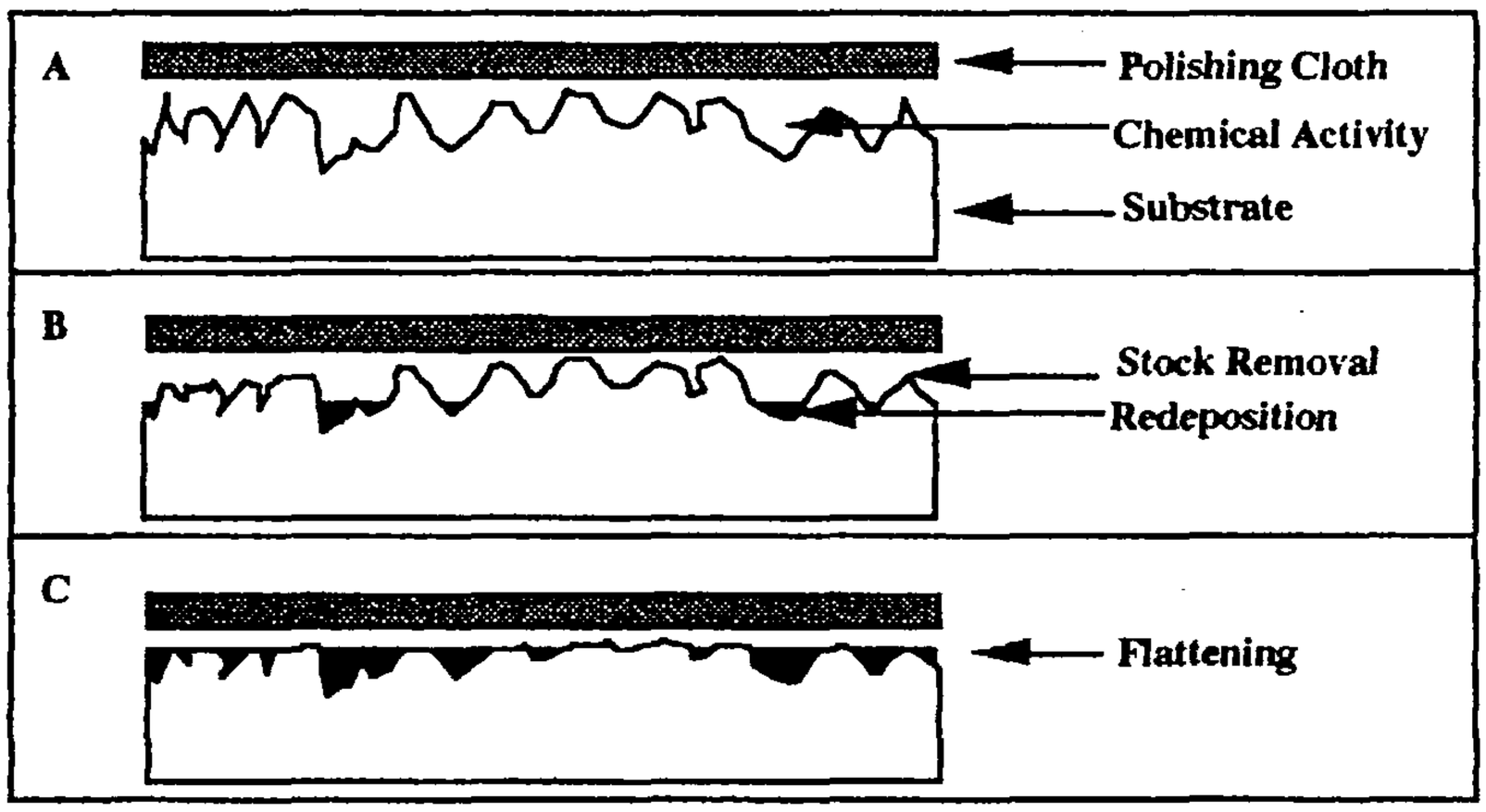

Figure 1.3.1: The Passivating Layer Model.

The mechanical action of the polishing cloth will operate first on the highest points of the surface, removing the products of chemical reaction from these areas and allowing build-up of products in the troughs between them. Some redeposition of material may also occur, leading to the formation of a 'protective' layer on the lowest parts of the surface. This protective layer modifies or slows reaction at the lowest points on the surface while allowing more vigorous reaction at the higher parts. This eventually leads to a flat surface when the remaining parts of the passivating layer are removed by the mechanical action of the polishing cloth.

If this model is an accurate description of how flat surfaces are achieved, the nature and solubility of the etch products will be critical to the surface quality which can be achieved on any material.

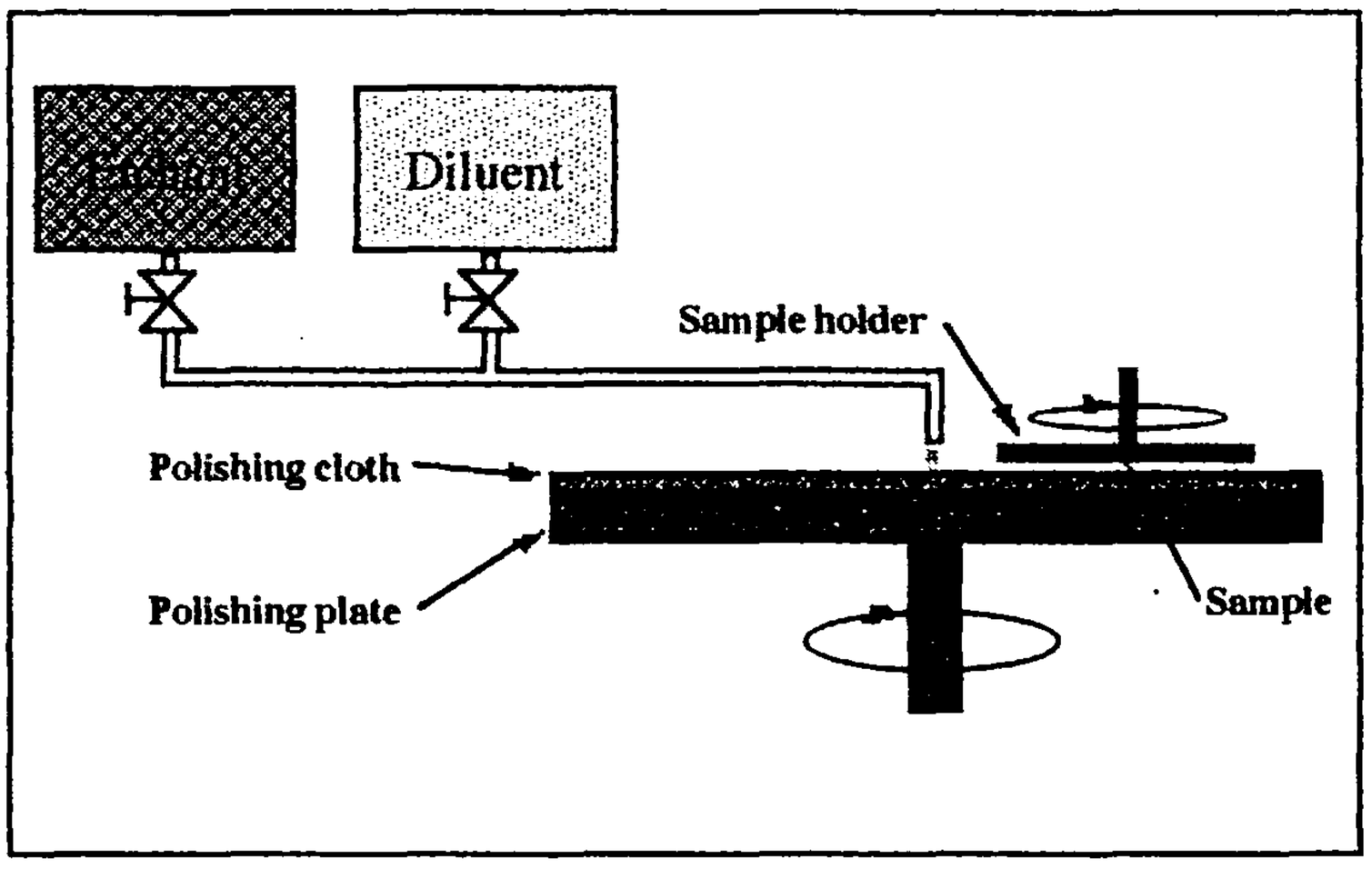

Figure 1.3.2: Schematic Representation of a Polishing Machine.

Figure 1.3.2 gives a schematic outline of the general equipment used in polishing. The sample is rotated over a revolving plate which is covered with a pad or cloth. A mixture of chemical etchant and solvent or diluent is dripped onto the rotating plate. The load on the sample can be varied using weights or a specially designed vacuum jig. The speed of the polishing plate can be varied up to a maximum of about 70 r.p.m. Dependent on the nature of the material to be polished, different types of polishing plates and pads can be employed. Paper cloths or polyurethane polishing plates can be used on harder materials such as silica or silicon, whereas softer materials like GaAs would normally require a softer, velvet-napped polishing cloth. Abrasive materials like cerium oxide and aluminium oxide can be employed as a slurry to improve stock removal.

The polishing process required to produce sub-nanometre smooth surfaces involves slow reaction and low stock removal rates. Thus if a large degree of thinning (>50μm) is required, the polishing process is preceded by a more vigorous mechanical action known as lapping. The lapping procedure employs a hard pad surface like glass or cast iron and abrasive materials of large particle size (9μm) to remove large amounts of material prior to polishing. A slightly convex plate is ideal for use in the lapping process, since it will produce a slightly concave sample, compensating for increased chemical reactivity at the wafer edges during chemomechanical polishing (Figure 1.3.3).

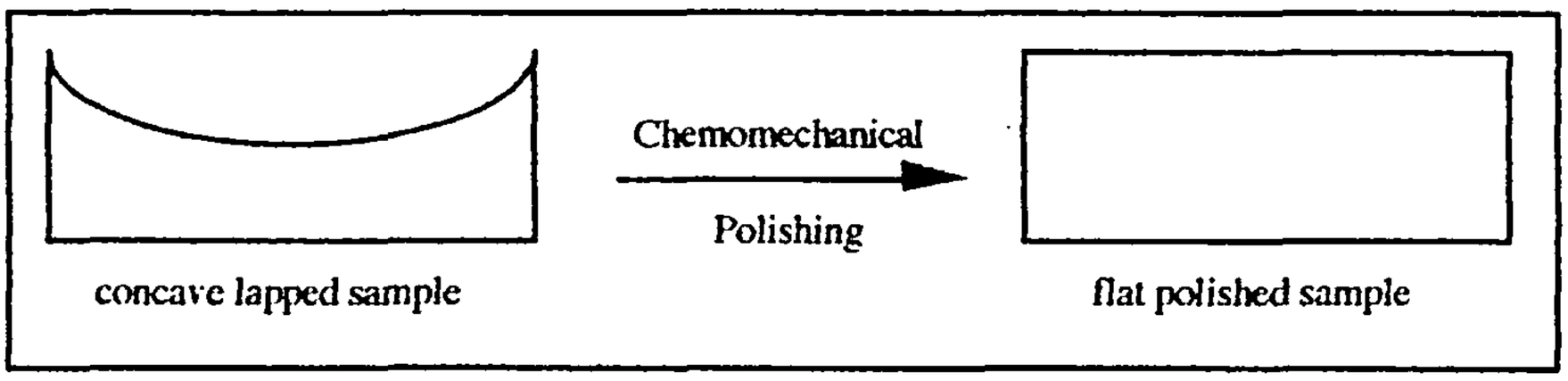

Figure 1.3.3: Compensation for Increased Reactivity at Wafer Edges.

The standard procedures used in lapping and polishing are well documented[16]. Considerable variation is possible, so specific procedures for a particular material and sample size are best referred to individually. The description of procedures that has been given here is therefore general and more detailed information is provided in Chapter Three.

1.4 CHEMICAL ETCHANTS EMPLOYED IN POLISHING.

Etchants for semiconductors can be acidic, basic or neutral and may operate by chemical reaction, usually oxidation, at the semiconductor surface. Etchants used in chemical or chemomechanical polishing will generally be liquids or solutions but solid or gas phase etchants are also feasible.

Gas phase etchants define the field of dry etching, which has developed almost independently of chemomechanical polishing. Dry etching techniques are most commonly used as part of the device fabrication process rather than in treatment of surfaces prior to fabrication. The term dry etching encompasses a vast realm of processes from reactive neutral bombardment[17-19], through reactive ion[20-22] and plasma

etching[23] to laser-induced chemical etching[24-26]. The terminology describes differences in delivery of the reagents onto the surface and subsequent enhancement of reaction using radiation, heat or ionisation. All dry etching processes, however, involve high temperature reactions, usually redox processes, between gaseous etchants and the semiconductor surface. Halogen etchants are the most commonly employed on GaAs[27].

Although much research has been undertaken on the dry etching of semiconductors with halogen-based reagents like dichlorine, dibromine[28] and hydrogen chloride[29], comparatively little work has been undertaken with regard to their room temperature reactions, either in the vapour phase or solution. A vast amount of literature has surfaced in the last 30 years, concerned with etch rates and selectivity of reagents like dibromine in methanol[30,31], hydrogen peroxide[32,33] and sodium hypochlorite[34,35] on various compound semiconductors. However, few of the aforementioned publications have ventured into the chemical mechanisms by which such reagents operate.

The reaction of dibromine on GaAs and CdTe is presumed to yield bromine-containing species which can then be dissolved or washed away in an appropriate solvent, such as methanol. Some authors have speculated on the production of cadmium dibromide and tellurium tetrabromide on CdTe[36]. There have also been tentative suggestions concerning the operation of NaOCl on GaAs[37]. The consensus of opinion is that 'active oxygen' in aqueous solutions can oxidise directly the GaAs surface to produce oxides in stoichiometric amounts, as shown in equation 1.4.1:

$$2GaAs + 6NaOCl \rightarrow Ga_2O_3 + As_2O_3 + 6NaCl \qquad .....(1.4.1)$$

Non-stoichiometric surfaces are then explained by differences in the solubilities of the oxides. Although most of these suggestions are largely sensible, few of them are supported by direct chemical evidence and the authors themselves seldom go as far as 'proving' the reactions in question. Hence, it is clear that a more rigorous investigation into the chemical operation of such etchants would be beneficial. The etchants under investigation in this project are among the most common employed commercially and are described in the following pages.

1.4.1 DIBROMINE.

Bromine (Br_2), named from the Greek 'bromos' meaning stink, has been used since the earliest of times in pigments and colourants. The earliest known reference is as a substituent on indigo to form a purple pigment mentioned in The Bible[38] and known to the Romans many years later as Tyrian purple. The element itself was not isolated until

1826, when Balard extracted it from liquors remaining after crystallisation of salts from the Montpellier salt marches. Bromine then became popular with influential chemists like Dumas[39], who used it in experiments with organic compounds[40]. Döbereiner, in 1829, recognised that bromine was part of a group of elements containing chlorine and iodine, and that in terms of physical properties and reactivity, bromine was the central member of this group[41].

Dibromine is a very dense, volatile , red-brown liquid, boiling at 332.8K. In the liquid state, the structure of dibromine is molecular, with a Br-Br bond distance of 228pm[42]. As a solid (melting point 266.10K) the dibromine molecules form a layer lattice structure, lengthening the Br-Br bond distance to 272pm. Dibromine is the only nonmetallic element which is a liquid at room temperature[9].

There are two naturally occurring isotopes of bromine, which are ^{79}Br (50.69%) and ^{81}Br (49.31%). There are three commonly used radioactive isotopes; ^{80m}Br ($t_{1/2}$ = 4.42h, γ-emitter), ^{80}Br ($t_{1/2}$ = 17.6 min, β^--emitter) and ^{82}Br ($t_{1/2}$ = 35.3h, β^--emitter)[9]. These isotopes are used in the study of isotope exchange reactions among others. [^{82}Br]-Labelled dibromine was used in this project to examine adsorption of dibromine onto surfaces.

The halogens in general are among the most reactive of all elements, being easily reduced to form the singly charged anion, which is stable with a filled valence shell. This reactivity makes dibromine a very effective oxidising agent for a wide range of materials. Dibromine will brominate most carbon or hydrogen bonds and is commonly employed to halogenate organic compounds[42], as in equation 1.4.2:

$$CH_2{=}CH_2 + Br_2 \rightarrow CH_2Br\text{-}CH_2Br \quad \text{.....(1.4.2)}$$

Bromine can also be used to produce high oxidation state metal centres like $ReBr_5$[42] by direct halogenation reactions. The oxidative power of bromine has also been employed and modified in organic complexes which contain a central Br^+ atom[43]. Such complexes have potential as chemical etchants because of the modification of their etching properties by chemistry and environment.

The reactivity of dibromine can often depend greatly on the solvent, since solvolysis or halogenation of the solvent may enhance or facilitate reaction. This is particularly relevant in a polishing situation, since the choice of diluent may be critical to the reactivity of bromine at the wafer surface. Methanol is the most common choice of diluent for use with bromine in polishing[30], since it allows even distribution of the halogen throughout

the solvent. A CH_3OH---Br-Br---CH_3OH chain structure is known to form between Br_2 and CH_3OH in the solid phase[44]. Methanol also allows dissolution of product materials (probably by hydrolysis) in the polish solution. Solutions are normally used in the concentration range 0.2-2.0% v/v, since stronger solutions yield too vigorous a reaction and lead to a rough surface with a texture resembling orange peel.

1.4.2 HYDROGEN PEROXIDE.

First prepared in 1818 by Thenard, by acidification of barium peroxide, this compound is now prepared on an industrial scale by autoxidation of alkyl anthraquinols[45]. Hydrogen peroxide (H_2O_2) is best known as a bleaching agent and this is still its largest application, used in textiles and the paper industry. It has found a niche in the treatment of domestic and industrial effluent.

Hydrogen peroxide is a colourless, viscous liquid at room temperature, boiling at 423K (Density = 1.44 gcm^{-3})[9]. In the liquid and solid phases, there is strong hydrogen bonding among the molecules, causing a decrease in the dihedral angle, $\angle_d$, from 111.8° in the gas phase to 90.2° in the solid phase, Figure 1.4.1.

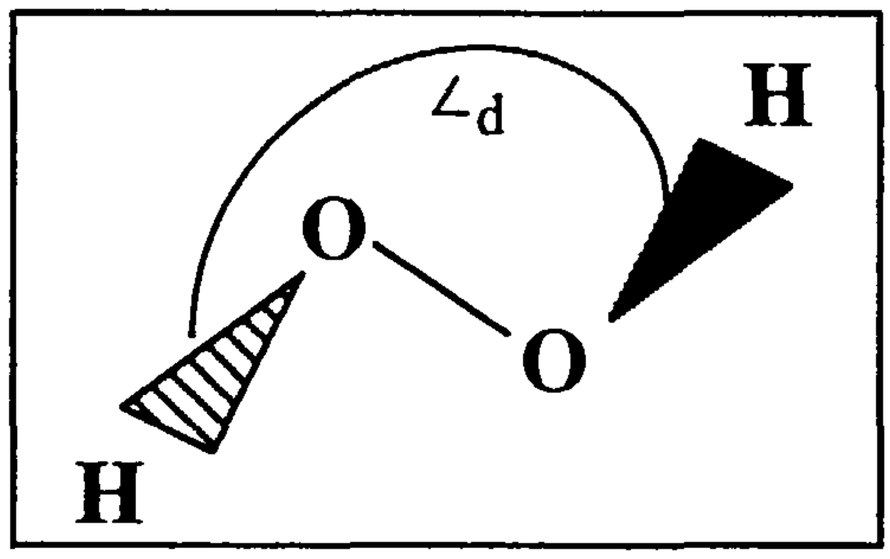

Figure 1.4.1 : The Structure of Free Hydrogen Peroxide.

Hydrogen peroxide evolves molecular oxygen on decomposition:

$$2H_2O_2 \rightleftharpoons 2H_2O + O_2 \quad .....(1.4.3)$$

This reaction occurs at room temperature if catalysed by small quantities of metal or alkali. The reaction is highly exothermic and can lead to explosions in very concentrated solutions. Its ease of decomposition means that the purity and freshness of H_2O_2 solutions are critical to their oxidative power.

Hydrogen peroxide is a very versatile reagent in that it can be used in both acidic (peroxonium salts, H_2OOH^+) and basic (hydroperoxides, OOH^-) forms. H_2O_2

solutions can also behave as both oxidising and reducing agents. The reactions below indicate the standard potentials of H_2O_2 for oxidation and reduction in acid solution[46]. These data indicate that H_2O_2 will not behave as a reducing agent in acidic solution i.e. in the acidic aqueous solution formed by H_2O_2, the compound behaves as a powerful oxidising agent.

$$2H^+ + H_2O_2 + 2e^- \rightarrow 2H_2O \qquad 1.776V \qquad \text{.....(1.4.4)}$$

$$H_2O_2 \rightarrow O_2 + 2H^+ + 2e^- \qquad -0.695V \qquad \text{.....(1.4.5)}$$

Hydrogen peroxide as an etchant is used as an oxidising agent which is usually employed in etchant mixtures rather than on its own. The reasons why peroxide is not effective on its own are not clearly understood. However, one possibility is that the oxidation products are not highly soluble in the acidic aqueous solution formed by H_2O_2 and another agent is required to complex or solvate the oxide, hence solubilizing the reaction products and allowing the oxidation to continue. This is the widely accepted view and is used to explain the etching behaviour of mixtures of H_2O_2 and phosphoric acid (H_3PO_4)[47] and sulphuric acid (H_2SO_4)[48,49] on GaAs and indium phosphide (InP)[50], although mechanistic details are seldom suggested. More detailed investigations have been carried out on alkaline hydrogen peroxide systems, where Kelly and Reynders[33] suggest that ammonia aids the reaction by complexation of insoluble gallium hydroxides at high pH:

$$\{Ga(OH)_3\}_{ads} + mNH_3 \rightarrow [Ga(NH_3)m]_{soln}^{3+} + 3OH^- \qquad \text{.....(1.4.6)}$$

This reaction is postulated by Kelly and Reynders, but no evidence for the existence of the product complex is provided and no precedent for such a system is available. However, regardless of the precise reactions in operation in these systems, it is clear that the solubility of oxides is critical to etching with hydrogen peroxide.

1.4.3 SODIUM HYPOCHLORITE

The history of hypochlorous acid (HOCl), the acid of which sodium hypochlorite (NaOCl) is a salt, began with its discovery by Scheele in 1774, when it was produced during experiments on chlorine (Cl_2). Hypochlorites in general have been widely used since for bleaching and sterilizing. Industrially, sodium hypochlorite (the most commonly known bleach) is prepared by the disproportionation of Cl_2 in cold alkali:

$$Cl_2 + 2NaOH \rightarrow NaOCl + NaCl + H_2O \qquad \text{.....(1.4.7)}$$

Most commercially available hypochlorite solutions will therefore contain one mole of chloride for each mole of hypochlorite. Sodium hypochlorite is unstable relative to other hypochlorites like calcium hypochlorite, $Ca(OCl)_2$ and cannot be isolated pure. Hypochlorous acid can be formed in the vapour phase by the equilibrium:

$$H_2O_{(g)} + Cl_2O_{(g)} \rightleftharpoons 2HOCl_{(g)} \qquad .....(1.4.8)$$

However, it is extremely unstable and is usually prepared in aqueous solution by the action of a mercuric oxide suspension on dichlorine.

The complex nature of the aqueous equilibria involved in hypohalite solutions means that the rate of decomposition is easily influenced by concentration, pH and temperature of solutions. Solutions of hypohalite will always contain several other species, including disproportionation products from the reaction shown in equation (1.4.9)[51]:

$$3[OCl]^- \rightleftharpoons 2Cl^- + [ClO_3]^- \qquad .....(1.4.9)$$

Fortunately, the disproportionation of hypochlorite, $[OCl]^-$, is slow at room temperature, so this reaction is not as critical to reagent purity as it is with other hypohalites like OBr^-. Hypohalous acids are also present in most hypohalite solutions:

$$[OCl]^- + H_2O \rightleftharpoons HOCl + OH^- \qquad .....(1.4.10)$$

This equilibrium lies well to the right because of the weak nature of hypohalous acids, so a significant amount of HOCl will be present in sodium hypochlorite solutions except at high pH values.

Both hypochlorite and hypochlorous acid are used for bleaching and sterilising because of their good oxidising power. Their standard reduction potentials are given in equations 1.4.11 and 1.4.12[46]:

$$[OCl]^- + H_2O + 2e^- \rightarrow Cl^- + 2OH^- \qquad 0.81V \qquad .....(1.4.11)$$

$$H^+ + HOCl + e^- \rightarrow 1/2Cl_2 + H_2O \qquad 1.61V \qquad .....(1.4.12)$$

The hypohalites and their acids are commonly used in both organic and inorganic chemistry. In organic chemistry, their main use is in the halogenation of aromatic and aliphatic compounds:

$$CH_2{=}CH_2 + HOCl \rightarrow CH_2Cl\text{-}CH_2OH \qquad .....(1.4.13)$$

In inorganic chemistry, they can be used to oxidise inorganic species by direct transfer of an oxygen atom[52,53]. This has led to the use of the term 'active oxygen' in many articles which discuss the etching chemistry of NaOCl[50], despite a lack of direct evidence that such a mechanism operates on 13-15 materials. As an etchant, sodium hypochlorite is widely employed in aqueous solution on gallium arsenide and indium phosphide[54] at various pH values and is also applied in the polishing situation[55].

1.5 AIMS OF THE PROJECT

The diversity of etchants used on GaAs and CdTe is very large, and the physical and chemical nature of the surfaces produced are, consequently, varied. However, even the most commonly employed reagents, such as dibromine in methanol or sodium hypochlorite, are not well understood with respect to the reactions occurring at the substrate surface. The initial aim of the project was to determine and clarify the reactions by which such reagents operate. Integral to this was the investigation of the dependence of etching and polishing on parameters like pH, concentration and abrasive type. From this position, further objectives involving the prediction of optimum polishing and etching conditions for older reagents already in use and the design of new reagents have developed.

The impression currently given in the literature is that the polishing process is different for each material and each reagent and is therefore more of an art , for experienced practitioners, than a science. However, in this work we have endeavoured to find general physical and chemical principles which can be applied to all etchants and substrates and to formulate a generalised scientific model for chemomechanical polishing.

1.6 APPROACH TO THE WORK.

The general approach to the work has been to combine model experiments using dip-etch and radiotracer techniques with *in situ* experiments using polishing equipment. This approach overcomes problems with the control of parameters and collection of results during the polishing process and has allowed the creation of conditions not possible in a polishing experiment, in order to determine initial reaction products and the effects of air and moisture.

The initial stages of the project involved dip-etching of GaAs and CdTe (as 'typical' 13-15 and 12-16 semiconductors) using the reagents described in Section 1.4. The nature of these reactions and their products was examined using mass loss determinations, atomic absorption spectroscopy analyses and various surface analysis techniques. These aqueous solution etches were executed in conjunction with some anhydrous etching experiments. The results of these general etching experiments were used to predict optimum polishing conditions and these hypotheses were tested *in situ* on both GaAs and CdTe. The outcome of polishing experiments was evaluated using mass decrease and various techniques for the measurement of surface roughness.

Radiotracer techniques employing radioactive isotopes of chlorine and bromine (^{36}Cl and ^{82}Br respectively) were used to verify presumptions made from dip-etch experiments. This technique also proved useful in the investigation of phenomena unique to the polishing process, such as the interaction between refractory oxide abrasives and certain chemical reagents.

The knowledge gained from a combination of dip-etch, polishing and radiotracer experiments was applied, in the latter stages of the project, to the development of new reagents for the etching and polishing of GaAs and CdTe.

CHAPTER TWO

SOLUTION ETCHING

2.1 INTRODUCTION.

Dip-etch experiments were employed in this section of the work to model the reactions occurring in a polishing situation. By using the reagent in a solution etch, it was possible to control carefully parameters such as pH, concentration and temperature and hence produce more reliable results. Important conclusions drawn from these model experiments were then tested in polishing experiments to check the validity of any extrapolations.

Dip-etches were used to examine a wide variety of reactions and conditions using the same very basic techniques. Etch solutions were analysed using iodometric titration, atomic absorption spectroscopy and electronic spectroscopy. The semiconductor surfaces were examined using various surface analysis techniques and the reactions were also evaluated in terms of mass differences in the wafers after etching. The same dip-etch techniques were used to determine the dependence of reactivity on pH and concentration and for the production of etched surfaces to allow surface analysis. One critical difference between this approach and that of previous authors[30-37] is that the progress of etch reactions was examined by a combination of atomic absorption analyses and mass decrease measurements. Since this approach does not confine the analysis to one technique, a cross-check was available to confirm the reliability of results. Some anhydrous etches were also undertaken to determine the effect of moisture on the reactions occurring.

2.2 GENERAL EXPERIMENTAL TECHNIQUES.

2.2.1 IODOMETRIC TITRATION

In order to determine the precise concentration of sodium hypochlorite (NaOCl) solutions prior to etching and to account for any decomposition during etching, it was necessary to titrate the solutions and ascertain the amount of available chlorine present. This was achieved using the standard technique of iodometric titration[56].

Sodium hypochlorite reacts with halide salts in acid conditions to release the halogen by oxidation. Thus, if an iodide salt is added to hypochlorite in acid conditions, iodine will be liberated, as in equation 2.2.1:

$$[OCl]^- + 2I^- + 2H^+ \rightleftharpoons Cl^- + I_2 + H_2O \quad \text{.....(2.2.1)}$$

The iodine liberated can then be titrated with standard sodium thiosulphate to determine the concentration of OCl^- present:

$$I_2 + 2S_2O_3^{2-} \rightarrow 2I^- + S_4O_6^{2-} \quad \text{.....(2.2.2)}$$

Thus, for every two moles of thiosulphate required for neutralisation, one mole of hypochlorite is present:

$$[OCl]^- \equiv I_2 \equiv 2S_2O_3^{2-} \quad \text{.....(2.2.3)}$$

It is advisable to use weak acids to acidify the analyte solution, since strong acids will react with small amounts of chlorate decomposition product to liberate extra iodine from the iodide salt:

$$[ClO_3]^- + 6I^- + 6H^+ \rightleftharpoons Cl^- + 3I_2 + 3H_2O \quad \text{.....(2.2.4)}$$

To standardise the hypochlorite solution, $1cm^3$ of NaOCl solution (12% w/v, BDH Spectrosol) was placed in a $250cm^3$ conical flask by micropipette and diluted up to $50cm^3$ with distilled water. Iodate-free potassium iodide (M&B Pronalys, approximately 2g) and glacial acetic acid (Prolabo Rectapur, 99-100%, $2cm^3$) were added to this and the liberated iodine was titrated with standard sodium thiosulphate solution ($0.1mol.dm^{-3}$, Volucon). As the solution turned pale yellow, a few drops of starch indicator were added

and some extra acid was added dropwise to check that pH was not the limiting factor. The endpoint was identified when the analyte mixture turned and remained colourless.

Table 2.2.1 shows some typical titration results from this type of standardisation experiment.

Titration	Start	Finish	Titre(cm^3)
1	7.79	43.38	35.59
2	8.76	44.10	35.34
3	6.70	40.68	33.98
4	9.82	44.16	34.34
5	7.78	42.98	35.20

Table 2.2.1: Standardisation of Hypochlorite.

The average titre here was 34.89cm^3 of 0.1$mol.dm^{-3}$ thiosulphate, containing 3.49 x 10^{-3} mol of thiosulphate in total. This is the amount required to neutralise 0.00175 mol of hypochlorite. Thus, if 1cm^3 of hypochlorite solution contains 0.00175 mol of OCl^-, the concentration of the solution must be 1.75 $mol.dm^{-3}$.

Such titrations were carried out prior to dip-etch experiments employing NaOCl as a concentrated solution. They were also employed to check the precise concentration of diluted samples where the etchant concentration was varied. Table 2.2.2 gives examples of the data from this type of experiment.

Dilution	Volume(cm^3)	Titre(cm^3)	Concentration ($mol.dm^{-3}$)
–	1	32.52	1.61
1:2	2	36.90	0.92
1:3	4	48.54	0.61
1:4	4	37.40	0.47
1:5	5	37.48	0.38
1:10	5	18.90	0.19
1:25	10	15.72	0.08
1:50	25	21.98	0.04
1:100	25	9.08	0.02

Table 2.2.2: Dilution and Standardisation of Hypochlorite.

2.2.2 ATOMIC ABSORPTION SPECTROMETRY

A) BASIC PRINCIPLES

The basis of atomic absorption spectroscopy is the absorption of radiation by atoms. The quantitative version of this technique allows the concentration of a given element to be determined by the quantity of a certain wavelength of radiation which is absorbed. The quantitative technique is referred to as atomic absorption spectrometry[57] (AAS). A schematic diagram of an atomic absorption spectrometer is shown in Figure 2.2.1.

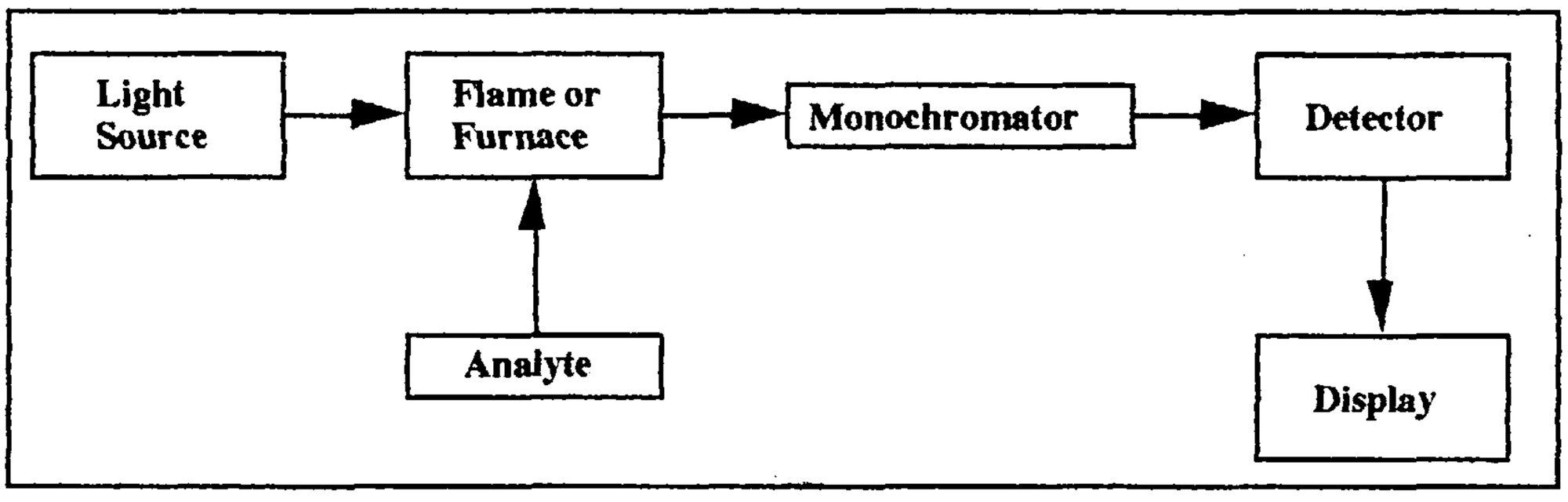

Figure 2.2.1: Components of an Atomic Absorption Spectrometer

The absorption of radiation in AAS occurs by the collision of photons with the valence shell electrons in the analyte atoms. The energy imparted by such a collision promotes electrons into higher energy levels and some of these excited state electrons will return to a lower energy level by the emission of a photon of light. The photon energies of the ultraviolet and visible radiation used in AAS mean that only the valence shell electrons are affected. At the temperatures of the flames (air/acetylene or nitrous oxide/acetylene) used in AAS, the majority of the atoms in the analyte will be in the ground state, making atomic absorption spectroscopy a very sensitive technique.

The spectrum obtained in an AAS experiment is measured in units of absorbance (A), which is equal to the logarithm of the ratio of incident light power (P_o) to transmitted light power (P) as in equation 2.2.5.

$$\mathbf{A = \log\ (P_o/P)} \qquad .....(2.2.5)$$

The transmitted light, P (Figure 2.2.2) will be affected both by the nature of the medium through which the light beam is passing and the path length, L, of the absorbing material.

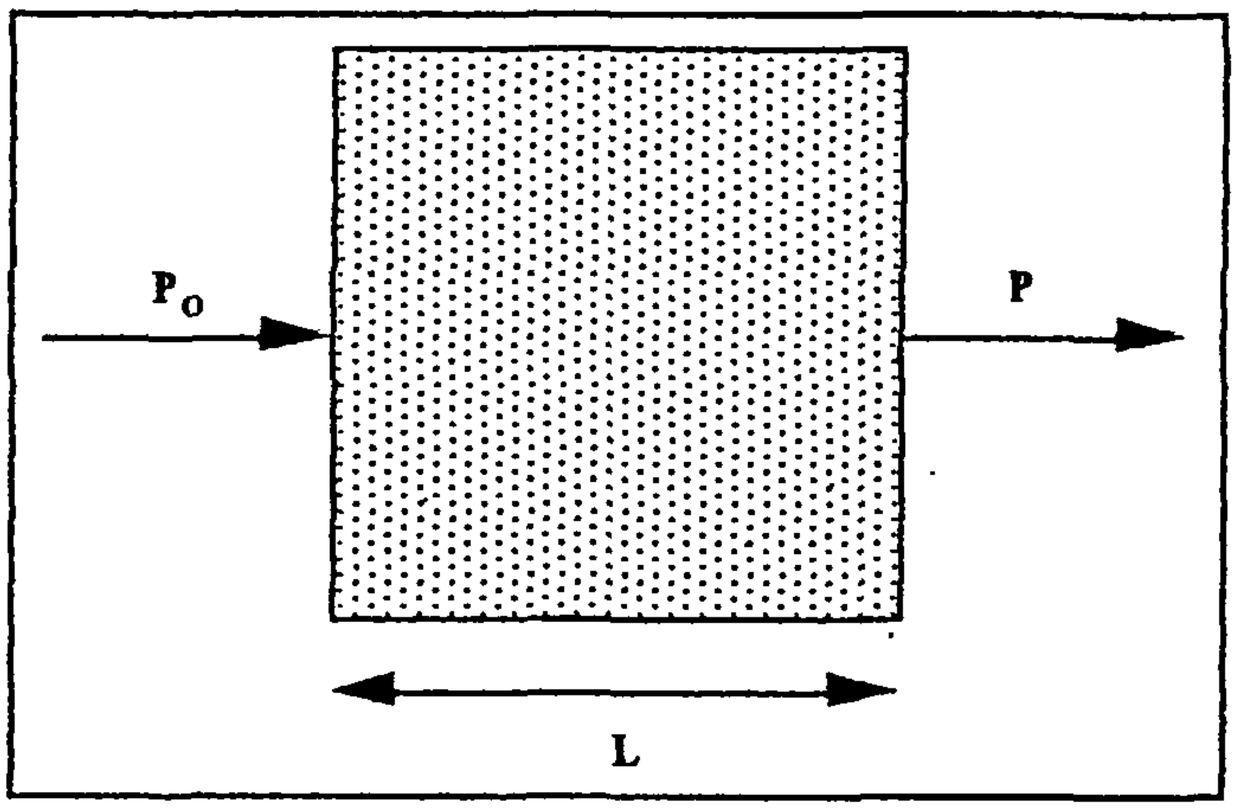

Figure 2.2.2: Absorption of Light by an Absorbing Medium of Path Length L

Thus, the relationship between transmitted and incident light power can be described as in equation 2.2.6:

$$P = P_o \exp(-kL) \quad .....(2.2.6)$$

where k is the absorption coefficient, which takes into account several parameters, such as the wavelength of the incident light and the density of the ground state atoms in the absorbing material.

The calculation of absorbance would be greatly simplified if k could be treated as a constant. However, k varies over the wavelength range incident on the detector. This means that k is very dependent on the accuracy of the incident wavelength and on the width of the emission profile from the light source. Thus, we require a light source which can produce radiation over a very narrow wavelength range which exactly matches that absorbed by the atoms we are trying to detect. The hollow cathode lamp (Figure 2.2.3) which is used in AAS best meets these criteria.

The inside of the hollow cathode is lined with the element whose emission spectrum is required and the lamp itself is filled with an inert gas such as argon or neon, at a pressure lower than atmospheric. Electrons released from the cathode cause ionisation of the fill-gas and subsequent collision of the newly-formed ions with the cathode lining leads to vaporisation of the constituent atoms. The collision of these atoms with the electrons, ions and atoms in the lamp leads to a characteristic, narrow width, emission spectrum. The fact that the light source is at lower temperature and pressure than the analyte means

that Doppler and Lorentz broadening[57] processes are minimised in the final absorption spectrum.

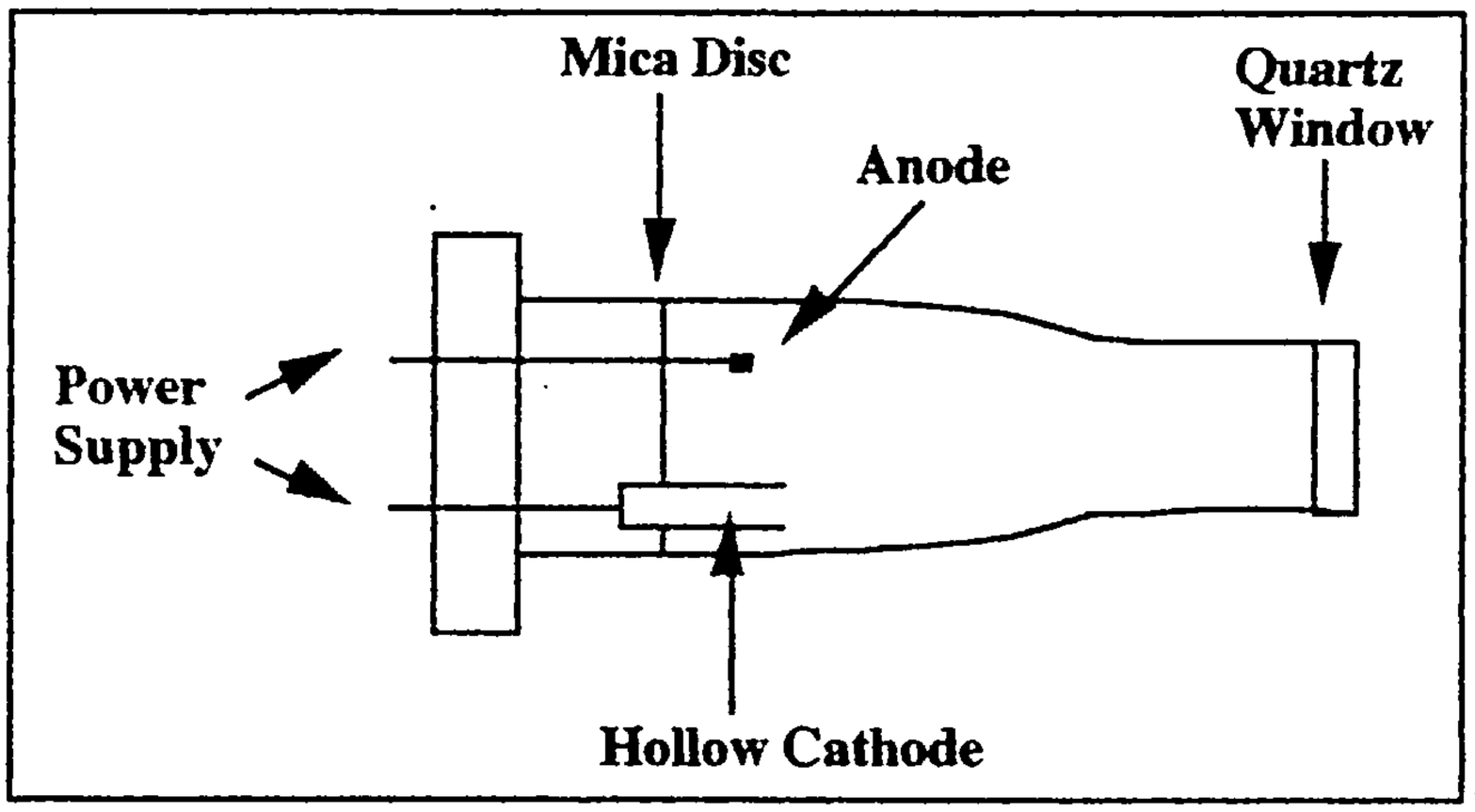

Figure 2.2.3: Hollow Cathode Lamp

Using this type of light source the absorption coefficient, k, is kept as constant as possible. However, it is still necessary to take various other broadening processes into account. These can be calculated and incorporated into a new constant, K. Hence, equation 2.2.6 becomes:

$$P = P_0 \exp(-KL) \quad .....(2.2.7)$$

The last factor which requires to be considered in the calculation of absorbance is the density of ground state atoms in the absorption medium. Since the ratio of excited state to ground state atoms is so small, the number of ground state atoms present per unit volume is approximately equal to the total number of atoms present per unit volume, N. Hence absorbance, A, can be calculated as shown in equation 2.2.8, and is therefore proportional to the concentration of given atoms in the analyte.

$$A = KLN \quad .....(2.2.8)$$

B) EXPERIMENTAL DETAIL

The atomic absorption spectrometer used throughout the project was a Perkin Elmer model 1100B instrument. The hydride generation analysis technique was used to determine the concentration of arsenic in etch solutions after dip-etch experiments. Other techniques can be used to determine different atoms. These are described in Chapter Three.

The hydride generation system involves the reaction of the borohydride anion BH_4^- with the element to form its hydride, which is then sprayed into an oxy-acetylene flame. This is a two-step reaction: The reductant reacts to liberate hydrogen, which in turn reduces the metal ions to a volatile hydride. An hydrogen stream flushes the hydride into a heated quartz cell where it decomposes and the absorptions of the metal can be measured.

$$As^{3+} + 4BH_4^- \rightarrow AsH_3 + 1/2H_2 + 2B_2H_6$$
$$\downarrow \Delta$$
$$As$$

.....(2.2.9)

In the experiments detailed, a 1ppm arsenic solution in 1.5% hydrochloric acid was used as a standard, injected in aliquots of 10, 25 and 50μl. The calibration volume was 10cm^3.

An example of the calibration graph obtained when employing these standards is given in Figure 2.2.4. All analyses were repeated at least twice and the average absorbance taken to calculate final concentration.

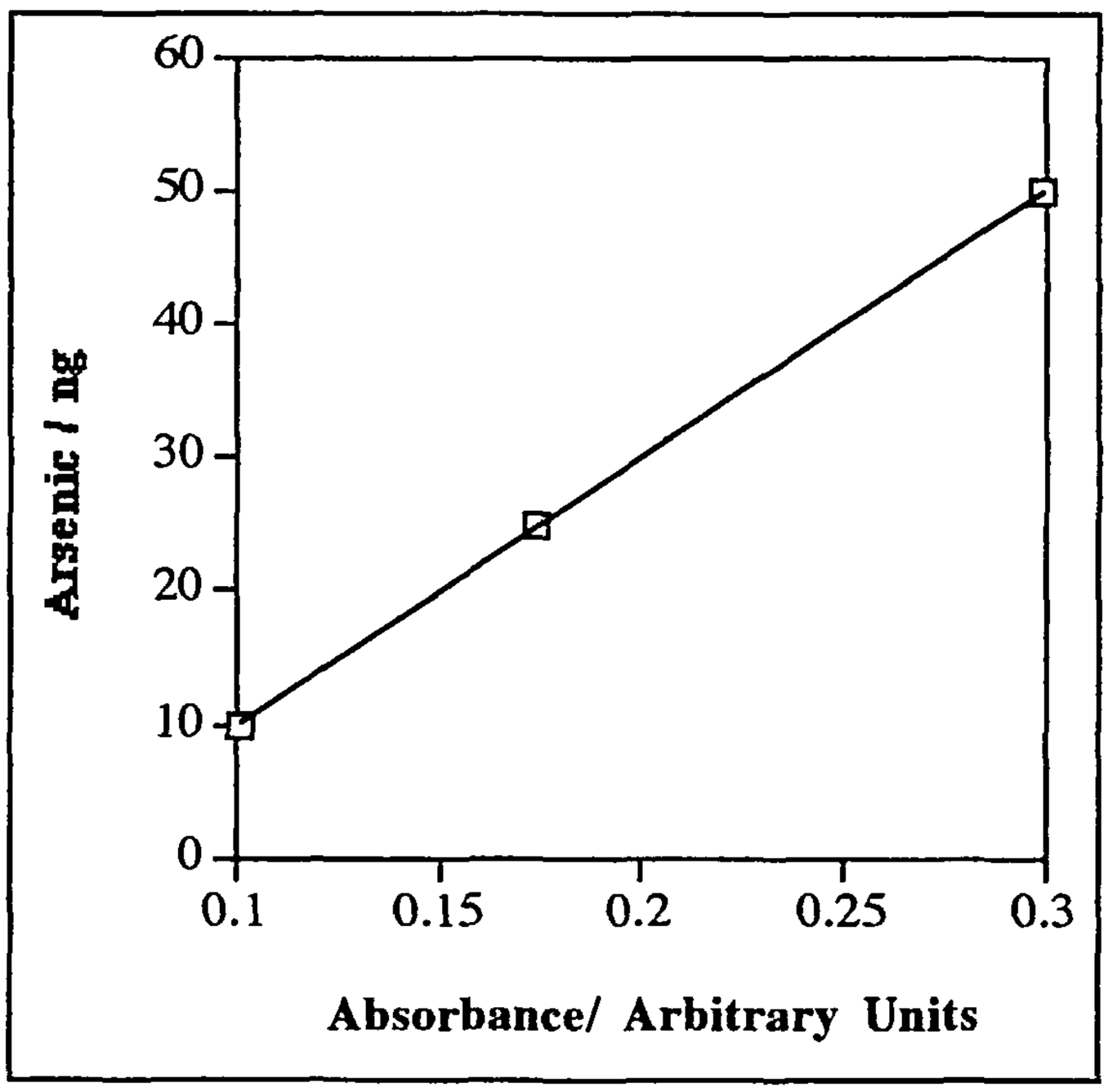

Figure 2.2.4: Calibration for Arsenic Standards in Hydride Generation

2.2.3 ELECTRONIC SPECTROSCOPY

Electronic spectroscopy was used to examine changes in the composition of sodium hypochlorite solutions.

A) BASIC PRINCIPLES

Electronic spectroscopy detects the transfer of electrons between different valence shell molecular orbitals. In absorption ultraviolet (UV) or visible spectroscopy, the sample is irradiated by a light source and the light emitted from such excitation is dispersed by a prism or grating before reaching the detector, as in Figure 2.2.5.

The light source in the visible region is a simple filament lamp and in the UV region is a high pressure hydrogen or deuterium lamp. A sample of any phase can be examined in this way, provided the correct sampling technique and an appropriate reference are used. For solids and liquids, absorption bands are usually broad (Figure 2.2.6) and spread widely across a maxima. However, gas phase samples often show rotational fine structure which can yield information about individual transitions between energy levels.

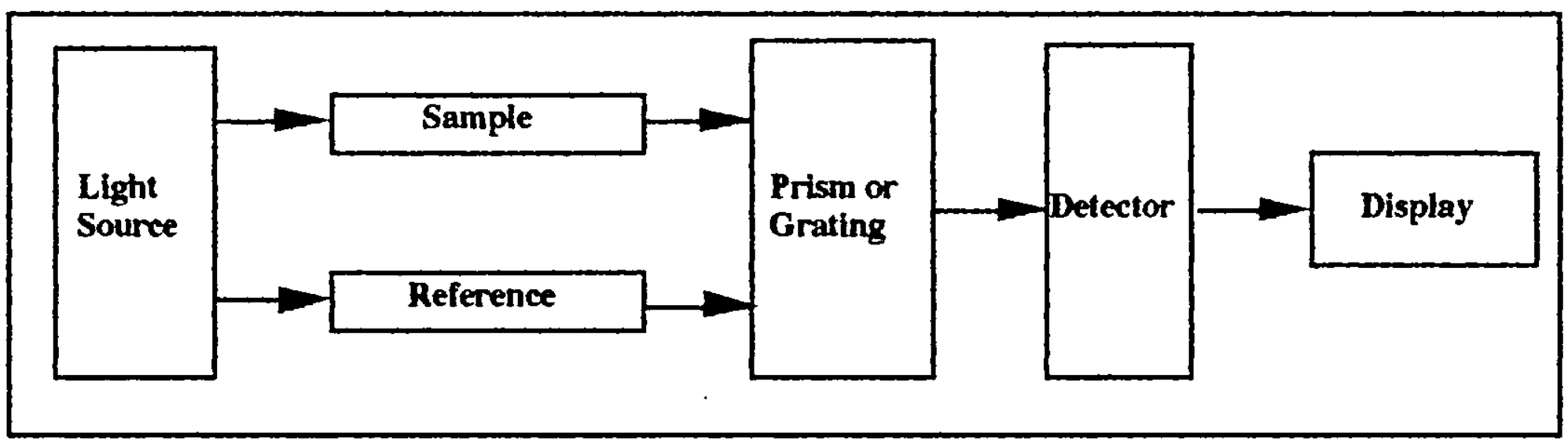

Figure 2.2.5: Schematic of a UV/Visible Spectrometer.

B) EXPERIMENTAL DETAIL

Qualitative experiments can be used to determine whether certain species are present, by identification of their absorbance maxima (λ_{max}). The conversion of one species to another can also be followed qualitatively with time.

i) pH Dependence of Hypochlorite Decomposition.

Six NaOCl solutions were prepared at pH values ranging from 5.4 to 8.1 using glacial acetic acid (Prolabo, Rectapur) and NaOCl (12% w/v BDH Spectrosol). The solutions

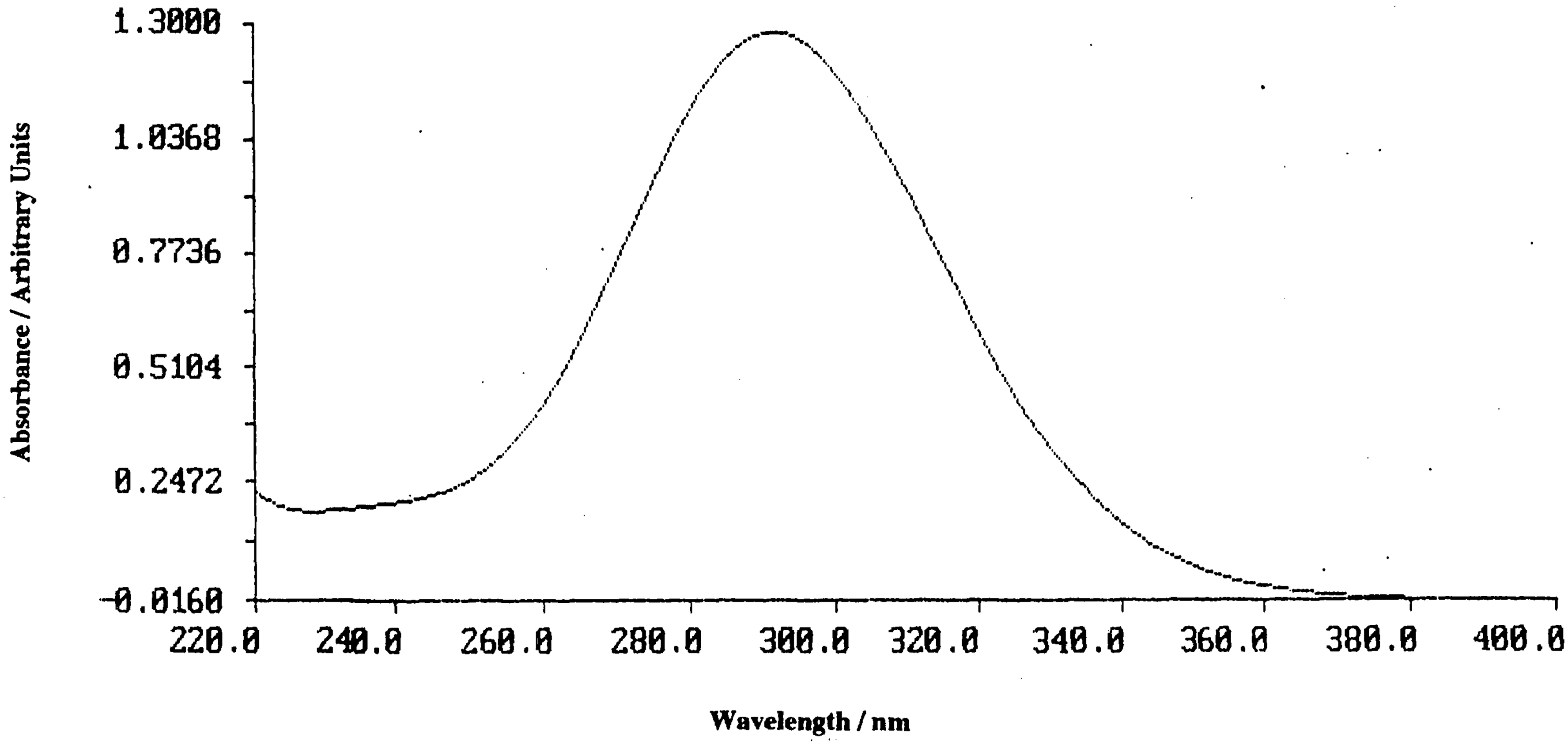

Figure 2.2.6: UV / Visible Absorption Spectrum of NaOCl Solution

were stored in airtight containers and their ultraviolet spectra were recorded after 5min., 120min. and 21h on a Perkin Elmer Lambda 9 UV/visible/near IR Spectrometer. The acidities of the solutions were determined using a standard pH electrode (Russell pH Ltd.) with an EIL 7050 meter. The spectra obtained after 5min. and 21h are shown in Figures 2.2.7 and 2.2.8. Table 2.2.1 shows the various absorbance values obtained for $[OCl]^-$ and HOCl at the different sampling times. After 5min., a clear increase in hypochlorite (λ_{max} 292nm)[51] and a decrease in hypochlorous acid (HOCl, λ_{max} 236nm)[51] is apparent as pH increases. This represents the shift in the equilibrium of equation 1.4.10 to $[OCl]^-$ at high pH After 21h, both $[OCl]^-$ and HOCl contents had levelled out significantly, indicating that decomposition was complete. The pH of all six solutions at this point had reduced to 4.5.

pH	Approximate Absorbance					
	5min.		120min.		21hrs.	
	NaOCl	HOCl	NaOCl	HOCl	NaOCl	HOCl
5.4	0.20	0.45	0.16	0.34	0.16	0.25
5.7	0.45	0.55	0.16	0.32	0.16	0.25
6.5	1.05	0.30	0.16	0.30	0.16	0.25
6.9	1.38	0.22	0.16	0.28	0.16	0.25
7.6	1.45	0.25	0.16	0.23	0.16	0.20
8.1	1.65	0.15	0.28	0.20	0.16	0.20

Table 2.2.1: Decomposition of NaOCl to HOCl with pH

Electronic spectroscopy can also be used quantitatively. The concentration of a certain species in solution can be determined according to the Beer-Lambert Law (equation 2.2.10)

$$A = \varepsilon c l \quad .....(2.2.10)$$

where A = absorbance
ε = molar extinction coefficient
c = concentration
and l = path length of cell (10mm).

ii) NaOCl Standards for Electronic Spectroscopy.

In order to quantify the amount of hypochlorite remaining in the sample solutions at a given time, it was necessary to produce a set of standards relating absorbance A (on the scale 0→1.0) to hypochlorite concentration in $mol.dm^{-3}$.

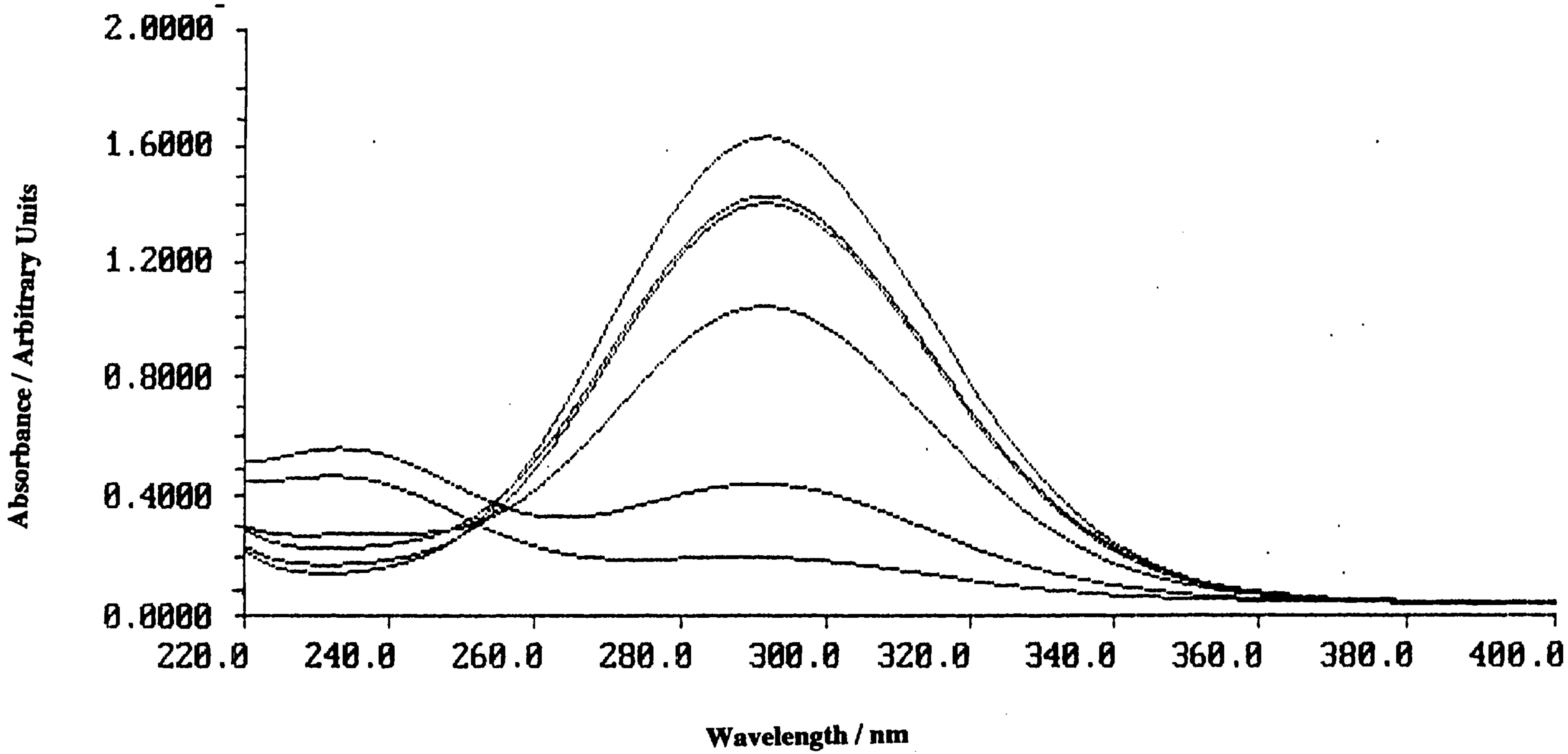

Figure 2.2.7: UV / Visible Absorption Spectra of NaOCl Solutions 5 min. After Acidification to pH Values Between 5.4 and 8.1

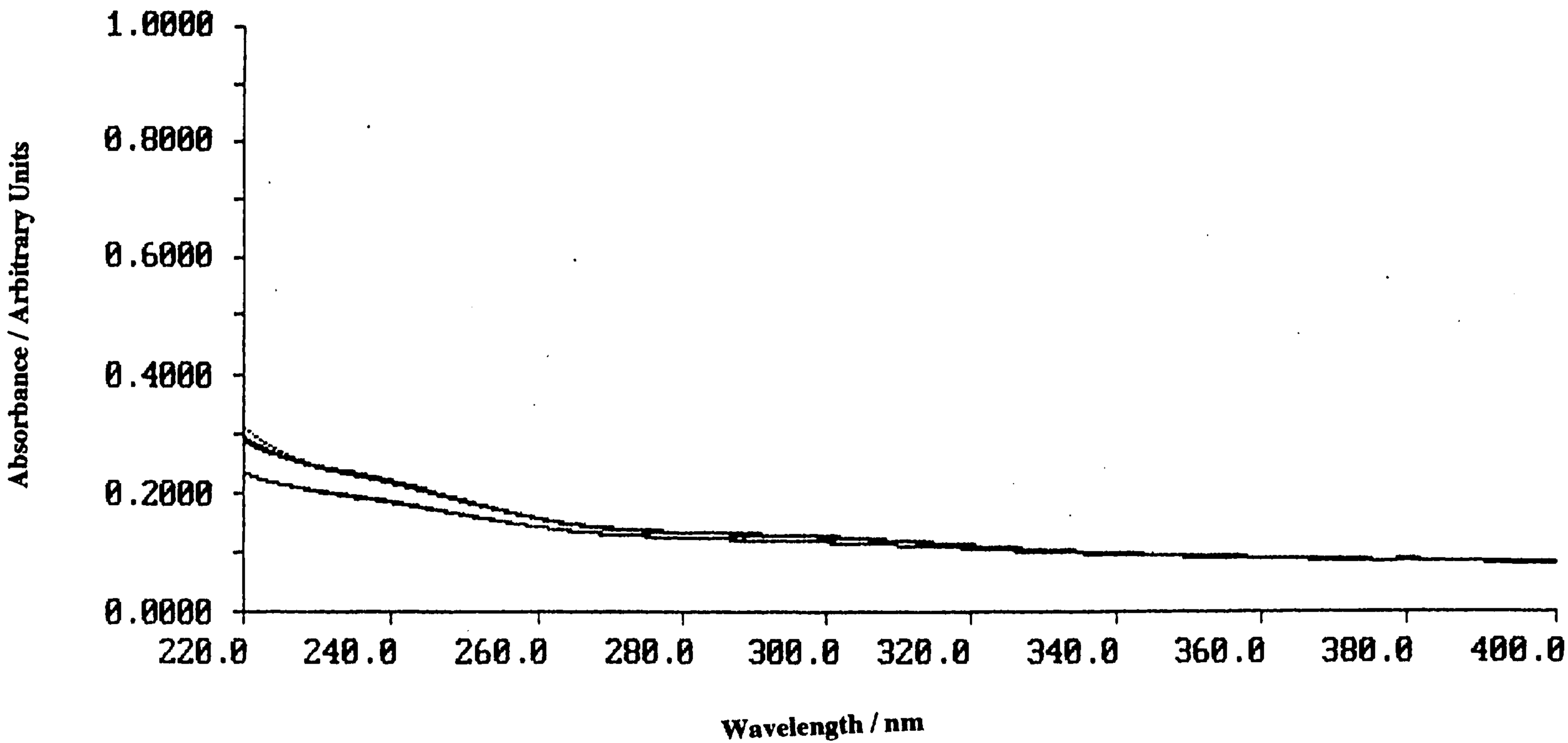

Figure 2.2.8: UV / Visible Absorption Spectra of NaOCl Solutions 21 h. After Acidification to pH Values Between 5.4 and 8.1

The bulk hypochlorite was standardised by iodometric titration first to determine its precise concentration. From this titre, the concentration of hypochlorite in the bulk solution was calculated to be 1.769 mol.dm^{-3}. This bulk solution was diluted to various degrees to give a range of absorbance intensities when analysed by UV/visible spectroscopy. The results from this procedure are given in Table 2.2.2.

Standard	µl NaOCl per 100cm^3	Absorbance	Concentration/ mol.dm^{-3} x 10^{-6}
1	140	0.9157	2.48
2	130	0.8570	2.30
3	120	0.7839	2.12
4	110	0.7452	1.95
5	100	0.6565	1.77
6	90	0.5837	1.59
7	80	0.5370	1.42
8	70	0.4814	1.24
9	60	0.4127	1.06
10	50	0.3615	0.89
11	40	0.2944	0.71
12	30	0.2401	0.53
13	20	0.1873	0.35
14	10	0.1069	0.18

Table 2.2.2: [OCl]$^-$ for UV/Visible Spectroscopy

Based on the linear relationship according to the Beer-Lambert Law, a plot of standard concentration versus absorbance A for the OCl$^-$ peak should give a straight line calibration plot with gradient equal to the product of ε and l. Such a calibration plot is shown in Figure 2.2.9.

2.2.4 SURFACE ANALYSIS TECHNIQUES

Wafer samples were examined after dip-etching to compare surfaces and, in some cases, to determine the composition of any surface product layer. Scanning electron microscopy and photoelectron spectroscopy techniques were employed.

A) X-RAY PHOTOELECTRON SPECTROSCOPY (XPS)

XPS techniques like Auger spectroscopy and ESCA (electron spectroscopy for chemical analysis) are high technology methods for determining the surface states present on a sample. The principle of ESCA is that electrons in lower energy bands or levels are

bombarded by X-rays from an aluminium (Al, 1487eV) or a magnesium (Mg, 1284eV) source. These electrons gain enough energy to leave the atom altogether (Figure 2.2.10) and are detected according to their residual kinetic energy (Equation 2.2.11).

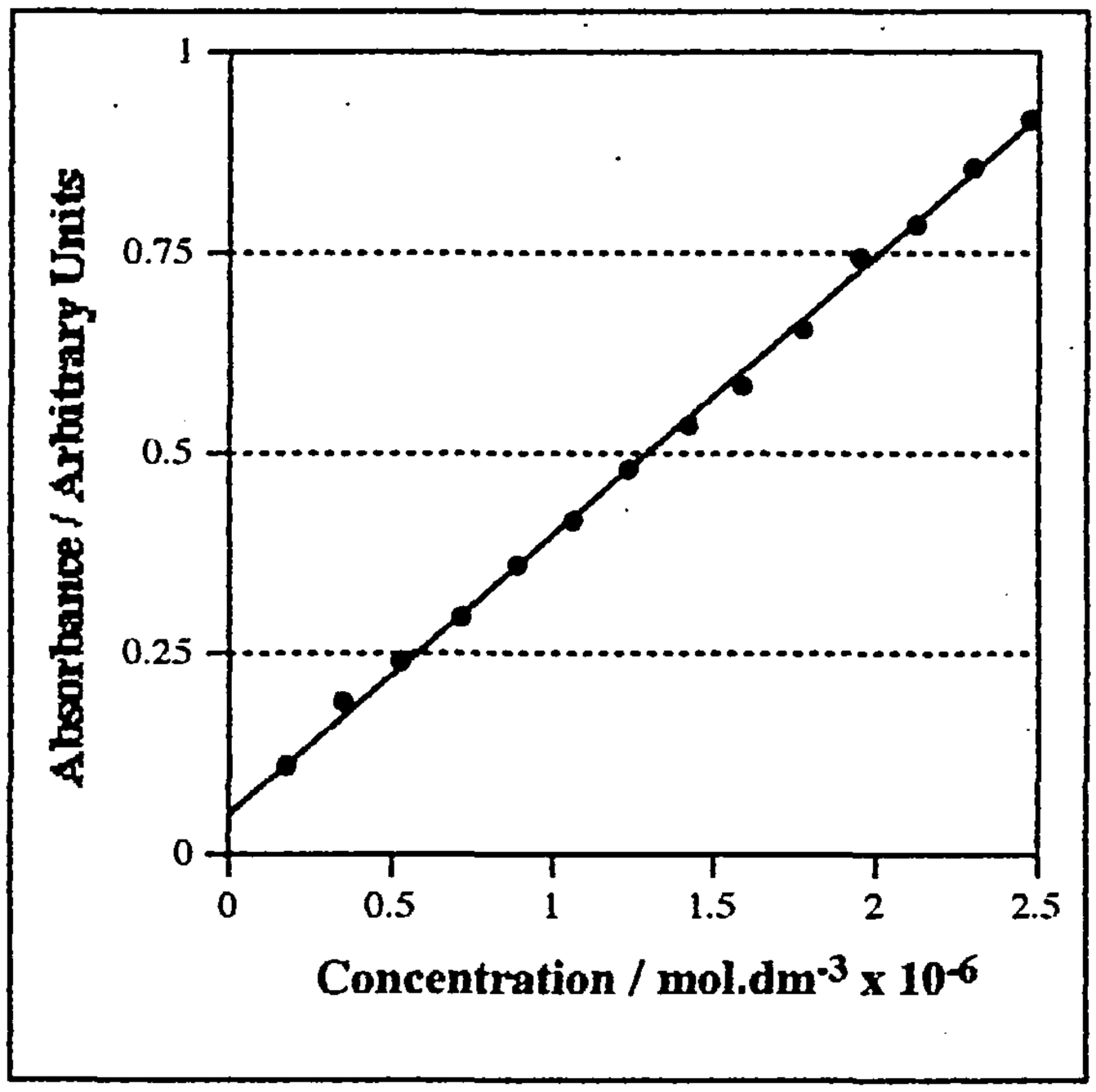

Figure 2.2.9: $[OCl]^-$ Calibration Graph for UV/Visible Spectroscopy

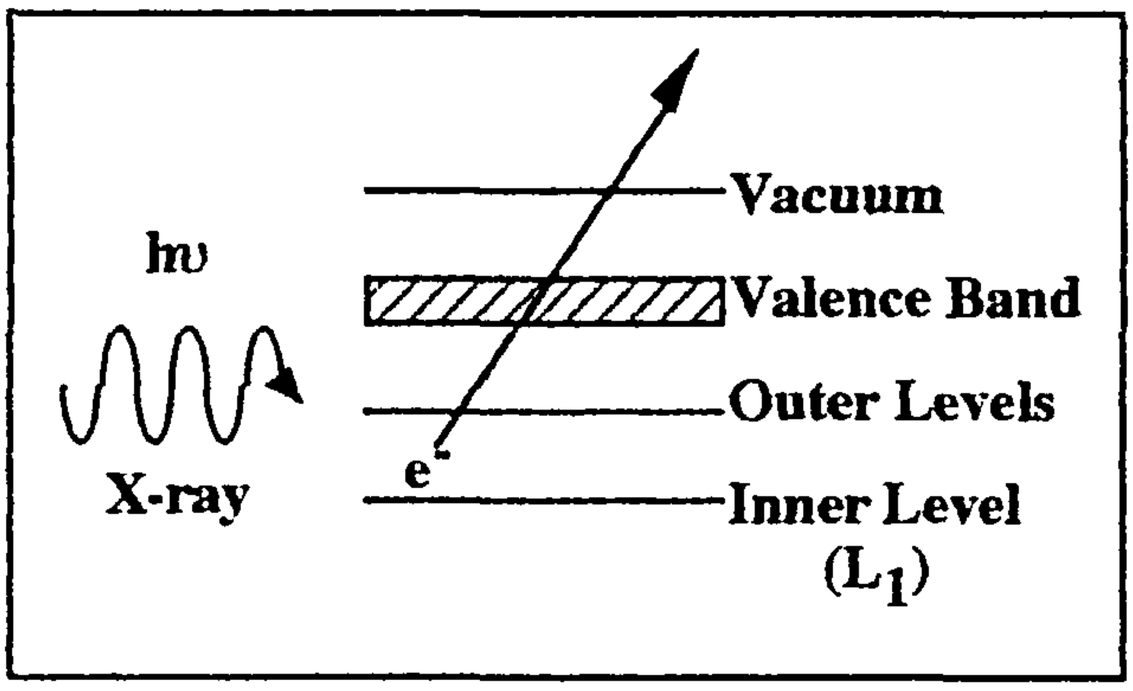

Figure 2.2.10: Ejection of Inner Shell Electrons in ESCA

$$\textbf{Kinetic Energy} = h\upsilon - E_{L_1} \qquad .....(2.2.11)$$

where E_{L_1} = the binding energy of an electron in an inner energy level.

Auger spectroscopy (Figure 2.2.11) works by a similar mechanism but the energy analysis is employed on secondary electrons. Secondary electrons are ejected from outer

shells, using energy provided when excited state electrons in lower energy levels relax back to their ground state. The residual kinetic energy is a function of the binding energies of the lower and outer shell electrons, as shown in equation 2.2.12.

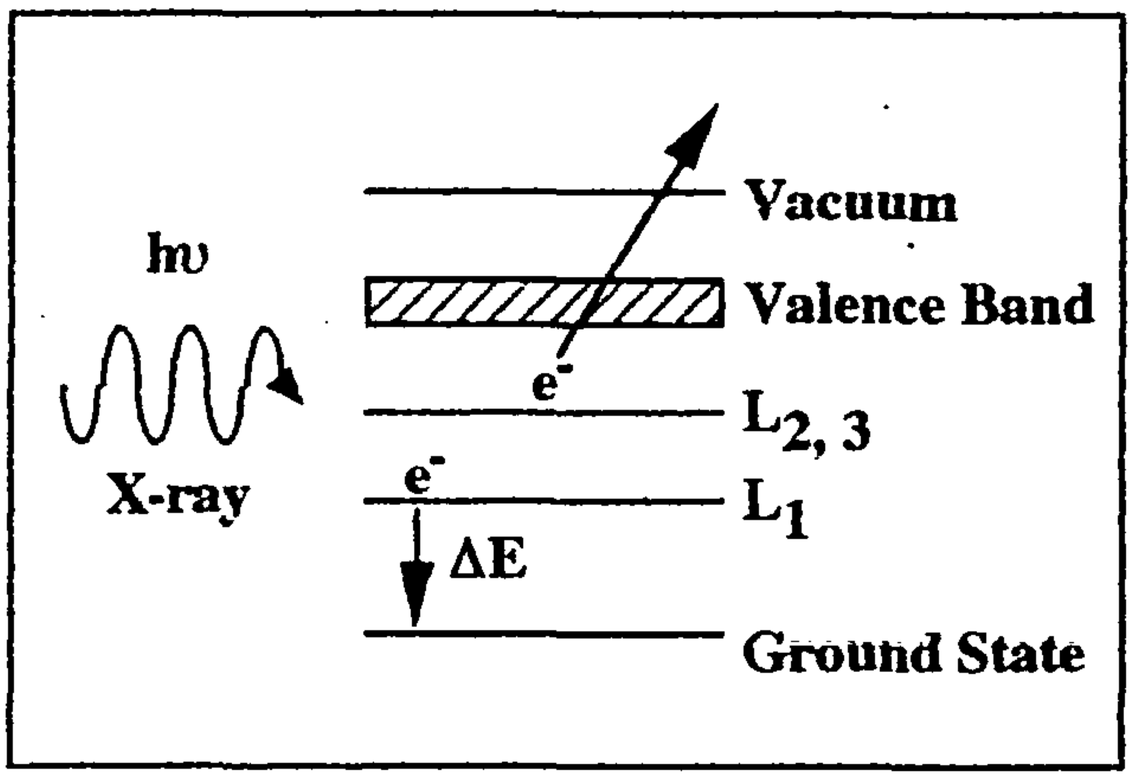

Figure 2.2.11: Ejection of Secondary Electrons in Auger Spectroscopy

$$\text{Kinetic Energy} = \Delta E - E_{L_{2,3}} \quad .....(2.2.12)$$

where $E_{L_{2,3}}$ = the binding energy of an electron in an outer energy level.

ESCA and Auger analyses were carried out on a Kratos XP 800 instrument using radiation from an Al source. Argon ion (Ar^+) sputtering used to etch the surfaces was carried out under a beam energy of 4kV. Auger analyses used a take-off angle of 90° normal to the sample surface. The base operating pressure, after loading the samples and pumping down, was ca. 9×10^{-10} Torr previous to Ar^+ sputter etching. The proportions of elements detected using Auger and ESCA techniques were determined using standard Scofield sensitivity factors[58].

B) SCANNING ELECTRON MICROSCOPY (SEM)

Scanning electron microscopy provides the lowest magnification of all the electron microscopy techniques but provides good depth of focus, allowing surface texture and topography to be examined. SEM is commonly used to study structures in the range 10^{-2} to 10^2 μm and so is ideal for examining surface features on etched wafer samples. Electrons from an electron gun are focused, using electromagnets, onto a small spot (50 to 100 Å) on the sample surface. Secondary electrons emitted from the surface are then used to build up an image which is very similar to an optical micrograph in appearance.

The scanning electron microscope used in this work was a Philips SEM500. Samples were examined at a tilt of 10° and the electron gun was operating at a potential of 3kV.

C) FOURIER TRANSFORM INFRARED MICROSCOPY

Infrared (IR) spectroscopy is a vibrational spectroscopic technique i.e. it detects the molecular vibrations of a sample. Any molecular vibration which produces an overall change in the electric dipole of a molecule can be detected by IR spectroscopy. The oscillating electric dipole produced when the molecule vibrates can interact with the electric vector of the electromagnetic (IR) radiation incident upon it. This interaction leads to the absorption of radiation at the same frequency as the molecular vibration. This absorption of radiation is then converted into a spectrum which can be viewed in terms of absorbed or transmitted frequencies. Such frequencies can range from 30 - 4000cm^{-1}, where cm^{-1} represents wavenumbers, equal to the reciprocal of the wavelength.

In older IR instruments, a dispersive element such as a prism or grating is used to separate the different frequencies of energy transmitted from a vibrating molecule. The newer technique of Fourier Transform IR uses an interferometer rather than a dispersive element. This allows all absorbed or transmitted frequencies to be measured quickly and simultaneously as an interference pattern or interferogram, which is then resolved into a spectrum using a mathematical function known as a Fourier Transform.

Infrared microscopy allows the convenience and specificity of microscopy to be combined with the versatility of the IR spectroscopic technique. The infrared beam can be focused onto a small region of the sample and an absorbance or transmittance spectrum for that region alone, rather than the whole sample area, can be obtained. FTIR microscopy was executed at Paisley University Chemistry Department on a BIORAD FTS 40 infrared spectrometer. Spectra were recorded in the range 4000cm^{-1} to 400cm^{-1} and averaged over 60 scans to analyse any given point on the wafer surface.

2.3 DIP-ETCH EXPERIMENTS

Initial work indicated that cadmium telluride was not etched by sodium hypochlorite solution and therefore model experiments using the dip-etch technique to investigate NaOCl as a reagent were limited to GaAs.

2.3.1 ETCHING OF GALLIUM ARSENIDE IN HYDROGEN PEROXIDE/AMMONIA SOLUTIONS AT VARIOUS pH VALUES

Ten sections ($1cm^2$) of the same GaAs (100) wafer were diamond scribed, cleaved and weighed on an analytical balance (precision 0.0001g). These wafer sections were then etched, for 30 minutes, in H_2O_2 (60 cm^3, AnalaR, BDH, 100vol. 33% wt./wt.) to which aqueous NH_3 (Pronalys, M&B, 33% wt./wt.) had been added to give a range of pH values as shown in Table 2.3.1.

Wafer Section	Initial Mass / g	pH
1a	0.3239	2.7
2a	0.3012	3.2
3a	0.3755	4.9
4a	0.3294	5.3
5a	0.3945	6.1
6a	0.2380	6.8
7a	0.2918	7.6
8a	0.3198	8.3
9a	0.2241	8.7
10a	0.3083	9.2

Table 2.3.1: GaAs Dip-Etch in Hydrogen Peroxide/Ammonia

The apparatus used for the dip-etch experiments is shown in Figure 2.3.1. Wafers were rinsed in distilled water, dried and weighed afterwards to determine any mass loss. Etch solutions were retained and analysed by hydride generation AAS to determine soluble arsenic.

2.3.2 ETCHING OF GALLIUM ARSENIDE IN SODIUM HYPOCHLORITE SOLUTIONS OF VARIOUS CONCENTRATION

Sections ($1cm^2$) of the same GaAs (100) wafer were cut and weighed on an analytical balance. Using the apparatus in Figure 2.3.1, these wafer sections were then etched, for 30 minutes, in NaOCl solution (60 cm^3, Spectrosol, BDH, 12% wt./wt.) diluted to a given concentration and standardised as described in Section 2.2.1.

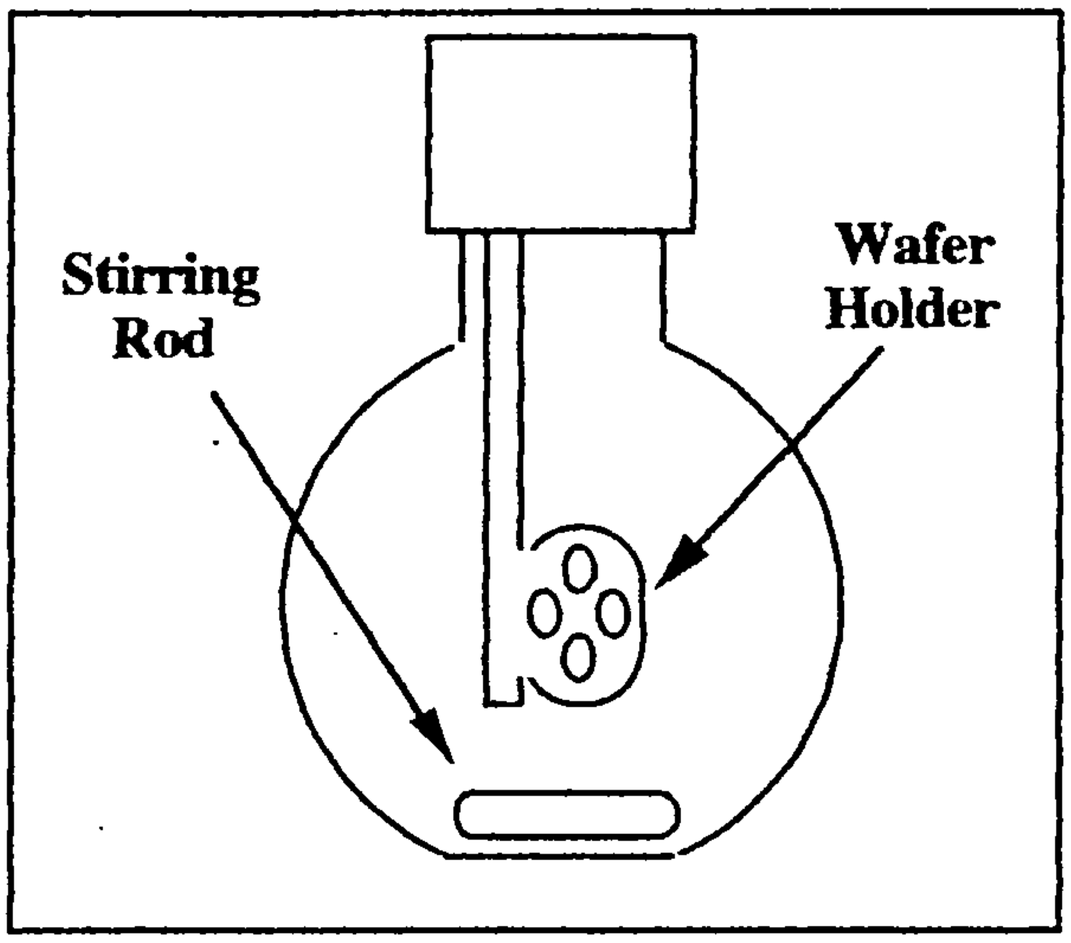

Figure 2.3.1: Dip-Etch Vessel

Wafer Section	Mass / g	NaOCl Concentration / $mol.dm^{-3}$
1b	0.2488	1.626
2b	0.2004	0.922
3b	0.2846	0.607
4b	0.2567	0.468
5b	0.2033	0.375
6b	0.1802	0.189
7b	0.1898	0.079
8b	0.1674	0.044
9b	0.2083	0.018

Table 2.3.2: GaAs Dip-Etch in NaOCl of Various Concentrations

Table 2.3.2 shows the concentrations of NaOCl employed and the initial masses of the wafer sections. Wafers were rinsed in distilled water, dried and weighed afterwards to determine any mass loss. Etch solutions were retained and analysed by hydride generation AAS to determine soluble arsenic.

2.3.3 Etching of Gallium Arsenide in Sodium Hypochlorite Solutions at Various pH Values

Sections ($1cm^2$) of the same GaAs (100) wafer were cut and weighed on an analytical balance. Using the apparatus in Figure 2.3.1, these wafer sections were then etched, for 30 minutes, in NaOCl solution. Acetic acid (Prolabo, Rectapur, 99-100%) was added

dropwise to the NaOCl solution prior to etching, until the desired pH was reached. The initial masses of the wafer sections and the pH values of the etchant solutions are given in Table 2.3.3.

Wafer Section	Mass / g	pH
1c	0.2255	13.0
2c	0.2924	10.9
3c	0.2895	9.6
4c	0.3125	7.5
5c	0.3530	5.1
6c	0.3065	3.4

Table 2.3.3: GaAs Dip-Etch in NaOCl at Various pH Values

Wafers were rinsed in distilled water, dried and weighed afterwards to determine any mass loss. Etch solutions were retained and analysed by hydride generation AAS to determine soluble arsenic.

2.3.4 MEASUREMENT OF HYPOCHLORITE DECOMPOSITION DURING GALLIUM ARSENIDE ETCHING IN SODIUM HYPOCHLORITE SOLUTIONS AT VARIOUS pH VALUES

Sodium hypochlorite solutions of various pH values were prepared as described in Section 2.3.3 and standardised (Section 2.2.1) to determine their precise concentration as shown in Table 2.3.4.

Solution	pH	NaOCl Concentration / $mol.dm^{-3}$
A	12.4	1.594
B	9.6	1.488
C	8.9	1.458
D	7.5	1.015
E	6.1	0.620
F	5.7	0.622

Table 2.3.4: GaAs Dip-Etch for Measurement of NaOCl Decomposition.

An aliquot ($60cm^3$) of each solution was then used in a standard dip-etch experiment on GaAs, as described in experiment 2.3.2. One aliquot ($60cm^3$) was kept as a control for the duration of the etch. Both the etch solution and the control were titrated after the etch to determine the extent of decomposition and to evaluate any enhancement of the decomposition which might be induced by the etching reaction.

2.3.5 ETCHING OF GALLIUM ARSENIDE IN SODIUM HYPOCHLORITE SOLUTION FOR VARIOUS ETCH PERIODS

Five sections ($2cm^2$) were cut from a GaAs (100) wafer and weighed on a 4-decimal place analytical balance. These sections were then etched, using the apparatus in Figure 2.3.1, in NaOCl solution ($1.6mol.dm^{-3}$). The wafer sections were etched for various time intervals ranging from 1h to 3h as shown in Table 2.3.5.

Wafer Section	Mass / g	Etch Time / h
1d	0.9493	1.0
2d	0.9665	1.5
3d	0.9511	2.0
4d	0.9108	2.5
5d	0.9519	3.0

Table 2.3.5: GaAs Dip-Etch in NaOCl for Various Etch Periods

The wafers were rinsed in distilled water, dried and weighed afterwards. Samples were retained for examination by scanning electron microscopy and photoelectron spectroscopy. A white precipitate formed overnight in the etchant solution from wafer section 5d and was filtered off. The precipitate did not melt below 300°C. The white solid was dissolved in water and treated with silver nitrate solution, yielding a dense white precipitate. These observations suggest the presence of NaCl.

2.3.6 ANHYDROUS ETCHING OF GALLIUM ARSENIDE IN A DIBROMINE/DICHLOROMETHANE SOLUTION

This experiment made use of a Pyrex glass vacuum line (10^{-2}Torr) to which a double-limbed Pyrex reaction vessel (Figure 2.3.3) was attached. The dibromine used was stored over phosphorus (V) oxide (P_4O_{10}) to ensure dryness and was regularly degassed

by cooling in a dry ice/dichloromethane bath to remove any hydrogen bromide. The dichloromethane used was dried over molecular sieves and also regularly degassed during the course of the experiment i.e. before each etch.

The double-limbed vessel was attached to the Pyrex vacuum line (Figure 2.3.2). It was evacuated, removed and degreased before weighing by suspension from a wire in an analytical balance. The vessel was then opened to the air and a GaAs wafer section inserted into one limb, before degassing and re-weighing to obtain the mass of GaAs used. The vessel was re-attached to the vacuum line and a quantity of dibromine was vacuum distilled into the remaining limb. The vessel was again removed, degreased and weighed to determine the mass of Br_2 present. This procedure was repeated, vacuum distilling a quantity of dichloromethane onto the dibromine and weighing to allow calculation of the concentration of the bromine solution.

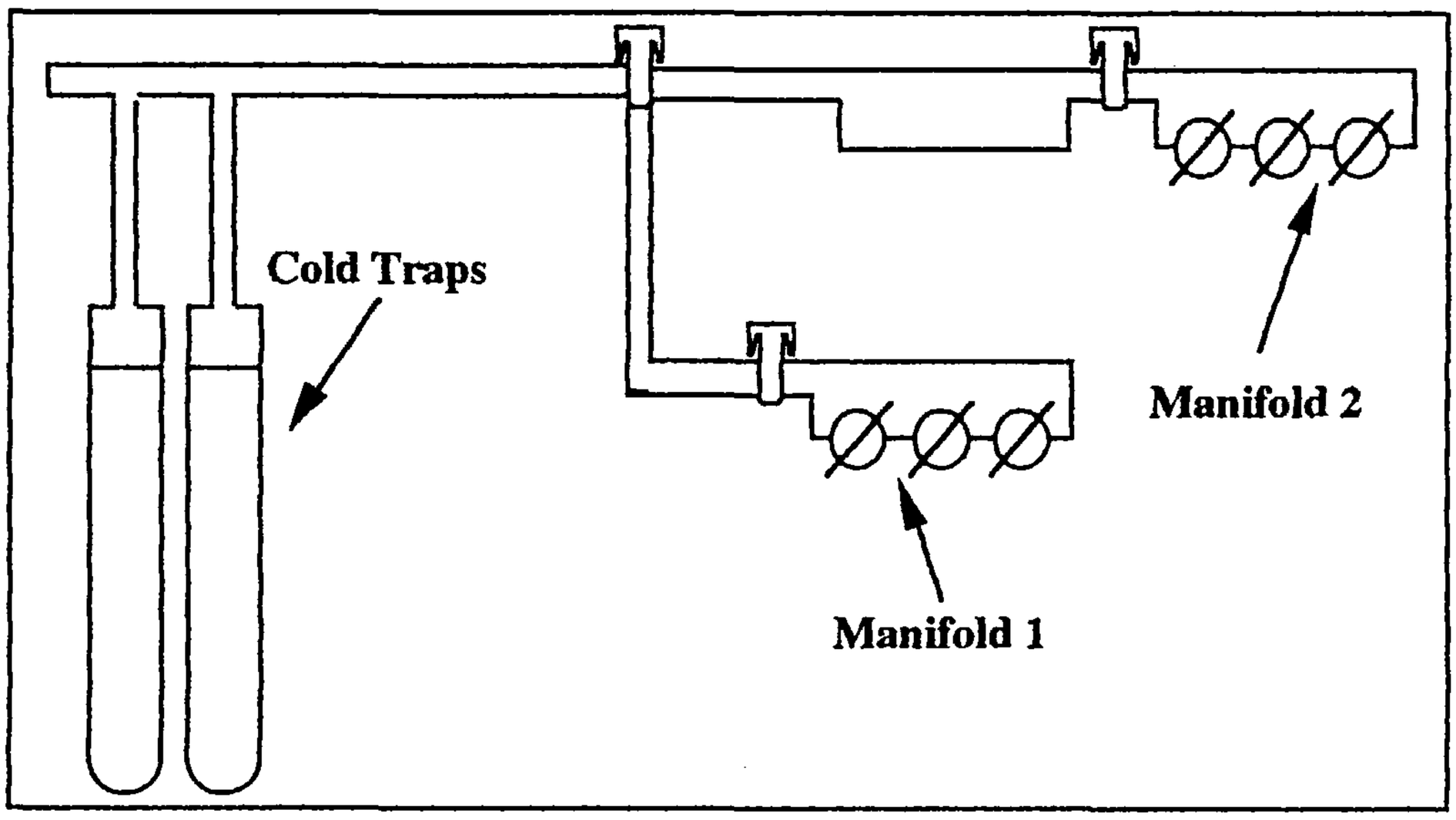

Figure 2.3.2: Pyrex Vacuum Line for Handling Dibromine

The central tap in the double-limbed vessel was opened and the vessel was inverted, allowing the dibromine solution to run over onto the GaAs. The solution was allowed to sit over the GaAs for 30 minutes before inverting the vessel again and removing the last traces of solution from the wafer limb by vacuum distillation. Both limbs of the vessel were then pumped out before a final vessel+wafer mass was recorded.

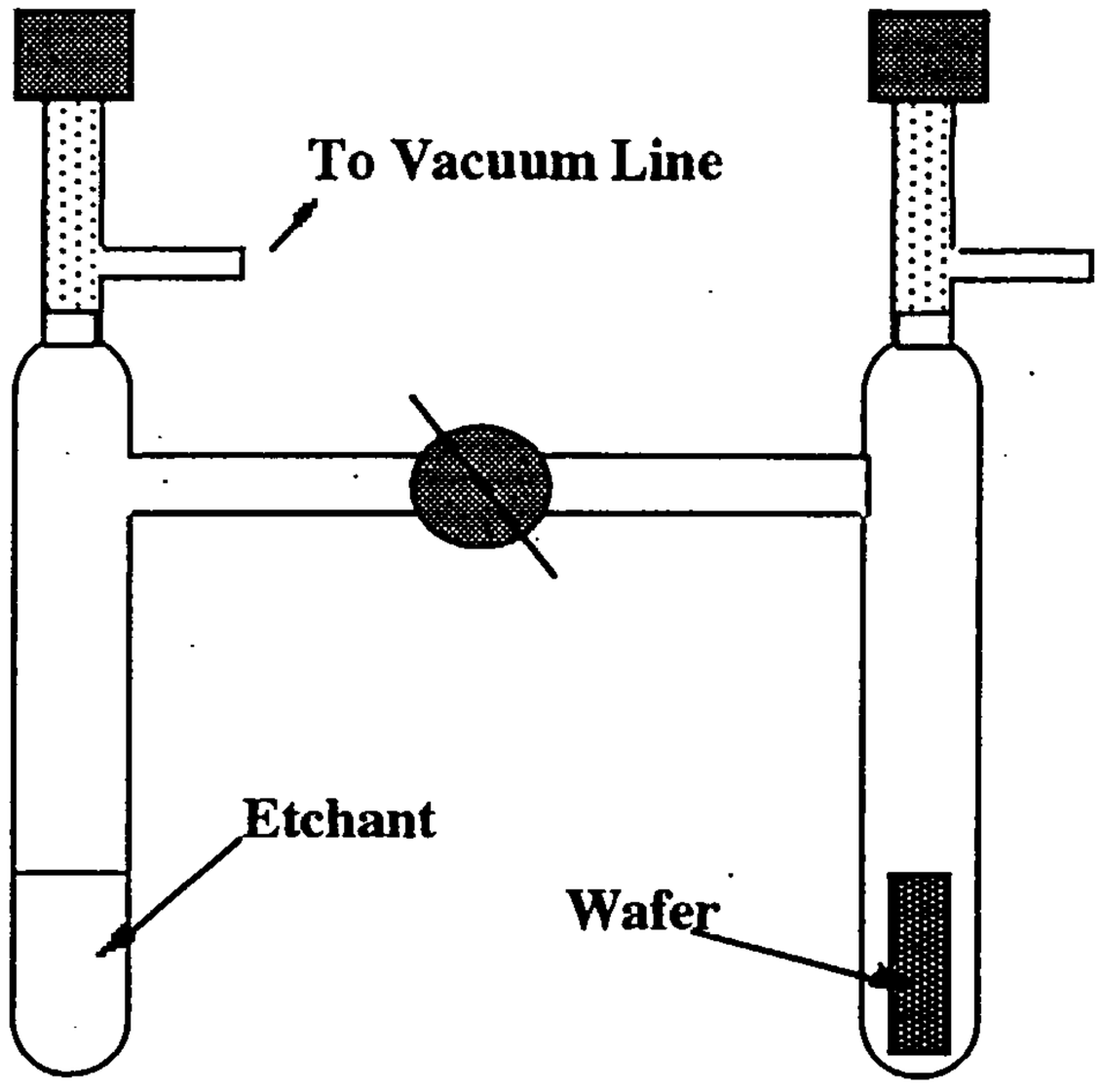

Figure 2.3.3: Double-Limbed Vessel

The initial mass readings for each GaAs section are given in Table 2.3.6 with the concentration (mol.dm^{-3}) of bromine in the solutions used to etch them.

Wafer Section	Mass / g	Dibromine Concentration / mol.dm^{-3}
1e	0.1645	0.049
2e	0.1740	0.123
3e	0.1662	0.145
4e	0.1078	0.394
5e	0.2010	0.457
6e	0.1542	0.475
7e	0.2164	0.802

Table 2.3.6: Anhydrous Dip-Etch of GaAs in Dibromine/Dichloromethane

2.4 RESULTS

2.4.1 ETCHING OF GALLIUM ARSENIDE IN HYDROGEN PEROXIDE/AMMONIA SOLUTIONS AT VARIOUS pH VALUES

The mass of GaAs removed from wafer segments etched in H_2O_2/NH_3 at pH values between 2.7 and 9.2 ranged from 0% to 64.9% of the initial wafer mass. The mass differences produced from ten different wafer sections are shown in Table 2.4.1.

Wafer Section	pH	Mass Loss / g	% Mass Loss
1a	2.7	0	0
2a	3.2	0	0
3a	4.9	0	0
4a	5.3	0.0003	0
5a	6.1	0.0004	0.1
6a	6.8	0.0003	0.1
7a	7.6	0.0017	0.6
8a	8.3	0.0063	2.0
9a	8.7	0.0363	16.2
10a	9.2	0.2001	64.9

Table 2.4.1: GaAs Etch in H_2O_2/NH_3 - Mass Loss Results

Analysis of the etch solutions for soluble arsenic yielded a similar trend with pH (Figure 2.4.1). 0.016mg of arsenic were found in $60cm^3$ of etch solution used at pH 2.7 and 47.4mg of arsenic were detected in the same volume of solution used to etch GaAs at pH 9.2. Mass loss results and soluble arsenic analyses both indicated that no significant reaction occurred until pH 7.5, where the etch rate began to rise sharply with pH. These results confirmed previous work carried out at Glasgow[59].

2.4.2 ETCHING OF GALLIUM ARSENIDE IN SODIUM HYPOCHLORITE SOLUTIONS OF VARIOUS CONCENTRATION

The mass of GaAs removed from wafer segments etched in NaOCl at concentrations between $0.018mol.dm^{-3}$ and $1.626mol.dm^{-3}$ ranged from 0% to 6.5% of the initial wafer

mass. The mass differences produced on nine different wafer sections are shown in Table 2.4.2.

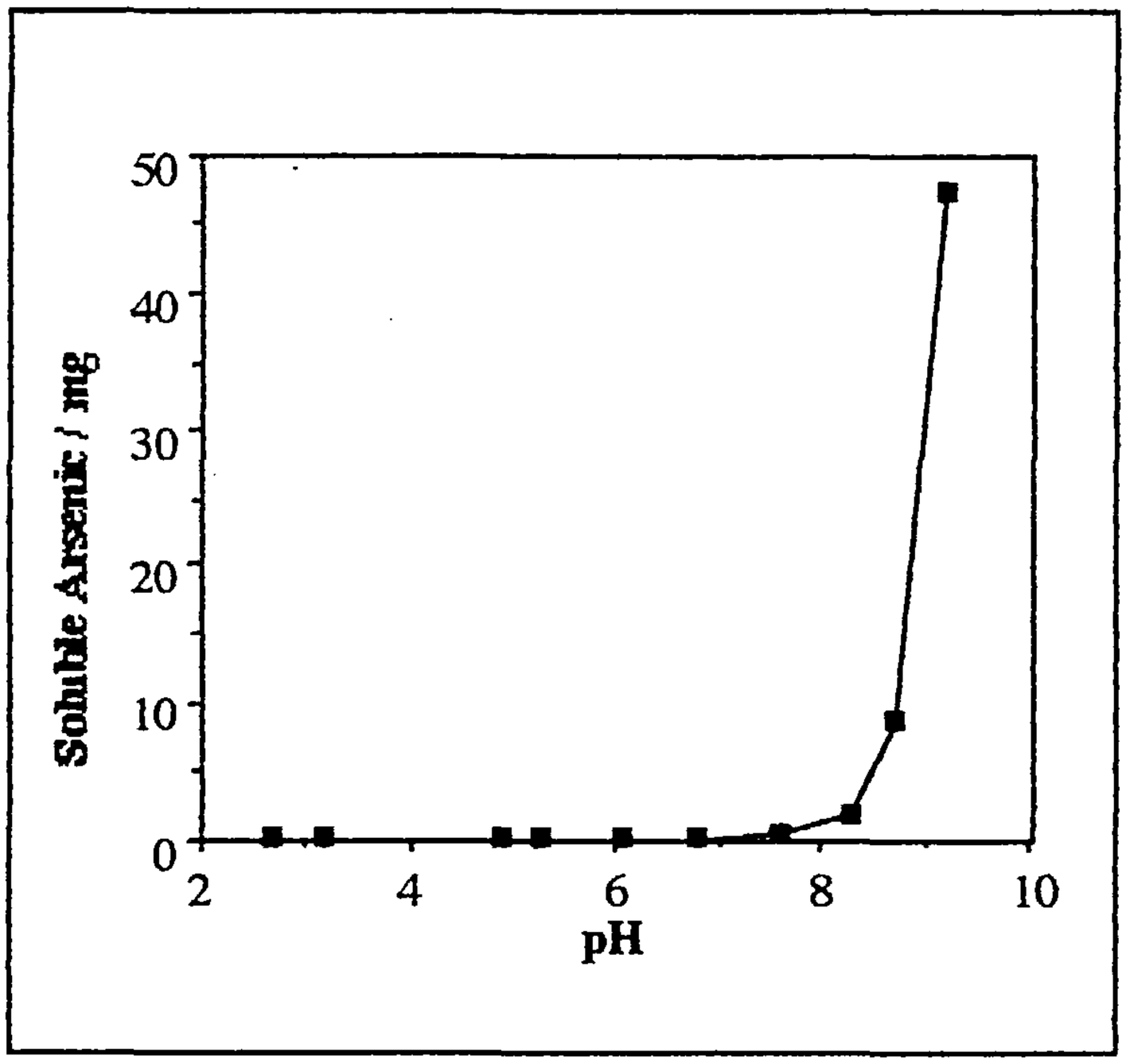

Figure 2.4.1: GaAs Etch in H_2O_2/NH_3 - Soluble As Results

Wafer Section	NaOCl Concentration / $mol.dm^{-3}$	Mass Loss / g	% Mass Loss
1b	1.626	0.0163	6.5
2b	0.922	0.0096	4.8
3b	0.607	0.0113	4.0
4b	0.468	0.0102	3.9
5b	0.375	0.0077	3.8
6b	0.189	0.0019	1.0
7b	0.079	0.0005	0.3
8b	0.044	0.0000	0
9b	0.018	0.0000	0

Table 2.4.2: GaAs Etch in NaOCl at Different Concentrations - Mass Loss Results

The apparently anomalous result for wafer 2b was probably the result of a failure in the magnetic stirrer at an unknown point during the 30min. etch. This would have resulted in a depletion in the concentration of reagent immediately in contact with the wafer and hence a reduced reaction rate. This result was therefore omitted when compiling the

results of the AAS analysis for soluble arsenic in the etch solutions. Figure 2.4.2 shows the total soluble arsenic in 60cm^3 etch solutions of various concentration.

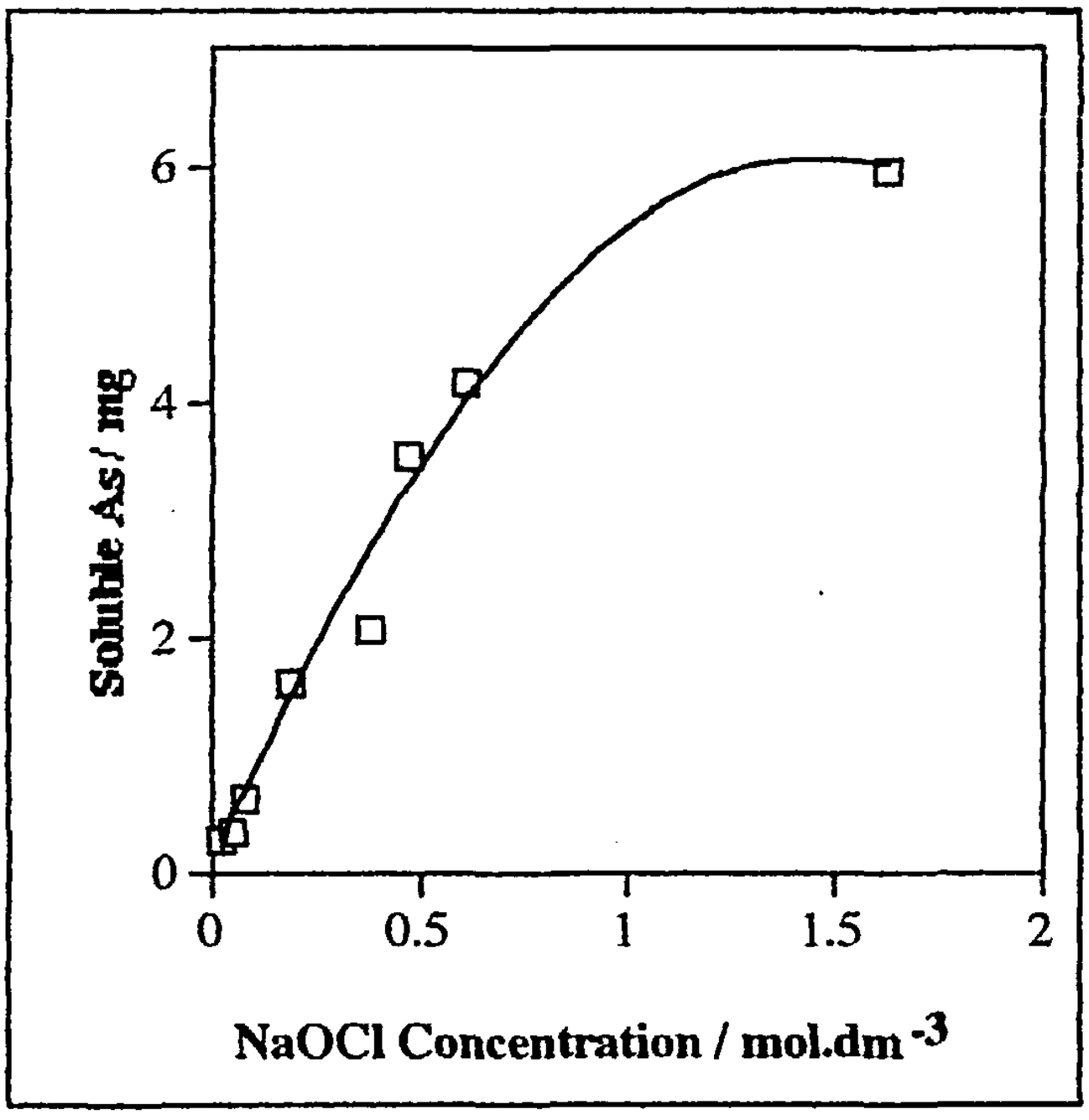

Figure 2.4.2: GaAs Etch in NaOCl at Different Concentrations - Soluble As Results.

Both mass loss and soluble arsenic results indicated that the general trend is for increased etching at higher concentrations. The trend at lower concentration (below 0.6mol.dm^{-3}) is fairly linear, but etch rate appears to level out at higher concentration, suggesting that reagent concentration is not the only factor determining stock removal. Diffusion of reagent to the surface or rate of product removal may become a limiting factor at higher concentration.

2.4.3 ETCHING OF GALLIUM ARSENIDE IN SODIUM HYPOCHLORITE SOLUTIONS AT VARIOUS pH VALUES

The mass of GaAs removed from wafer segments etched in NaOCl at pH values between 3.4 and 13.0 ranged from 0.5% to 16.4% of the initial wafer mass. The mass differences produced from six different wafer sections are shown in Table 2.4.3.

Wafer Section	pH	Mass Loss / g	% Mass Loss
1c	13.0	0.0370	16.4
2c	10.9	0.0210	7.2
3c	9.6	0.0210	7.3
4c	7.5	0.0030	1.0
5c	5.1	0.0015	0.4
6c	3.4	0.0016	0.5

Table 2.4.3: GaAs Etch in NaOCl at Different pH Values - Mass Loss Results

The mass loss results showed a plateau in the general trend of increasing mass loss with increasing pH. This phenomenon was confirmed in the atomic absorption analyses (Figure 2.4.3) which also revealed a plateau between pH 9 and 11. This buffering effect may be due to the effect of pH on the solubilities of the reaction products, or the phenomenon may be due to the appearance of a different reaction mechanism as pH is increased. It is important to note that the initial steep rise in stock removal in this reaction is similar to that for the reaction between GaAs and the H_2O_2/NH_3 reagent. A second sudden rise in stock removal occurs at pH 11 and may represent the onset of another reaction mechanism altogether.

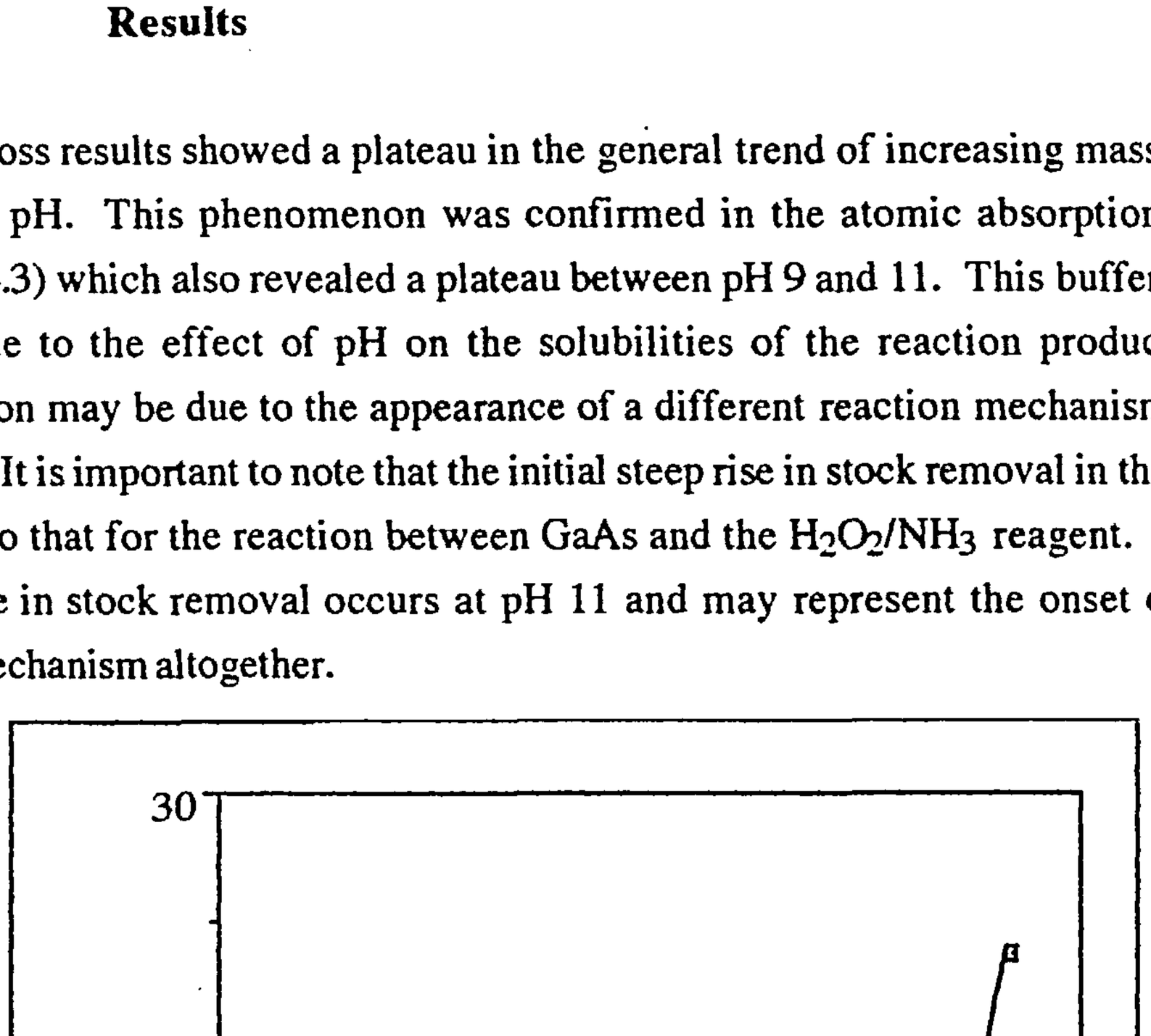

FIGURE 2.4.3: GaAs Etch in NaOCl at Different pH Values - Soluble As Results

2.4.4 HYPOCHLORITE DECOMPOSITION DURING GALLIUM ARSENIDE ETCHING IN SODIUM HYPOCHLORITE SOLUTIONS AT VARIOUS pH VALUES

All the etch solutions showed a decrease in available chlorine content after a 30 minute etching reaction. The final concentrations of all seven etch solutions are given in Table 2.4.4 alongside the final concentrations of control solutions which were identical in concentration to the etch solutions prior to the experiment.

Solution	Initial $[OCl]^-$ Concentration /mol.dm $^{-3}$	Final $[OCl]^-$ Concentration /mol.dm $^{-3}$	$[OCl]^-$ Control Concentration /mol.dm $^{-3}$
A	1.594	1.385	1.369
B	1.488	1.455	1.442
C	1.458	1.193	1.133
D	1.015	0.235	0.238
E	0.620	0.365	0.365
F	0.622	0.370	0.379

Table 2.4.4: Decomposition of NaOCl Solution During GaAs Etch

The results show that, although some decomposition has occurred during the etch, especially around neutral pH, this is a consequence of the etchant pH, not the etching reaction itself. The final concentrations of the etch solutions were very similar to those solutions which had not been employed in an etching experiment.

2.4.5 ETCHING OF GALLIUM ARSENIDE IN SODIUM HYPOCHLORITE SOLUTION FOR VARIOUS ETCH PERIODS

GaAs wafers etched in NaOCl solution (1.6mol.dm^{-3}, pH 13) for 30 min. or more were shiny in appearance, with a darkened, glassy layer on the surface. Unlike the underlying crystalline GaAs, this layer was not electrically conductive. Mass decreases ranged from 24.9% to 60.4% of the initial wafer mass. Table 2.4.5 gives details of the amount of material removed in the different etching reactions.

Examination by scanning electron microscopy (Figure 2.4.4) revealed the formation of a distinct product layer which was different in structure and appearance from the substrate

GaAs. The material which appears white under the microscope takes the form of a black, glassy layer.

Wafer Section	Etch Time / h	Mass Loss / g	% Mass Loss
1d	1.0	0.2365	24.9
2d	1.5	0.2373	24.9
3d	2.0	0.6300	63.8
4d	2.5	0.3739	41.7
5d	3.0	0.5754	60.4

Table 2.4.5: GaAs Etching in NaOCl - Mass Loss Results

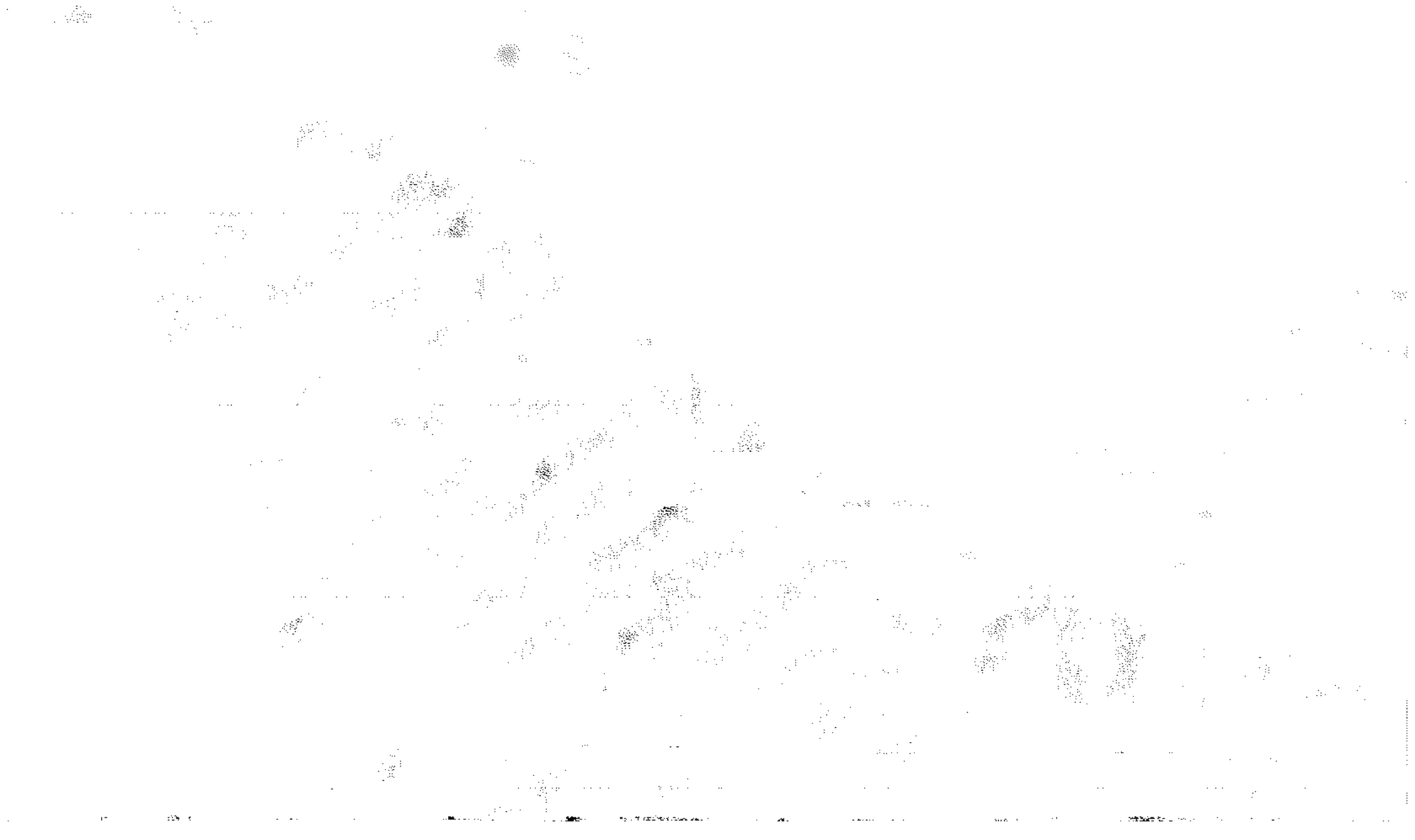

Figure 2.4.4: Scanning Electron Micrograph of GaAs Etched in NaOCl for 3h. (Bar = 10μm)

ESCA and Auger analysis revealed the presence of surface carbon (C), oxygen (O) and sodium (Na) contamination, but mild Ar^+ ion bombardment cleared the surface of superficial contamination. Double peaks were observed in the As 3d, 3p and Auger peaks, consistent with the presence of elemental As and arsenic (III) oxide. However, no

such doubling was observed in the Ga 3d, 3p, 3s or Auger peaks, suggesting the absence of any form of Ga oxide.

Table 2.4.6 shows the percentages of each species on the surface of samples 1d and 5d, in two separate analyses, prior to any surface cleaning or etching.

Wafer Section	Ga	As	As Oxide	O	C	Na
1d	4.5	3.1	1.3	25.3	65.8	0
5d	23.1	6.2	8.1	34.2	26.7	1.7

Table 2.4.6: Auger Analyses of GaAs Surfaces (Atom %)

These results show that for the sample which had been etched longer, there is a greater difference in the Ga:As ratio, and there is more As_2O_3 relative to elemental As present on the surface.

Auger etching down through the surface layer on sample 5d produced a rapid decrease in carbon detected and revealed the presence of a discontinuous oxide layer between 300Å and 600Å thick. A schematic of the surface layer structure is shown in Figure 2.4.5. The thicknesses shown are approximate, since the precise Auger etch rate on the material was not determined. However, the figure is qualitatively correct in that the order and nature of the detected layers are reliable.

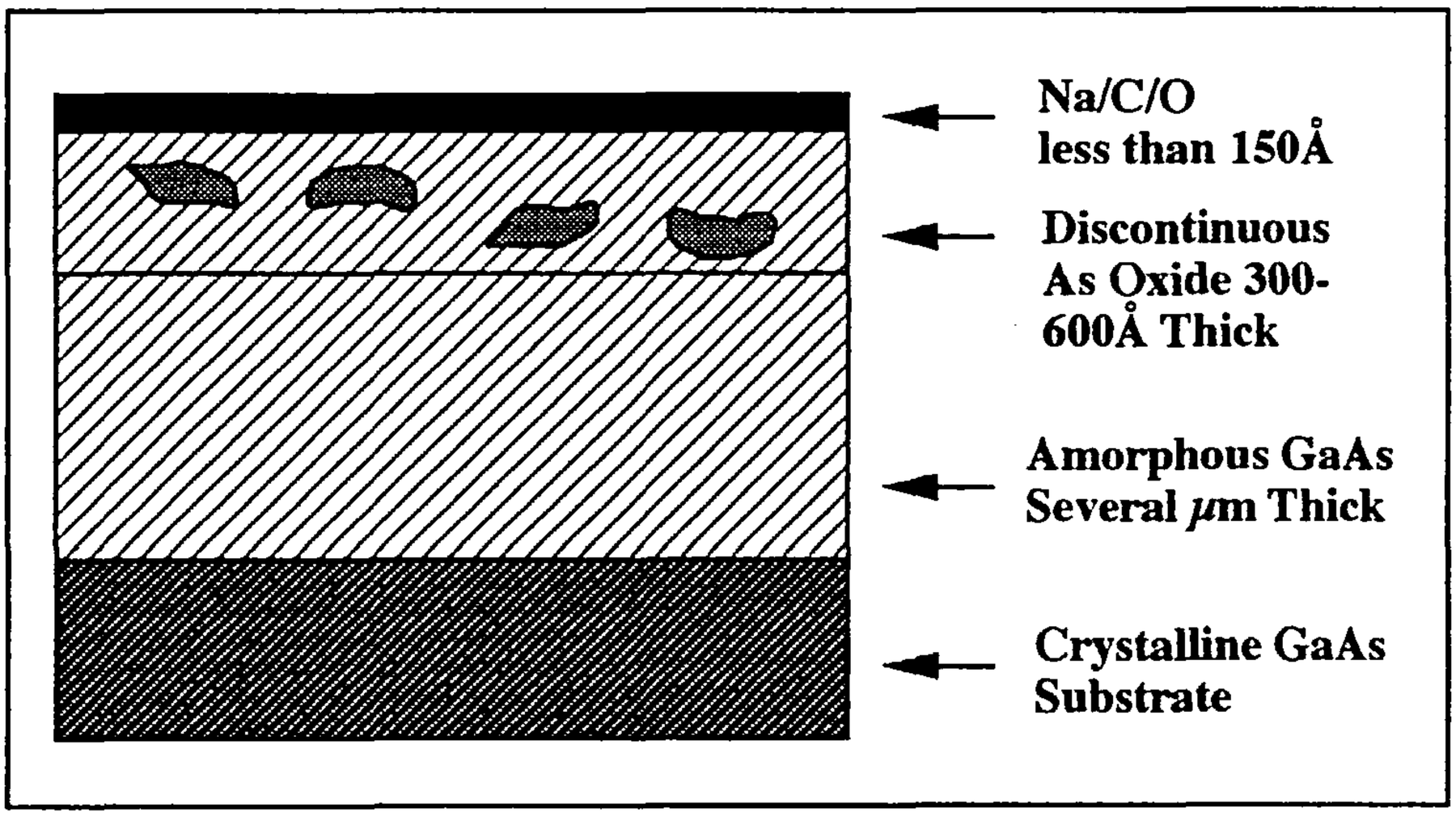

Figure 2.4.5: Surface Layer formed on GaAs Etched in NaOCl Solution for 3h.

Examination of the sample surfaces by Fourier transform infrared microscopy revealed very few surface hydroxyl species except directly above etch pits, where some degree of surface hydration could be detected.

2.4.6 ANHYDROUS ETCHING OF GALLIUM ARSENIDE IN A DIBROMINE/DICHLOROMETHANE SOLUTION

Etching of GaAs in anhydrous conditions using a solution of dibromine in dichloromethane produced no significant reduction in the mass of the wafer. Indeed, in most cases a small increase in the mass of the vessel+wafer after reaction was detectable. The mass differences from all seven wafer sections are shown in Table 2.4.7.

Wafer Section	Dibromine Concentration / $mol.dm^{-3}$	Mass Increase / g
1e	0.049	0.02
2e	0.123	0.00
3e	0.145	0.00
4e	0.394	0.02
5e	0.457	0.01
6e	0.475	0.01
7e	0.802	0.02

Table 2.4.7: Mass Increases on GaAs Etched in Dibromine / Dichloromethane

The magnitude of the results and the errors inherent in measuring such small mass differences in a reaction vessel weighing approximately 131g make the precise values inconclusive. However, it is helpful to note that the large mass differences traditionally found when etching and polishing GaAs with dibromine in ambient atmosphere[60] are not in evidence under anhydrous conditions. This suggests that moisture may be important in the removal of reaction products from the surface, thereby allowing etching to continue.

2.5 DISCUSSION

The dip-etch experiments described in this chapter have proved to be a useful way of determining the general behaviour of polishing reagents on gallium arsenide in particular. The effects of pH on hydrogen peroxide and on sodium hypochlorite have been determined and these experiments have yielded information on the possible mechanisms by which the etchants operate. Dip-etch experiments have also been used as a stepping-stone to other techniques, which have yielded information regarding the products which may form at the polishing cloth/wafer interface during a polishing experiment.

The effect of reagent concentration on stock removal has been determined for Br_2 and H_2O_2 in previous work[59,60]. For both of these reagents, stock removal increases linearly with the concentration of the active etchant in reagent mixtures such as dibromine in methanol and hydrogen peroxide with ammonia. Hence, the result shown in Figure 2.4.4 for NaOCl solution on GaAs is surprising, in that the stock removal appears to plateau at high concentration. This phenomenon indicates that, as concentration increases, etchant availability in solution ceases to be the limiting factor in the etching reaction. Other factors, such as the formation of a product layer as a barrier to diffusion, may become important. It should also be noted that the removal of As to solution by NaOCl solution is much slower than with Br_2 in methanol or with H_2O_2/NH_3. Dibromine in methanol ($0.5 mol.dm^{-3}$) removes 140 mg of arsenic to solution over the period of a 30min. etch. The gentler action of NaOCl solution is probably an advantage in the polishing situation where slower stock removal often leads to higher surface quality.

The pH of etch solutions such as H_2O_2/NH_3 and NaOCl is critical to their etching behaviour because of factors such as composition/oxidising ability of the reagent and solubility of the resultant products. Comparison of Figures 2.4.1 and 2.4.3 shows similarities in the pH dependence of H_2O_2 and NaOCl as etchants, indicating a possible common factor in the pH dependence of both reagents. It is feasible that the oxidation products formed by H_2O_2 and $[OCl]^-$ are a common factor and their dissolution, allowing further reaction, is dependent on given pH conditions. To examine this possibility, it is necessary to determine what such products are likely to be. Analysis of the substrate surface by ESCA and Auger techniques has gone some way towards this.

With regard to oxidising ability, it is true that both reagents are more efficient etchants at high pH (c.f. Sections 1.4.2 and 1.4.3). However, it is unlikely that the pH at which

oxidation begins would coincide exactly for both reagents. Nevertheless, consideration should be given to changes in the composition or oxidising ability of a reagent with pH to explain effects such as the plateau in Figure 2.4.3. This effect is not observed in the H_2O_2 curve and so probably relates to the reagent itself rather than the products of the oxidation reaction. Radiotracer experiments to determine changes in the etchant composition of NaOCl solutions at various pH values, and to trace pH dependent reactions with GaAs were undertaken later in the project (c.f. Chapter Four).

Qualitative surface analyses by ESCA/Auger techniques indicate that oxide forms during the etching of GaAs by NaOCl solution at high pH. However, this oxide is not a mixture of Ga and As oxides which form directly on the crystalline GaAs substrate. ESCA results show the presence of As (III) oxide in a discontinuous layer near the surface, but no Ga oxides of any description. Also, the As_2O_3 product layer is separated from the crystalline GaAs substrate by an amorphous layer containing more Ga than As. Hence, some surface reconstruction occurs during the etching reaction at high pH. During this reconstruction more Ga than As is left on the substrate surface.

It is possible that the oxidation of As on the wafer surface leads to a high degree of lattice disruption, yielding a highly damaged sub-surface layer. The high Ga:As ratio might be explained by an almost exclusive selectivity of the oxidising agent for As. This postulation obviously depends on As being more easily oxidised than Ga in the conditions of the etch solution. In fact, the converse is true; an examination of the standard reduction potentials for the likely reactions occurring (Equations 2.5.1 to 2.5.7)[46] reveals that Ga is more easily oxidised in alkaline aqueous solution. Indeed, the reaction to form As_2O_3, detected in the product layer, has a positive reduction potential, suggesting this oxide as a far less likely product than, for example, $H_2GaO_3^-$.

$\mathbf{As_2O_3 + 6H^+ + 6e^- \rightarrow 2As + 3H_2O}$	**0.234V**	.....(2.5.1)
$\mathbf{HAsO_2 + 3H^+ + 3e^- \rightarrow As + 2H_2O}$	**0.248V**	.....(2.5.2)
$\mathbf{AsO_2^- + 2H_2O + 3e^- \rightarrow As + 4OH^-}$	**-0.68V**	.....(2.5.3)
$\mathbf{GaOH^{2+} + H^+ + 3e^- \rightarrow Ga + H_2O}$	**-0.498V**	.....(2.5.4)
$\mathbf{H_2GaO_3^- + H_2O + 3e^- \rightarrow Ga + 4OH^-}$	**-1.219V**	.....(2.5.5)
$\mathbf{Ga^{3+} + 3e^- \rightarrow Ga}$	**-0.549V**	.....(2.5.6)
$\mathbf{Ga^+ + e^- \rightarrow Ga}$	**-0.2V**	.....(2.5.7)

One other feasible explanation for the product layer formed is that a mixture of oxides and oxohydroxides, of the type detailed in equation 2.5.1 to 2.5.7, is formed during the etching reaction. The oxides and hydroxides of As are generally more soluble in aqueous solutions than those of Ga, although both Ga and As oxides/hydroxides will dissolve to

some degree in alkali. The lower solubility of the Ga oxidation products would explain retention of more Ga than As in the product layer. The presence of elemental Ga and As in a sub-surface amorphous layer is more difficult to rationalise, but may be explained by further redox processes after formation of an insoluble oxide layer. These redox processes may lead to redeposition of elemental substrate material and would be consistent with the fact that etching appears to continue within the layer, when fresh etchant is no longer able to penetrate to the substrate surface. Without more detailed information about the products formed instantaneously at the etchant/substrate interface, it is difficult to differentiate between selective oxidation and selective dissolution in the production of a non-stoichiometric product layer.

The reaction of NaOCl with GaAs at high pH produces a non-stoichiometric product layer in a static dip-etch experiment. However, there is no evidence that polishing GaAs with NaOCl based reagents produces a non-stoichiometric surface. The role of the polishing pad and abrasive must therefore be critical in altering this product layer or in preventing its formation. This phenomenon, and the possible passivating effects of the product layer require *in situ* investigation in polishing experiments.

CHAPTER THREE

CHEMOMECHANICAL POLISHING

3.1 INTRODUCTION

The dip-etch experiments described in Chapter Two suggested certain optimum conditions for the use of hypochlorite in a polishing experiment. The experiments in this chapter were designed to test these predictions and evaluate the best surface finishes which could be achieved using sodium hypochlorite as a reagent. Previous work using hydrogen peroxide and bromine determined the best conditions for polishing with these reagents[59].

Refractive oxides such as ceria (CeO_2) and α-alumina are commonly employed as abrasives in the polishing process, to improve stock removal and help maintain geometry across the wafer surface. The use of a fine particle abrasive prevents increased chemical reactivity at the wafer edges and helps reduce rounding of the wafer sample. Sodium hypochlorite solution is often used in a slurry (with α-alumina), which is dripped onto the polishing cloth. However, this process is messy and requires fresh slurries to be prepared regularly. Logitech Ltd. are developing a process in which the abrasive is incorporated into the polishing pad. This pad was tested with sodium hypochlorite and dibromine in methanol as reagents, to determine any effects on the reagent and/or any improvement in the surface finish which could be achieved using this system. The effect of regular pad conditioning on the process was also investigated.

The results of polishing experiments were evaluated in terms of surface quality as well as mass removed and/or soluble material in the etch solution. Techniques such as stylus measurement of surface roughness and optical microscopy to observe surface topography were also employed.

3.2 GENERAL EXPERIMENTAL TECHNIQUES

3.2.1 LAPPING AND POLISHING

Before lapping or polishing a sample, it is necessary to mount the wafer or wafer segment on a flat substrate to allow even polishing of the sample. The wafer samples were wax bonded to flat glass substrates on a hot plate. Excess wax was pressed out from under the sample before any remaining around the wafer edges was removed using a solvent such as acetone.

For the purpose of lapping a wafer segment or for polishing on certain types of polishing machine, the glass substrate and bonded wafer sample were mounted onto a Logitech PP5GT precision lapping and polishing jig (Figure 3.2.1)

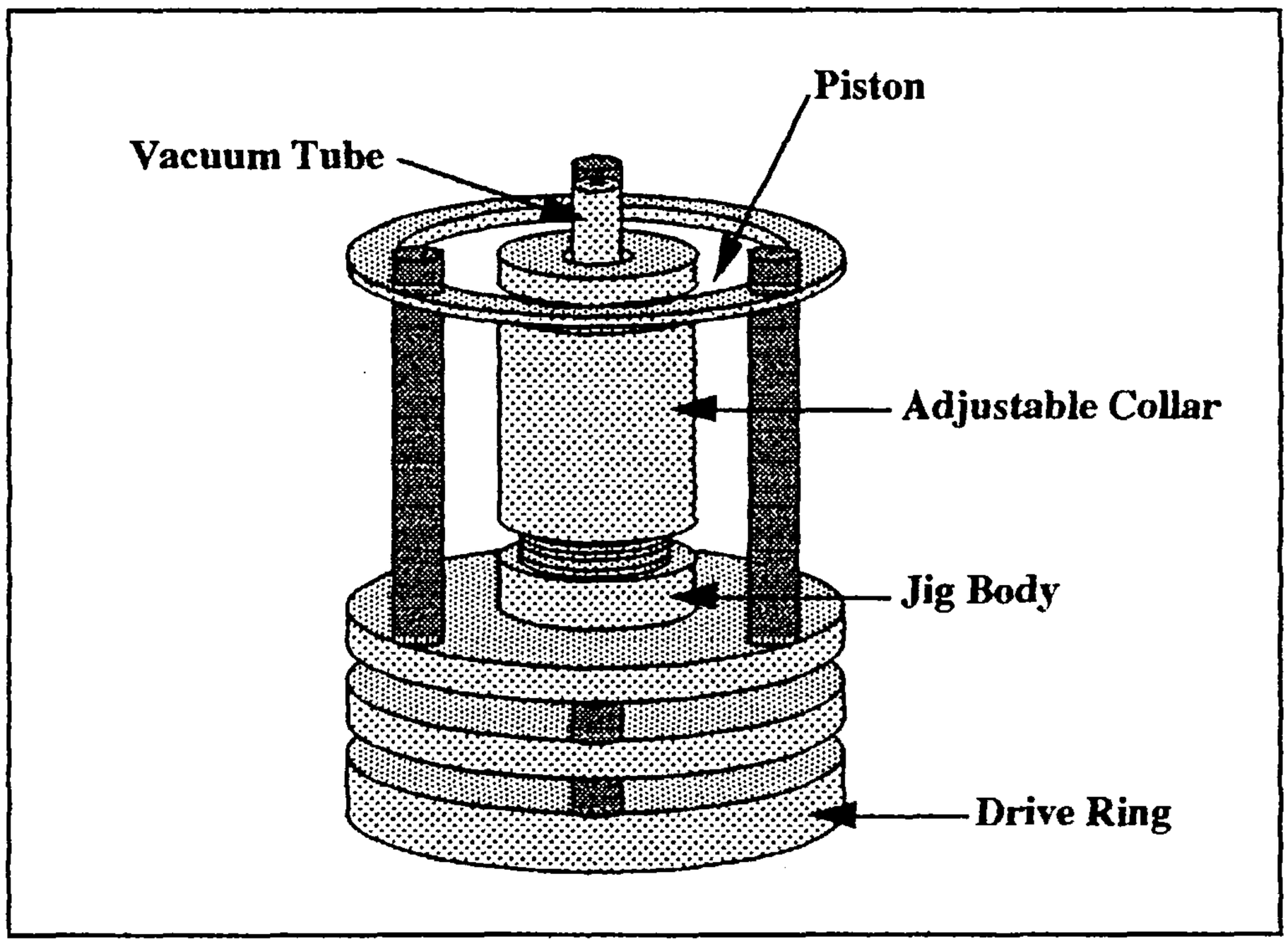

Figure 3.2.1 : Logitech PP5GT Vacuum Jig

The wafer sample was mounted on the chuck face, which was adjustable with respect to the drive ring, providing optimum contact with the polishing plate. A dial was attached to the jig, allowing measurement of the amount of material being removed. This has been omitted from the diagram for clarity. The glass substrate was held onto the chuck face by vacuum and the load on the sample was varied by lowering or raising the adjustment collar, imparting movement to the piston and hence to the vacuum chuck (Figure 3.2.2).

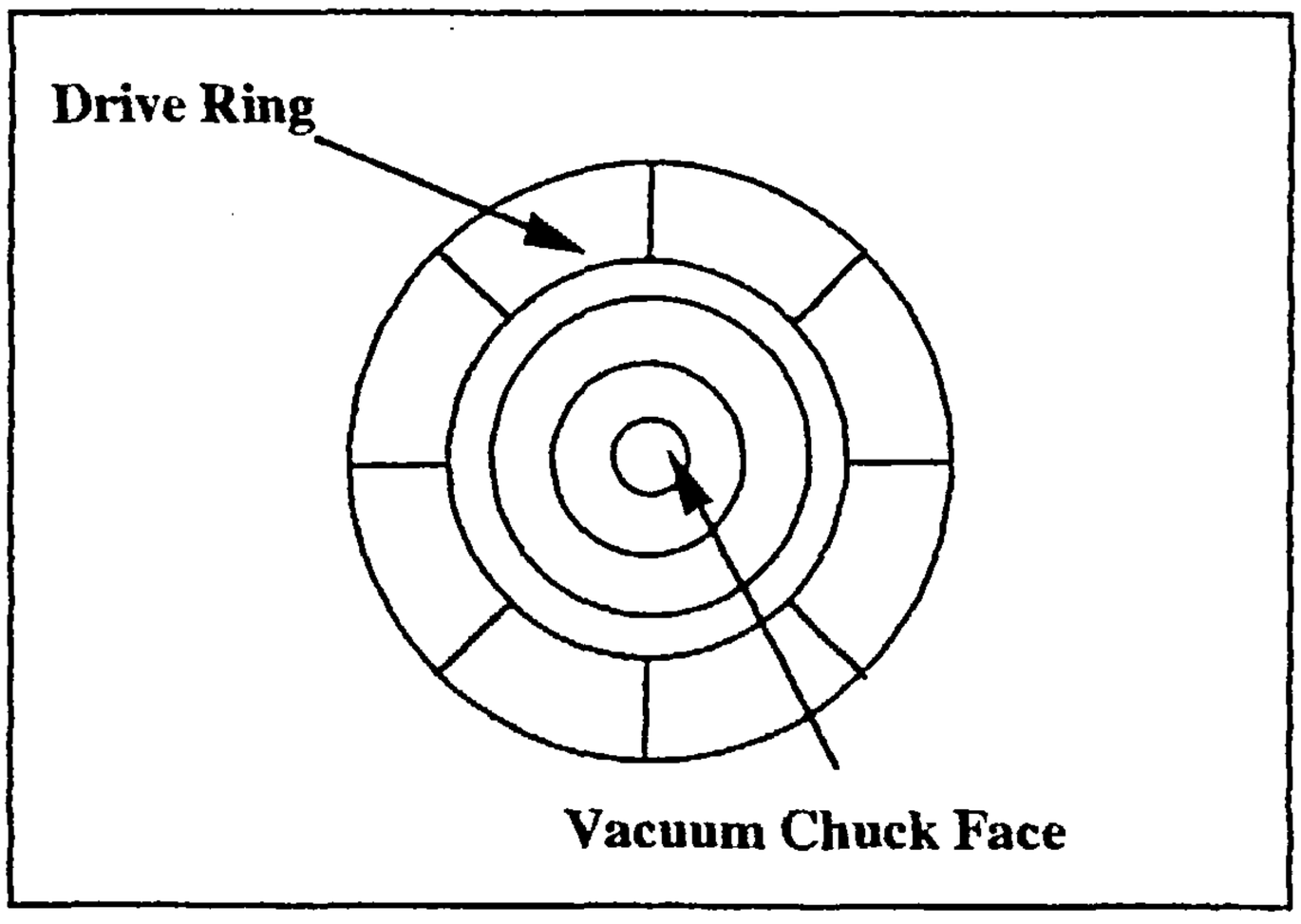

Figure 3.2.2 : Chuck Face of Logitech PP5GT Vacuum Jig

Logitech PM2A polishing equipment was used to lap the wafer samples and to polish with hypochlorite solution in some experiments. This machine consists of a simple geared turntable to which various polishing plates can be attached. The speed of the plate can be varied from 0-70 rpm. For lapping of GaAs and CdTe, a glass lapping plate with scores to allow the run-off of abrasive solution was used (Figure 3.2.3a). A 3μm α-alumina slurry was generally used. Larger particle sizes (e.g.. 9μm) can be used where faster lapping is desired.

For polishing GaAs or CdTe with NaOCl, a Chemcloth polishing pad (Figure 3.2.3b) was glued to a plain finish polishing plate and attached to the PM2A polishing machine. The Chemcloth polishing pad had a velvet napped, absorbent surface to allow a more gentle polish.

Alumina-impregnated pads were tested on different polishing apparatus, since the metal construction of the Logitech PM2A machine was easily corroded under the action of bromine. The Logitech CP2000 chemical polishing machine was constructed of polypropylene and other plastics.

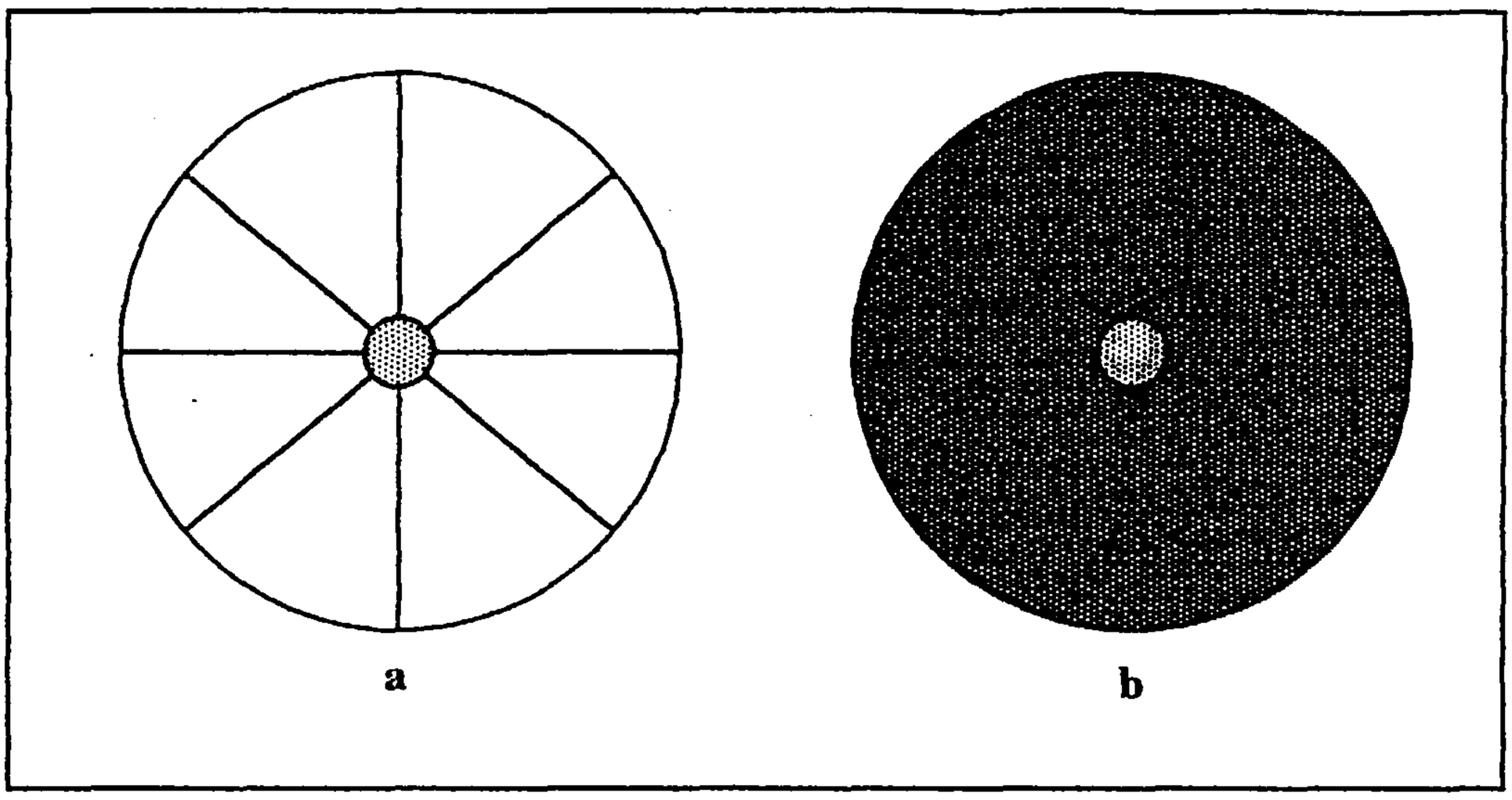

Figure 3.2.3: Polishing Plates for the PM2A used for a) Lapping and b) Polishing with NaOCl

The polishing plate or pad was covered by a polishing deck, as shown in Figure 3.2.4, which was fitted with a gearing system to rotate the samples in the opposite direction to the plate. Etchant solution was dripped onto the centre of the plate and the samples were held firmly in small plastic holders which rotated within the gearing mechanism. Metal weights were placed onto the sample holders, as a simple alternative to an adjustable load vacuum jig.

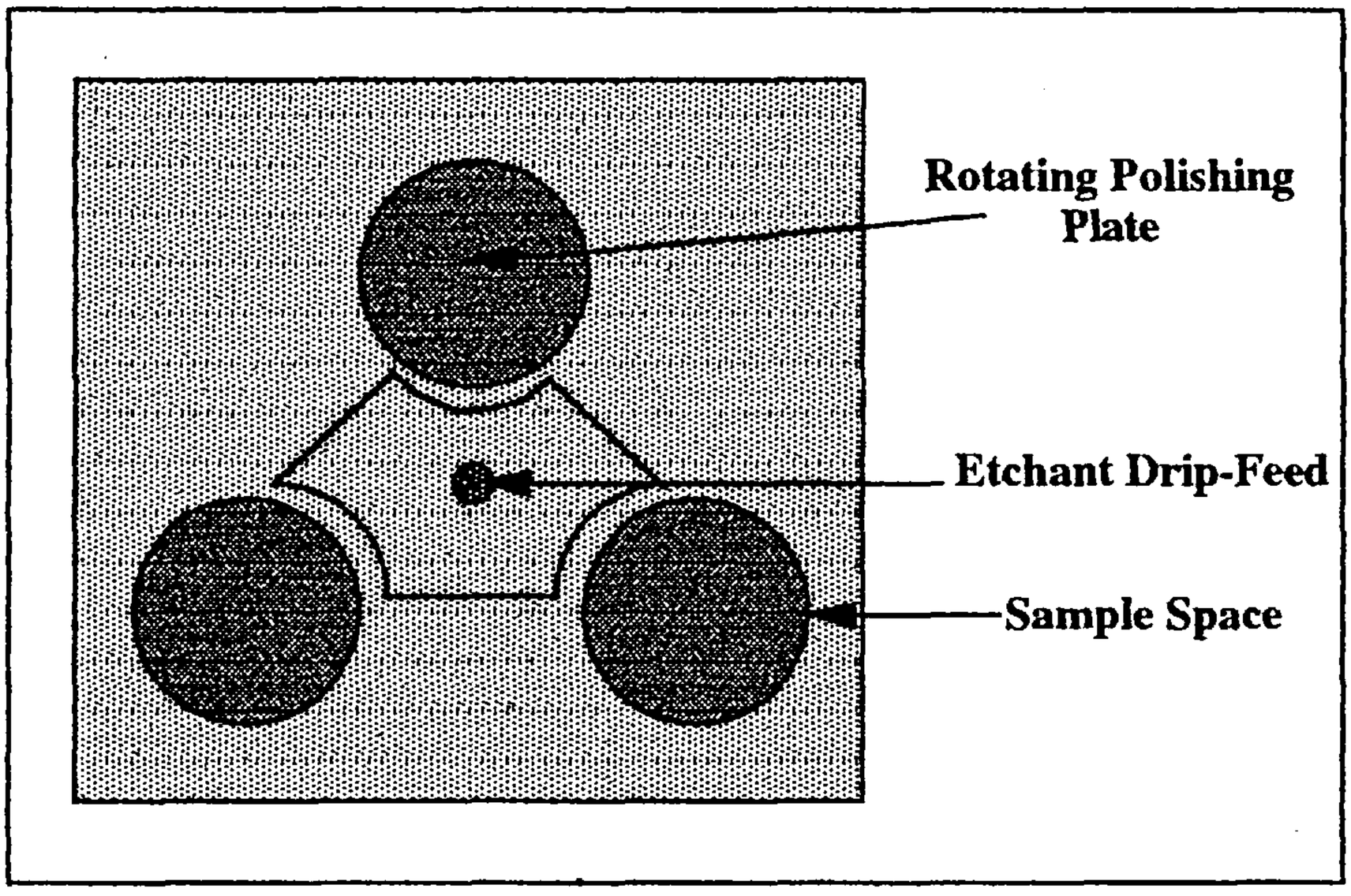

Figure 3.2.4: Logitech CP2000 Polishing Deck

The alumina-impregnated polishing pads were manufactured commercially for Logitech Ltd by mixing 3μm α-alumina into polyurethane polymer before cold-curing. The structure of the pads is shown in Figure 3.2.5, showing the grid pattern (1cm^2 blocks) of scores to allow run-off of etchant and products.

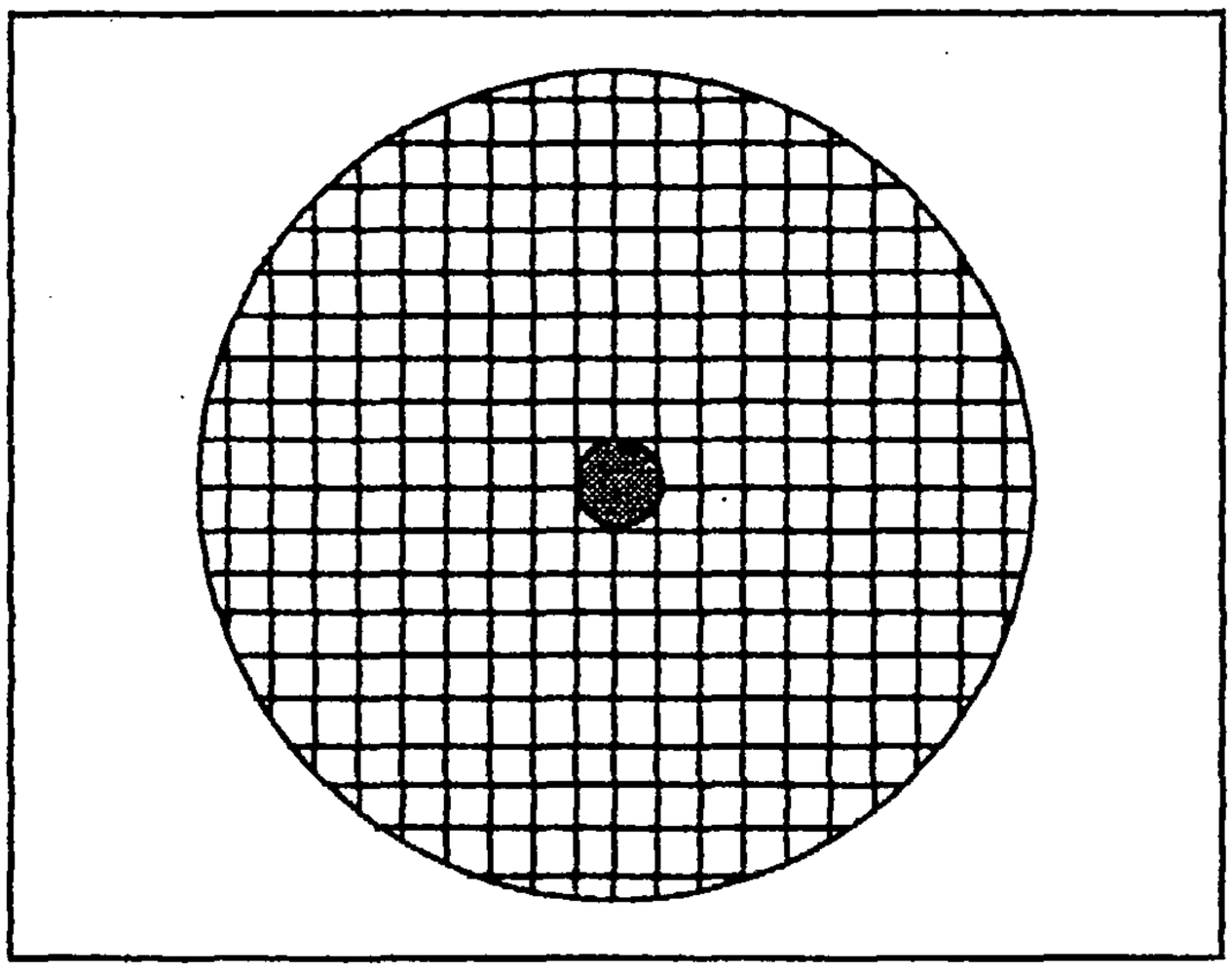

Figure 3.2.5: Surface of an Alumina-Impregnated Pad

To release the alumina from the polymer and make the pad surface more mobile, the pad was conditioned before use, using a diamond-impregnated polyurethane conditioner (Figure 3.2.6).

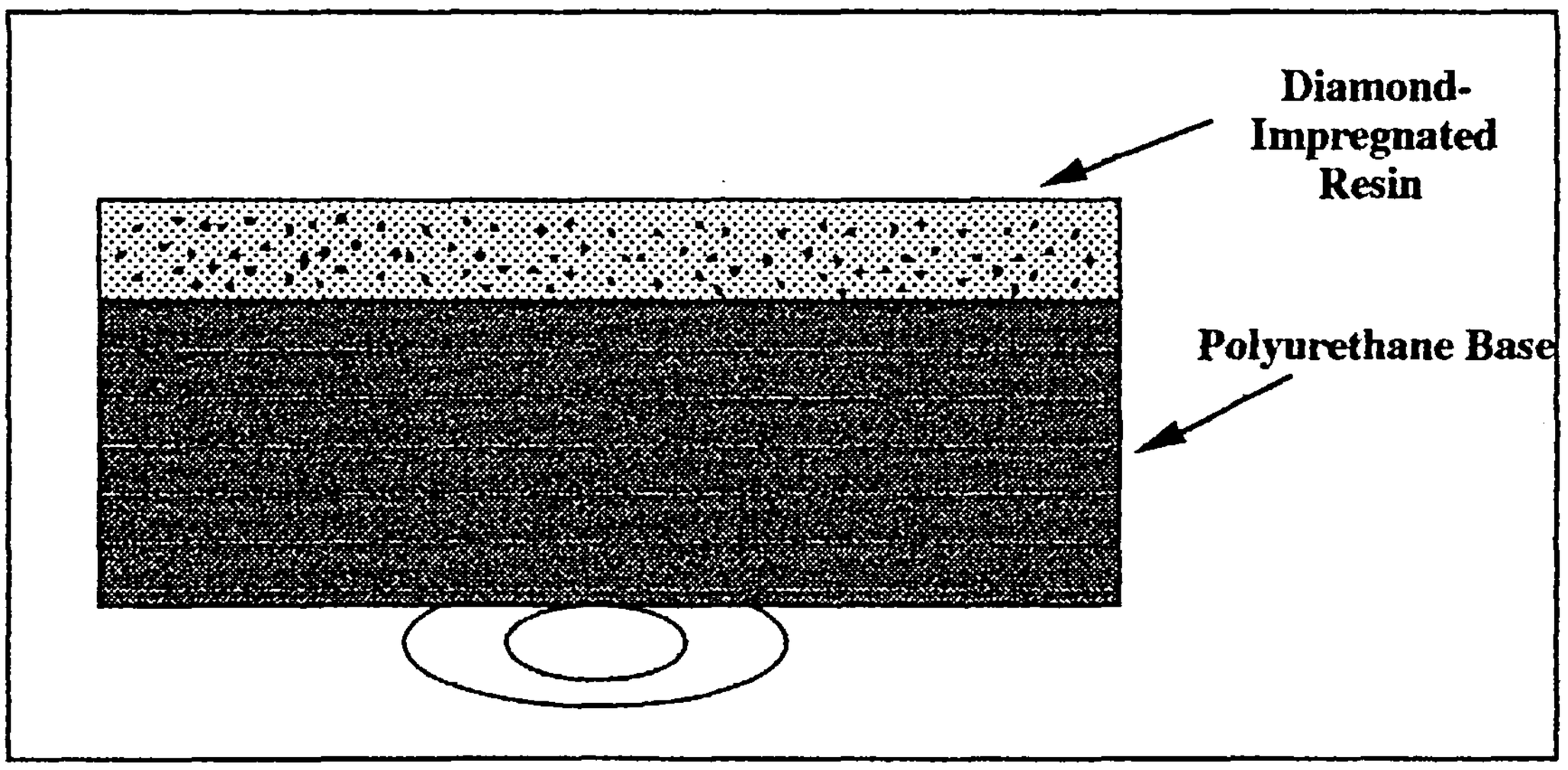

Figure 3.2.6: Diamond Conditioner for Alumina Impregnated Pads

3.2.2 OPTICAL MICROSCOPY AND SURFACE ROUGHNESS

After polishing, samples were viewed under a Zeiss optical Nomarski microscope. The microscope was used as a normal light reflectance microscope for the detection of etch pits and scratches on the wafer surface. The Nomarski polarisation facility was used to distinguish any height differences across the wafer sample and thereby indicate any loss of geometry or selective etching effect in operation during the polishing process.

Samples which appeared smooth under the microscope were then placed in a Rank Taylor Hobson Talystep instrument and their surface roughness measured using a 2μm stylus tip. The stylus tip lightly traced the wafer surface and a profile of the surface topography was obtained. The magnification on the instrument could be changed to make the system more or less sensitive to small features on the wafer surface. Average surface roughness (R_a) is the root mean square average of the sizes of the peaks and troughs across a given distance on the surface. The R_a value was calculated from an optimum 'zero' line on the surface and was corrected to account for any global loss of planarity across the wafer. For example, a trace obtained as in Figure 3.2.7a would be corrected and the calculation carried out on the data as shown in Figure 3.2.7b.

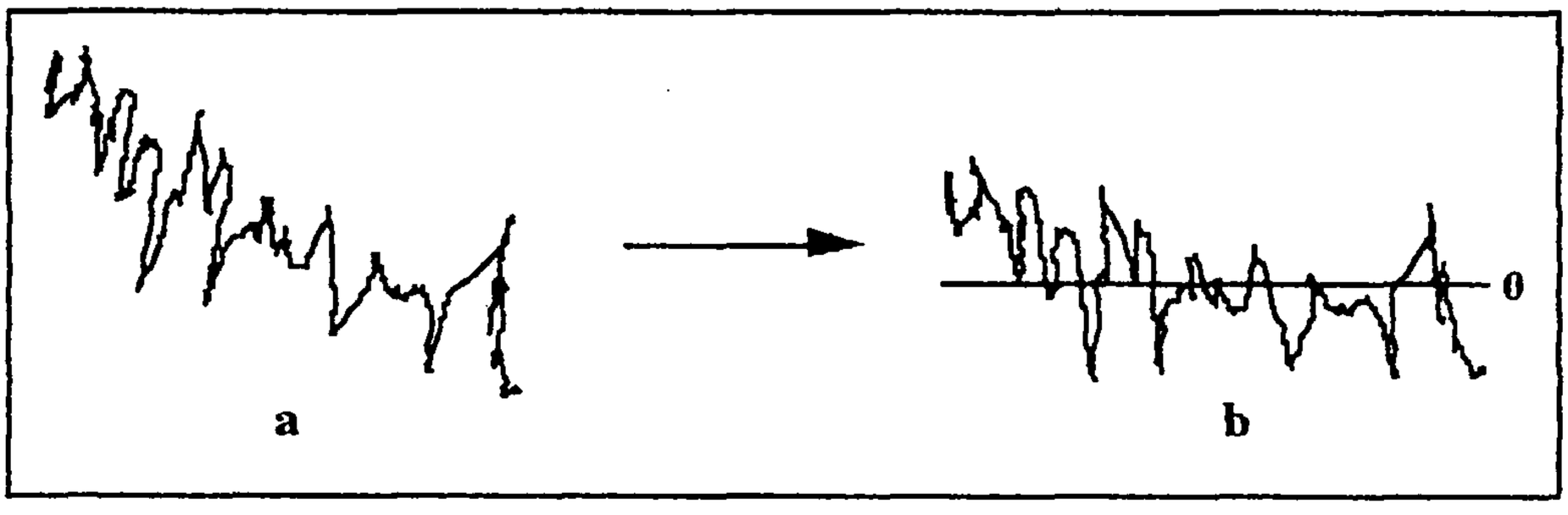

Figure 3.2.7: Talystep Correction for Lack of Surface Planarity

The measurement of surfaces which are believed to be smooth on the 1-10 nm scale with a 2μm stylus tip has obvious disadvantages. For this reason, it is essential to view all R_a values cited as comparative and not an indication of the absolute roughness of the surface. This is true for Talystep measurements cited in the scientific literature in general when they are used to evaluate such small features on a surface. However, the technique is useful for examining trends and distinguishing optimum conditions for the use of a reagent or process.

3.2.3 ATOMIC ABSORPTION SPECTROSCOPY (AAS)

The basic principles behind AAS were described in Chapter Two. No cadmium or tellurium determinations were required in the solution etching work because of the lack of reactivity between CdTe and NaOCl in a dip-etch. However, polishing of CdTe with NaOCl produced very different results. The techniques used for the determination of Cd and Te by AAS are different form the hydride generation method described in Chapter Two and are described below.

i) Flame Method

This technique was employed for cadmium and tellurium analyses. Using the flame method, the sample are sprayed by a pneumatic nebulizer into a flame, where the droplets are dried. The resulting solid particles then thermally decompose to give gaseous molecules that dissociate to free atoms. These processes occur within a few milliseconds as the 'cloud' passes through the flame. This technique is obviously limited to liquid phase samples.

Standard solutions of 0.5, 1.0, 1.5 and 2.0 ppm were used to calibrate for cadmium (Figure 3.2.8) and 5.0, 10.0 and 15.0 ppm standards were used for tellurium. All analyses were carried out in triplicate.

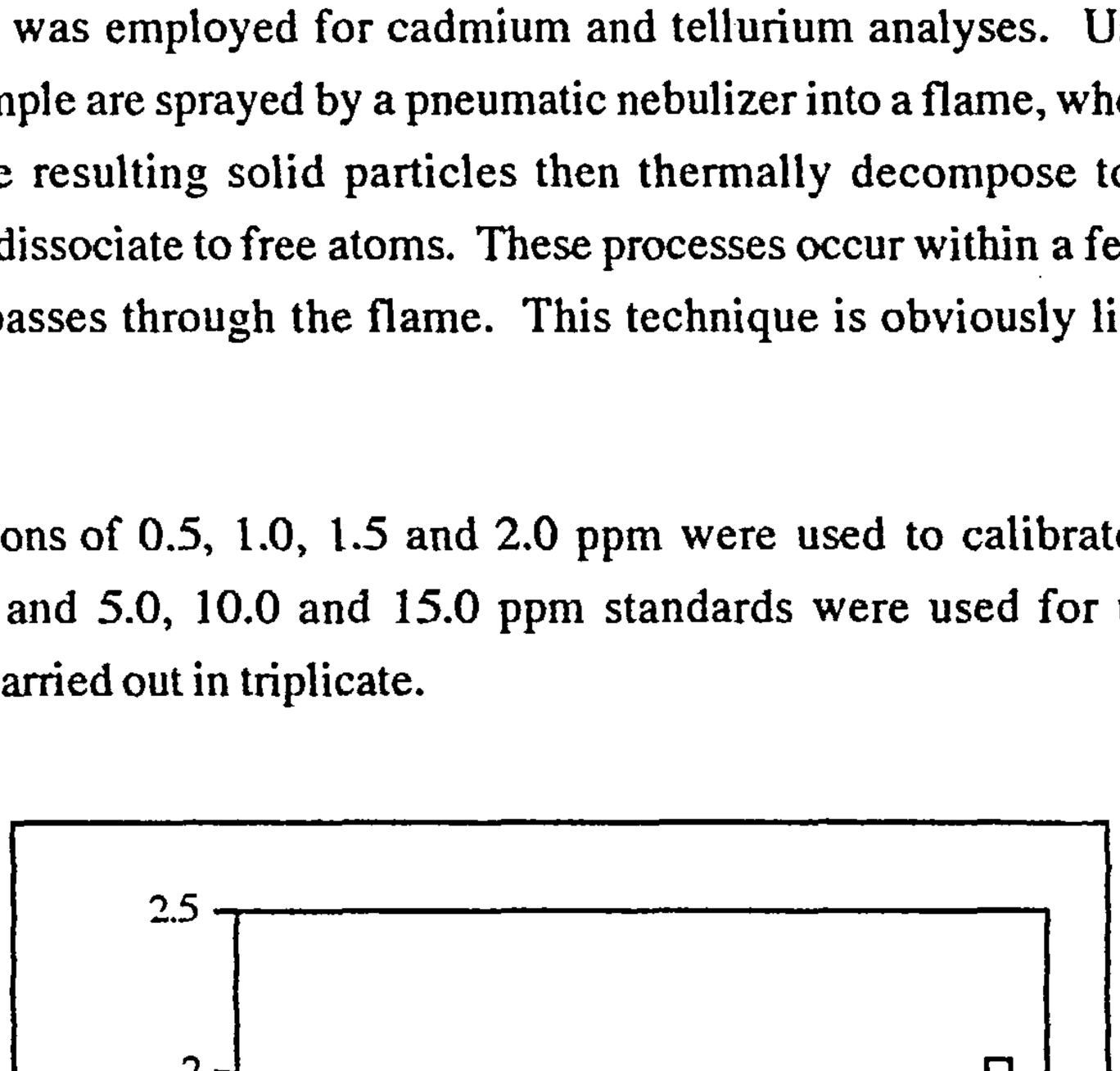

Figure 3.2.8: Calibration for Cadmium Standards using Flame Technique

iii) Graphite Furnace

This method was attempted for tellurium analysis, since the flame technique is far less sensitive to Te than to Cd. The graphite furnace is a small graphite tube which can be heated electrically. The temperature can be increased stepwise to separate the processes of drying, thermal decomposition and atomisation. During the first two stages, an inert gas purges the tube to remove solvent and matrix vapours. The gas stream is halted during atomisation, allowing the free atoms to remain in the flame for a much longer period than with the flame technique. This improves the sensitivity of the method greatly and allows a much lower detection limit.

Four standards of 0.5, 1.0, 1.5 and 2.0 ppm tellurium solutions were used in 30μl aliquots. The calibration graph is shown in Figure 3.2.9.

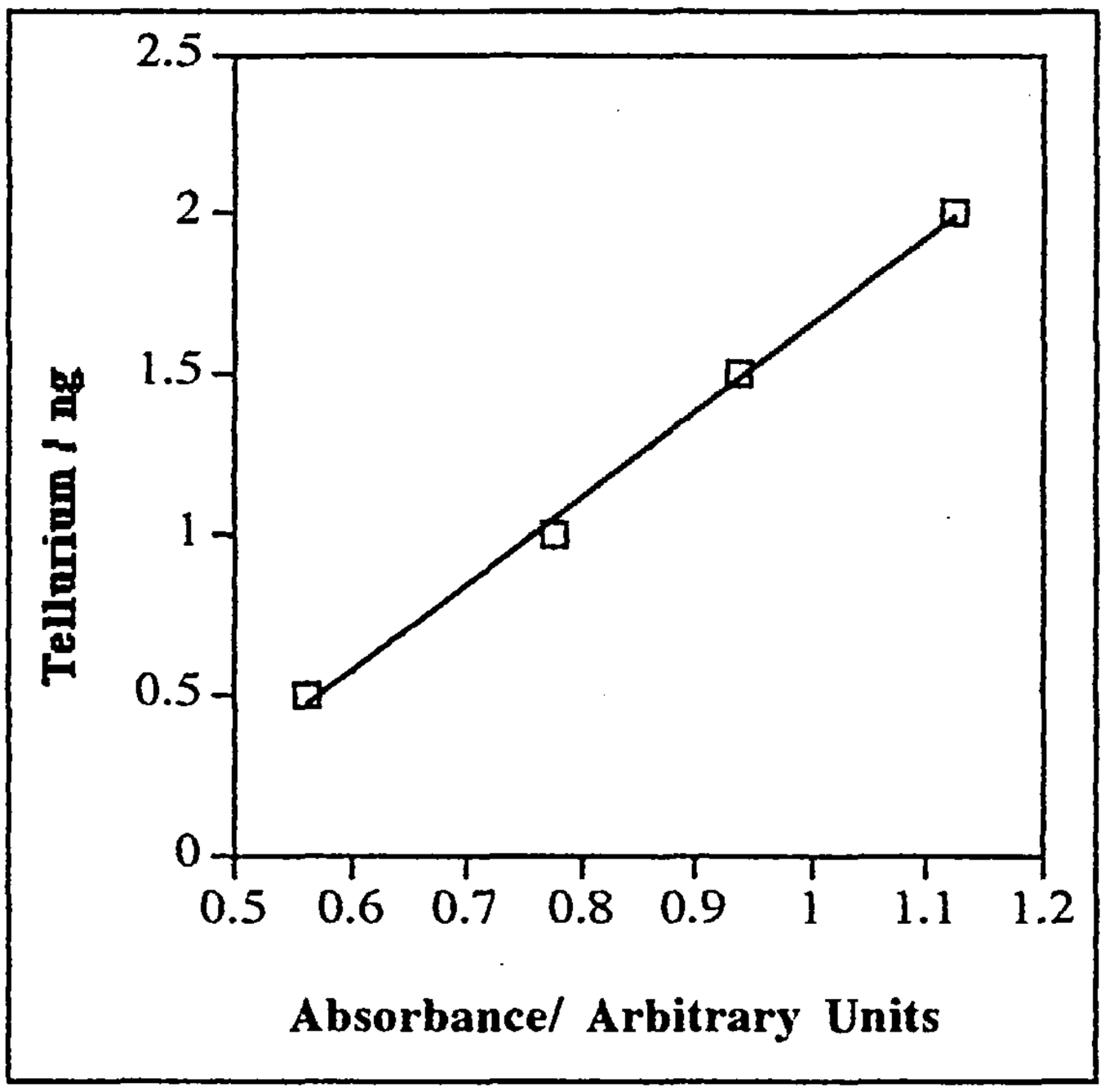

Figure 3.2.9: Calibration for Tellurium Standards using Graphite Furnace

3.3 POLISHING EXPERIMENTS

3.3.1 POLISHING OF GALLIUM ARSENIDE WITH SODIUM HYPOCHLORITE AT VARIOUS PH VALUES

The sodium hypochlorite solutions were prepared and their pH determined as described in Chapter Two. The pH was altered by the dropwise addition of glacial acetic acid. A

range of solutions was prepared, as shown in Table 3.3.1. Each solution was freshly prepared immediately prior to the polishing experiment in which it was used.

Wafer Section	Etchant Volume / cm^3	pH
1f	98	12.3
2f	124	9.2
3f	112	8.3
4f	156	8.0
5f	147	7.6
6f	128	6.4

Table 3.3.1: GaAs Polish in NaOCl at Various pH Values

This series of experiments employed a Logitech PM2A polishing machine. A Chemcloth polishing pad was applied to the plate, which rotated at 30rpm with no extra applied load on the sample. The wafers were lapped for 10 minutes before each polish, using a glass lapping plate rotating at 40rpm and a slurry of 3μm α-alumina in water. NaOCl solution (100cm^3) was prepared initially and each wafer was polished for 30 minutes. If the etchant solution ran out before the end of the polish, it was replenished to ensure that the polishing cloth remained moist. Wafer samples used were approximately 2cm x 2cm.

After the polish, the surfaces was examined by optical Nomarski microscopy and the better surfaces were investigated by Talystep measurements. All polish solutions were retained for later analysis by AAS.

3.3.2 POLISHING OF CADMIUM TELLURIDE WITH SODIUM HYPOCHLORITE AT VARIOUS PH VALUES

Wafer Section	Etchant Volume / cm^3	pH
1g	98	12.3
2g	85	10.6
3g	98	9.2
4g	98	8.8
5g	11	8.3
6g	129	8.0
7g	146	7.2

Table 3.3.2 CdTe Polish in NaOCl at Various pH Values

The method used for this experiment was identical to that described in Section 3.3.1. The pH values for the solutions used and the volume of etchant required in each case are given in Table 3.3.2.

3.3.3 POLISHING OF GALLIUM ARSENIDE USING AN ALUMINA IMPREGNATED POLYURETHANE PAD

This series of experiments used a Logitech CP2000 polishing machine and a specially prepared polyurethane pad impregnated with 3μm α-alumina. The wafers were lapped for 10 minutes before each polish. The alumina impregnated pad was used at first without any conditioning, then conditioned with a diamond conditioner for 30 minutes to break up the surface prior to later polishes. The plate was rotated at 30 rpm and no load was used on the samples. Table 3.3.3 lists the reagents used, their volume, the polish duration and whether or not the pad was conditioned immediately prior to the polish. All etchant solutions were freshly prepared for each polish. The NaOCl solution was prepared to a desired pH rather than to any given concentration.

Wafer Section	Etchant	Concentration / mol.dm $^{-3}$	Volume / cm ^{3}	Duration / min	Conditioned
1h	0.5% Bromine/MeOH	0.087	90	30	x
2h	1% Bromine/MeOH	0.173	107	30	x
3h	1% Bromine/E.G.	0.173	78	15	x
4h	1% Bromine/MeOH	0.173	11	10	√
5h	1% Bromine/E.G.	0.173	74	10	√
6h	NaOCl/Acetic Acid pH 8	----	98	30	√

Table 3.3.3: GaAs Test Polish with Alumina Impregnated Pad (MeOH ≡ Methanol and E.G. ≡ Ethylene Glycol)

An aliquot (100cm^3) of etch solution was prepared initially and this was topped up if the etchant ran out before the end of the polish. Polish solutions were retained for analysis by AAS.

3.3.4 POLISHING OF GALLIUM ARSENIDE USING AN ALUMINA IMPREGNATED POLYURETHANE PAD AND A DIAMOND CONDITIONER

This experiment used the same apparatus as described in Section 3.3.3. Initially, the polyurethane pad was conditioned for 1 hour on a PM2A machine with a stainless steel/diamond conditioner to remove any contamination from previous reagents.

The method was the same as that used in Section 3.3.3, except that the resin-bonded diamond conditioner (Figure 3.2.6) remained on the pad for the whole period of the polish and the plate speed was increased to 50 rpm to facilitate the breakdown of the pad surface. The pad was conditioned on the PM2A for 1 hour before a change of reagent to ensure a fresh, clean pad surface. The details of etchant and polish duration are given in Table 3.3.4.

Wafer Section	Etchant	Concentration / mol.dm $^{-3}$	Volume / cm ^{3}	Duration / min	Mass GaAs / g
1i	1% Bromine/MeOH	0.173	40	15	0.2901
2i	1% Bromine/MeOH	0.173	112	30	0.3313
3i	1% Bromine/MeOH	0.173	56	45	0.3907
4i	1% Bromine/E.G.	0.173	67	15	0.4237
5i	1% Bromine/E.G	0.173	81	30	0.4142
6i	1% Bromine/E.G.	0.173	106	45	0.4605
7i	NaOCl/Acetic Acid pH 8	——	130	30	0.2475
8i	NaOCl/Acetic Acid pH 8	----	333	45	0.3475
9i	NaOCl/Acetic Acid pH 13	----	287	45	0.3390

Table 3.3.4: GaAs Polish with Alumina Impregnated Pad and Diamond Conditioner (MeOH ≡ Methanol and E.G. ≡ Ethylene Glycol)

Wafers were weighed before and after each polish to determine mass loss and polish solutions were retained for analysis by AAS. Surfaces were examined by optical Nomarski microscopy and those which appeared smooth were investigated by Talystep measurement.

3.4 RESULTS

3.4.1 POLISHING OF GALLIUM ARSENIDE WITH SODIUM HYPOCHLORITE SOLUTION AT VARIOUS PH VALUES

Gallium arsenide was polished by NaOCl solution at all the pH values used, to produce a shiny, mirror-like surface, although some rounding was visible at the wafer edges. The amount of soluble arsenic detected in solution generally increased with increasing pH, as shown in Table 3.4.1. The data given in the Table refer to the total amount of soluble arsenic in the etchant solution.

Wafer Section	pH	Total Soluble As / mg	R_a / nm
1f	12.3	18.05	-----
2f	9.2	12.45	10.29
3f	8.3	11.24	0.99
4f	8.0	3.85	11.69
5f	7.6	4.25	3.75
6f	6.4	5.00	-----

Table 3.4.1: AAS and Talystep Results from the Polishing of GaAs with NaOCl at Various pH Values.

Talystep measurements were attempted for samples 2f, 3f, 4f and 5f. The resulting R_a values were all indicative of good surface finishes, but varied greatly even over a small pH range. It was easiest to produce a consistently good finish at pH values of 8 or less.

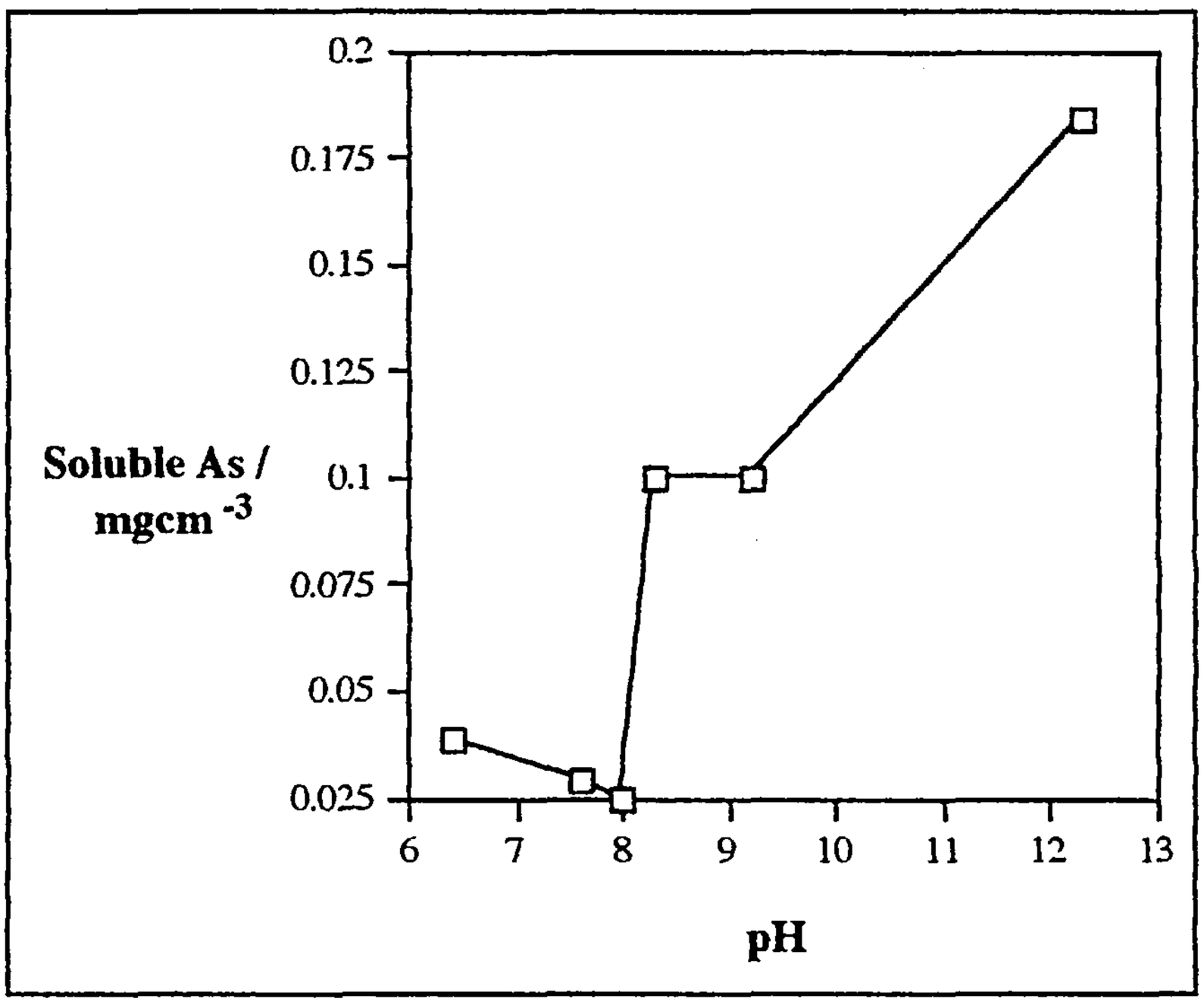

Figure 3.4.1: Soluble As per Unit Volume for the Polishing of GaAs with NaOCl at Various pH Values.

A better indication of the efficiency of the etchant in a polish was to consider the amount of material removed per cm^3 of etchant solution. Figure 3.4.1 shows a plot of soluble arsenic per cm^3 of etchant solution versus pH. This plot shows a similar pattern to that found in the dip-etch experiment (Section 2.4.3). The removal of material dropped at pH 8 and a plateau appeared in the plot before product removal increased again at high pH.

These results substantiated further the hypothesis that two etching mechanisms were competing across the pH range of the experiment. The best surface finishes appeared to be achieved when the removal of material to solution was slow.

3.4.2 POLISHING OF CADMIUM TELLURIDE WITH SODIUM HYPOCHLORITE SOLUTION AT VARIOUS PH VALUES

Cadmium telluride was polished by NaOCl solution at all the pH values used. The quality of the surfaces, even to the naked eye, varied greatly over the pH range. The amount of soluble cadmium detected in solution generally decreased with increasing pH, as shown in Table 3.4.2. Tellurium determinations by graphite furnace were inconclusive because of the effect of the NaOCl matrix on the absorbance. Flame analysis was possible, but could not detect the amounts of Te present (< 0.5 mg per 100 cm^3). Hence, significantly more cadmium than tellurium must have been removed from the sample.

Wafer Section	pH	Total Soluble Cd / mg	R_a / nm
1g	12.3	<0.3	-----
2g	10.6	0.38	23.17
3g	9.2	0.83	51.85
4g	8.8	1.24	4.60
5g	8.3	1.47	-----
6g	8.0	1.98	-----
7g	7.2	1.53	-----

Table 3.4.2: AAS and Talystep Results from the Polishing of CdTe with NaOCl at Various pH Values.

Talystep measurements were attempted for samples 2g, 3g and 4g. Note that the R_a value for sample 4g was obtained after a 60 min. polish. The CdTe was very difficult to polish to a flawless surface because of the polycrystalline nature of the material. The best R_a value obtained was after a 60 minute polish in NaOCl solution at pH 8.8.

To evaluate the efficiency of the etchant in removing material to solution, soluble Cd per cm^3 of etchant solution was plotted against pH (Figure 3.4.2). This plot suggested a maximum Cd removal around pH 8.5, before stock removal reduced again as pH was increased. This type of behaviour may also be indicative of two different etching mechanisms which 'buffered' when the NaOCl solution was used around pH 8. It is

interesting to note that the pH dependence of the CdTe/NaOCl reaction was opposite to that for the GaAs/NaOCl reaction.

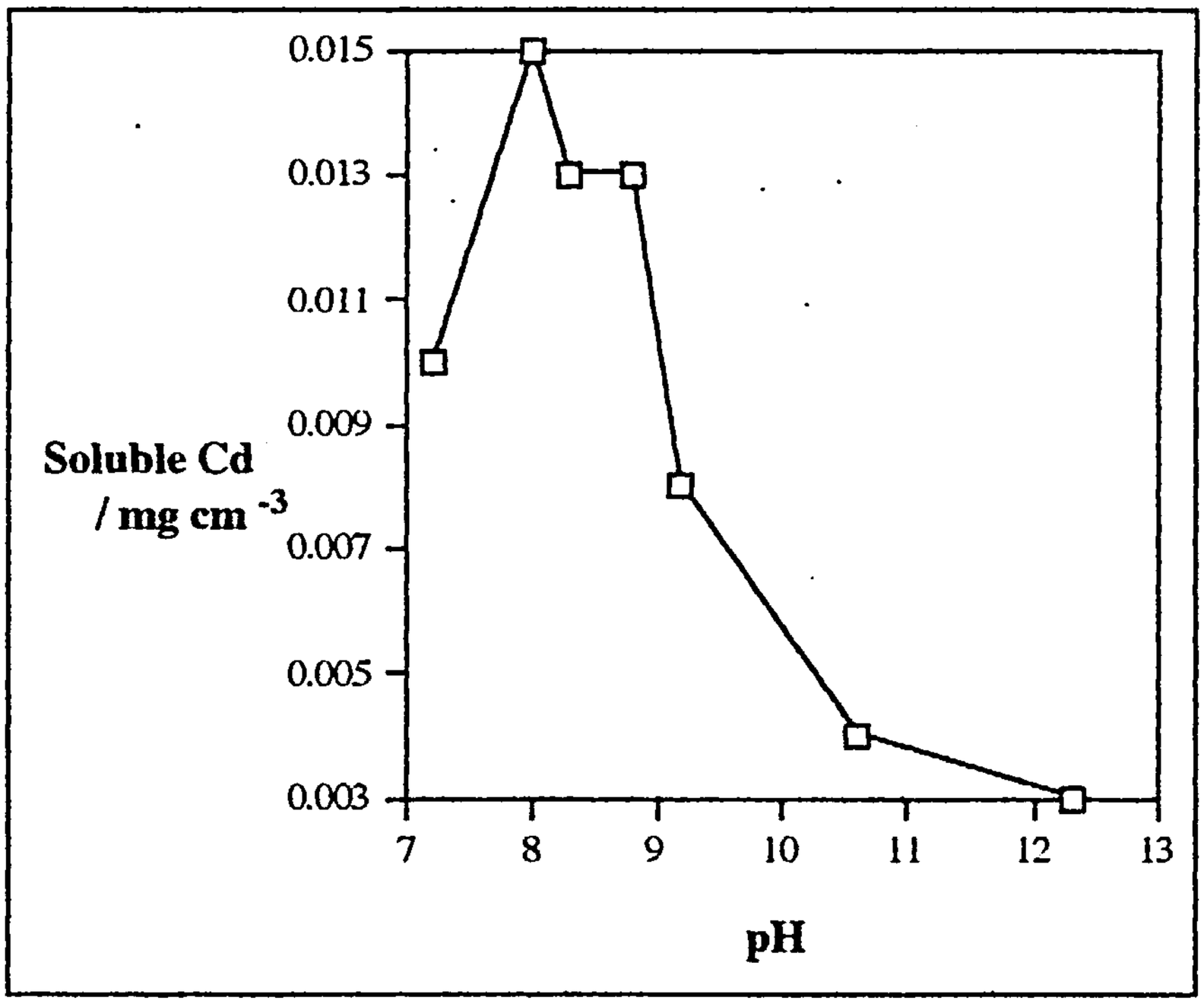

Figure 3.4.2: Soluble Cd per Unit Volume for the Polishing of GaAs with NaOCl at Various pH Values.

3.4.3 POLISHING OF GALLIUM ARSENIDE USING AN ALUMINA IMPREGNATED POLYURETHANE PAD

The results of AAS analysis of polish solutions from the polishing of GaAs with alumina impregnated pads, using various reagents, are shown in Table 3.4.3.

Wafer Section	Etchant	Concentration / mol.dm $^{-3}$	Duration / min	Conditioned	Soluble As / mg
1h	0.5% Bromine/MeOH	0.087	30	x	8.38
2h	1% Bromine/MeOH	0.173	30	x	47.72
3h	1% Bromine/E.G.	0.173	15	x	5.94
4h	1% Bromine/MeOH	0.173	10	√	6.08
5h	1% Bromine/E.G.	0.173	10	√	3.13
6h	NaOCl/Acetic Acid pH 8	-----	30	√	5.14

Table 3.4.3: AAS Results from the Polishing of GaAs with NaOCl using an Alumina Impregnated Pad. (MeOH = Methanol and E.G. = Ethylene Glycol)

The patterns visible when using the alumina impregnated pad were similar to those observed with a Chemcloth pad[59,60]. A 1% bromine/methanol solution removed significantly more material than a 0.5% solution over the same period. Ethylene glycol modified the action of the bromine and led to a lower stock removal than the same concentration of bromine in methanol. The levels of soluble arsenic detected were of the same order of magnitude as those found from Chemcloth polishing experiments.

Conditioning of the pad immediately prior to a polish did not make any real difference to the quantity of arsenic removed to solution but did affect the surface quality. Wafers polished on a newly conditioned pad appeared significantly better to the naked eye, although some surface scratching was still visible. After using bromine on the pad, the surface remained badly stained, even after conditioning, indicating that some bromine was retained on the pad surface.

3.4.4 POLISHING OF GALLIUM ARSENIDE USING AN ALUMINA IMPREGNATED PAD AND A DIAMOND CONDITIONER

Samples polished with dibromine/methanol or NaOCl (pH 8), on the new pads with a diamond conditioner, reached a smooth, polished finish within 45 minutes. The samples polished with bromine/methanol were dimpled in appearance with the 'orange peel' effect characteristic of bromine polishing in general. The results of soluble arsenic determinations and mass loss measurements for all of the samples are shown in Table 3.4.4.

Wafer Section	Etchant	Duration / min	% Mass Loss	Soluble As / mgcm $^{-3}$
1i	1% Bromine/MeOH	15	1.86	0.092
2i	1% Bromine/MeOH	30	18.2	0.238
3i	1% Bromine/MeOH	45	6.0	0.050
4i	1% Bromine/E.G.	15	1.4	0.016
5i	1% Bromine/E.G	30	0.6	0.005
6i	1% Bromine/E.G.	45	10.9	0.174
7i	NaOCl/Acetic Acid pH 8	30	0.8	0.103
8i	NaOCl/Acetic Acid pH 8	45	3.6	0.032
9i	NaOCl/Acetic Acid pH 13	45	38.5	0.009

Table 3.4.4: AAS and Mass Loss Results from the Polishing of GaAs with NaOCl using an Alumina Impregnated Pad and Diamond Conditioner.

The results were very inconsistent in terms of mass loss or soluble arsenic versus polish time. This reflects the fact that it was very difficult to obtain reproducible results using

the polyurethane pads. The application of a heavy load on the samples improves the reproducibility of the polishing process using these pads.

Wafer Section	Etchant	Duration	R_a / nm
1i	1% Bromine/MeOH	15	9.8
2i	1% Bromine/MeOH	30	13.5
3i	1% Bromine/MeOH	45	7.56
8i	NaOCl/Acetic Acid pH 8	45	3.56

Table 3.4.5: Talystep Results from the Polishing of GaAs with NaOCl using an Alumina Impregnated Pad and Diamond Conditioner.

The best surfaces achieved using the alumina impregnated pads were examined by Talystep to determine their average surface roughness (Table 3.4.5). The R_a values achieved were comparable with those achievable on a Chemcloth pad but were inconsistent with respect to polish time.

3.5 DISCUSSION

The experiments detailed in this chapter have shown that NaOCl solution polishes GaAs and CdTe in the absence of refractive oxide abrasives. Surface finishes measured on GaAs indicate that the etchant on its own can produce a better quality surface than an abrasive slurry, if it is employed at the correct pH. This is advantageous since it reduces the probability of scratching and sub-surface damage which can result from the disruption of the crystal structure when using an abrasive. However, some rounding was visible at the wafer edges because of the purely chemical nature of the polish. The use of an abrasive helps prevent this loss of geometry.

Polishing experiments on GaAs confirmed the hypothesis from the dip-etch work, that an optimum surface finish would be achieved around pH 8. Soluble As determinations revealed a similar pattern to those from the dip-etch experiments. The presence of a plateau confirmed that two different etching mechanisms were contributing to the reaction, dependent on pH. This hypothesis was tested further by investigation of the interaction of dichlorine with GaAs at room temperature and these experiments are detailed in Chapter Four.

Polishing experiments on CdTe revealed that, despite the lack of reactivity between CdTe and NaOCl in a dip-etch, a reasonable finish can be achieved using NaOCl on CdTe in a polishing situation. Thus, the action of the pad must be critical in removing some protective layer from the CdTe surface, and allowing etching to proceed. The layer protecting the CdTe surface in the dip-etch experiment is likely to be oxide formed in ambient atmosphere, which was removed by the action of the pad in the polishing experiment. The results of AAS analysis for Cd and Te indicated that more Cd than Te was removed from the CdTe surface. This behaviour is consistent with the action of dibromine on CdTe[36]. The phenomenon may be a solubility effect due to the fact that the Te products formed in both NaOCl and Br_2 reactions are less soluble than their Cd counterparts.

The use of alumina impregnated polyurethane pads to polish GaAs afforded very little advantage over other polishing methods. The wafer samples did not show any rounding at the edges, indicating that the pad did help maintain geometry during polishing. However, the surface quality which could be achieved was not comparable with that from a Chemcloth pad, and scratches were still visible on some samples from lapping damage. Scratching on the surface was probably due to the polymer matrix on the pad, since alumina is itself commonly used in slurries without such surface damage. The traditional use of an alumina slurry in NaOCl is more effective in maintaining geometry while still affording a reasonable surface finish. The use of a softer polymer may produce a more mobile pad surface and improve polish quality. Circular drainage grooves on the pad surface, rather than a sharp-cornered grid pattern, may also improve results.

The interaction of dibromine with the alumina impregnated pad may have significance to the use of aluminas as oxide abrasives in polishing reagents. The chemisorption of halogens onto aluminas is well-documented[61-64], so the role of alumina during the polishing process may involve a chemical interaction as well as the physical action of an abrasive, especially if used in conjunction with bromine or chlorine containing etchants. Any chemical interaction may be of use in formulating an abrasive/etchant system and so this hypothesis was investigated further in adsorption experiments on α and γ-alumina, detailed in Chapter Four

CHAPTER FOUR

HALOGEN ETCHING AND RADIOTRACER EXPERIMENTS

4.1 INTRODUCTION

Solution etching and polishing experiments, described in Chapters Two and Three, have produced results which suggest that NaOCl may etch by different reactions dependent on pH. Dichlorine gas is evolved rapidly from NaOCl solution at low pH (<8) and so there is a possibility that Cl_2 is in fact the active etchant in hypochlorite solutions which are employed at low pH. At higher pH values, direct oxidation by $[OCl]^-$ is more likely, as found in NaOCl etching experiments described in Chapter Two, Section 2.4.5. To test whether dichlorine was a likely etchant at low pH, it was necessary first to determine whether dichlorine reacts with GaAs at room temperature and to identify the products which form in this reaction. Thus, an experiment reacting GaAs with Cl_2 under anhydrous conditions was undertaken and the reaction products were identified by infrared and Raman spectroscopy.

Another phenomenon which required to be investigated further was the interaction of halogens and halogen-containing reagents with alumina. Work in this department has shown that dibromine is readily adsorbed onto a calcined γ-alumina surface[61,64]. Further adsorption experiments, examining the uptake of Cl_2 and Br_2 onto both α and γ-alumina, are detailed in this chapter. The effect of α and γ-alumina on NaOCl

decomposition has also been determined, using electronic spectroscopic techniques.

This chapter introduces the use of radioisotopes in this work, to trace reactions and measure uptake of reagents onto surfaces. These techniques adapt well to the work because of the small amounts of material involved and their use *in vacuo* permits the elimination of moisture from the system, preventing rapid hydrolysis of any products, as would occur in a polishing situation.

Radioactivity was discovered by Becquerel in 1896[65], when he discovered that uranium salts spontaneously emit radiation without being exposed to bright light beforehand. Becquerel recognized the difference between this type of radiation and normal fluorescent radiation, where light is later emitted from a previously excited substance. Rutherford found, in 1897, that some types of radiation could penetrate matter to a greater extent than others. He named the less penetrating rays alpha (α) rays and the more penetrating rays beta (β) rays. Later workers, including Madame Curie, proved that the 'rays' were in fact material particles. They could be deflected by a magnetic field, showing that they carried an electrical charge. Since α- and β-radiation take the form of particles which can interact with matter, it is possible for them to lose momentum during collisions with nuclei and be 'stopped' in a sufficiently thick sample of solid. Villard, in 1900, found a third type of radiation which proved to be even more penetrating than either alpha or beta radiation. These rays, named gamma (γ) rays are not deflected by a magnetic field i.e. they carry no charge.

Alpha particles are positively charged and are effectively helium nuclei which are emitted from certain radioactive materials during decay, as shown in Equation 4.1.1:

$$^{238}_{92}U \longrightarrow {}^{234}_{90}Th + {}^{4}_{2}He \qquad .....(4.1.1)$$

where the helium nucleus is the emitted alpha particle. Alpha particles can travel several centimetres in air but are easily stopped by a few millimetres thickness of aluminium foil. They have a definite range in an absorber (e.g.. aluminium) which is dependent on their energy, as shown in Figure 4.1.1:

The interaction of beta particles with matter is not as strong as that of alpha particles, hence β-particles are more penetrating than α-particles and it is possible to detect β-radiation through aluminium foil and even glass. The absorption of β-radiation is more complex than α-particle absorption, being approximately exponential until a certain thickness of absorber is reached, at which point absorption becomes complete.

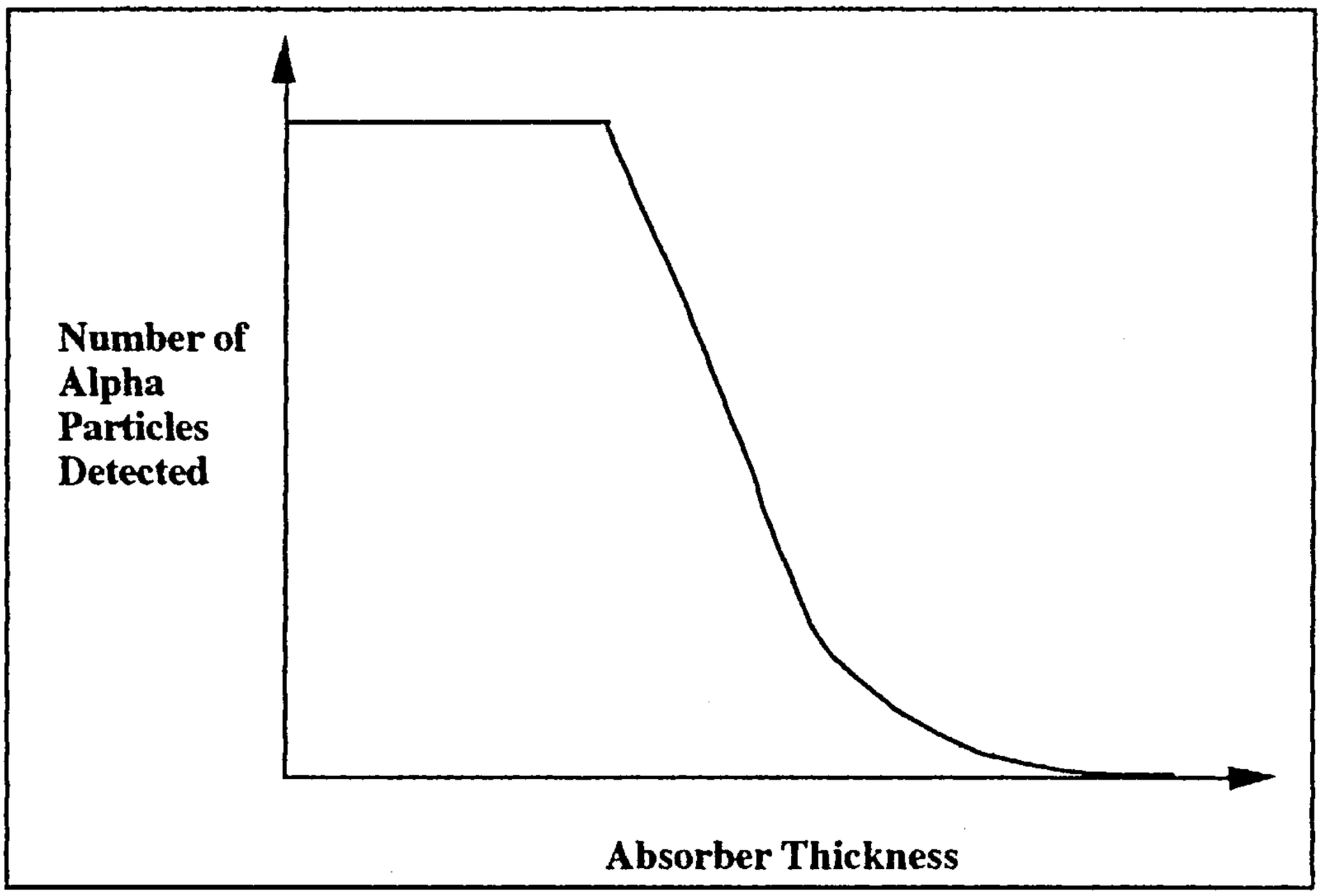

Figure 4.1.1: Absorption of Alpha Particles.

If alpha or beta particles are produced during radioactive decay in a sample of bulk solid, it may prove difficult to detect them using standard techniques such as a Geiger-Müller (GM) tube. This is due to a phenomenon known as self-absorption, where particles produced are stopped in the bulk solid before they reach the surface. As beta particles are absorbed in a material, some of their energy is converted into x-rays known as bremstrahlung and hence will not be detected using methods such as the GM tube which detect charged particles.

Beta particles are high energy electrons and can be emitted from a nucleus at various velocities from zero to a maximum value determined by the emitting nucleus. An uncharged particle called a neutrino is emitted in conjunction with the beta particle, allowing conservation of energy and momentum regardless of the velocity of the emerging beta particle. Some radioactive isotopes also emit positively charged beta particles known as positrons. The symbols β^+ and β^- signify the charge of the particle.

Gamma rays represent the third type of radioactive decay. They are not deflected by a magnetic field, indicating that they are not charged particles. Gamma rays are, rather, a form of electromagnetic radiation of very short wavelength. A gamma ray photon is emitted from a nucleus as it decays from a high energy state to one of lower energy and they have energies characteristic of the nucleus from which they are emitted. Gamma

emission often accompanies both alpha and beta emissions.

The various isotopes of bromine, including common radioactive nuclei, are described in Chapter One, Section 1.4.1. [^{82}Br]-Labelled Br_2 (β^-, γ) was used in this work to measure the uptake of Br_2 onto α-alumina. There are 17 known isotopes of chlorine[66] although only two occur naturally; ^{35}Cl (75.77% abundant) and ^{37}Cl (24.23% abundant). ^{36}Cl is the most commonly used radioactive isotope of chlorine, with a half-life of 3.0×10^5 years. Most radioactive isotopes of chlorine have half-lives of less than one hour and so are much less useful as radiotracers. [^{36}Cl]-Labelled Cl_2 (β^-) and NaOCl were used in this work to measure uptakes on GaAs and alumina.

4.2 General Experimental Techniques

4.2.1 Vacuum Line Calibration

Pyrex glass vacuum lines were used extensively in this work to investigate reactions in the absence of moisture. The basic apparatus used to measure adsorption of a gas onto a solid surface in shown in Figure 4.2.1. Before the apparatus could be used for experimental purposes, it was necessary to determine the volumes of different parts of the line. This calculation permits the determination of how much gas is present above the wafer at any given time.

The volume of the line was determined by expanding a known volume of air at a measured pressure into a section or manifold on the line. The pressure reading on a gauge attached to the manifold was recorded and the volume of the manifold (V_2) was calculated using the relation:

$$\mathbf{P_1V_1 = P_2V_2} \quad \text{.....(4.2.1)}$$

Where P_1 = atmospheric pressure

V_1 = the initial known volume of air expanded into the manifold (cm^3)

P_2 = the pressure reading from the gauge (Torr).

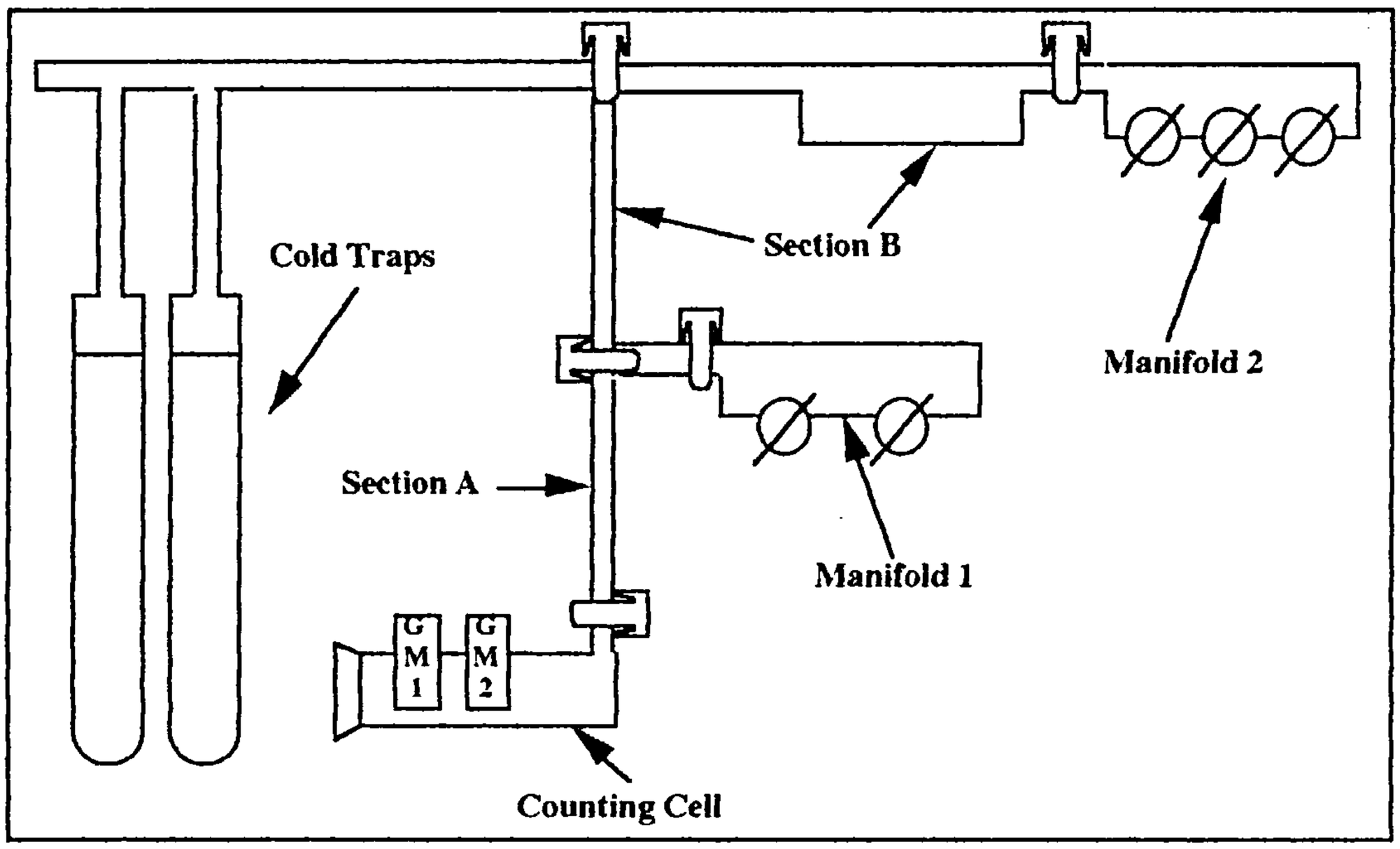

Figure 4.2.1: Schematic of Chlorine Vacuum Line.

During counting, it is convenient to convert pressures into a known quantity of gas in moles or millimoles, to calculate the stoichiometry of the reaction. This procedure was carried out for manifold 1, progressively opened to section A and then the counting cell. The results are shown in Table 4.2.1

SECTION	P_2 / Torr	V_2 / cm^3	1mmol =
Manifold 1	350	207.6	89.6Torr
Section A	312	46.5	72.8Torr
Counting Cell	158	416.1	27.7Torr
Section B	111	358.2	
Manifold 2	97	173.8	

Table 4.2.1: Calibration of Chlorine Vacuum Line.

4.2.2 THE GEIGER-MÜLLER COUNTING TECHNIQUE

A) THE PLATEAU REGION

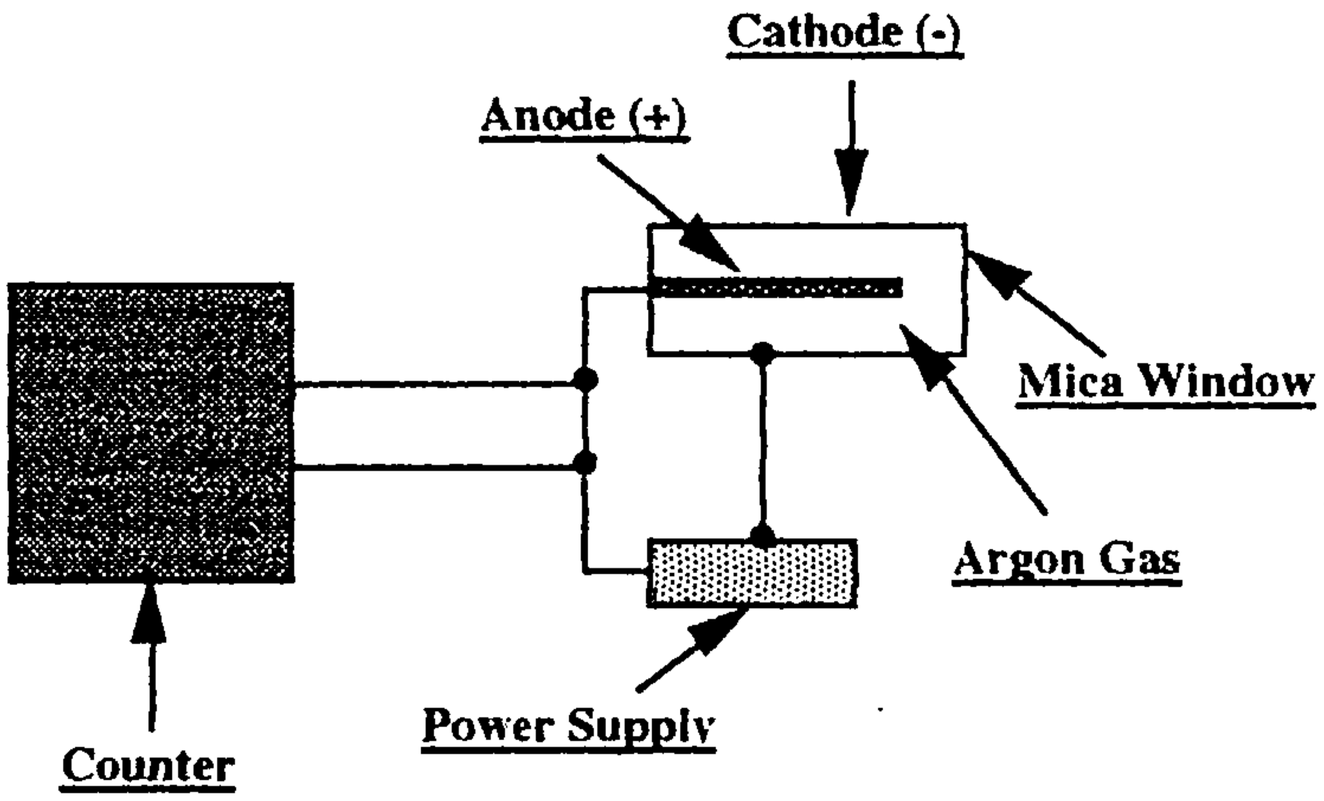

Figure 4.2.2: Geiger-Müller Counter.

Geiger-Müller tubes are used to detect ions produced when α and β particles come into contact with matter. They were used in this project to count ^{36}Cl (β^-) activity. When using a Geiger-Müller tube (Figure 4.2.2) to detect ionising radiation a threshold voltage (V_O), known as the Geiger threshold, exists below which no counts are recorded. This is because the applied voltage on the tube must be large enough to attract the free electrons produced to the tube.

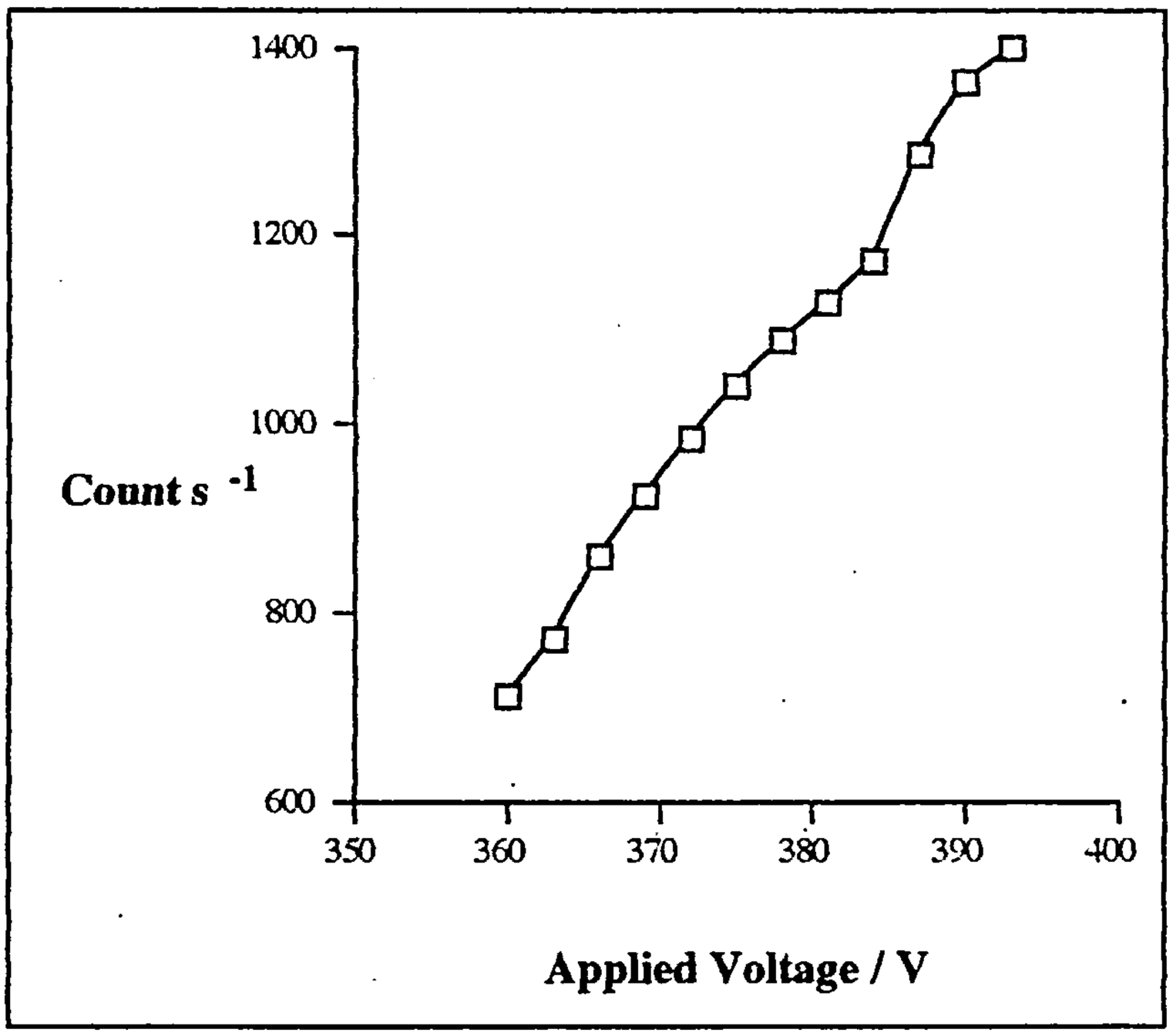

Figure 4.2.3: Plateau Curve.

Above the threshold voltage, counts rise rapidly and then begin to level slightly over a 'plateau' until spurious discharges cause another steep rise. It is desirable to work at a voltage in the middle of the plateau region, since this is where the counter is most accurate. In many modern GM tubes, this region is not manifested by a discernible flat region but by a gradual drop in the gradient of the plot around the optimum voltage (Figure 4.2.3) The plateau region was determined for both Geiger-Müller (GM) tubes used, by constructing a plot of counts obtained from a ^{60}Co source .

B) DEAD TIME DETERMINATION

The decay in activity of a radioactive isotope can be described by the relationship:

$$\mathbf{A_t = A_o \exp(-\lambda t)} \qquad .....(4.2.2)$$

where A_o = the initial activity

A_t = the activity at time t

λ = the decay constant (per unit time, dependent on the units of A)

Hence, a plot of $\ln A_t$ vs. t should give a straight line of slope $-\lambda$, with a y-intercept of $\ln A_o$. If such a plot is attempted using a Geiger-Müller tube, a curve is obtained. This is because each pulse from a Geiger-Müller tube is followed by a period in which no particles can be detected (the dead time). This period lasts until positive ions surrounding the central anode move far enough away to allow an output pulse large enough to operate the recording equipment. In accurate counting experiments, it is necessary to correct for counts lost in dead time, especially if the count rate is high.

The dead times of both Geiger-Müller tubes were determined by counting a sample of [^{18}F]-labelled caesium fluoride for 330 minutes (Figure 4.2.4). The linear portion of the plot was extrapolated back to t = 0 using the half-life of the radioisotope (109.72 min). This extrapolated line gives N_t, the true count rate, which is related to the observed count rate, N_o by the relation shown in Equation 4.2.3:

$$\mathbf{N_t = \frac{N_0}{1 - N_0 \tau}} \qquad .....(4.2.3)$$

Where τ = dead time.

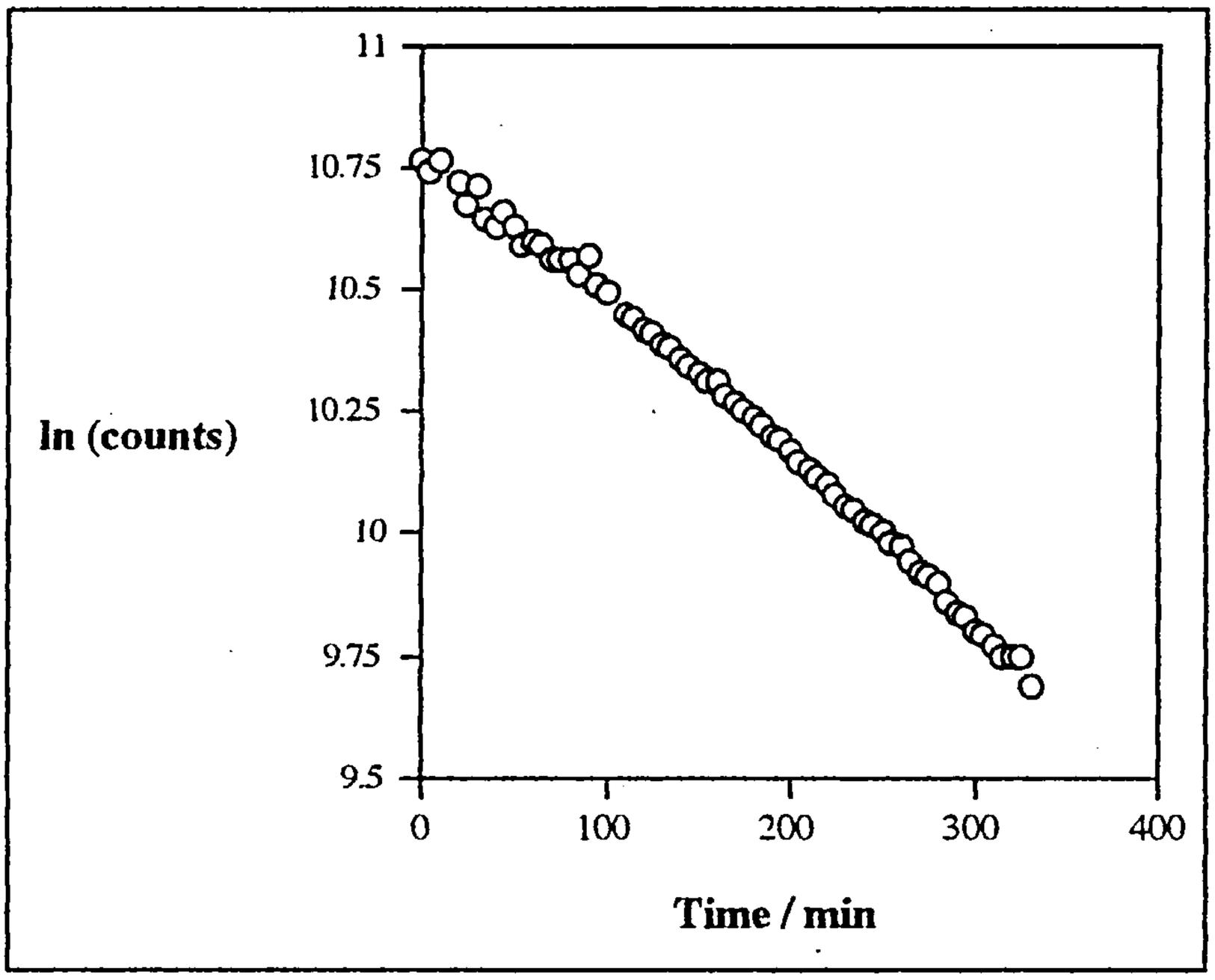

Figure 4.2.4: Dead Time Curve.

The dead times determined for GM1 and GM2 were 1.30 x 10^{-4} s and 2.01 x 10^{-4} s respectively. In reality these numbers probably represent the dead times of the respective scalers since the scaler ratemeters are designed to have larger dead times than the GM tubes.

c) INTERCALIBRATION OF GM TUBES

Geiger-Müller tubes should be intercalibrated regularly by measuring the activity of varying pressures of radioactive gas. A sample of radioactive gas was necessary to intercalibrate the two Geiger-Müller tubes. To prepare anhydrous [^{36}Cl]-chlorine labelled HCl ($H^{36}Cl$), [^{36}Cl]-labelled aqueous NaCl (2.5cm^3, 62.5μCi, Amersham International) was diluted with 34.5% w/v hydrochloric acid (10cm^3, Fisons). This solution was added dropwise to concentrated sulphuric acid (15cm^3, BDH). The reaction was carried out in a specially designed flask attached to a series of moisture / impurity traps and a collection vessel[59]. The $H^{36}Cl$ gas was used at various pressures to determine the count rate from both GM tubes in the counting cell.

A graph of pressure versus counts yielded a straight line through the origin. When the counts from both tubes were plotted against each other, a straight line was obtained,

with a gradient equal to the counting ratio between the two tubes (Figure 4.2.5). For the graph shown, GM2 was found to be a more efficient counter than GM1, with an intercalibration ratio of 1.36 between the two.

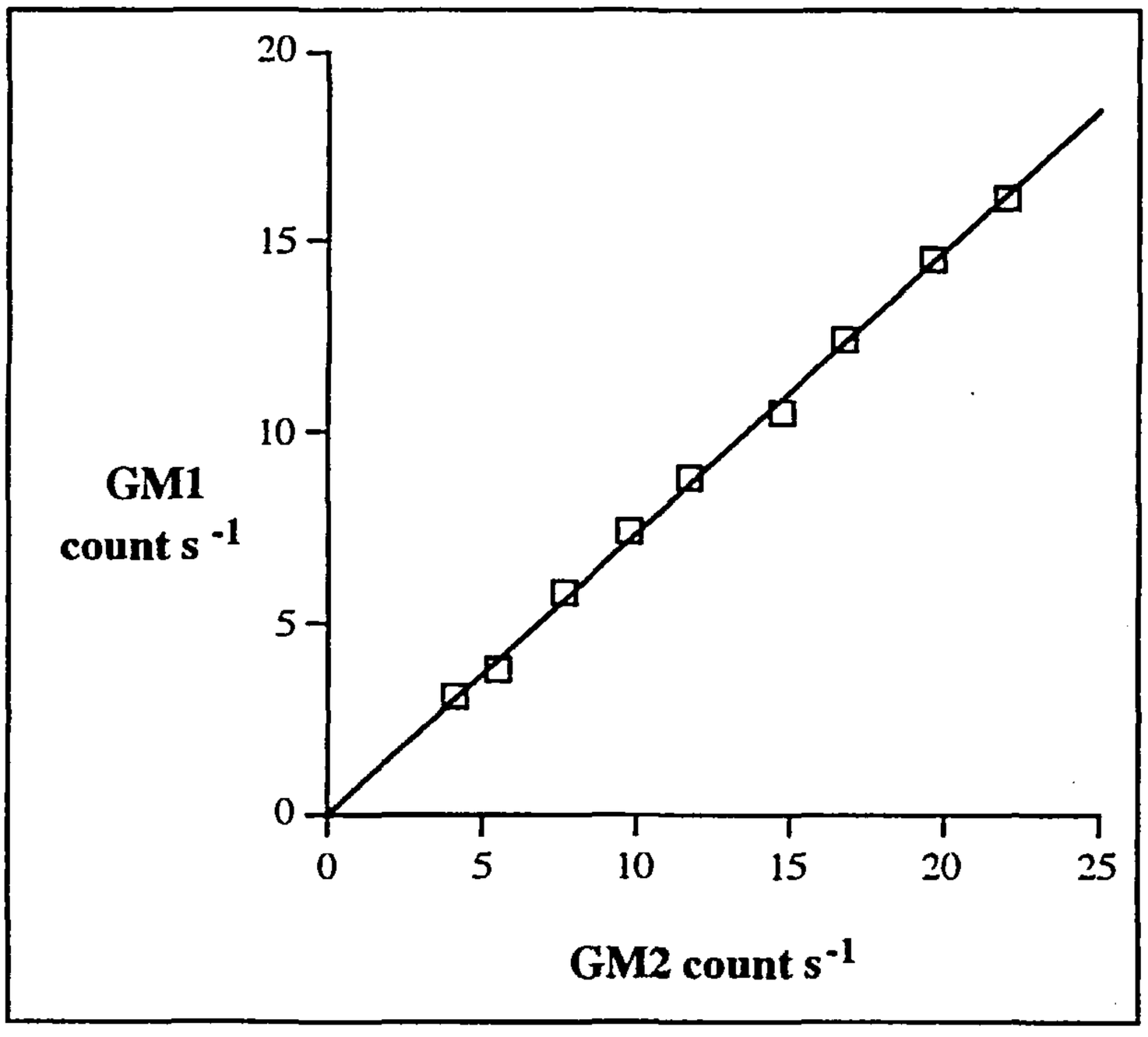

Figure 4.2.5: Intercalibration Plot.

4.2.3 THE SCINTILLATION COUNTING TECHNIQUE

The GM counting technique is only useful for detecting charged particles such as α and β-radiation. To detect γ-radiation, a different technique is necessary. One commonly used detector for γ-radiation is the scintillation counter. Placement of a large impurity ion like thallium (Tl^+) in a crystal such as sodium iodide (NaI) causes lattice strain. This strain is relieved by interaction with a γ-ray and a photon is released which is proportional in energy to the original γ-ray. These photons are detected then amplified using a photomultiplier and can be measured using a scaler ratemeter. An NE sodium iodide scintillation counter and scaler ratemeter were used in this work.

A) CALIBRATION OF THE SCINTILLATION COUNTER

It is possible to vary the operating voltage of a scintillation counter to obtain an optimum signal within a certain range of photon energies. The purpose of this

calibration exercise was to ascertain the optimum operational voltage of the counter and to calibrate the threshold potentiometer to allow direct reading of the γ-ray energy (kilo electron volts keV) rather than threshold potential (millivolts mV). This process was carried out in accordance with the manufacturer's handbook, using the 662keV gamma peak of a small ^{137}Cs (caesium 137) source. The operating voltage on the counter was varied (at a fixed threshold) until a maximum count rate was reached (Figure 4.2.6). This maximum was accurately located (± 2V) and the operating voltage was fixed at this optimum value.

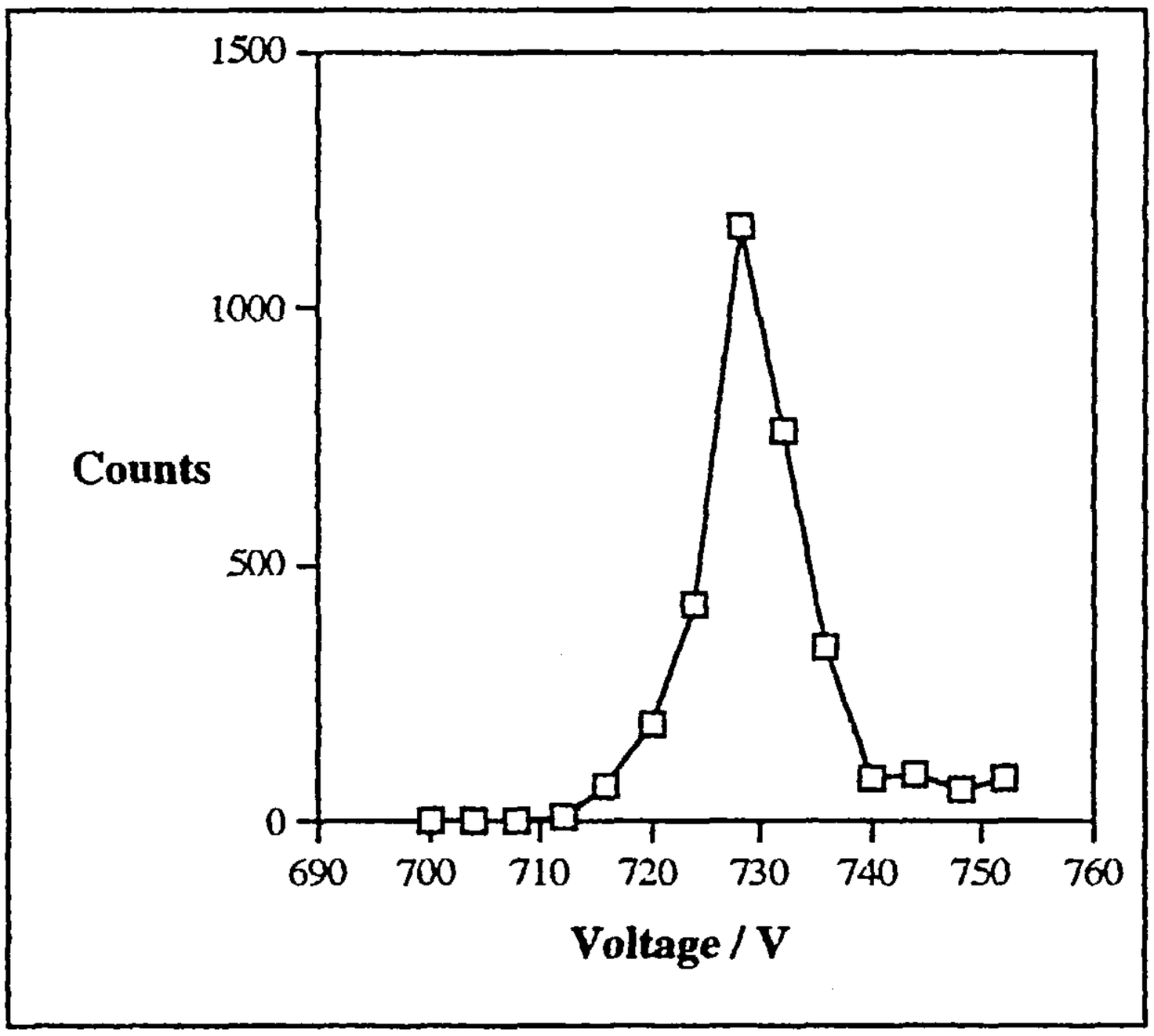

Figure 4.2.6: Operational Voltage Calibration of a NaI Scintillation Counter Using a ^{137}Cs Source

The threshold potentiometer was then calibrated (at the fixed voltage of 728V) to allow direct measurement of γ-ray energy between 10keV and 1000keV.

B) THE γ-RAY SPECTRUM OF ^{82}Br

The scintillation counter was used in this project to determine the activity of ^{82}Br in a sample. Before using an [^{82}Br]-labelled sample in an experiment, the purity of the sample, in terms of radioisotopes present, was determined by obtaining a γ-ray spectrum of the material. Having calibrated the counter to allow direct measurement of energy in keV, it was possible to scale through the energies and determine the isotopes present in a sample by their unique γ-ray energies. ^{82}Br has several γ-ray energy peaks between

500 and 1500keV[66].

The operating voltage was set at 728V and 0.0574g (0.359mmol) of [^{82}Br]-labelled Br_2 in chloroform (1cm^3) was placed in the well of the scintillation counter. The threshold was varied from 500keV to 1000keV at 10keV intervals and the count rate was determined at each point. Counts were corrected for background radiation and were decay corrected, since the spectrum was accumulated over two days. The spectrum obtained is shown in Figure 4.2.7.

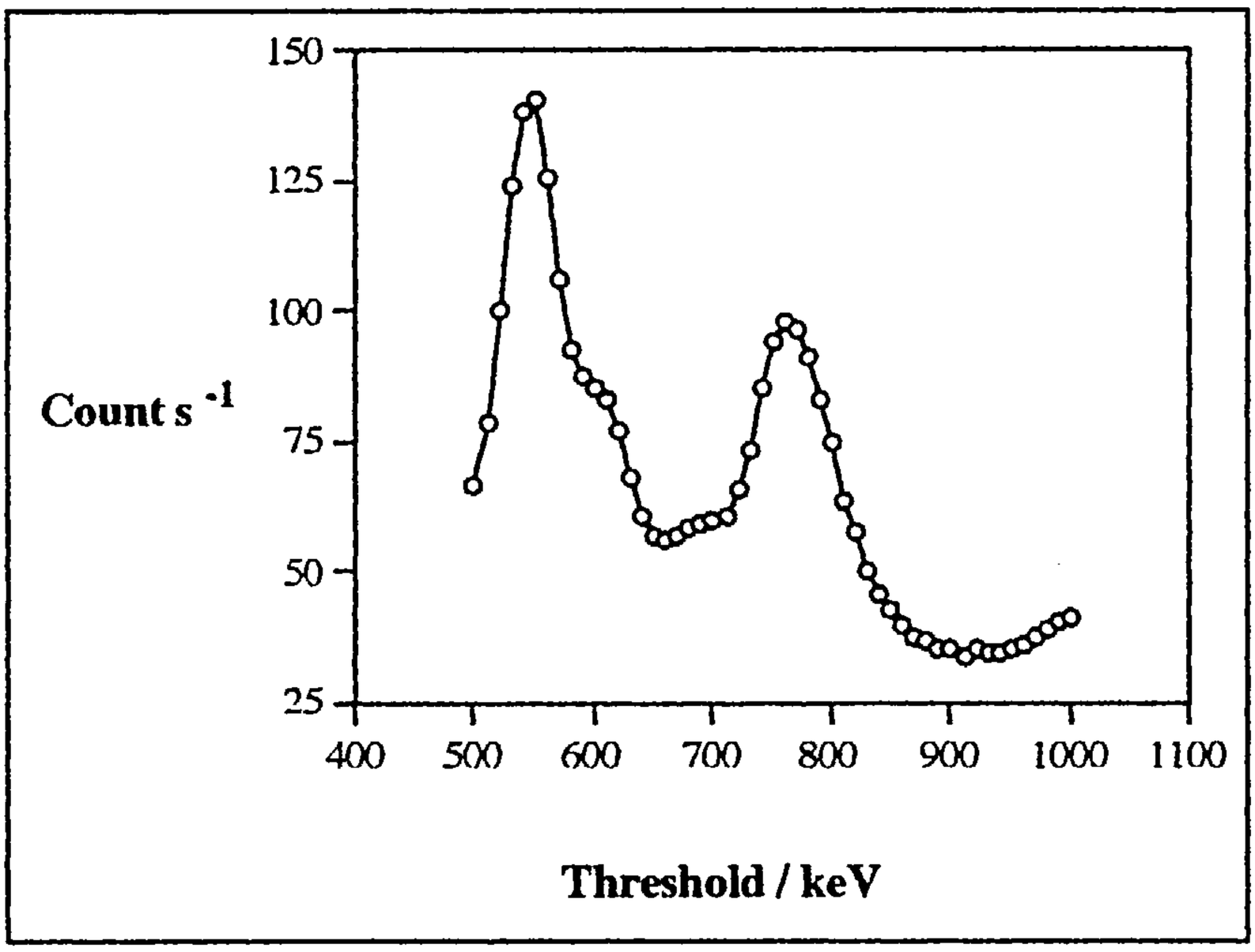

Figure 4.2.7: γ-Ray Spectrum of ^{82}Br-Labelled Br_2

The peak at 770keV is the clearest distinguishable maximum in the spectrum, so the threshold potentiometer was set at 770keV for counting ^{82}Br disintegrations.

C) HALF-LIFE OF ^{82}Br

Determination of the half-life of a sample is another way of checking its radiochemical purity. Half-life can be determined using a combination of equations 4.2.2 and 4.2.5.

$$t_{\frac{1}{2}} = \frac{\ln 2}{\lambda} \qquad .....(4.2.5)$$

where

λ = the decay constant (h^{-1})

and

$t_{1/2}$ = half-life (h)

From equation 4.2.2, a plot of lnA against t should give a straight line of gradient -λ (Figure 4.2.8). λ, determined from such a plot, can then be used in equation 4.2.5 to determine the half-life of the sample. For the plot shown in Figure 4.2.8, $t_{1/2}$ = 34.67h. The given literature half-life for ^{82}Br is 35.3 hours[66]. The lower half-life value for our sample indicates the presence of other bromine isotopes, of shorter half-life, produced during the activation process. Although most of these isotopes will have decayed during the 48 hour delay in sample collection, sufficient amounts of ^{*80}Br ($t_{1/2}$ =4.74h), for example, will be present to reduce the half-life of the sample by this amount. However, the half-life value of 34.67h obtained, confirms that ^{82}Br is the major isotope present. Also, the reaction times used in our experiments far exceed 4.74h, so isotopes of this half-life will not significantly affect the results.

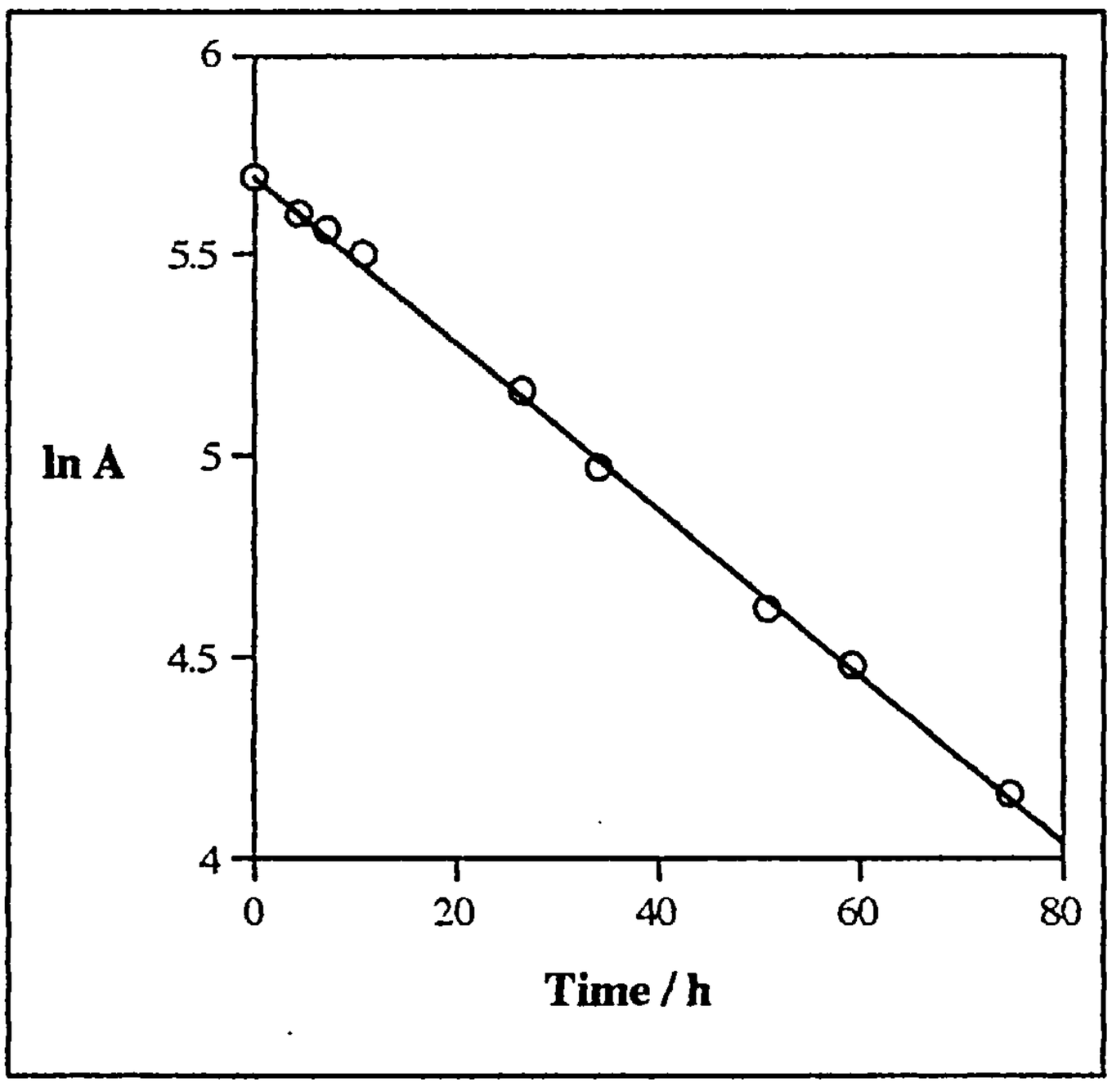

Figure 4.2.8: Half-life Determination for ^{82}Br

D) SPECIFIC ACTIVITY OF ^{82}Br

To convert count rate in an uptake experiment into the amount of bromine adsorbed (in mmol or mg atom) it was necessary to determine the specific activity of a Br_2 sample (in count s^{-1} (mg atom Br)$^{-1}$) before use. The specific activity of the bromine was

determined by counting a known mass of dibromine in a solution of chloroform ($1cm^3$). The count rates given in Table 4.2.2 are for 0.0859g (0.537mmol) of Br_2. The counts and count rates were corrected to account for decay. From the table, the average count rate was 270.9 count s^{-1} for 0.537mmol, yielding a specific activity value of 504.5 count s^{-1} (mmol Br_2)$^{-1}$ or 252.2 count s^{-1} (mg atom Br)$^{-1}$. This process was undertaken for each sample of ^{82}Br prepared and the data are typical of several experiments.

Time / h	Count	Count s^{-1}
0	27181	271.81
2.50	27191	271.91
2.53	27261	272.61
2.57	27008	270.08
2.60	27121	271.21
2.63	27132	271.32
2.67	26955	269.55
2.70	27002	270.02
2.73	27304	273.04
2.77	26817	268.17
2.80	26998	269.98
2.83	27062	270.62

Table 4.2.2: Specific Activity Determination for ^{82}Br

4.2.4 RAMAN SPECTROSCOPY

Raman spectroscopy, like infrared spectroscopy, is a vibrational spectroscopic technique i.e. it yields a spectrum based on the vibrational energies of a molecule. However, radiation is scattered rather than directly absorbed and the incident radiation is normally of much higher frequency than the vibrational frequencies of the molecule.

In Raman spectroscopy, the electron cloud of the molecule is polarised by the electron vector of incident electromagnetic radiation. Thus, any molecular vibration which leads to a change in the polarizability of a molecule will produce a band in a Raman spectrum. When a photon of frequency υ interacts with a Raman active vibration, a short-lived excited state is created. Relaxation back to the ground state is accompanied by the release of a second photon. This second photon will have a frequency equal to ($\upsilon \pm \omega$), where ω is the frequency of the molecular vibration. The photons of frequency ($\upsilon - \omega$) are used to produce a Raman spectrum consisting of the photon emissions (known as Stokes emissions) at various frequencies. The photons of frequency ($\upsilon + \omega$) are known as anti-Stokes emissions, appearing at a frequency higher than the incident radiation. These bands are usually very weak since very few of the analyte molecules

will initially be in an excited state. The frequencies of the emissions are separated from the frequency of the incident light by the vibrational frequencies of the molecule. Thus, a final spectrum can be produced showing the Stokes lines at wavenumbers (cm^{-1}) appropriate to the molecular vibration which they represent.

A basic Raman spectrometer usually uses a monochromatic laser beam, operating at a visible wavelength, as the light source. The sample is placed between the beam and a visible light spectrophotometer which measures the Raman-shifted light from the sample. One advantage of using visible light sources is the use of glass optics, mirrors and sample containers. This allows analysis of air sensitive samples in sealed glass containers. In this work, Raman spectra were obtained using a Spex Ramalog spectrometer (514.6nm excitation), from reaction products sealed *in vacuo* into thin glass capillaries.

4.3 THE REACTION OF DICHLORINE WITH GALLIUM ARSENIDE

4.3.1 IDENTIFICATION OF PRODUCTS FROM THE REACTION OF DICHLORINE WITH GALLIUM ARSENIDE

This experiment used anhydrous chlorine gas. The apparatus was a simple glass reaction vessel (Figure 4.3.1) attached to a vacuum manifold. Three moles of Cl_2 (Linde Gas UK Ltd.) were employed for every mole of GaAs used, assuming the reaction shown in equation 4.3.1.

$$\mathbf{2GaAs + 6Cl_2 \rightarrow 2AsCl_3 + Ga_2Cl_6} \quad .....(4.3.1)$$

Dichlorine gas was vacuum distilled from a reservoir obtained from a cylinder, after the reservoir had been degassed to remove any air. The Cl_2 was degassed in a dry ice/dichloromethane bath (193K) before vacuum distilling into a degassed storage vessel containing potassium permanganate ($KMnO_4$) to remove any trace hydrogen chloride. After warming to room temperature, the Cl_2 was distilled into the final storage vessel containing phosphorus (V) oxide to keep the Cl_2 dry.

A section of GaAs wafer (1.84mmol) was transferred into the reaction vessel, which was degassed on a vacuum manifold. Cl_2 gas (5.5mmol) was condensed into the vessel

from the reservoir. The reaction vessel was allowed to warm slowly back to room temperature. When reaction began, and heat from the reaction started to warm the vessel, a cold Dewar containing liquid nitrogen was used as a heat sink around the vessel for safety. This was replaced by a cold, empty Dewar as reaction proceeded. Once at room temperature, the reaction mixture was allowed to continue overnight to ensure complete reaction. No wafer segment was visible when reaction was complete. A yellow/brown liquid product was obtained which appeared cloudy. After a further 24 hours, white crystals precipitated out leaving a murky yellow liquid.

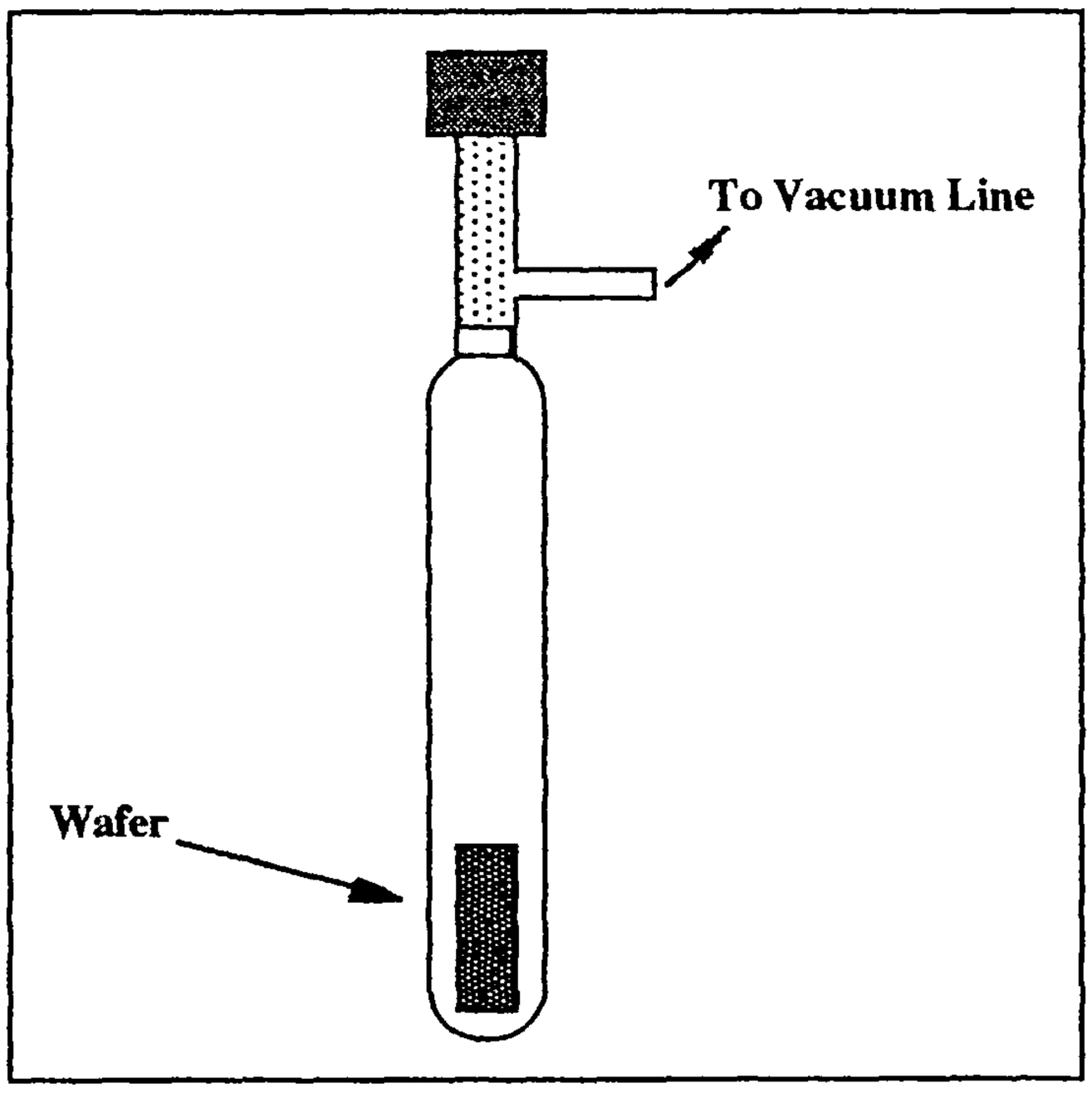

Figure 4.3.1: Glass Reaction Vessel

The product mixture was separated into its constituents by very slow vacuum distillation. A transparent, colourless liquid and a white crystalline solid were obtained. The white solid was prepared as a Nujol mull in a nitrogen glove box, and both the mull and the colourless liquid were analysed between silicon windows on a Philips PU9800 infrared spectrometer. The products were also analysed by Raman spectroscopy in sealed glass capillaries.

4.3.2 ADSORPTION OF [^{36}Cl]-LABELLED DICHLORINE ONTO GALLIUM ARSENIDE

To prepare [^{36}Cl]-chlorine labelled dichlorine ($Cl^{36}Cl$), a solution of [^{36}Cl]-labelled sodium chloride in aqueous hydrochloric acid (2.4cm^3, 60μCi, Amersham International)

was added to hydrochloric acid ($30cm^3$, 35.4% w/v, Fisons) and heated to 333K before the dropwise addition of a saturated solution of $KMnO_4$ ($250cm^3$). The reaction involves oxidation of the chloride in acid solution, as shown in equation 4.3.2.

$$MnO_4^- + 8HCl \rightarrow Mn^{2+} + 4H_2O + 3Cl_2 + 2Cl^- \quad .....(4.3.2)$$

However, the characteristic brown colour of MnO_2 was visible in the reaction vessel after reaction is complete. This implies that a further oxidation reaction occurs, whereby some of the dichlorine formed in the above reaction is reduced back to the chloride, as shown in equation 4.3.3.

$$Cl_2 + Mn^{2+} + 2H_2O \rightarrow MnO_2 + 4H^+ + 2Cl^- \quad .....(4.3.3)$$

The overall reaction can be represented as shown in reaction equation 4.3.4:

$$MnO_4^- + 2HCl + 2H^+ \rightarrow MnO_2 + 2H_2O + Cl_2 \quad .....(4.3.4)$$

The reaction was carried out in a round-bottomed flask attached to a series of moisture / impurity traps and a collection vessel[67,68]. The dichlorine liberated was distilled through the series of traps into the collection vessel and then distilled from 193K to 77K and stored over phosphorus (v) oxide in a Monel metal bomb to ensure dryness.

Adsorption experiments to measure ^{36}Cl uptake on the GaAs surface were carried out in the counting cell on the chlorine vacuum line. A more detailed diagram of the counting cell is shown in Figure 4.3.2.

A section of GaAs (2.33mmol) was placed in the reaction boat under GM1 and the line opened to the vacuum pump. A pressure of [^{36}Cl]-labelled dichlorine gas was collected in manifold 1 (Figure 4.2.1) and the manifold was then opened up to section A and the counting cell. The gauge was allowed to settle for about one minute, to allow for equilibration of pressure throughout the line, before the reading shown in Table 4.3.1 was taken. Aliquots of gas were added at intervals of about 30 minutes and the time interval noted accurately. The background count rates for GM1 and GM2 were 0.95 and 0.80 count s^{-1} respectively.

Due to the low activity of the [^{36}Cl]-labelled dichlorine, counts were accumulated over 30 min. (1800 s.) to ensure the statistical reliability of the count rates. Counts from GM2 (gas only) and GM1 (gas + solid) were recorded simultaneously. After reaction

appeared complete, the counting cell was opened to the vacuum pump (via cold traps) and any drop in count rate was noted.

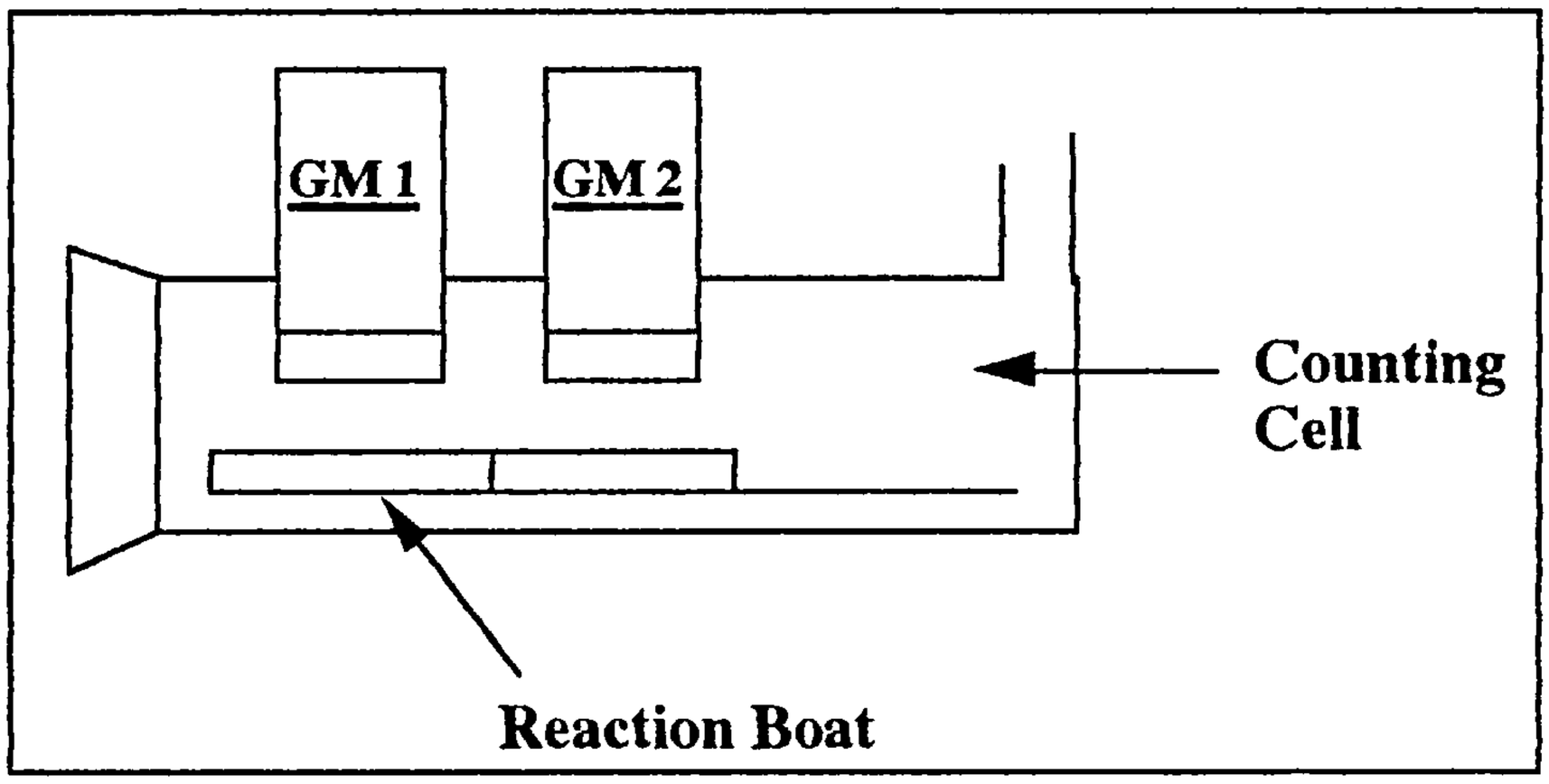

Figure 4.3.2: Counting Cell for the Chlorine Vacuum Line

Time / sec	Accumulated Pressure of $^{36}ClCl$ in Counting Cell / Torr
0	10
1800	30
3660	45
5580	50

Table 4.3.1: Aliquots of [^{36}Cl]-Labelled Cl_2 Added to GaAs

4.3.3 Adsorption of [^{36}Cl]-Labelled Dichlorine, Evolved from Acidified Sodium Hypochlorite Solution, onto Gallium Arsenide

A GaAs wafer section (2.54mmol) was placed in the counting cell under GM1 and the vacuum line opened to the pump. Sodium hypochlorite solution (14%, BDH, 40cm^3) was placed in the reaction vessel shown in Figure 4.3.3 and the vessel was attached to the vacuum manifold

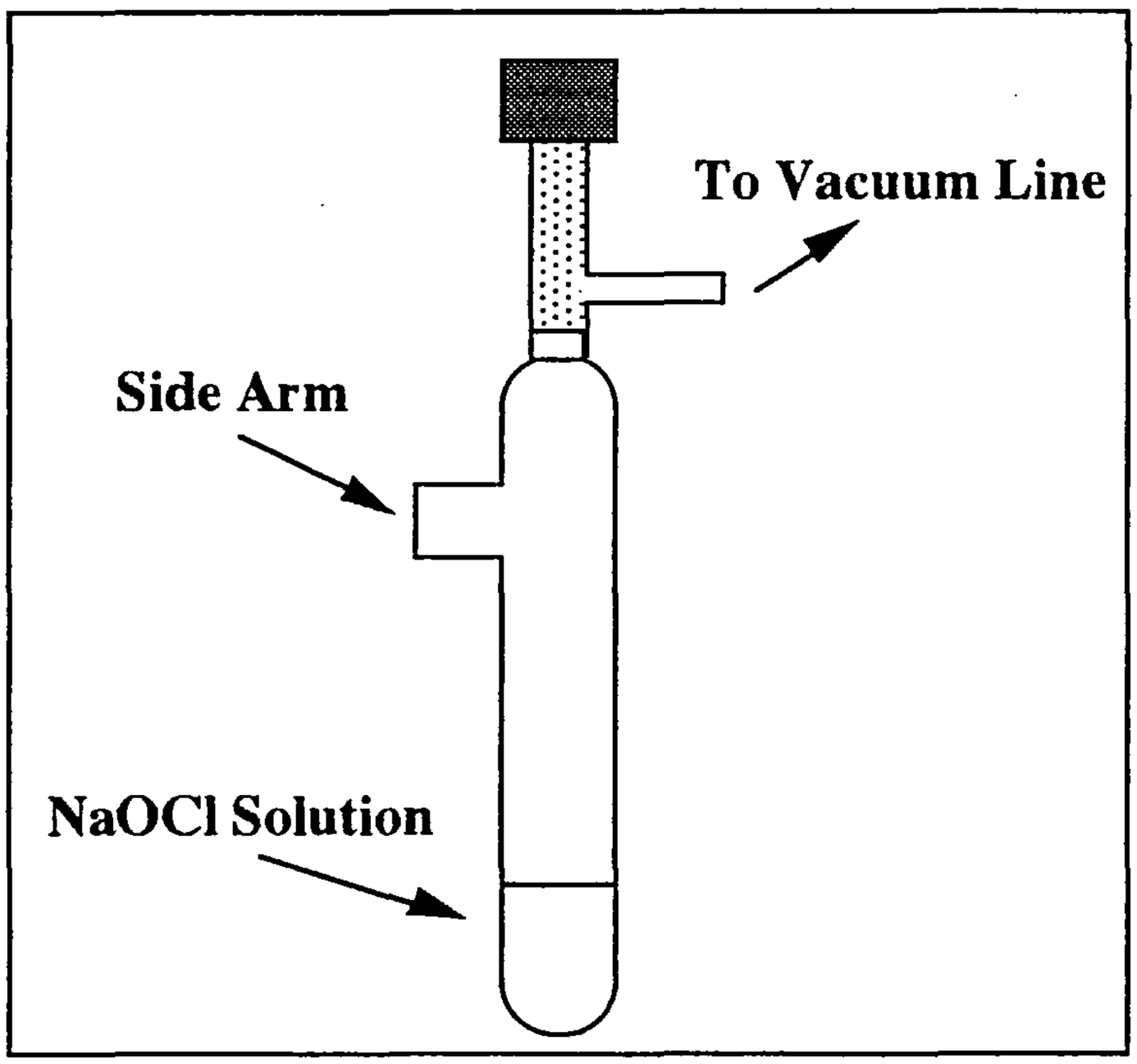

Figure 4.3.3: NaOCl Reaction Vessel

The pressure in the reaction vessel was reduced by opening to an evacuated manifold (but not to the pump) and allowing the air in the vessel to expand into the manifold. This process was repeated until the NaOCl solution began to bubble. [^{36}Cl]-labelled NaCl solution in HCl (1cm^3) was injected, via a rubber septum on the side-arm, into the reaction vessel. This allowed labelling of the NaOCl, as shown in equation 4.3.5 and reduction of pH in one step without disrupting the reduced pressure atmosphere inside the reaction vessel. The solution was stirred using a magnetic stirring bar throughout the reaction.

$$2[OCl]^- + 4H^{36}Cl \rightarrow 3^{36}Cl_2 + 2H_2O \quad .....(4.3.5)$$

After the acid had been added, the reaction vessel was opened to the vacuum manifold but not the pump and a pressure of 400Torr was allowed to accumulate in the manifold. The manifold was then opened to section A and the counting cell (Figure 4.2.1). Counts were accumulated for 300s periods, at intervals of 15 min., simultaneously from GM1 and GM2. After reaction was complete, the counting cell was opened to the vacuum pump and any drop in count rate was recorded.

4.4 INTERACTION OF HALOGEN CONTAINING REAGENTS WITH α AND γ-ALUMINAS

4.4.1 EFFECT OF α-ALUMINA AND γ-ALUMINA ON SODIUM HYPOCHLORITE DECOMPOSITION.

Aliquots ($25cm^3$) of NaOCl solution were pipetted into 3 small conical flasks containing magnetic stirrer bars. The pH of each solution was reduced to 8.5 using glacial acetic acid. α-Alumina (0.5g was added to one sample and γ-alumina (0.5g) was added to another. The third sample was used as a control solution. The samples were made airtight and stirred to ensure even distribution of the acid.

Samples ($0.001cm^3$) of each solution were taken at regular intervals, using a micropipette, and analysed by UV/visible spectroscopy. The sample size was increased as the concentration of OCl^- anion in the solutions became difficult to detect. Absorbances were corrected to allow for the effect of the alumina present in the aliquots. The absorbances were matched to concentrations per $100cm^3$ using an experimentally determined calibration (Section 2.2.3). These values were converted into molarities ($mol.dm^{-3}$) for the bulk solutions.

4.4.2 ADSORPTION OF [^{36}Cl]-LABELLED DICHLORINE, EVOLVED FROM SODIUM HYPOCHLORITE, ON α-ALUMINA AND γ-ALUMINA

A) ADSORPTION ON α-ALUMINA

A quantity of α-alumina (1.09g) was placed in a glass reaction vessel, degassed on a Pyrex vacuum line, and calcined for 8 hours at about 523K using a cylindrical surround furnace. The glass reaction vessel was then transferred to the counting cell and the α-alumina was decanted into the appropriate compartment of the reaction boat. This process was carried out without the alumina coming into contact with the air, using the procedure shown in Figure 4.4.1..

[^{36}Cl]-Labelled dichlorine was evolved from NaOCl solution as described in Section 4.3.3. A larger quantity of HCl ($3cm^3$) was added to encourage rapid evolution of Cl_2

gas. Once a significant pressure had built up in manifold 1, the counting cell was opened to the manifold. Counts were taken for 500 second periods at intervals of 15 minutes, simultaneously from GM1 and GM2. Counts were corrected for background radiation and intercalibration ratio.

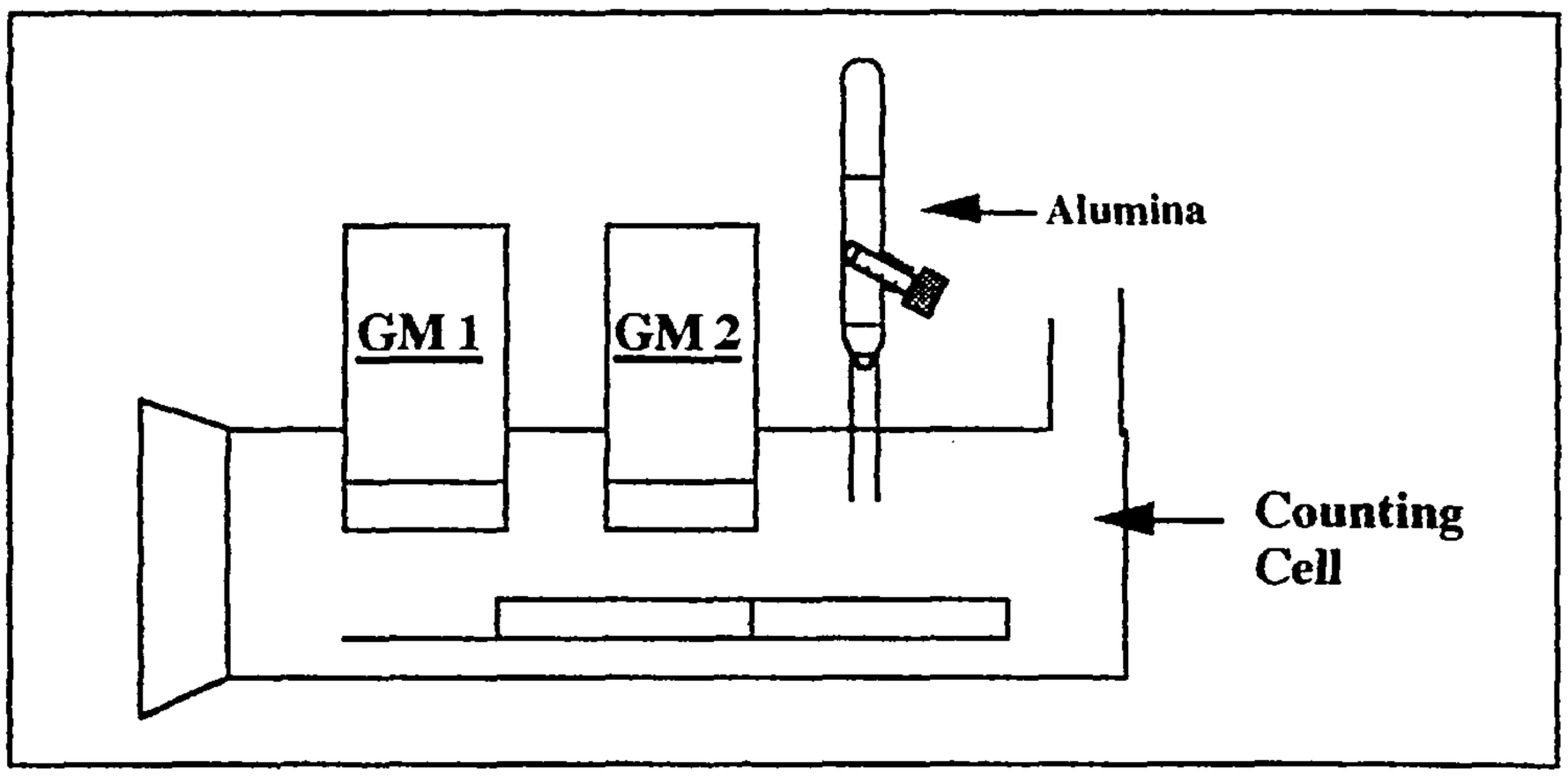

Figure 4.4.1: Transferance of Alumina to the Counting Cell

B) ADSORPTION ON γ-ALUMINA

The light, voluminous nature of the γ-alumina (0.1g) made it impossible to use the same quantity as was employed in the α-alumina experiment. The calcination and adsorption experiment were carried out in an identical manner to that described in section 4.4.2 A).

4.4.3 ADSORPTION OF [^{82}Br]-LABELLED DIBROMINE ONTO α-ALUMINA

[^{82}Br]-Labelled dibromine was produced from [^{82}Br]-labelled ammonium bromide (NH_4Br) by reaction with H_2SO_4 *in vacuo*. Neutron irradiations, ^{81}Br (n,γ) ^{82}Br, were carried out in the Scottish Universities Reactor Research Centre, East Kilbride, with a neutron flux of 3.6×10^{12} neutron $cm^{-2}s^{-1}$ for 3h. The activity of the [^{82}Br]-labelled NH_4Br was ca. 100mCi. Labelled solids were transferred to Glasgow ca. 24h after irradiation to allow decay of short-lived isotopes.

To prepare [^{82}Br]-labelled dibromine, solid NH_4Br (0.5g, BDH, analytical grade) and the [^{82}Br]-labelled NH_4Br (2mg) were placed in a pressure equilibrated vessel and

H_2SO_4 (5cm^3, Fisons, general purpose) was allowed to drip slowly onto this mixture. The vessel was connected to a vacuum system (0.01Torr) with two storage vessels attached. The [^{82}Br]-labelled dibromine which was liberated was vacuum distilled into the first storage vessel using liquid nitrogen (77K) and was allowed to reach 263K in a dry ice/dichloromethane slush bath. The storage vessel was degassed to remove any hydrogen bromide (HBr) or sulphur dioxide (SO_2) impurities. The dibromine was distilled into the second storage vessel which contained phosphorus (v) oxide and was stored at 77K until required.

[^{82}Br]-Labelled Br_2 uptake on α-alumina (1.3g) used a thin glass, double-limbed Pyrex counting vessel (Figure 2.3.3) with a central stopcock allowing isolation of one limb from the other. [^{82}Br]-labelled Br_2 (0.082mmol) was introduced into one limb and counted, before opening the central stopcock and measuring uptake on the degassed, calcined alumina in the other limb. Both limbs were counted alternately until uptake ceased. At this point, the contents were degassed and any [^{82}Br]-activity retained on the alumina was quantified.

4.5 RESULTS

4.5.1 IDENTIFICATION OF PRODUCTS FROM THE REACTION OF DICHLORINE WITH GALLIUM ARSENIDE

Dichlorine reacted overnight with GaAs to give a yellow viscous liquid. If any of the GaAs wafer remained, this liquid proved difficult to separate into individual components. In the absence of any residual GaAs, after reaction with excess dichlorine, the yellow liquid was separated into two components by careful and prolonged vacuum distillation. A colourless liquid and a white crystalline solid were obtained. The most probable identities of these products were considered to be arsenic trichloride ($AsCl_3$, melting point 257K) and gallium trichloride (Ga_2Cl_6, melting point 351K) respectively.

Some controversy surrounds the identification of both these species by vibrational spectroscopy. $AsCl_3$, $GaCl_3$ and Ga_2Cl_6 have been studied extensively and their spectra are well documented. However, most authors disagree with one another on some aspect of the interpretation. The study of species in different phases and the possible presence of hydrolysis products complicates the literature further.

Gallium trichloride has been studied as the monomer ($GaCl_3$) at high temperature[69] and as the dimer (Ga_2Cl_6) in a Nujol mull, solution and as a vapour[70]. Balls et al[71] reported a comprehensive study of the vibrational spectrum of the solid dimer in 1967. Their interpretation was challenged by Beattie et al[70], who undertook a combined IR/Raman study of the dimer, also in 1967. Beattie followed this with a study of the monomer, in collaboration with J.R. Horder, in 1969[72]. There were apparently no significant new developments on the subject until a study by Sjøgren et al in 1984[69]. This most recent study is also the most extensive, listing 15 bands in all. A comparison of the IR bands in all three studies of the dimer is given in Table 4.5.1.

Intensity Maxima (ν_{max}) / cm^{-1}			
Sjøgren et al[69]	**Beattie et al[70]**		**Balls et al[71]**
vapour	**vapour**	**solid**	**solid**
619w			609w
590w			
565w	548mw		
530w			
475vs	477s	464s	466s
453sh			
415m			420s
398s	400ms	390s	394vs
341vw			365w
309m	310ms	{300s	303s
278vs	280s	broad	274vs
201vw	202w	obscured}	
170vw	170w sh		
154w	155m	156m	
120m	120ms	114s	123s
			73m

Table 4.5.1: Literature Values for the Analysis of Ga_2Cl_6 by Infrared Spectroscopy. (w = weak, s = strong, m = medium, v = very and sh = shoulder)

In general, Sjøgren's paper agrees with Beattie's with regard to assignment of the strongest bands. Sjøgren finds five extra, weak bands not observed by Beattie, which he attributes to combination bands from weaker vibrational modes. There is good evidence that this explanation also applies to some weaker bands assigned by Beattie as residual monomer ($GaCl_3$) bands. Most of the assignments given by Balls et al. are disputed by both Beattie and Sjøgren, although most of the stronger bands appear at the same wavenumbers. Table 4.5.2 lists the bands which were observed in the spectrum for this work and compares them with the values and assignments given by Beattie and

Sjøgren.

Intensity Maxima (ν_{max}) / cm^{-1}			Symmetry Assignment
Sjøgren et al[69]	Beattie et al[70]	This Work	
vapour	solid	solid	
		608	
475	464	468	$\upsilon_8\ B_{1u}$
398	390	395	$\upsilon_{16}\ B_{3u}$
309	{300 broad	304	$\upsilon_{13}\ B_{2u}$
278	obscured}	278	$\upsilon_{17}\ B_{3u}$

Table 4.5.2: Symmetry Assignments for Vibrational Fundamentals in Ga_2Cl_6

The band at 608 cm^{-1} was not reported by Beattie but a band at 609 cm^{-1} was reported by Balls et al in earlier work. There is a possibility that these bands correspond to that at 619 cm^{-1} in the vapour phase spectrum of Sjøgren et al. This is assigned as a weak combination band ($\upsilon_2+\upsilon_{13}, A_{1g}+B_{2u}$).

Another possibility which must be considered is that some of the bands observed in the spectra may be due to hydrolysis products from the reaction of Ga_2Cl_6 with water or other contaminants. This is especially probable in the case of the very weak band at 608cm^{-1}, which is the only controversial band observed in this work. However, any hydrolysis of Ga_2Cl_6 would immediately yield distinctive HCl bands in the IR spectrum. No evidence of such bands was found. A Raman spectrum of the white crystalline solid was attempted but the sample decomposed under the laser beam.

It is clear from this discussion that the study of Ga_2Cl_6 is not a simple matter. However, given that the interpretation and assignments of Sjøgren and Beattie appear to be reliable, the IR analysis in this project clearly identifies the white crystalline solid from the reaction of dichlorine with GaAs as dimeric Ga_2Cl_6. All five of the bands observed in this work were also observed in a Nujol mull of commercial Ga_2Cl_6 (Alfa, Johnson Matthey).

The analysis of the colourless liquid product by IR and Raman spectroscopy was less

complicated than the identification of the solid. The assignment of bands in both the IR and Raman spectra was based on IR studies by Davis and Oetjen[73] in 1958 and Lunelli et al.[74] in 1983. This was possible because all 4 vibrational fundamentals in the pyramidal (C_3v) $AsCl_3$ are both IR and Raman active. Table 4.5.3 shows that the authors cited above find bands in approximately the same regions for υ_1, υ_2 and υ_4. It is important to bear in mind the values cited for Lunelli et al are band centres for spectral features which are broad and are complicated by combination bands etc not due to the fundamental vibrations. Also, Lunelli et al attempted to assign fundamentals separately according to isotopomer, but could only find all four separate fundamentals for $As^{35}Cl_3$. These are the values shown in the table.

The one band in dispute is υ_3, which is assigned as 306.7cm^{-1} by Davis and Oetjen and at 396.0cm^{-1} by Lunelli et al. Lunelli et al do not explain this disagreement with the previous authors, but their detailed list of intensity maxima shows that, in fact, they only observed a very weak band in this region. In retrospect, it is perhaps prudent to give more credence to the assignments of Lunelli et al since their study is by far the most detailed and has the advantage of higher resolution spectroscopy combined with better purification and sample handling techniques. It is certainly possible that the band observed by Davis and Oetjen at 307cm^{-1} may have been due to an hydrolysis product or impurity and that any band above 390cm^{-1} may have been masked by the very strong υ_1 band at 412cm^{-1}.

Symmetry Assignment	Intensity Maxima (ν_{max}) / cm^{-1}	
	Davis & Oetjen[73]	Lunelli et al[74]
υ_1 A_1	411.8 ± 1.0	423.0
υ_2 A_1	193.6 ± 0.5	193.5
υ_3 E	306.7 ± 0.5	396.0
υ_4 E	155.3 ± 0.7	152.0

Table 4.5.3: Literature Values for the Analysis of $AsCl_3$ by Infrared Spectroscopy

In this project, only two strong bands were observed in the infrared analysis, at 412cm^{-1} and 371cm^{-1}. However, a satisfactory Raman spectrum was obtained and is shown in Figure 4.5.1. The results of both analyses are given in Table 4.5.4. The values

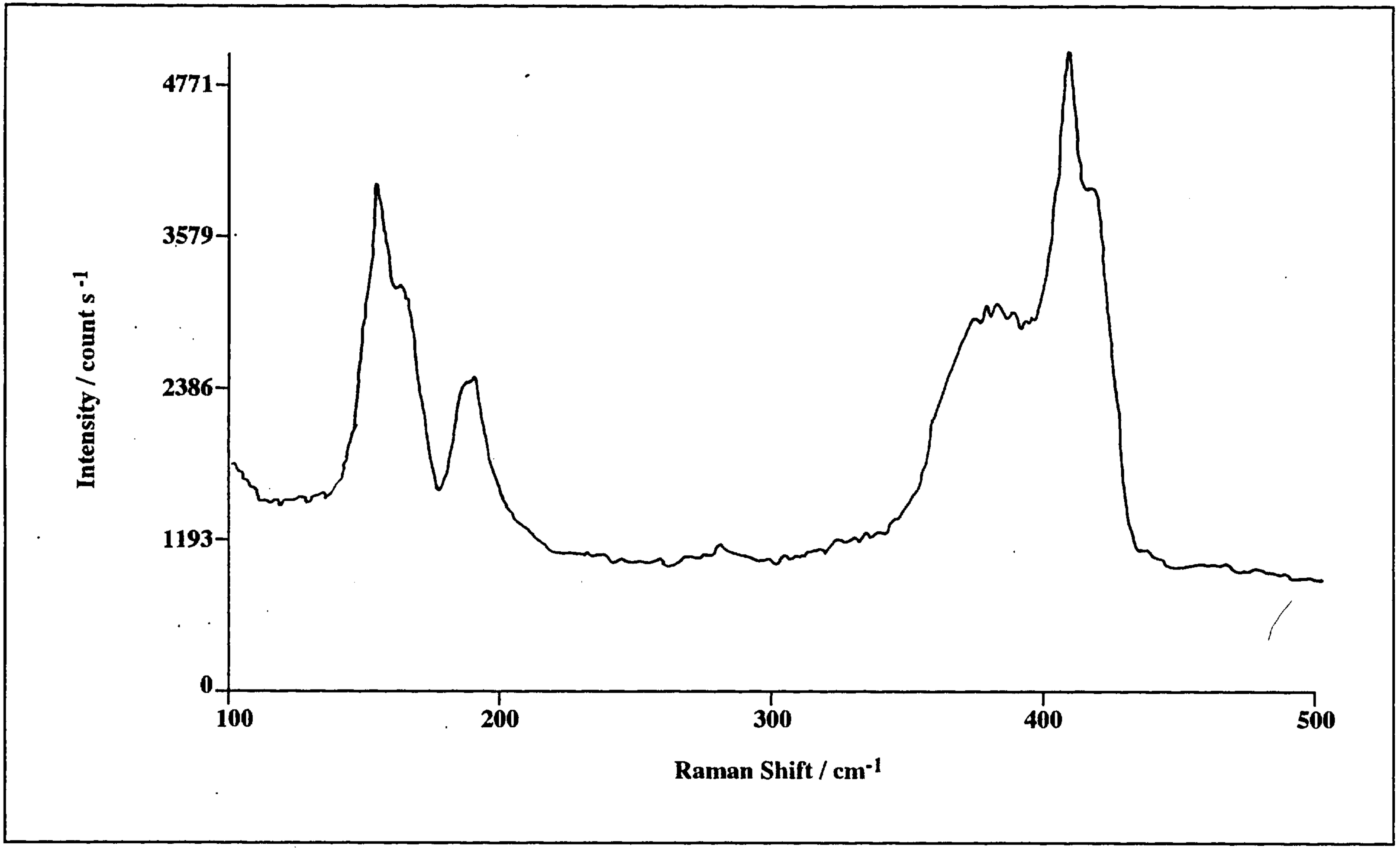

Figure 4.5.1: Raman Spectrum of Colourless Liquid from the Reaction of Dichlorine with GaAs

correlate closely enough with those of previous authors to allow a positive identification of the liquid product as $AsCl_3$. It is interesting to note the broad band at 370cm^{-1}, which overlaps with the $\upsilon_1(A_1)$ band at 406cm^{-1}. It is likely that this peak represents the $\upsilon_3(E)$ vibration, but it is not well resolved.

Symmetry Assignment	Intensity Maxima (ν_{max}) / cm^{-1}	
	Infared Spectrum	Raman Spectrum
$\upsilon_1 A_1$	412	406 414sh
$\upsilon_2 A_1$		191
$\upsilon_3 E$	371	370 broad
$\upsilon_4 E$		156 164sh

Table 4.5.4: Results for the Analysis of $AsCl_3$ by IR and Raman Spectroscopy

Reference spectra taken from a commercial sample of $AsCl_3$ (Janssen Chimica) confirmed the presence of all the bands observed in the Raman and the IR.

4.5.2 Adsorption of [^{36}Cl]-Labelled Dichlorine onto Gallium Arsenide

Having established that dichlorine reacts with GaAs to produce Ga_2Cl_6 and $AsCl_3$ the reaction was repeated using [^{36}Cl]-labelled Cl_2 gas. This experiment was designed to enable the behaviour of the labelled reactant and resultant products on the wafer surface to be traced and to predict the nature of any product layer which might form. It would be predicted, from previous radiotracer experiments using [^{82}Br]-labelled Br_2 on GaAs[60], that the solid product (Ga_2Cl_6) would be retained on the surface after pumping out the counting cell. The more volatile product (in this case $AsCl_3$) would be expected to be pumped away.

The activity of the [^{36}Cl]-labelled Cl_2 gas produced did not allow a continuous uptake to be measured, since a 30 minute counting period was required to accumulate a statistically acceptable number of counts. For this reason, the [^{36}Cl]-labelled Cl_2 was added in aliquots and the gas phase and solid phase counts were recorded over a 30 minute period before addition of the next aliquot.

Exposure of the GaAs wafer to [^{36}Cl]-labelled Cl_2 gas resulted in the detection of radioactivity on the surface after about an hour. This was followed by a gradual uptake, which continued for more than an hour after the final aliquot had been added. After addition of the second aliquot, a yellow, viscous liquid began to form on the wafer surface. This surface layer increased as further aliquots were added.

The count rates for solid and gas (corrected for background radiation and intercalibration ratio) for the uptake of radiolabelled dichlorine on GaAs are given in Table 4.5.5. They are correlated with initial pressure of gas added and the pressure drop over the measurement period. The * and + represent condensation of chlorine back into the reservoir and opening of the system to a vacuum pump, respectively.

TIME/ min	PRESSURE/ Torr	PRESSURE DROP/ Torr	SOLID / count s^{-1}	GAS / count s^{-1}
0	10	0	0	0.43
30	30	2	0	1.41
61	45	9	1.00	1.66
93	50	22	2.01	1.77
168		5	3.27	1.12
199		2	3.63	0.92
233		0	3.68	0.88
267	*		3.46	0.32
298	+		3.50	0.23

Table 4.5.5: Count Rates for the Uptake of ^{36}ClCl on GaAs

The pressure recorded as each aliquot was added dropped significantly over the 30 minute counting period. It is, therefore, difficult to ascertain exactly how many mmols of Cl_2 were taken up by the GaAs during each stage of the experiment. After about 4 hours, the reaction was complete and solid and gas counts began to stabilise. The total amount of Cl_2 used in the experiment was 62Torr (3.28mmol). The pressure fell to 19Torr after the reaction was apparently complete. In total, this means that about 2.28mmol of Cl_2 had been adsorbed by the GaAs.

Figure 4.5.2 presents the data in terms of total counts accumulated in the 30 minute counting period, corrected for background counts and intercalibration ratio. After about 5 hours, the counting cell was opened to the vacuum pump to remove any volatile species from the product mixture. Table 4.5.5 and Figure 4.5.2 show that, apart from

the removal of excess gas from above the wafer surface, there is no significant drop in activity on opening the counting cell to the pump. This result is surprising in that it contradicts observations made from the reaction of Br_2 with GaAs. $AsCl_3$ is even more volatile than its bromine counterpart $AsBr_3$[9] and so would be expected to pump away immediately on degassing the counting cell. Therefore, there must be some unique property of the GaAs/Cl_2 system which stops the volatile component being removed from the product layer.

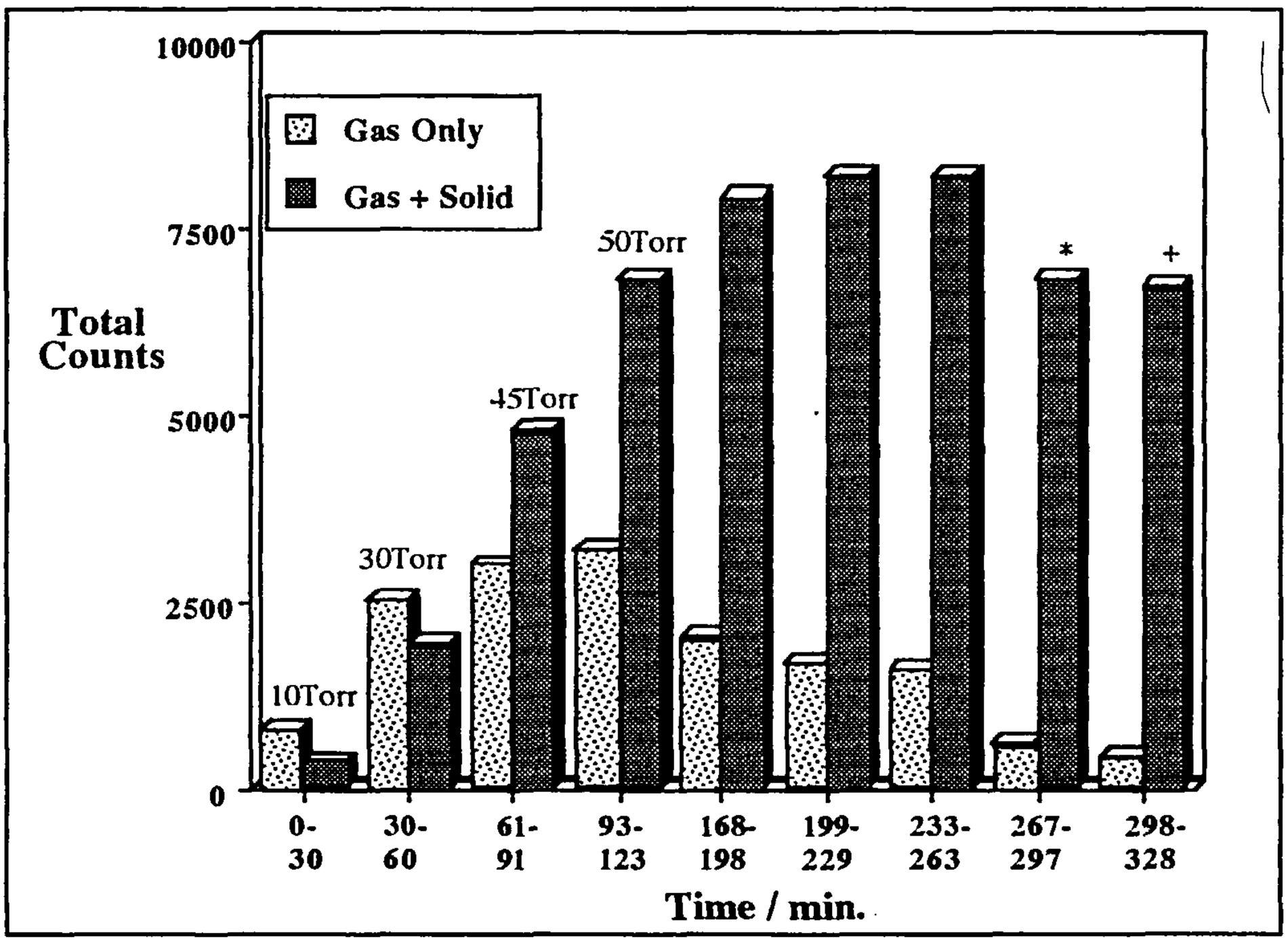

Figure 4.5.2: Total Counts for the Uptake of $^{36}ClCl$ on GaAs

4.5.3 Adsorption of [^{36}Cl]-Labelled Dichlorine, Evolved from Sodium Hypochlorite, onto Gallium Arsenide

This experiment was designed to confirm the results described in Section 4.5.2 using a system which more closely resembles the GaAs/NaOCl etching system. The experiment was designed to fulfil two important functions. Firstly, it was necessary to confirm that dichlorine evolved from acidified sodium hypochlorite solution would interact with the GaAs surface. Secondly, direct evolution of [^{36}Cl]-labelled Cl_2 from the NaOCl solution yielded a high activity sample of the gas, allowing continuous monitoring of the uptake.

Figure 4.5.3 shows the results of [^{36}Cl]-labelled Cl_2 uptake on GaAs, on evolution of labelled dichlorine from an acidic NaOCl reservoir. The values plotted are corrected for background radiation and intercalibration ratio. The daggers represent the count rates after opening the system to the vacuum pump.

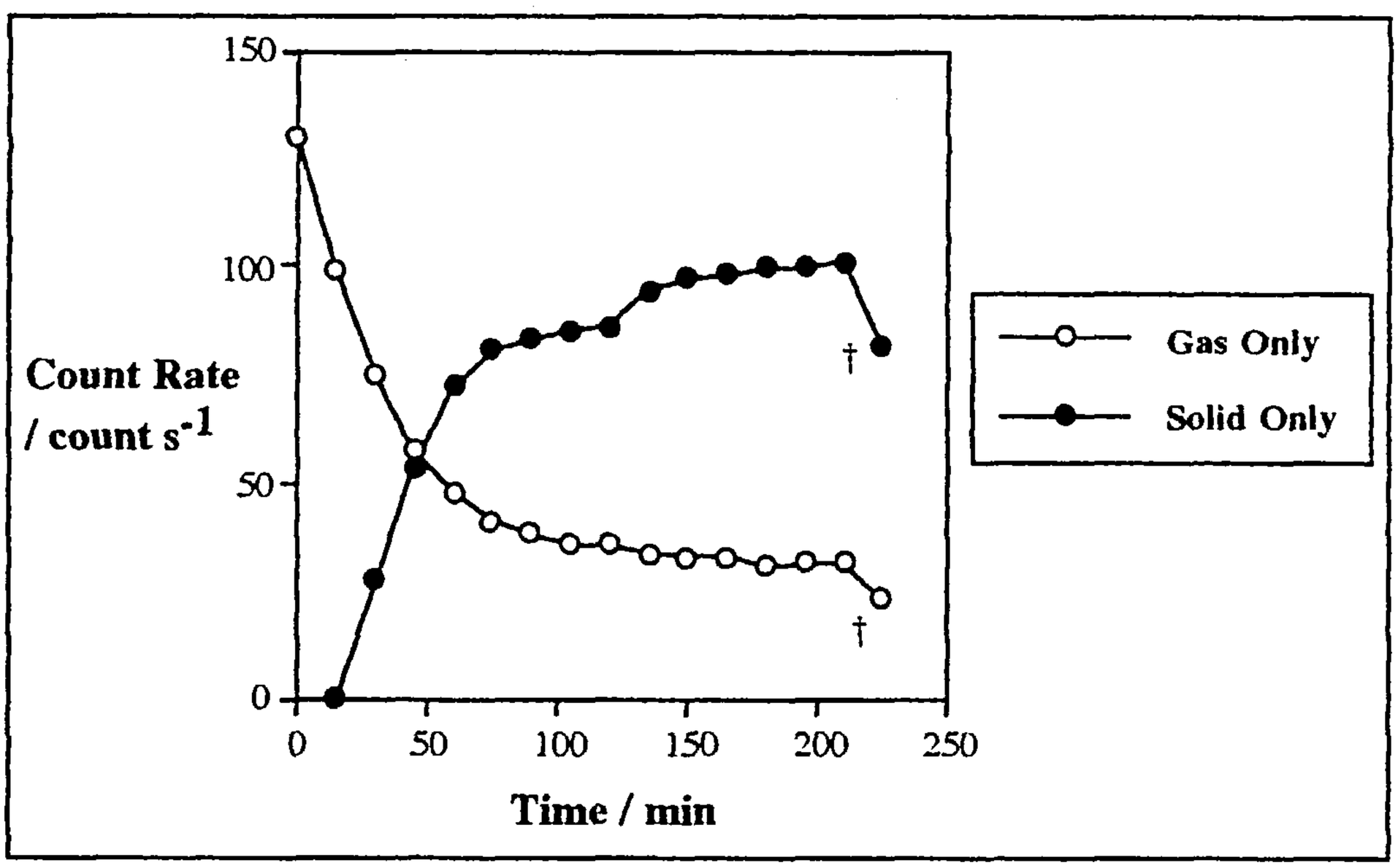

Figure 4.5.3: Uptake of ^{36}ClCl, Evolved from NaOCl, on GaAs

The pattern in this graph reflects the results obtained from experiment 4.5.2 and confirms the fact that dichlorine, evolved from NaOCl at low pH, is active in etching GaAs. The behaviour of the system on opening to vacuum is also reproducible, yielding no significant drop in count rate relative to total counts and the drop in gas phase count rate.

4.5.4 Effect of α-Alumina and γ-Alumina on Sodium Hypochlorite Decomposition.

The results of UV/visible spectroscopic analysis of acidic solutions of NaOCl, containing α-alumina and γ-alumina, are shown graphically in Figure 4.5.3. The three decomposition curves show that the presence of alumina in the solution has a small but instantaneous effect on the NaOCl composition. The concentration of $[OCl]^-$ anion was determined from a calibration of the $[OCl]^-$ peak intensity at $\lambda_{max} = 292nm$.

At time zero, immediately on addition of the acetic acid, the sample containing γ-alumina shows a smaller concentration of $[OCl]^-$ anion than the one containing α-alumina. Both samples containing alumina show less $[OCl]^-$ present than in the control sample. This trend continues until decomposition is complete after about 2.5 hours. Thus, the aluminas have a small promoting effect on the decomposition of $[OCl]^-$. γ-Alumina is a more effective promoter than α-alumina.

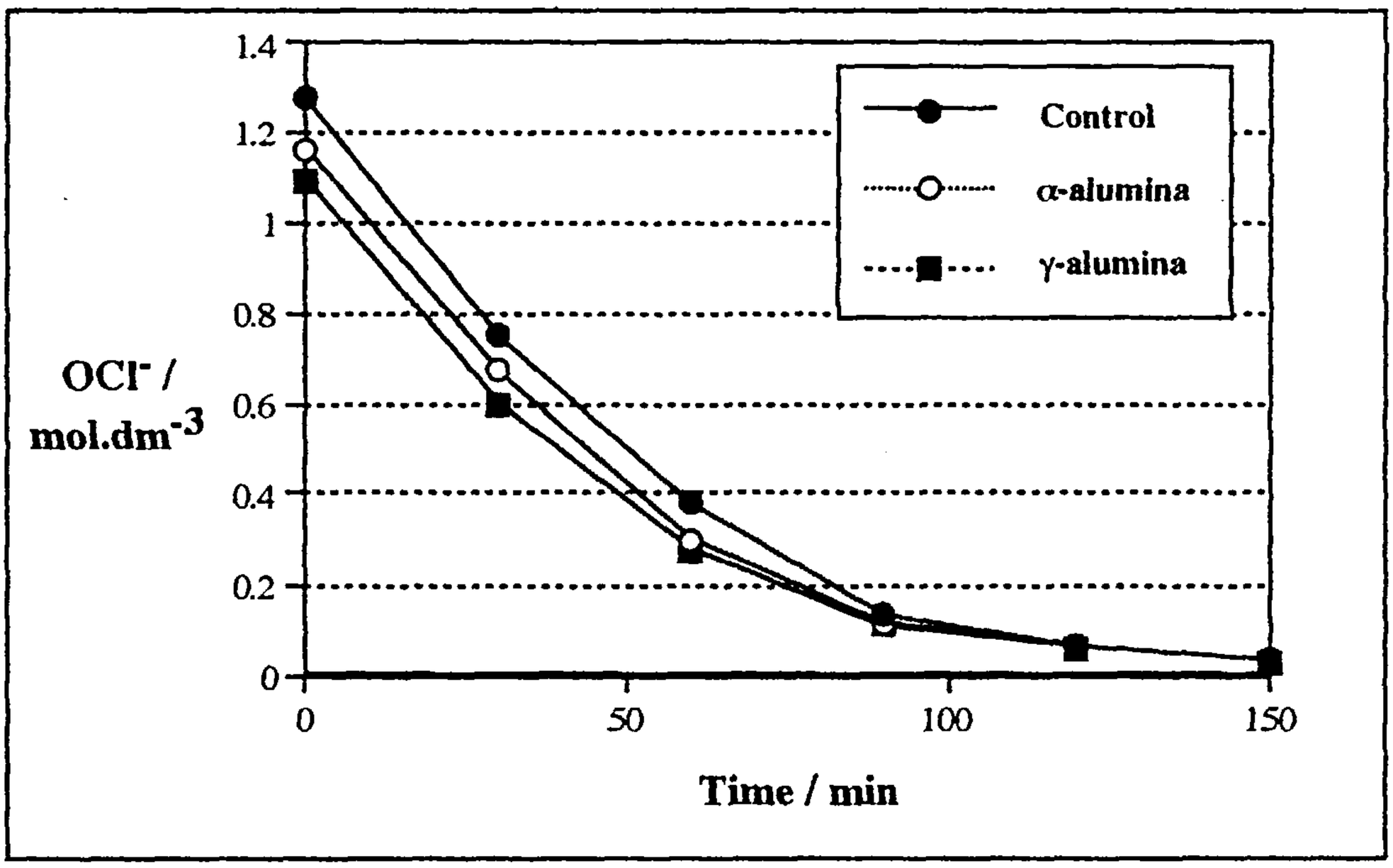

Figure 4.5.3: Decomposition of Hypochlorite in the Presence of Aluminas

4.5.5 Adsorption of [^{36}Cl]-Labelled Dichlorine, Evolved from Acidified Sodium Hypochlorite Solution, on α-Alumina and γ-Alumina

The exposure of α-alumina (1.09g) to [^{36}Cl]-labelled Cl_2 (4.66mmol), did not lead to any detectable change in [^{36}Cl] count rate from vapour or solid, for the duration of a 2.5h experiment (Figure 4.5.4). Both count rates returned to their original background value when the [^{36}Cl]-labelled Cl_2 was removed from the system. Any interaction between the Cl_2 evolved and α-alumina can therefore be deemed negligible.

Exposure of γ-alumina (0.1g) to [^{36}Cl]-labelled Cl_2 (7.94mmol), led to a gradual decrease in the [^{36}Cl] activity of the vapour, but no corresponding increase in the solid phase count rate. A drop in vapour phase count rate of 19.7% suggests that Cl_2 is

adsorbed onto the alumina surface. The lack of any detectable increase in the activity of the solid may be attributable to self-absorption of β^- particles in the bulk solid. The adsorption of Cl_2 gas onto calcined γ-alumina has been observed in previous work in this department[67] and so a significant increase in solid phase count rate, with a concomitant decrease in gas phase count rate, would have been predicted. However, it should be noted that the [^{36}Cl]-labelled Cl_2 evolved from acidified NaOCl solution would be very 'wet' i.e. would also contain water vapour, leading to hydration of the γ-alumina surface and hence poor adsorption of the halogen. This phenomenon reflects the *in situ* polishing situation, where NaOCl solution at pH<8 is more likely to hydrate the alumina than chlorinate it. Thus, any interaction between γ-alumina and the active etchant in a low pH NaOCl polishing solution is likely to be negligible.

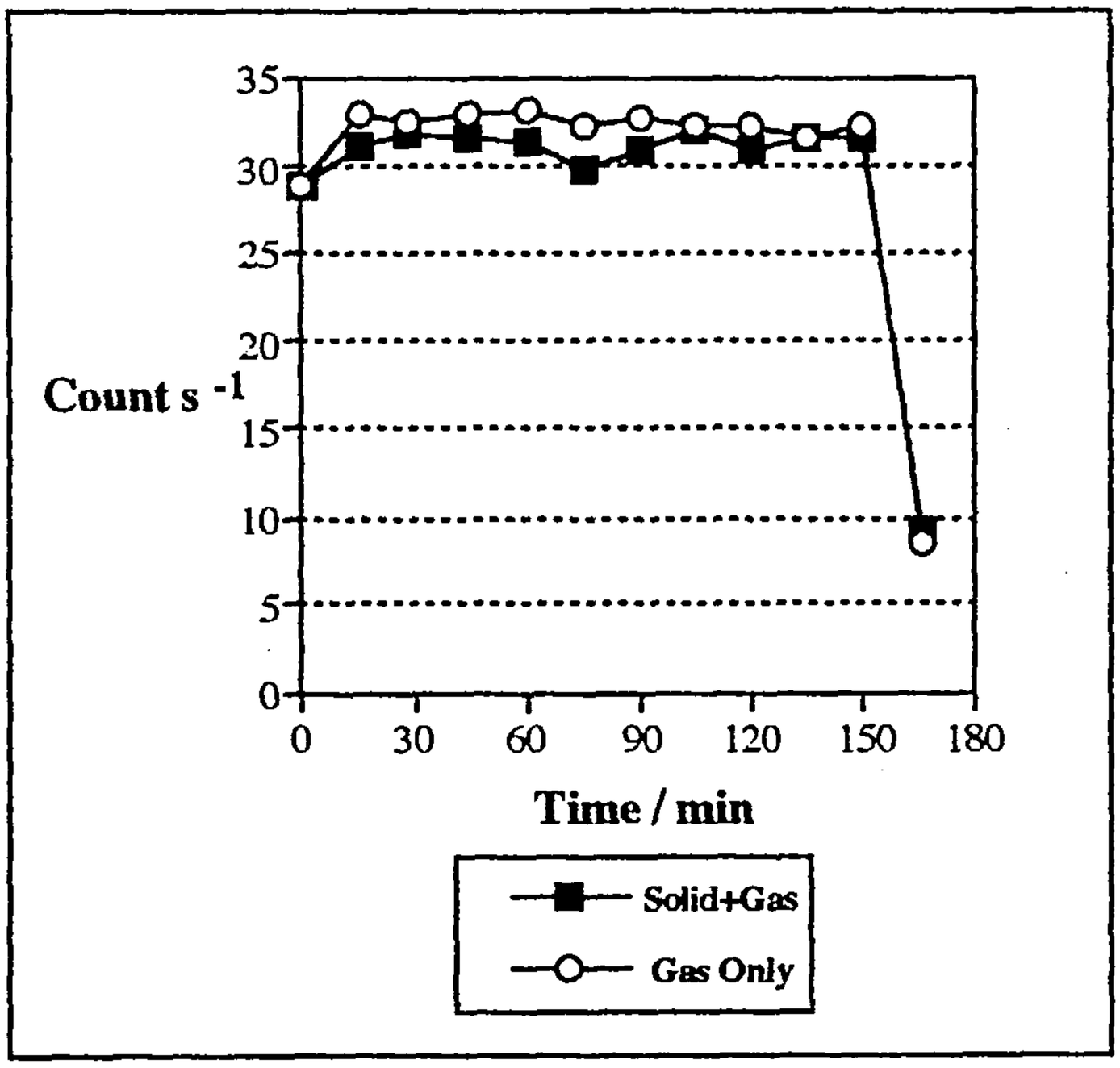

Figure 4.5.4: Interaction of ^{36}ClCl, Evolved from NaOCl, with α-Alumina

4.5.6 ADSORPTION OF [^{82}Br]-LABELLED DIBROMINE ONTO α-ALUMINA AND γ-ALUMINA

The results obtained from the exposure of α-alumina (1.3g) to [^{82}Br]-labelled Br_2 (0.082mmol) are given in Table 4.5.3. The asterisk represents the count rate obtained from the ^{82}BrBr in the solid state. The table shows that the count rate detectable in the alumina limb remained approximately constant at 4.5-4.7 count s^{-1} and was not

significantly higher than that detectable in the bromine limb. If the α-alumina had adsorbed all the available Br_2, a count rate of 40 count s^{-1} would have been detectable in the alumina limb and the count rate in the bromine limb would have dropped during the experiment. Hence, there was no significant uptake of Br_2 onto the α-alumina.

Similar experiments using [^{82}Br]-labelled Br_2 (1.36mmol) on γ-alumina (0.065g) in this department[75] have shown a significant interaction between Br_2 and γ-alumina. This was characterised by a gradual increase in the count rate of the solid, which reached a plateau after approximately 120 hours. Specific uptake, determined for the specific count rate of [^{82}Br]-labelled Br_2 and the solid count rate after 119h, was 17.1 mg atom Br (g γ-alumina)$^{-1}$.

Time / h	Dibromine Limb / count s^{-1}	Alumina Limb / count s^{-1}
0	41.4*	----
0.08	-----	4.69
0.17	-----	4.73
0.25	-----	4.81
0.33	-----	4.87
0.50	-----	4.65
0.75	4.13	----
1.00	----	4.51
1.50	----	4.61
1.75	3.88	----
2.00	----	4.72
2.77	-----	4.74
5.00	-----	4.59
5.38	3.47	-----
6.13	-----	4.66
6.97	-----	4.72

Table 4.5.3: Interaction of ^{82}BrBr with α-Alumina

4.6 DISCUSSION

The experiments detailed in this chapter have confirmed many of the hypotheses made in Chapters One to Three and form the basis for a new understanding of how NaOCl operates as an etching and polishing reagent.

Radiotracer experiments have shown that Cl_2 is evolved from aqueous NaOCl solutions at low pH and etches GaAs to produce a viscous product layer. Extensive analysis of this product by IR and Raman spectroscopy, combined with critical interpretation of the literature, have confirmed $AsCl_3$ and Ga_2Cl_6 as the components of this layer. Radiotracer experiments have also shown that the $AsCl_3/Ga_2Cl_6$ product mixture which forms on GaAs has unusual properties: $AsCl_3$ is volatile relative to Ga_2Cl_6 and its bromine counterpart $AsBr_3$ and so should be removed easily from an $AsCl_3/Ga_2Cl_6$ mixture by pumping (10^{-4} Torr). If this were the case, about 50% of the solid count rate in a $^{36}ClCl$/GaAs adsorption experiment (Section 4.5.3) should be removed when the system is opened to the pump. This is indeed the case in an $^{82}BrBr$/GaAs adsorption experiment[60]. However, the $AsCl_3/Ga_2Cl_6$ mixture does not separate easily by vacuum distillation or pumping and the separation is made even more difficult if some of the GaAs wafer is still present. This phenomenon implies some form of unique interaction between the chlorinated products which does not occur between $AsBr_3$ and Ga_2Br_6 and which is encouraged in some way by the presence of the GaAs substrate. The formation of complexes by gallium trichloride is well documented in the literature[76]. Although the existence of an electronic interaction between $AsCl_3$ and Ga_2Cl_6 is unlikely, it is impossible on the basis of this work to rule one out, or indeed to rule out a weak electronic interaction between the mixture and the GaAs itself. However, the properties of $AsCl_3$ as an effective covalent solvent are also well known[77], and this may account for the formation of a particularly stable product mixture.

The formation of a product layer on GaAs when it reacts with Cl_2 is an important consideration in the polishing of GaAs with NaOCl solution at low pH (<8). Figure 4.6.1 shows the surface of a GaAs wafer after etching in Cl_2 gas. The striations visible on the wafer surface indicate where liquid product has built up during reaction. hindering further reaction at these points on the surface. This passivation effect will also occur, to a lesser extent, in the polishing process before the chlorinated products are hydrolysed in the etchant solution. This phenomenon is likely to contribute to the high quality finish which can be achieved using low pH NaOCl solution on GaAs. The short-lived passivating layer modifies reaction sufficiently to prevent very vigorous reaction, producing a slow but very high quality polish. Such passivating layers have been identified in other polishing work and are thought to promote surface quality generally[78,79].

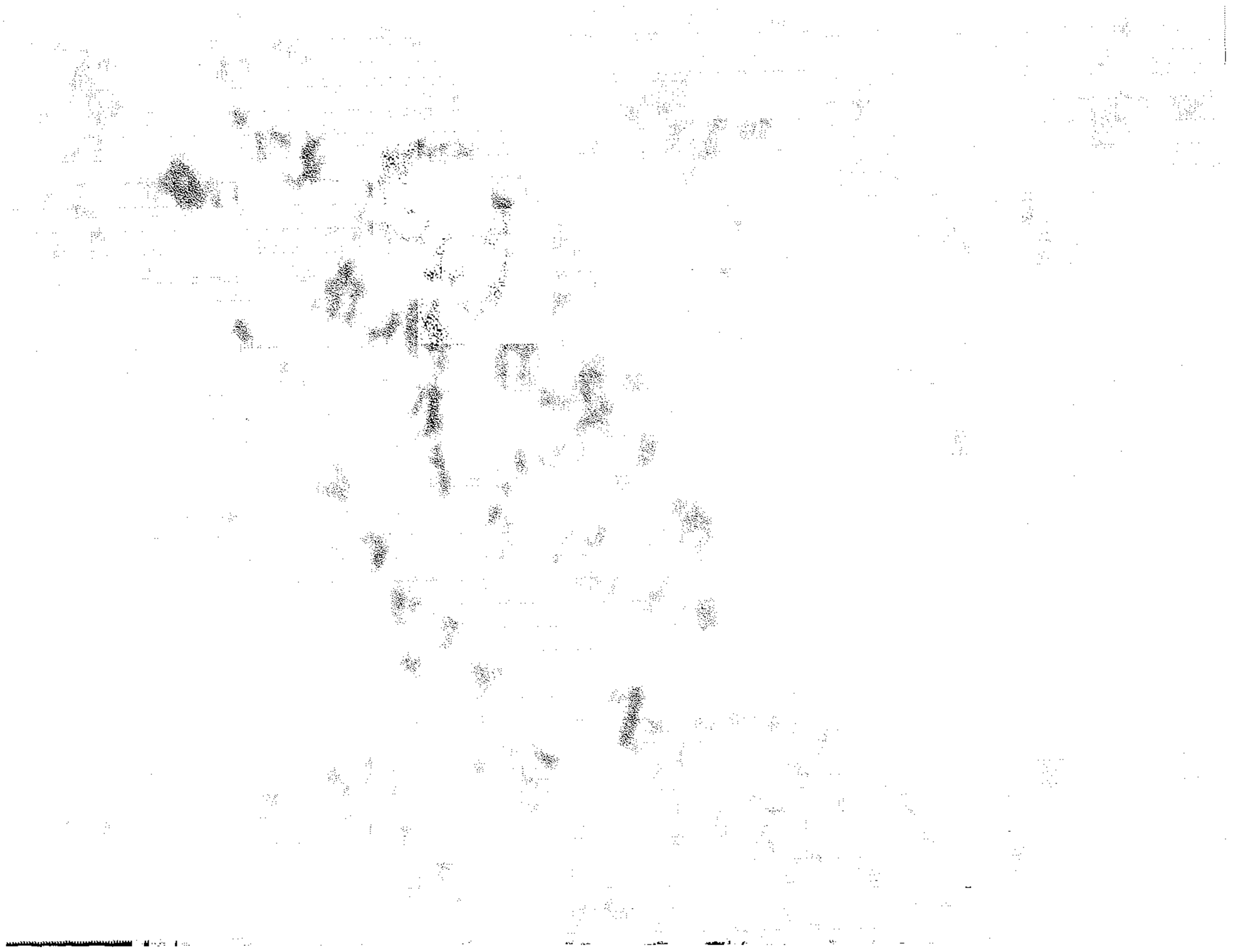

Figure 4.6.1: Electron Micrograph of a Glass Surface after Etching in Dichlorine Gas (Standard Procedure)

Experiments on α-alumina and γ-alumina have shown that they do interact to some extent with the halogen-containing reagents commonly used in polishing. The decomposition of NaOCl to Cl_2 in acid solution (Equations 4.6.1 and 4.6.2) is enhanced to a small extent by both α-alumina and γ-alumina.

$$[OCl]^- + H^+ \rightleftharpoons HOCl \qquad .....(4.6.1)$$

$$HOCl + Cl^- + H^+ \rightarrow Cl_2 + H_2O \qquad .....(4.6.2)$$

This effect is most visible in the case of γ-alumina and may be a consequence of the formation of acid sites on the alumina surface, providing an active surface for the reaction 4.6.1 to occur on. The effect of such an interaction would be expected to be very small, since reactions 4.6.1 and 4.6.2 will occur freely in solution. Dibromine and dichlorine were both adsorbed by γ-alumina but α-alumina showed no significant reaction with either Cl_2 or Br_2. These observations, using NaOCl solution and the

polishing process, since it produces positive effects with Br_2, Cl_2 and NaOCl etchants. However, the positive effects produced in the etchants by γ-alumina are very small relative to the advantages of α-alumina as an efficient abrasive. Any interaction between alumina and halogen in a polishing situation would also be greatly reduced by hydration of the alumina in an aqueous solution. For the purposes of this research, any chemical role of alumina abrasives during polishing with halogen-based reagents may be considered negligible and certainly secondary to their mechanical role as abrasives.

CHAPTER FIVE

MODIFIED BROMINE REAGENTS

5.1 INTRODUCTION

Dibromine is one of the most general reagents for the etching and polishing of semiconductors, for the reasons discussed in Chapter One (Section 1.4.1). One disadvantage in using Br_2 is that it often produces a surface which is dimpled in appearance, known as 'orange peel'. This phenomenon is, ironically, due to the effectiveness of Br_2 in etching materials such as GaAs. The etching reaction is so fast that the polishing pad cannot properly moderate the removal of material and an uneven surface results. An ideal etchant would be one which retains the generality of Br_2 but is gentler, so avoiding the orange peel effect.

This chapter describes the synthesis and use of various compounds for the etching and polishing of GaAs and CdTe. The strategy in this section of the work was to incorporate bromine (in various oxidation states) into organic molecules and to investigate the etching and polishing properties of the resultant compounds.

The compounds which were synthesised were chosen to provide different Br oxidation states and environments. Various ligand sizes and shapes were used to allow comparison of the moderating influence of different steric effects on the reactivity of the Br etchant in the compounds. Comparisons were made between bulky and smaller ligands and macrocycles were compared with aromatic and aliphatic ligands. Nitrogen-donor ligands such as quinoline were used to determine how easily reaction could be controlled using

pH and the reactivity of these compounds was compared with weaker oxygen-donor compounds.

Five ligands were chosen for use in these experimental etchant compounds and they are shown in Figure 5.1.1. Many of the compounds which were synthesised from these ligands were not previously documented and hence characterisation of the compounds was important. For some of the compounds conclusive characterisation of structure was not possible in the time available. However, in these cases similar literature precedents were used to make reasonable assumptions concerning structure. In addition to differences in the ligands employed, the compounds synthesised yielded bromine in its molecular form and also in positively and negatively charged forms. The range of compounds produced provided an overview of the many parameters which may influence the etching properties of an halogen in an organic environment.

5.2 Synthesis and Characterisation of Modified Bromine Reagents.

5.2.1 Bis(Quinuclidine) Bromonium Bromide

a) Background.

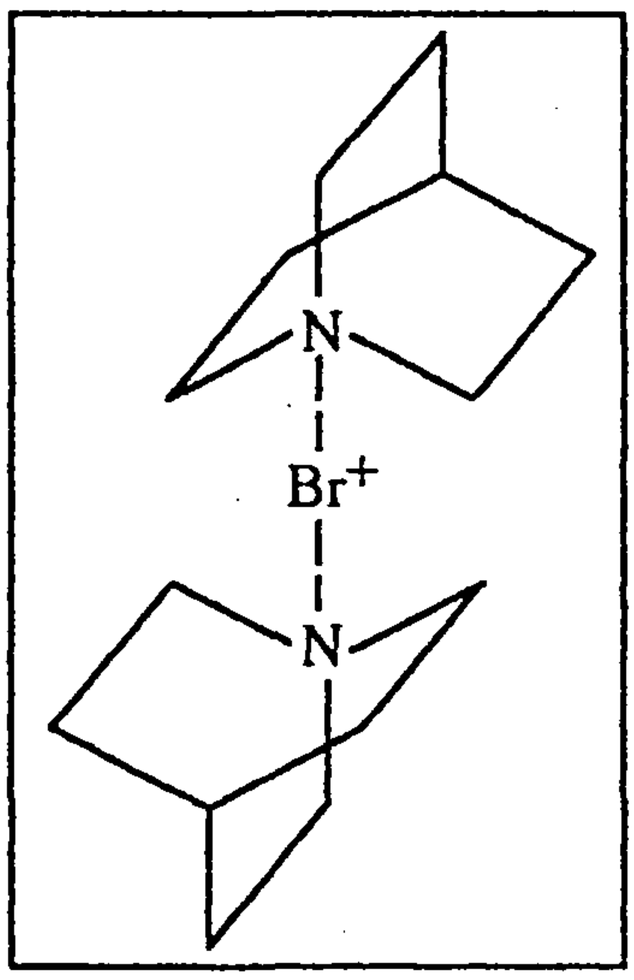

Figure 5.2.1: Bis(Quinuclidine) Bromonium Cation

This complex was first synthesised by Blair et al[43] as part of the preparation of the corresponding tetrafluoroborate (BF_4^-) salt. A crystal structure of the BF_4^- complex was obtained, but the bromide (or possibly tribromide) has not been well characterised. The

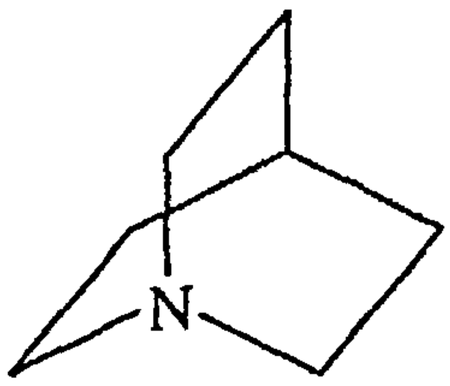

Quinuclidine

(Azabicyclo[2.2.2.]octane)

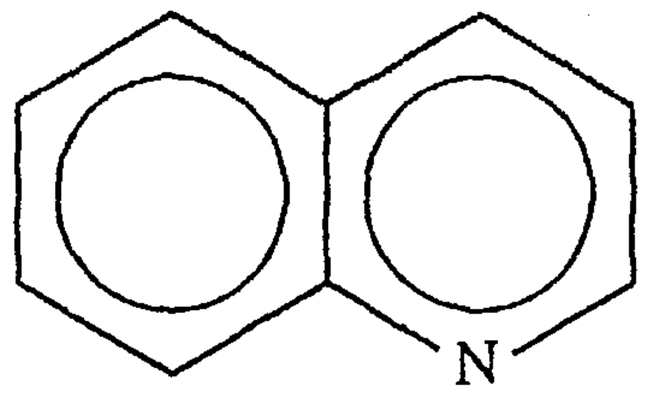

Quinoline

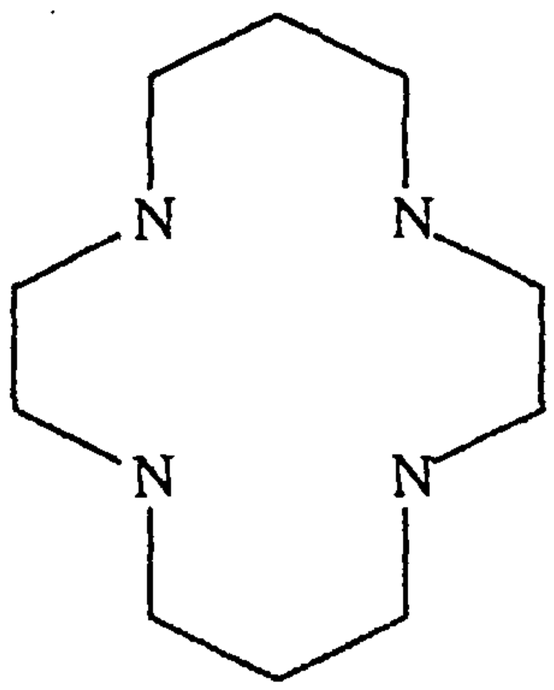

Cyclam

(1,4,8,11-Tetraazacyclotetradecane)

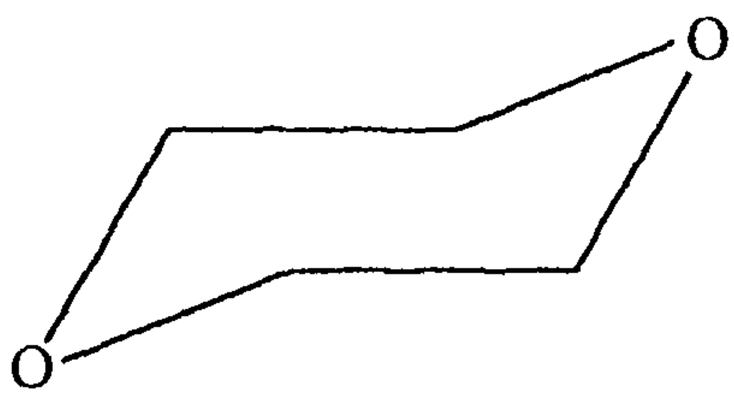

1,4 - Dioxane

(1,4-Dioxocyclohexane)

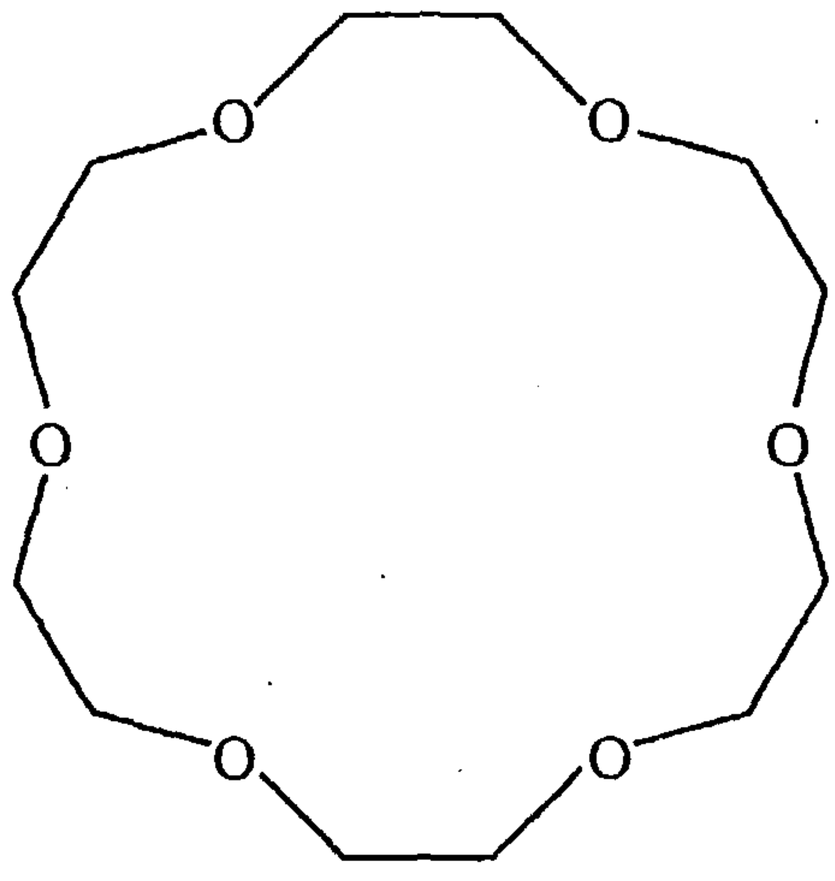

18 - Crown - 6

Figure 5.1.1: Ligands for Bromine Compounds

bromide compound prepared by Blair et al decomposed over the range 410K to 433K. The crystal structure of the tetrafluoroborate indicated a linear N-Br-N arrangement and staggered ring structure in the cation, as illustrated in Figure 5.2.1.

B) SYNTHESIS.

The preparation of this compound followed a similar method to that employed by Blair et al[43] in their paper, using the apparatus illustrated in Figure 5.2.2.

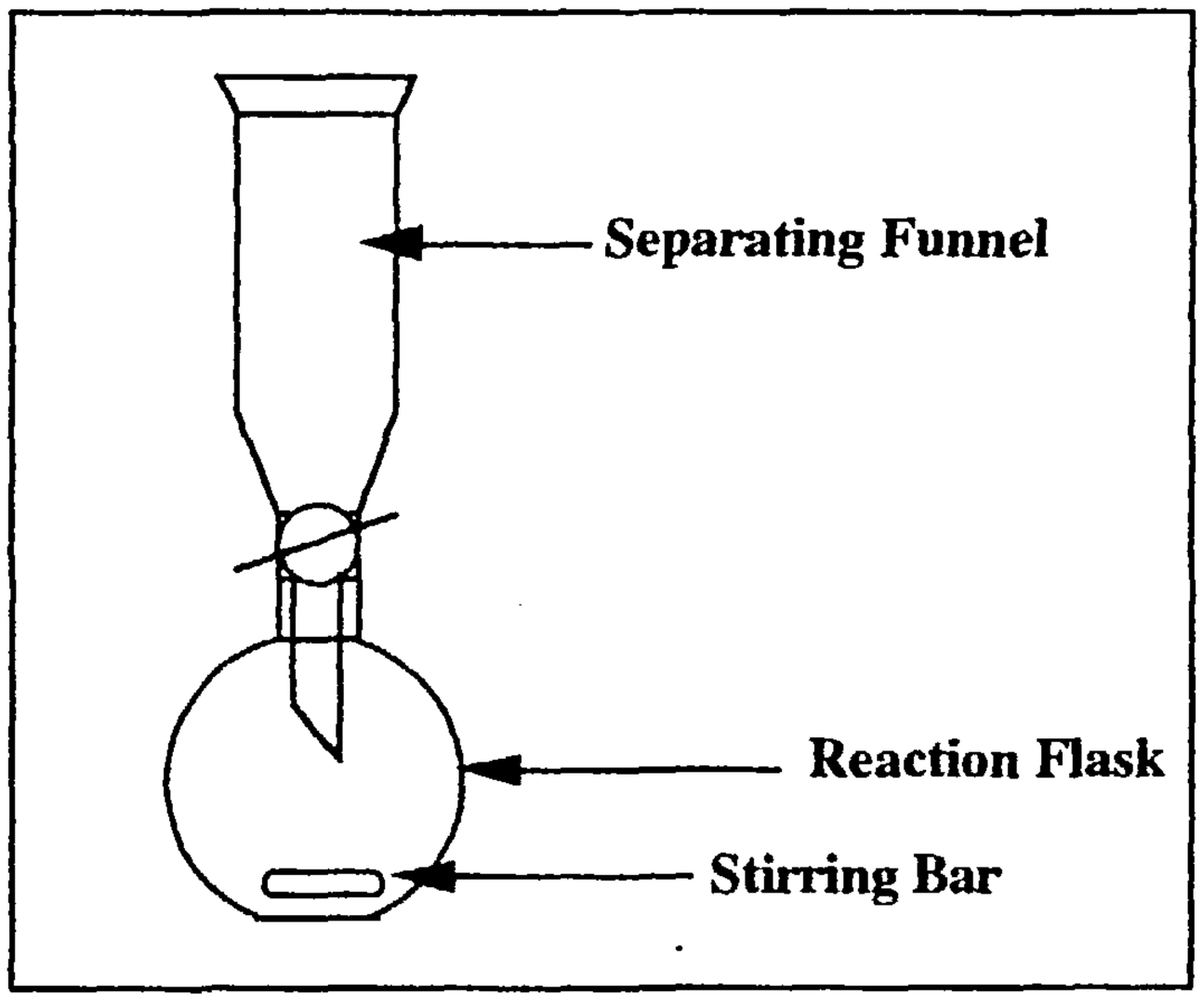

Figure 5.2.2: Apparatus for Synthesis of Bromine Compounds

Dichloromethane (15cm^3, Fisons Analytical) was used to dissolve quinuclidine (5.0g, 45mmol, Fluka) in a round-bottomed flask (50cm^3). A solution of Br_2 (5.6g, 35mmol, BDH) in CH_2Cl_2 (5cm^3) was added dropwise, over 3 hours, to the quinuclidine solution, with stirring. A few crystals began to form towards the end of the addition and the rest were precipitated out by stirring with diethyl ether (20cm^3, Fisons Analytical). This product was filtered and dried under vacuum before weighing.

C) CHARACTERISATION.

After drying under vacuum overnight, a soft yellow powder (10.8g) was obtained. Iodimetric titration indicated an oxidising bromine content of 8.6%. For the formation of the bromonium tribromide complex ($Br^+ Br_3^-$), an oxidising bromine content of 14.8% would be expected. For formation of the bromonium bromide ($Br^+ Br^-$), an oxidising bromine content of 21.0% would be expected. The colour of the compound suggested some retention of excess dibromine, since the product was described by Blair et al as a white solid. An attempted recrystallisation from acetonitrile led to a damp solid which

was difficult to dry, even under vacuum, and did not yield any significant improvement in the titre.

In order to verify the integrity of the quinuclidine molecule within the complex, a solid phase (KBr disc) spectrum of the solid was obtained. This spectrum is shown in Figure 5.2.3. The spectrum illustrates C-H stretching bands from methylene and N-CH_2 at 3000-2850cm^{-1} and 2800-2780cm^{-1} respectively[80]. These bands, with the corresponding deformation bands at lower wavenumbers, are characteristic of quinuclidine and confirm that the quinuclidine molecular unit remained intact during the reaction.

A crystal structure would be necessary to determine whether the complex exists with a bromide or tribromide anion. This distinction, however, may well be only philosophical since, in the presence of excess dibromine, some Br_3^- formation is likely to occur:

$$\mathbf{Br_2 + Br^- \Leftrightarrow Br_3^-} \qquad .....(5.2.1)$$

Based on formation of the bromide, the reaction shown in equation 5.2.2 below would produce a maximum yield of 8.6g of complex from 45mmol of quinuclidine in an excess (35mmol) of dibromine.

$$\mathbf{Br_2 + 2\ Quinuclidine \rightarrow [Bis(Quinuclidine)Br]^+\ Br^-} \qquad .....(5.2.2)$$

Based on the formation of the tribromide, the reaction shown in equation 5.2.3 below would produce a maximum yield of 18.97g of complex from 35mmol of dibromine in an excess (45mmol) of quinuclidine.

$$\mathbf{2Br_2 + 2\ Quinuclidine \rightarrow [Bis(Quinuclidine)Br]^+\ Br_3^-} \qquad .....(5.2.3)$$

If credence is given to this argument, it would appear from the 10.8g yield obtained in our experiment, that the reaction shown in equation 5.2.3 occurred to form the tribromide complex. However, practical observations suggested that the product was impure and the proportion of oxidising bromine in the complex was not consistent with this conclusion. Both bromide and tribromide species are likely to be present and the discolouration of the complex in comparison with Blair's white solid represents the presence of Br_2. This could occur either directly from an excess of dibromine in reaction 5.2.2, or indirectly from dissociation of Br_3^- formed in reaction 5.2.3.

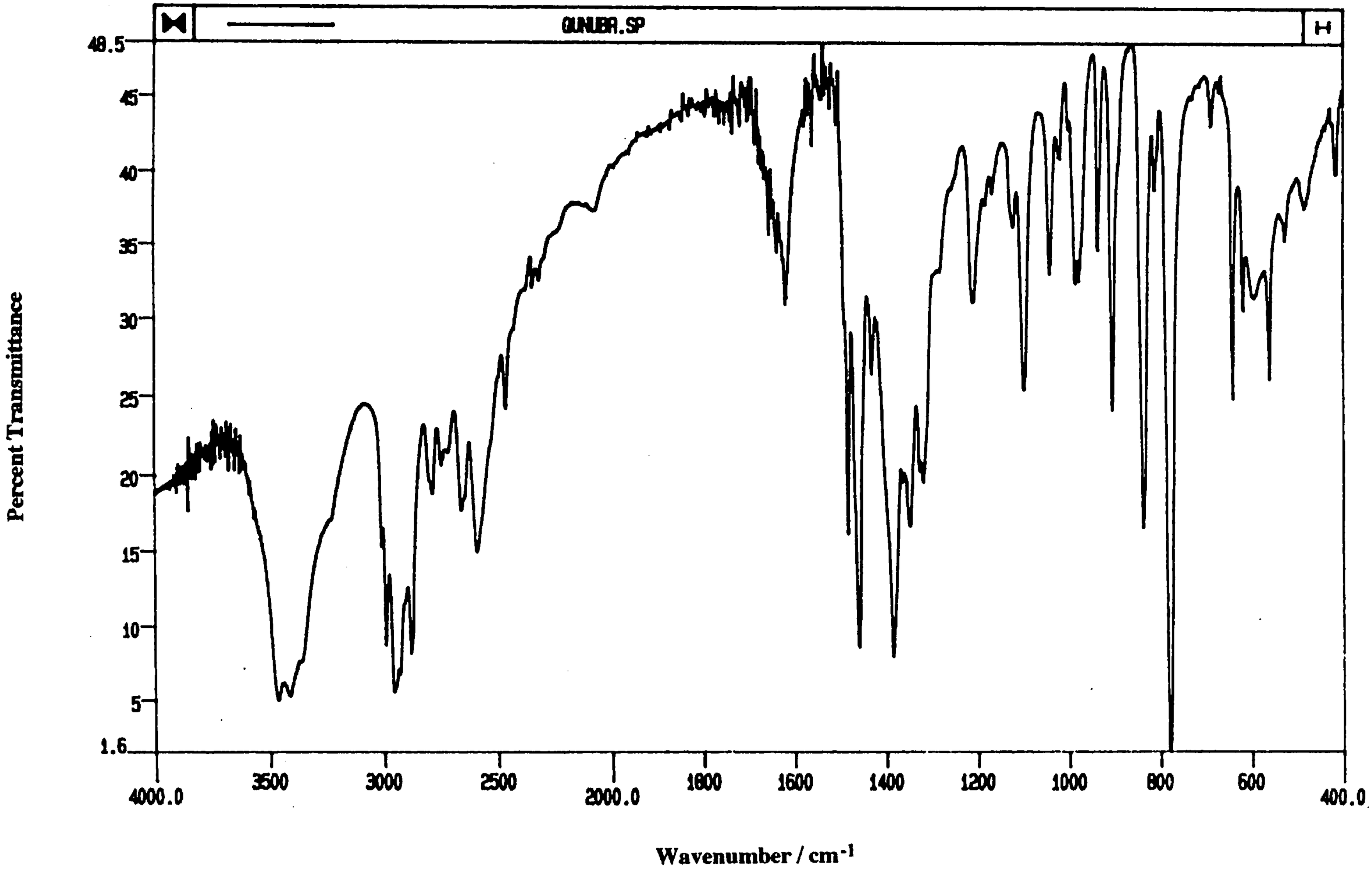

Figure 5.2.3: KBr Disc Infrared Spectrum of Bis(Quinuclidline) Bromonium Bromide

An accurate melting point for the complex could not be obtained as decomposition occurred between 403K and 423K. This is consistent with the observations of Blair et al[43].

5.2.2 BIS(QUINOLINE) BROMOMIUM BROMIDE

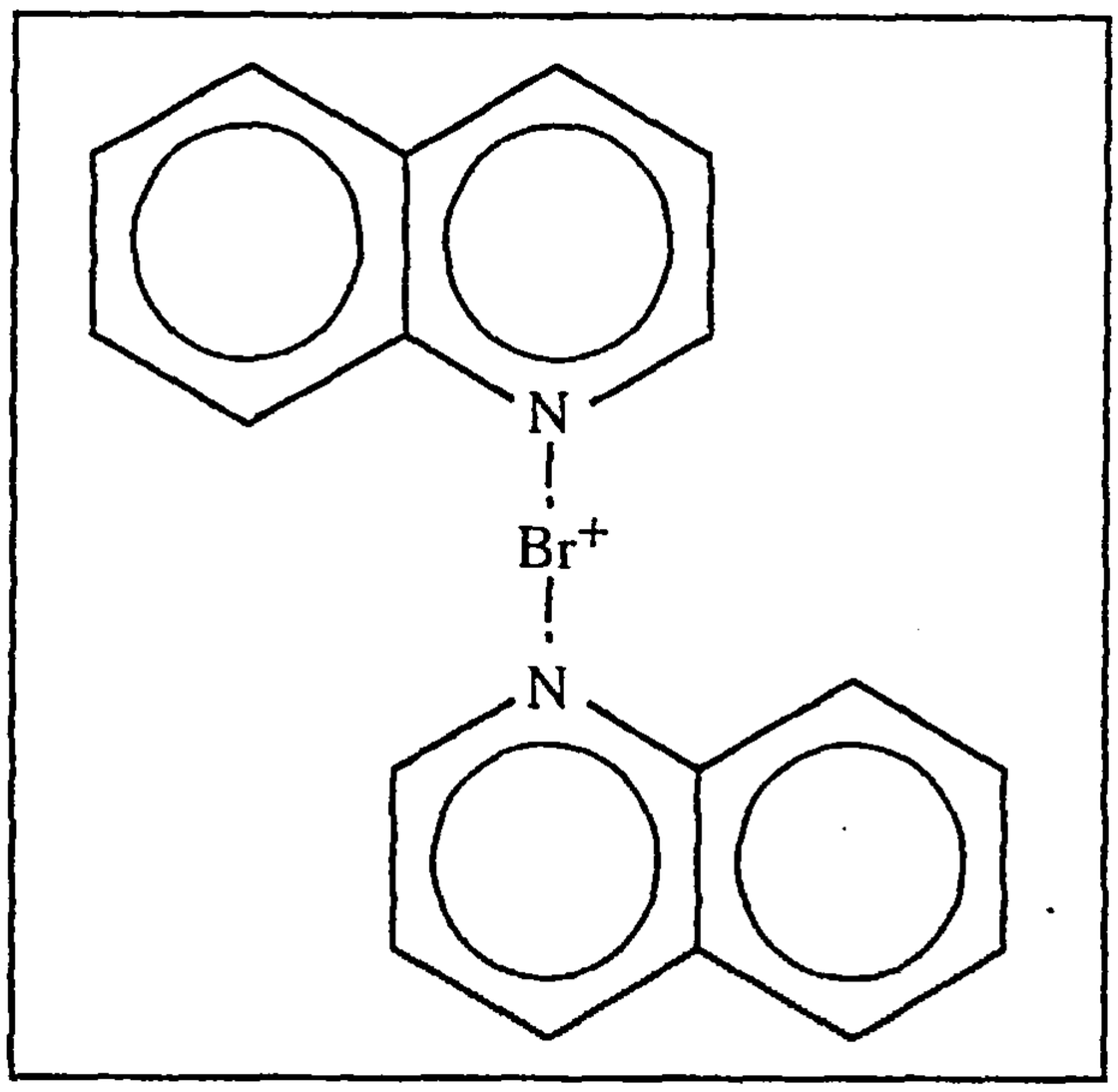

Figure 5.2.4: Bis(Quinoline) Bromonium Cation

A) BACKGROUND

The bis(quinoline) bromine cation has been previously reported by Alcock and Robertson[81] as part of a study of its perchlorate salt $[(qu)_2Br]^+[ClO_4]^-$, but no precedent was found in the literature for the synthesis of the bromide or tribromide. Alcock and Robertsons' study of the cation shows the N-Br-N arrangement to be linear, with one long (2.165Å) and one short (2.100Å) Br-N bond. Figure 5.2.4 shows a general representation of the cation

B) SYNTHESIS

The method used to synthesise bis(quinoline) bromonium bromide was a modification of that detailed in Section 5.2.1. Dichloromethane ($20cm^3$, Fisons Analytical) was used to dissolve dibromine (12.8g, 0.08mol, BDH Analar) and this was added dropwise to a solution of quinoline (10.32g, 0.08mol, Fluka) in CH_2Cl_2 ($30cm^3$). The addition took 3h and used the apparatus shown in Figure 5.2.1. The solid product was left to crystallise out overnight and excess solvent was removed by vacuum distillation the following day. A brick red solid (13.4g) was obtained.

c) CHARACTERISATION

Iodimetric titration indicated an oxidising bromine content of 25.3%. The value required for the tribromide complex would be 13.8%, and 19.1% for the bromide. However, microanalysis of the solid showed a significant amount (8%) of chlorine present from the CH_2Cl_2 solvent. Thus, the iodimetric titration was likely to be inaccurate due to solvent impurity in the sample. The solid melted in the range 346K to 351K. To confirm formation of the complex, an infrared spectrum was attempted but the solvent impurity in the solid made it difficult to obtain a clear spectrum. To overcome this problem, the tetrafluoroborate complex was synthesised from the bromide in order to produce a purer, more stable product for IR investigation of the cation. The BF_4^- complex of this cation is not documented in the literature. The synthesis of the complex followed the method detailed by Blair et al[43] for the preparation of bis(quinuclidine) bromonium tetrafluoroborate.

Quinoline (5.19g, 0.04mol) was dissolved in CH_2Cl_2 ($10cm^3$) before adding a solution of sodium tetrafluoroborate (1.5g, 0.014mol) in CH_2Cl_2 ($5cm^3$), stirring continuously. About 1 hour into the addition, solid began to precipitate into the orange solution. This solid was filtered off, yielding an orange/brown sticky substance, which was redissolved in the filtrate with the addition of diethyl ether ($20cm^3$). This procedure yielded a finer solid. Paler crystals (presumed to be sodium bromide) were also now visible.

To remove the NaBr, the solid was redissolved in the filtrate, which was then shaken with distilled water and the organic layer collected. The filtered product was rinsed with hot water several times to remove any remaining NaBr and then placed in a glass vessel and pumped out (10^{-4}Torr) overnight to dry. The solid remaining (3.69g) was granular and brick-red in colour. Figure 5.2.5 shows the KBr disc IR spectrum obtained from this solid. The spectrum shows bands at $3050cm^{-1}$ and $1250\text{-}1220cm^{-1}$ characteristic of aromatic C-H stretching and deformation respectively. Also present are the bands at $1620cm^{-1}$ (C=N conjugated cyclic) and $1450\text{-}1300cm^{-1}$ (C=C aromatic) characteristic of quinoline. The set of bands between $1140cm^{-1}$ and $1020cm^{-1}$ are unique to the BF_4^- anion. These bands confirm the integrity of the quinoline structure within the complex. The spike visible at $1590cm^{-1}$ is due to the Christiansen effect found in many solid phase IR spectra[70].

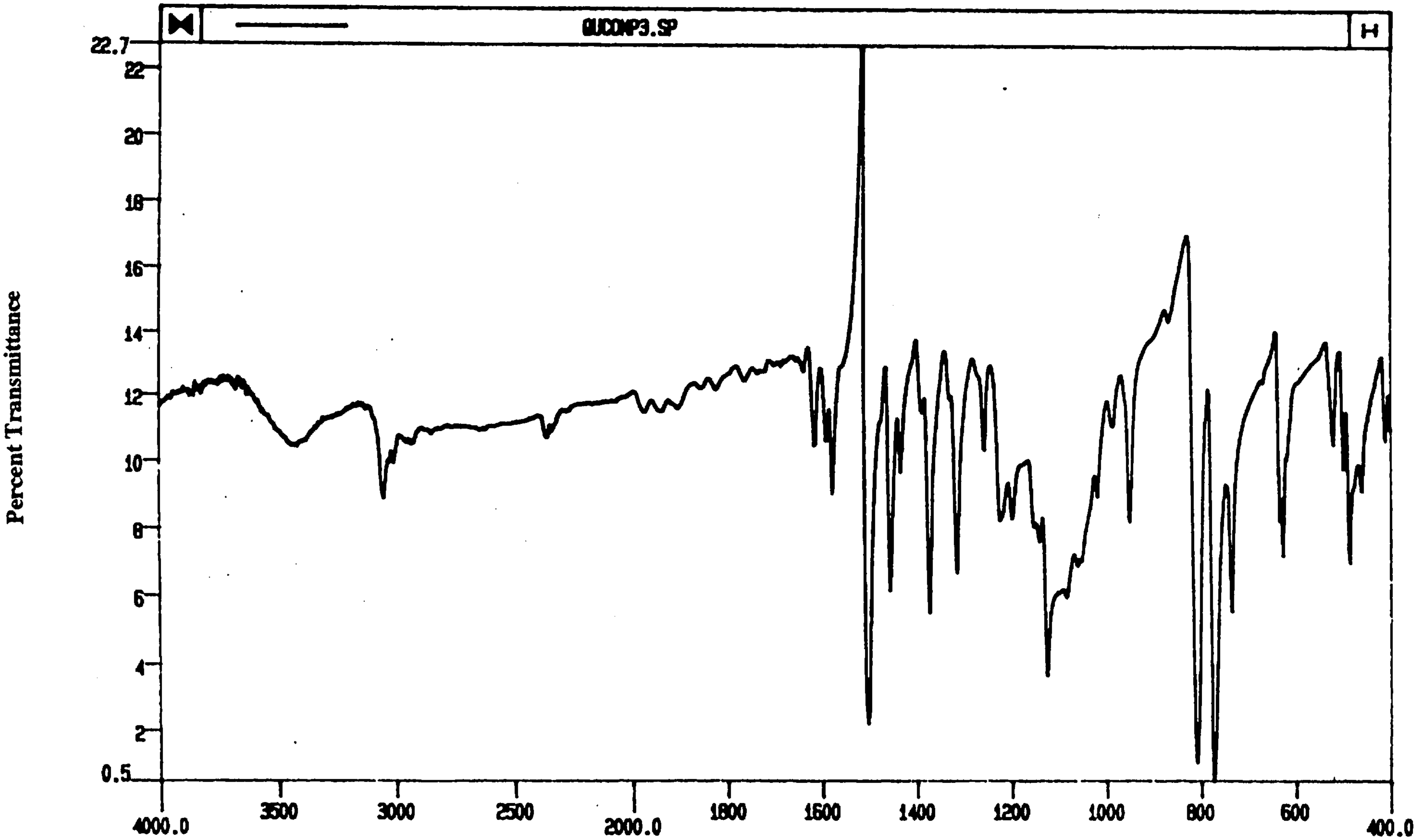

Figure 5.2.5: KBr Disc Infrared Spectrum of Bis(Quinoline) Bromonium Tetrafluoroborate

5.2.3 CYCLAM - DIBROMINE ADDUCT

A) BACKGROUND

The complex formed on reaction of 1,4,8,11-tetraazacyclodecane (cyclam) with dibromine has been prepared previously at Glasgow University[82]. The adduct is formed in a 1:2 stoichiometry of cyclam : Br_2 which suggests, by analogy with its iodine counterpart[82], the formation of a bromonium cation and tribromide anion. However, in the case of the bromine complex there is no definitive evidence of such a structure. The complex loses Br_2 in solution and is easily hydrolysed in air, perhaps implying the formation of a weak molecular adduct. No attempt to characterise the compound further was made in this work. However, it was expected that the choice of this adduct would provide a more labile source of bromine than the quinoline and quinuclidine complexes detailed in Sections 5.2.1 and 5.2.2, since the electrostatic interaction between N-donor and molecular dibromine should be weaker than that for Br^+.

B) SYNTHESIS

Since cyclam itself is hygroscopic and the complex itself is also moisture sensitive, the preparation was executed *in vacuo* on a Pyrex vacuum line and transferences were undertaken in a nitrogen atmosphere glove box. The CH_2Cl_2 used as a solvent in the reaction was dried over molecular sieves (activated at 400K for about 1 hour). Dry Br_2 (0.334g, 2mmol, BDH) was distilled into a vessel and degassed on the vacuum line. Cyclam (0.2g, 1mmol, Fluka) was loaded into a double limbed reaction vessel (Figure 2.3.3) in the glove box and the vessel was degassed. The CH_2Cl_2 ($5cm^3$) was vacuum distilled onto the cyclam and the mixture was allowed to warm to room temperature. The cyclam solution was shaken vigorously to ensure a homogenous suspension before further vacuum distillation of the Br_2 onto the solution. The reaction mixture was allowed to warm to room temperature very slowly. The yellow/orange complex was obtained by decanting the supernatant liquid and any remaining volatiles were removed by vacuum distillation. The solid was left open to the vacuum pump overnight to dry.

C) CHARACTERISATION

Microanalysis yielded the following: C 22.3, H 4.5, Br 60.1 and N 9.5. The required values for an adduct of cyclam with a 2:1 ratio of dibromine to cyclam molecules are C 23.1, H 4.7, Br 61.5 and N 10.8. Due to the small yield of product obtained (< 0.5g) and the requirement for concentrated etchant solutions in the dip-etch experiments, no further characterisation was undertaken.

5.2.4 1,4-DIOXANE - DIBROMINE ADDUCT

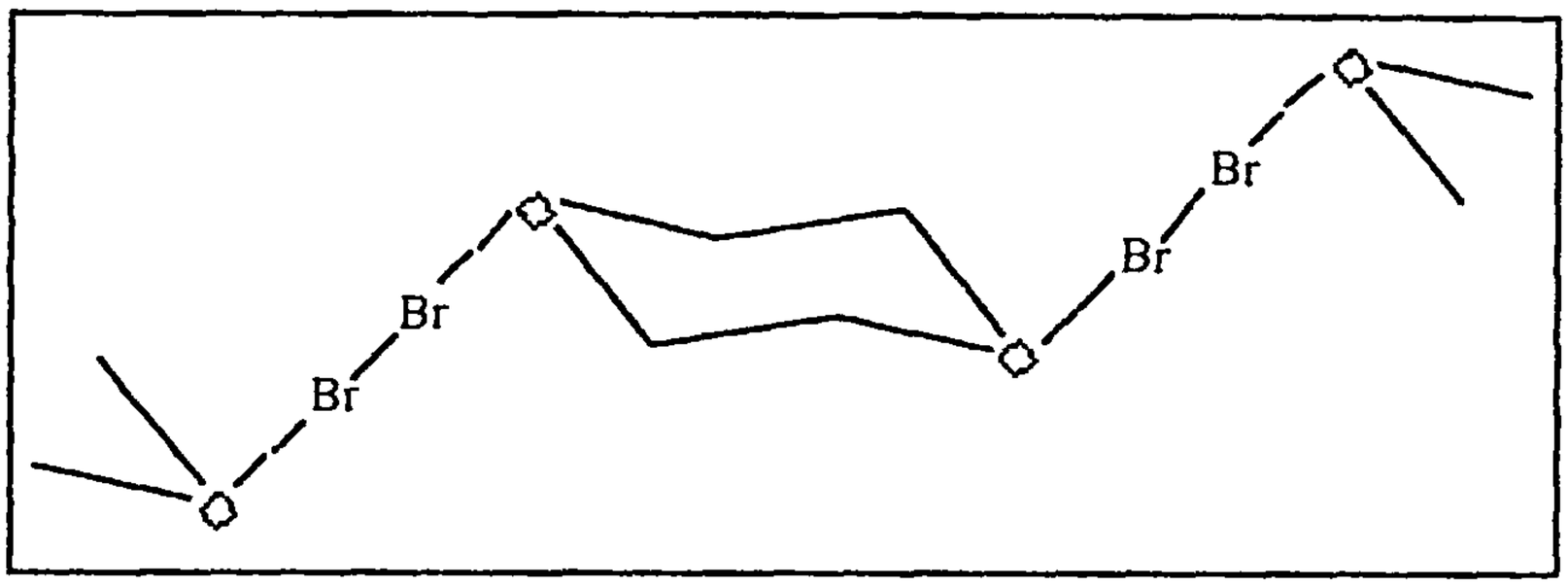

Figure 5.2.6: Br_2-Dioxane Adduct

A) BACKGROUND

This compound is often cited in the textbooks as an example of a molecular bromine adduct[83] and is illustrated in Figure 5.2.6. This structure was determined by x-ray crystallography[84]. The choice of this structure allows comparison of an adduct with oxygen donor atoms with the nitrogen-donor adducts detailed in Sections 5.2.1 to 5.2.3. Based on electronegativity considerations, oxygen atoms should form weaker complexes than their nitrogen donor equivalents. Hence, it would be expected that this adduct should easily give up its dibromine in solution, providing a more vigorous etchant than the N-donor ligands also being investigated.

B) SYNTHESIS

The adduct was prepared by simple dropwise addition of Br_2 (8g, 0.05mol, BDH) to 1,4 - dioxane (4.56g, 0.02mol, Fisons) using the apparatus in Figure 5.2.2. The addition was carried out over a 4 hour period to avoid overheating of the reaction mixture and coagulation of the product. An orange/brown solid was obtained.

C) CHARACTERISATION

The orange brown solid obtained slowly lost dibromine if left in air. This led to a slightly damp solid when left over 24 hours, probably due to the presence of excess 1, 4 - dioxane. The dry product melted between 336K and 338K. The ease with which the adduct lost Br_2 made microanalysis impossible and the solid decomposed under the laser beam when analysis by Raman spectroscopy was attempted.

5.2.5 18-CROWN-6 - DIBROMINE ADDUCT

A) BACKGROUND

No reference to this adduct or similar crown ether / Br_2 adducts could be found in the literature. Such a compound was thought to be useful in this work as an oxygen donor compound analogous to the cyclam adduct detailed in Section 5.2.3. The use of crown ethers as potential etchants also adds an extra dimension to the investigation, since such compounds are renowned fro their ability to 'capture' selectively certain metals dependent on the size of the macrocycle[85].

B) SYNTHESIS

18-Crown-6 (1.3855g, 5mmol, Fluka) was dissolved in CH_2Cl_2 ($5cm^3$). A solution of Br_2 (0.9g, 0.05mol, BDH) in CH_2Cl_2 ($5cm^3$) was added to the 18-crown-6 solution dropwise over 1 hour using the apparatus in Figure 5.2.2. The mixture was stirred for a further 3 hours. The solid product was obtained by vacuum distillation of most of the solvent, leaving a viscous orange solution. The remaining CH_2Cl_2 (ca. $2cm^3$) was allowed to evaporate slowly from the mixture, in an evaporating dish, over 2 days. The resulting solid was very damp and consisted of transparent orange platelets. These were blotted between two filter papers and allowed to dry for a further 48 hours.

C) CHARACTERISATION

A melting point was attempted but the solid decomposed between 348K and 363K. Microanalysis yielded the following values: C, 34.10%; H, 6.28%; Br, 35.40%. These values are consistent with an adduct of molecular Br_2 with the crown ether ($C_{12}H_{24}Br_3O_6$ requires C, 34.0%; H, 5.66%; Br, 37.7%) rather than a complex with a central Br^+ and a Br_3^- anion. The possibility of an ionic complex incorporating Br^+, with a Br^- anion, cannot be ruled out but is unlikely in the light of literature analyses of other halogen containing crown ether compounds[86].

5.3 ETCHING AND POLISHING WITH BROMINE COMPOUNDS

5.3.1 ETCHING OF GALLIUM ARSENIDE AND CADMIUM TELLURIDE WITH QUINOLINE AND QUINUCLIDINE BROMINE COMPOUNDS

The bis(quinoline) bromonium bromide and bis(quinucildine) bromonium bromide are both fairly soluble in water. The compounds (0.6g) were used in aqueous solution ($80cm^3$) to etch GaAs and CdTe for 1 hour etch periods, using the apparatus shown in Figure 2.3.1. Concentrated trifluoroacetic acid was added to some of the etch solutions to determine whether lowering pH would yield a more effective etchant. Table 5.3.1 lists the conditions used for each etch.

Wafer	Bromine Complex	Acid / cm^3	Material	Mass Wafer / g
1j	Quinoline	0	GaAs	0.4311
2j	Quinuclidine	0	GaAs	0.4331
3j	Quinoline	1.0	GaAs	0.4979
4j	Quinuclidine	1.0	GaAs	0.4507
5j	Quinoline	2.0	CdTe	0.5529
6j	Quinuclidine	2.0	CdTe	0.5100

Table 5.3.1: Etching with Quinoline and Quinuclidine Bromine Complexes

The wafer samples were weighed afterwards to determine mass loss. Etch solutions were retained for analysis by atomic absorption spectroscopy.

5.3.2 SOLUBILITY OF QUINOLINE AND QUINUCLIDINE BROMINE COMPOUNDS IN VARIOUS CARRIER FLUIDS.

To examine different methods of delivering solid organic etchants to the wafer surface during polishing, it was necessary to find out which diluents would be best for use in a slurry. Small amounts (ca. 0.1g) of each compound were added to different potential carrier fluids to estimate, qualitatively, how well they dissolved. About $1cm^3$ of concentrated trifluoroacetic acid was added to evaluate any further dissolution or effect on the suspension. The solvents examined were water, light paraffin oil, isopropyl alcohol

(IPA), ethanol and ethane diol. All solvents were commonly used commercial diluents supplied by Logitech Ltd.

5.3.3 POLISHING OF GALLIUM ARSENIDE WITH QUINOLINE AND QUINUCLIDINE BROMINE COMPOUNDS

Polishing experiments were undertaken on a Logitech PM2A polishing machine (Section 3.2.1) using a Chemcloth polishing pad. The samples ($2cm^2$) were mounted on a Logitech PP5GT polishing jig with minimal load and polished at a plate speed of 70rpm.

A) POLISHING WITH BIS(QUINUCLIDINE) BROMONIUM BROMIDE

Three different polishes were carried out using this compound. The first used 1.0g of the solid in a $200cm^3$ aqueous solution. The wafer was polished for 30 minutes with dropwise addition of the solution and for a further 10 minutes while washing the pad with distilled water. The second polish used 2.0g of the solid spread directly onto the polishing pad with a spatula. A 2.5% v/v concentrated sulphuric acid solution was dripped onto the pad during the 15 minute polish. The third method used 1.0g of solid in a $200cm^3$ aqueous solution containing 2.5% v/v concentrated sulphuric acid. This solution was dripped onto the pad throughout the 30 minute polish.

B) POLISHING WITH BIS(QUINOLINE) BROMONIUM BROMIDE

Bis(quinoline) bromonium bromide (4.0g) was suspended in 1 litre of commercial ethanol diluent in a rotating drum with drip-valve attached. This suspension was dripped onto the polishing pad concurrently with a 0-2% concentrated triflic acid solution (Table 5.3.2). The wafer was examined at 15 minute intervals using optical Nomarski microscopy and surface roughness measurements. The wafer sample was pre-polished for 20 minutes using a 0.2% v/v bromine/methanol solution to produce the usual orange peel surface.

Time / min	Triflic Acid / % v/v
0	-----
15	0.4
30	1.0
45	2.0
60	1.0

Table 5.3.2: Polishing with Bis(quinoline) Bromonium Bromide

5.3.4 ETCHING OF GALLIUM ARSENIDE AND CADMIUM TELLURIDE WITH CYCLAM - DIBOMINE ADDUCT

The only solvent which dissolved the cyclam complex to any extent was acetonitrile (CH_3CN). On addition of the CH_3CN ($80cm^3$) to the solid, the solution became yellow immediately but most of the complex remained undissolved. The etches were carried out for 1 hour etch periods using the apparatus in Figure 2.3.1. Concentrated trifluoroacetic acid was added to some of the solutions to determine whether protonation would speed up reaction. The details of each etch are given in Table 5.3.3

Wafer	Mass Complex / g	Acid / cm^3	Material	Mass Wafer / g
1k	0.2324	0	GaAs	0.5442
2k	0.0910	2	GaAs	0.5769
3k	0.0610	2	CdTe	0.4710

Table 5.3.3: Etching with Cyclam - Dibromine Adduct

The wafer samples were weighed afterwards to determine mass loss. Etch solutions were retained for analysis by atomic absorption spectroscopy.

5.3.5 ETCHING OF GALLIUM ARSENIDE AND CADMIUM TELLURIDE WITH 1, 4-DIOXANE - DIBROMINE ADDUCT

The Br_2 - dioxane adduct dissolved in a wide range of solvents, so several different etch solutions were tried. Etches were carried out in $80cm^3$ of solution for 1 hour etch periods using the apparatus in Figure 2.3.1. No acid was added to any of the etch solutions. The details of each etch are given in Table 5.3.4. The wafer samples were weighed afterwards to determine mass loss. Only the solution from sample 1l was analysed by atomic absorption spectroscopy. The organic matrix in the other samples made analysis using standard AAS techniques difficult and satisfactory data were not obtained.

Wafer	Mass Adduct / g	Solvent	Material	Mass Wafer / g
1l	0.4711	Water	GaAs	0.5019
2l	0.6800	Dichloromethane	GaAs	0.5543
3l	0.6694	Dichloromethane	CdTe	0.5478
4l	0.7090	Methanol	GaAs	0.5095

Table 5.3.4: Etching with Dibromine/Dioxane Adduct

5.3.6 ETCHING OF GALLIUM ARSENIDE AND CADMIUM TELLURIDE WITH 18-CROWN-6 - DIBROMINE ADDUCT

The yield of this adduct from the preparation was quite low, so substantially less was employed in each etch than was used in some of the other dip-etches. The etches were carried out in CH_2Cl_2 solution ($80cm^3$) for 1 hour etch periods using the apparatus in Figure 2.3.1. The details of the etches are given in Table 5.3.5.

Wafer	Mass Adduct / g	Material	Mass Wafer / g
1m	0.1716	GaAs	0.5626
2m	0.1534	CdTe	0.5069

Table 5.3.5: Etching with Dibromine/18-Crown-6 Adduct

The wafer samples were weighed afterwards to determine mass loss.

5.3.7 ETCHING OF GALLIUM ARSENIDE WITH [^{82}Br]-LABELLED ADDUCT OF DIBROMINE WITH 1, 4-DIOXANE

This experiment was undertaken to determine whether the Br_2 - dioxane adduct remained intact during the etching process. This was essential to determine whether there is any advantage in using the solid in solution rather than a simple solution of Br_2 in methanol. The [^{82}Br]-labelled Br_2 was prepared as described in Section 4.4.3 and its specific activity was determined as 305.2 count s^{-1} (mg atom Br)$^{-1}$. The [^{82}Br]-labelled Br_2 - dioxane adduct was prepared, and the etching reaction carried out, in a double-limbed Pyrex counting vessel with central stopcock (Figure 2.3.3).

A volume of [^{82}Br]-labelled Br_2 was vacuum distilled into one limb of the evacuated, weighed vessel. The vessel was degassed and re-weighed to give the mass of Br_2

present (0.228g). A slight excess of 1, 4-dioxane was weighed out (0.147g) and placed in the other limb before degassing this limb on the vacuum line. The central tap was opened and the bromine was decanted onto the dioxane. The remaining bromine was vacuum distilled onto the dioxane and the central tap was closed. Patches of solid product formed over the limb, sticking to the glass. Dry CH_2Cl_2 ($3cm^3$) was distilled into the limb to wash down the Br_2 - dioxane adduct ready for use in the etching experiment.

The limb in the reaction vessel which had been used to contain the active bromine was evacuated and then opened to the air to allow insertion of a section (0.2558g, 1.76mmol) of GaAs. The vessel was closed and this limb degassed. The central tap was opened and the etch solution was decanted onto the wafer sample. The limb containing the Br_2 - dioxane/CH_2Cl_2 solution was placed in the well of the scintillation counter and counted before the etch was started. After 30 minutes and 1 hour, the etch solution was decanted back into the other limb and the wafer and the etch solution were counted. At the end of the 1 hour etch, the solution was vacuum distilled into the other limb and the wafer limb was degassed. The ^{82}Br activity retained on the wafer was determined after each operation.

5.4 RESULTS

5.4.1 ETCHING OF GALLIUM ARSENIDE WITH ORGANIC BROMINE COMPOUNDS

Gallium Arsenide mass loss results from the experiments detailed in Sections 5.3.1 and 5.3.4 to 5.3.6 are compared in Figure 5.4.1. The results show that, in general, only small amounts of material are removed from GaAs, relative to normal etches using Br_2 in methanol.

Acidification of the etch solutions of bis(quinoline) bromonium bromide and bis(quinuclidine) bromonium bromide significantly improved the amount of material removed from the wafer segment. The Br_2-dioxane adduct in methanol and dichloromethane yielded mass losses comparable with solutions of Br_2 in the same solvents, suggesting that the dioxane was not moderating the Br_2 at all, or that the adduct was breaking down in solution. The Br_2-dioxane in H_2O produced very poor results,

probably due to hydrolysis of the dibromine within the compound, breaking down the adduct.

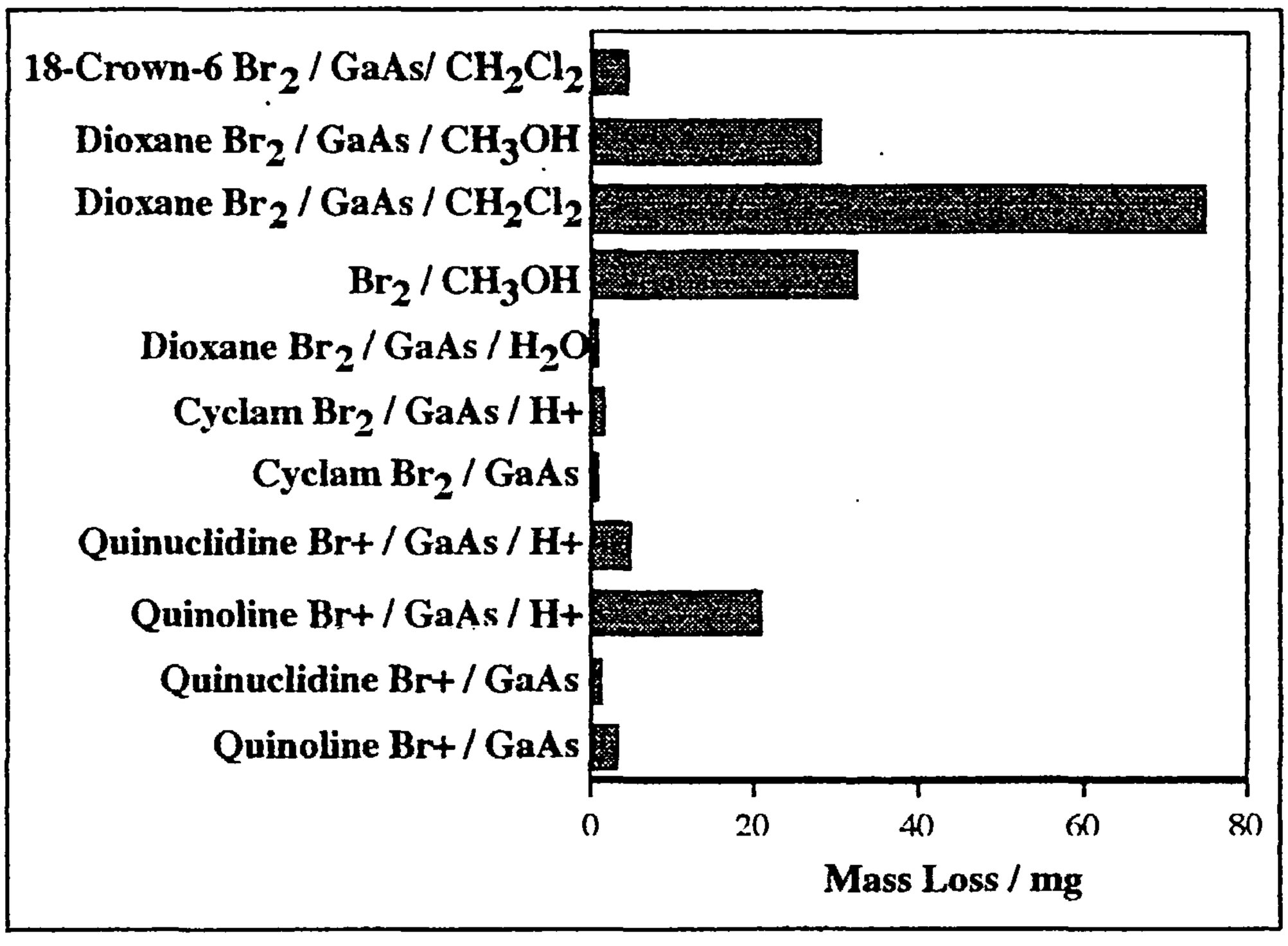

Figure 5.4.1: Mass Loss Results from GaAs Etches using Bromine Compounds

Soluble As results, from the etches where such analyses were possible, are shown in Table 5.4.1.

Wafer	Etchant	Total As / mg	As / μgcm^{-3}
1j	Quinoline Br+/Water	0	0
2j	Quinuclidine Br+/Water	0.02	0.4
3j	Quinoline Br+/Water/H+	2.19	1.4
4j	Quinuclidine Br+/Water/H+	2.49	1.2
1k	Dibromine-Cyclam/Acetonitrile	0.20	2.5
2k	Dibromine-Cyclam/Acetonitrile/H+	0.40	5.0
1l	Dibromine-Dioxane/Water	0.007	0.09

Table 5.4.1: Soluble As Results from GaAs Etches using Bromine Compounds

In general, the soluble As results reflect mas loss results well. However, despite the fact that bis(quinoline) bromonium bromide yields much higher mass loss results than its quinuclidine counterpart, the quinuclidine complex produces a much higher level of As in solution. This may be due to the 'trapping' of As in the quinoline complex e.g. the brominated arsenic product may interact with the quinoline, preventing hydrolysis and therefore the presence of soluble As in solution. Another possibility is that there is some selectivity between Ga and As in the case of the bis(quinuclidine) bromonium bromide.

5.4.2 ETCHING OF CADMIUM TELLURIDE WITH ORGANIC BROMINE COMPOUNDS

Cadmium telluride mass loss results for the experiments detailed in Sections 5.3.1 and 5.3.4 to 5.3.6 are compared in Figure 5.4.2.

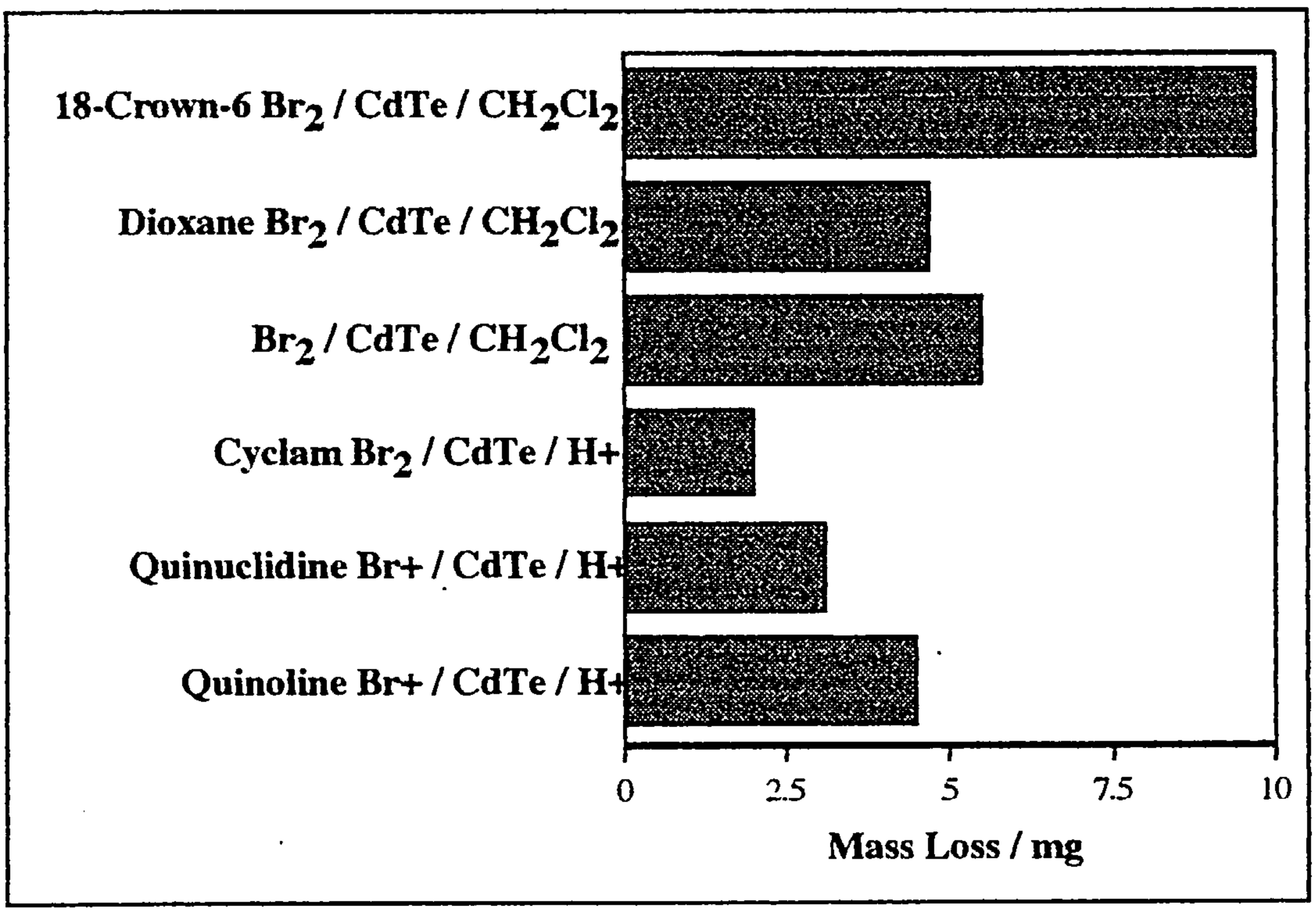

Figure 5.4.2: Mass Loss Results from CdTe Etches using Bromine Compounds

The results show that, in general, the compounds remove less material from CdTe than from GaAs (Figure 5.4.1). This result is expected, since bromine itself is a less effective etchant on CdTe than on GaAs[60]. Soluble Cd and Te results from the etches where such analyses were possible, are shown in Table 5.4.2.

These results are surprising in that they show consistently more Te being removed to solution than Cd. This contradicts the usual trend observed with Br_2 in methanol[60] or Br_2 and hydrobromic acid[36]. One possible explanation may be selective trapping of the smaller Cd atom in the solid, preventing its detection in solution.

Wafer	Etchant	Te/ μgcm^{-3}	Cd / μgcm^{-3}
5j	Quinoline Br+/Water/H+	44.7	34.5
6j	Quinuclidine Br+/Water/H+	16.7	12.5
3k	Br_2-Cyclam/Acetonitrile/H+	12.5	9.4

Table 5.4.2: Soluble Cd and Te Results from CdTe Etches using Bromine Compounds

5.4.3 POLISHING OF GALLIUM ARSENIDE WITH BIS(QUINOLINE) BROMONIUM BROMIDE AND BIS(QUINUCLIDINE) BROMONIUM BROMIDE

Experiments to determine the best carrier fluid for polishing with Br^+ complexes showed that none of the diluents tried completely dissolved either bis(quinoline) bromonium bromide or bis(quinuclidine) bromonium bromide. Since a suspension of the solid etchant was desired, rather than a solution, this observation was to our advantage. However, it was desirable that addition of acid should encourage dissolution of the complex, allowing control of the polishing process by pH. The best choice of carrier fluid appeared to be ethanol for the quinoline complex and ethane diol or water for the quinuclidine complex. Since ethane diol is known to moderate Br_2 as an etchant, water was used as the diluent for the quinuclidine complex.

Polishing of a lapped GaAs wafer with bis(quinuclidine) bromonium bromide in aqueous solution did not produce a shiny surface, even after a 40 minute polish. Addition of acid to the solution improved the result but still did not lead to a significantly polished surface. Spreading the solid directly onto the pad and dripping acid onto the pad during the polish produced by far the best results. A polish was beginning to appear around the edges of the wafer within 15 minutes. This result shows that the method of etchant delivery is critical to the quality of the polish. Delivery of the complex to the wafer surface as a solid is important in order to exploit any advantage over a simple solution of bromine.

Polishing of a pre-polished, orange-peel GaAs surface with bis(quinoline) bromonium bromide in ethanol showed some improvement in surface quality over a 30 minute polish. Addition of a 0.4% v/v triflic acid solution dropwise onto the polishing pad yielded the best results. Table 5.4.3 summarises the observations made and the surface roughness measurements at each stage of the experiment.

Polish Time / min	**Triflic Acid / %v/v**	**Optical Microscope**	**R_a / nm**
0	----	Orange Peel	----
15	0.4	Orange Peel	16.12
30	1.0	Smoother	10.70
45	2.0	Smoother	11.20
60	1.0	Same	11.93

Table 5.4.3: Observations During a 1 Hour Polish of GaAs with Bis(Quinoline) Bromonium Bromide

The results indicate a limit to the improvement which can be achieved using the complex. This is likely to depend on the quality of the original polish. However, an improvement of at least 5nm surface roughness was achieved in this case.

5.4.4 ETCHING OF GALLIUM ARSENIDE WITH [^{82}Br]-LABELLED Br_2-DIOXANE ADDUCT

The [^{82}Br]-activity retained on a GaAs wafer surface during etching with Br_2-dioxane adduct in CH_2Cl_2, at various stages of the reaction, is shown in Table 5.4.4. The retention of activity is expressed in terms of the % of the total counts available. Counts were taken for 100 second periods and were corrected for decay. The * and † represent vacuum distillation of the etch solution from the wafer limb and opening of the wafer to the vacuum pump, respectively.

The results show a decrease in the activity retained on the GaAs as the etching reaction proceeds. Thus, the activity retained is unlikely to be due to solid product building up on the wafer surface and is more likely due to the solid etchant being left behind as the solution is decanted. Although the experiment was not conclusive as to the nature of the etching reaction, it did suggest that the adduct remained intact in the CH_2Cl_2 solution.

Time / min	Wafer Count	Solution Count	% Retained
0	----	83792	
35	2828	-----	3.7
37	-----	76277	
69	2503	-----	3.3
71	-----	75672	
74*	2794	-----	3.3
76	-----	84074	
81†	2691	-----	3.2
83	-----	84362	

Table 5.4.4: Etching of GaAs with [^{82}Br]-Labelled Br_2-Dioxane Adduct

5.5 DISCUSSION

The experiments detailed in this chapter have illustrated further the principle, maintained throughout the project, that etching and polishing reactions can be controlled if enough is known about the chemistry of the etchant. This principle has been extended, in this chapter, to the design of new etchants with predictable general properties.

Experiments using bis(quinoline) bromonium bromide and bis(quinuclidine) bromonium bromide have shown that vigorous etchants like bromine can be moderated by changing their immediate chemical environment. The use of bulky ligands slows the action of bromine considerably, making the complexes useful in the elimination of orange peel effects produced from polishes in Br_2 solutions. These experiments also illustrated the controllability of such ligands, using the basic nature of the N donor atom to release the bromine faster on addition of acid. Such control is only possible in conventional etchants by changing the concentration of the etchant solution, which is less immediate and more difficult to control.

It might be predicted that faster solid etchants would be possible if a weaker ligand-halogen interaction was employed. The use of oxygen donor ligands in this work has shown this to be the case. The use of a Br_2-dioxane adduct yielded stock removals on GaAs and CdTe which were comparable with Br_2 solutions. This is despite the fact that the adduct appears to remain intact in solution. The use of an adduct like this, rather than a simple Br_2 solution, may be advantageous in maintaining geometry and 'distributing' the active etchant over the substrate surface more evenly.

The use of macrocyclic ligands has shown that it is also possible to design selectivity into an etchant. 18-Crown-6 is an ideally sized crown ether for the capture of Cd and this effect was shown to operate in the etching of CdTe with an adduct of 18-crown-6 and Br_2. As the etchant reacted with the CdTe, the 18-crown-6 was able to trap Cd and this led to a higher stock removal on CdTe than would otherwise be expected.

All of the etchants used in this chapter were chosen as representatives of molecules or complexes with similar properties. Since the behaviour of such etchants could be predicted easily, it is likely that other compounds in their classes will behave similarly. Thus, there is little limit to the series of etchants which could be designed to meet specific needs of speed, surface quality, selectivity and controllability.

CHAPTER SIX

DISCUSSION

6.1 INTRODUCTION

The overall objectives of this work were stated in Chapter One. They were to determine and/or clarify the reactions by which hydrogen peroxide, dibromine in methanol and sodium hypochlorite solutions operate on compound semiconductors. This has been investigated specifically on GaAs and CdTe. The main parameters which have been used to assess these reactions are mass loss and soluble semiconductor material, measured against varying reaction conditions such as pH and concentration.

After establishing the basic chemistries of these etchants, this knowledge was applied in the optimisation of current etching and polishing processes, specifically those employed by Logitech Ltd. The optimisation involved systematic research into the effects of reagent concentration and pH, polishing pad design, abrasive type and even etchant phase.

The latter stages of the project brought together the results of earlier experiments with the synthesis of new compounds designed to produce varying effects on reaction rate, geometry and surface quality during an etching or polishing experiment. The chemistries

of these compounds were predicted on the basis of knowledge gained during the preliminary stages of the work and these predictions were tested in etching and polishing experiments using the novel compounds synthesised.

The success of the project as a whole will be discussed, with regard to what has been learnt about etching and polishing chemistry and how this can be applied in practical terms to improve current etching and polishing procedures. Section 6.2 contains an in-depth discussion of the reaction chemistries of the various etchants employed in the work, including an explanation of the effects of these reactions on the semiconductor surface. In section 6.3, the role of abrasives and polishing pad in the chemomechanical polishing process is discussed. All of the previous discussion is brought together in Section 6.4, which presents the General Model for Chemomechanical Polishing, based on the assumption that the range of etchants investigated in this project can be generalised to cover most of the etchants employed in compound semiconductor etching / polishing. This assumption is justified in Section 6.5, which discusses in detail the results of etching and polishing experiments using modified bromine reagents as 'designer' etchants. The main conclusions of the project, and suggestions for further work in the area, are presented in Section 6.6.

6.2 Etching and Polishing Reactions on Gallium Arsenide and Cadmium Telluride.

The etching behaviours of Br_2, Cl_2, NaOCl and H_2O_2 have all been investigated to some extent as part of this work. Before etching can occur using these reagents on either GaAs or CdTe, a chemical reaction must occur at the semiconductor surface. Experiments using etchants in the gas phase (Br_2, Cl_2) and in solution (Br_2, NaOCl, H_2O_2) have shown that in most cases this reaction involves oxidation of the semiconductor material by the etchant. In the case of dibromine, either in the gas phase or in solution, this oxidation reaction produces bromides, e.g.

$$\mathbf{2GaAs + 6Br_2 \rightarrow Ga_2Br_6 + 2AsBr_3} \qquad .....(6.2.1)$$

$$\mathbf{CdTe + 3Br_2 \rightarrow CdBr_2 + TeBr_4} \qquad .....(6.2.2)$$

Evidence for the initial interaction between etchant and substrate was obtained using [^{82}Br]-labelled Br_2. In the case of GaAs, the brominated products have been positively

identified by Raman spectroscopy[87]. For the reaction of CdTe with Br_2, the brominated products cited in equation 6.2.2 have been suggested by various authors[36,88] but have not been identified beyond doubt. However, both of these etching reactions appear to operate by oxidation of substrate material by bromine, e.g.

$$6Br_2 + 12e^- \rightarrow 12Br^- \quad .....(6.2.3)$$

$$2As \rightarrow 2As^{3+} + 6e^- \quad .....(6.2.4)$$

$$2Ga \rightarrow 2Ga^{3+} + 6e^- \quad .....(6.2.5)$$

The redox reactions shown above may be an oversimplification. Indeed, in the case of the reaction Br_2 + CdTe, it is thought to be the complex electrochemistry in operation which eventually leads to a non-stoichiometric CdTe surface after etching[88]. Tellurium in the 4^+ oxidation state is believed to form when CdTe is oxidised by Br_2. This Te^{4+} may be reduced, via a series of redox reactions in solution, to form Te^0, which if deposited would lead to a non-stoichiometric surface. Such redox reactions, as with those given in equations 6.2.3 to 6.2.5 for GaAs, probably form part of a more complex redox system. However, this simple model adequately represents the reactions occurring between Br_2 and GaAs. The oxidation of GaAs by Cl_2, present in large quantities in low pH solutions of hypochlorite, produces similar products:

$$2GaAs + 6Cl_2 \rightarrow Ga_2Cl_6 + 2AsCl_3 \quad .....(6.2.6)$$

Again, this reaction can be adequately modelled using simple redox pairs, e.g.

$$3Cl_2 + 6e^- \rightarrow 6Cl^- \quad .....(6.2.7)$$

$$2As \rightarrow 2As^{3+} + 6e^- \quad .....(6.2.8)$$

When considering aqueous solutions of NaOCl and H_2O_2, the situation becomes complicated by the many equilibria in operation and by the influence of pH on such equilibria. This is compounded by the fact that, in solution, it is impossible to identify the products which form instantaneously at the etchant/semiconductor interface. In the case of halogenated species in particular, such products are easily hydrolysed by any water in the solution and hence will not be detectable in their initial form. For example, the products of the reaction of H_2O_2 with GaAs in basic conditions are often cited as

gallium and arsenic oxides and hydroxides[33]. However, it is just as probable that the initial reaction products are simple oxides, e.g.

$$2GaAs + 8H_2O_2 \rightarrow Ga_2O_3 + As_2O_3 + 8H_2O + O_2 \quad .....(6.2.9)$$

Some of the most likely oxide and hydroxide products formed on GaAs at high pH are listed in equations 2.5.1 to 2.5.7. The issue with regard to polishing or etch rate is the ease with which species such as As_2O_3 and $H_2GaO_3^-$ are removed from the surface to allow the etching reaction to continue.

In the case of NaOCl solution, the situation is complicated still further, since pH affects not only the speed of reaction, but also the composition of the etchant. In acidic conditions, the main component of the etchant solution is dichlorine, formed by the reaction of residual chloride with hypochlorous acid:

$$HOCl + Cl^- + H^+ \rightarrow Cl_2 + H_2O \quad .....(6.2.10)$$

This chlorine is the active etchant at low pH and oxidises the GaAs as shown in equations 6.2.7 and 6.2.8. In basic conditions, hypochlorite anion becomes the main component of the etchant solution and so the OCl^- oxidises the surface directly:

$$2GaAs + 6OCl^- \rightarrow Ga_2O_3 + As_2O_3 + 6Cl^- \quad .....(6.2.11)$$

These and other oxides may become hydrated in aqueous solution to produce a mixture of Ga and As oxides and hydroxides.

After oxidation of the semiconductor surface, the next stage of the etching or polishing process must involve the removal or reaction products to allow fresh reagent to reach the substrate surface. The efficiency of this removal is critical to the quality of the surface produced. Dibromine is the most common polishing reagent for both GaAs[6,16,30,31,89] and CdTe[16,90], yet the surface it produces on each of these substrates is often unsatisfactory.

On cadmium telluride, the nature of the crystal surface is entirely altered during polishing with dibromine-based reagents. This 'surface reconstruction' occurs because of differences in the solubilities and electrochemistry of the brominated products. An excess of Te is left on the CdTe surface. Reconstruction of this sort may be beneficial in producing an optically smooth surface, but is likely to have undesirable effects on the electronic properties (e.g. surface potential) of the substrate. At the device fabrication stage, the reconstructed surface is removed by etching, before growing an epitaxial CdTe

film, in an expensive and time-consuming process. It is therefore beneficial if the extent of such surface reconstruction is minimised. This was the one of the objectives in the design of new bromine-based reagents (Section 6.5).

On gallium arsenide, the surface which remains after polishing in e.g. dibromine in methanol is probably reconstructed to some degree[91], but appears to remain in an approximately 1:1 Ga:As stoichiometry. However, problems of surface topography are prevalent in GaAs, and solutions of Br_2 in methanol which contain more than 2% dibromine often lead to the production of an 'orange peel' effect on the surface. This dimpling effect is thought to occur because of selectivity in the reagent e.g. faster etching in certain crystal directions or at defects on the surface. This selectivity will of course still be present in solutions of lower Br_2 concentration, but its effect is minimised. This is because, if the etching reaction is slower, there is greater opportunity for redistribution of passivating material and mechanical modification of the surface by the polishing pad.

Hydrogen peroxide in ammonia solution can be used to polish GaAs and CdTe satisfactorily. However, the surface produced on both materials in a static etching experiment appears dull and slightly blackened. In such a static experiment, product removal is not aided by the polishing pad and so this dull appearance is produced by product build up on the surface. The rate of removal of reaction products from the substrate surface in such a case depends on the solubility of the products in the etchant solution. This solubility effect may explain the high polishing times required to produce a satisfactory polish on CdTe using H_2O_2/NH_3: Ga and As oxides and hydroxides are all soluble in alkali, whereas both Cd and Te oxides/hydroxides are insoluble in alkali, although some Te oxides (TeO, TeO_2 and TeO_3) can be dissolved in hot potassium or sodium hydroxides[9]. Hence, in a polishing situation, all the products from the $CdTe/H_2O_2$ reaction are removed by the mechanical action of the polishing pad, leading to a much increased polishing time and an inferior polished surface. A far better polished surface is achieved where the reaction products are soluble in the etchant solution and the mechanical action of the pad is required only to maintain the geometry of the substrate. Such maintenance of geometry is achieved at the wafer/pad interface by the passivation effect (Section 1.3). Hence, there is an optimum situation where the reaction products are insoluble enough to allow passivation, but soluble enough to prevent excessive polishing times and/or mechanical damage.

The substrate surfaces achieved using NaOCl solution as a polishing reagent on CdTe and GaAs were identical in appearance to those achieved using H_2O_2/NH_3. This was predictable since, at high pH, the products of the reaction are again oxides and hydroxides. Extensive surface reconstruction occurs when GaAs is etched by NaOCl

solution at high pH. This surface reconstruction leads to the formation of an amorphous, insoluble GaAs layer which incorporates As_2O_3 (Section 2.4.5). However, at low pH, the substrate surface appeared entirely different after polishing. The surface produced on GaAs by polishing in OCl^- solution at pH<8 was smooth and highly reflective and surface roughness measurements indicated that the surface quality was superior to that achievable at high pH values without an abrasive. At low pH, chlorides produced initially at the wafer surface (equation 6.2.6) are then hydrolysed in aqueous solution and removed by the polishing solution. In the case of chloride products, this process appears to have more of a modifying effect on the etching reaction than in the case of bromide production: No orange peel effect is observed on the substrate surface when polishing with NaOCl at pH<8, even when using 14% NaOCl solution. The improved surface quality is a consequence of better passivation of the GaAs surface by the trichloride products than by the tribromides (Figure 4.6.1). This is not intuitively obvious, since the trichlorides should dissolve more readily in aqueous solution than Ga and As tribromides do in methanol. Arsenic tribromide and trichloride hydrolyse in water and the Ga trihalides dissolve readily in aqueous solution. However, the results of ^{36}Cl adsorption experiments have shown that Ga_2Cl_6 and $AsCl_3$ in combination on a GaAs substrate appear to be more persistent than would be predicted (Section 4.6). This phenomenon may well be reflected at the wafer/etchant interface in a polishing situation. The degree of surface reconstruction occurring when GaAs is oxidised by Cl^- is not clear. However, the slower reaction and greater passivation of the surface by Cl^- suggest that it should compare favourably with $[OCl]^-$.

6.3 Mechanical Aspects of the Polishing Process

The largest part of this project has concentrated on the chemical aspect of the chemomechanical polishing process. However, to formulate an overall model and predict the effect of certain etchants on the polishing process, it was necessary to consider the influence of the abrasive and pad on the chemical reaction and on the final semiconductor surface.

Experimental work undertaken in this project has shown that there is a weak chemical interaction between alumina, the most commonly employed abrasive, and some etchants. However, the major role of the abrasive in the chemomechanical polishing process is in the maintenance of sample geometry and in the removal of product material.

The maintenance of sample geometry in chemomechanical polishing is a two tier effect. There are global and local effects of the etching reaction on the sample geometry. The global effect of the reaction leads to sample rounding at the wafer edges. This effect is especially predominant at cleaved edges, where a high concentration of defects leads to a much increased reaction rate. The polishing pad is the tool used to maintain sample geometry on this global level, since it will contact higher areas of the sample first, aiding product removal in the centre of the wafer and hence balancing reaction rate between the centre and the outside edges of the sample.

On a more local level, the abrasive and pad are both essential to the production of a smooth, flat surface (Section 1.3). This is the conventional passivation theory, where product material builds up in local 'troughs' in the surface and the polishing pad and abrasive contact the higher areas of the surface, removing them before contacting the lower areas. In fact, the evidence of this work is that the abrasive aids the passivation process further by building up in lower areas of the surface and protecting them from etchant until the pad reaches these areas and removes all residual material.

The different pad designs used in the project illustrate this simple model of geometry maintenance. The alumina-containing polyurethane pad (Figure 3.2.5) was designed to allow the release of alumina at the pad/sample interface during polishing i.e. as the alumina was required to remove product from the surface. This pad met the criteria of sample geometry on the global scale i.e. there was no edge rounding observed. However, the surface quality was poorer and the reaction itself slower than when using an alumina slurry. The illustrates the role of the abrasive both in product removal and in the improvement of surface quality by passivation. It is necessary to provide enough free alumina to fulfil both functions in order to achieve a good quality surface finish. For this reason, the traditional slurry mix of etchant and abrasive is more likely to produce a high quality finish than a polymer matrix containing abrasive. A more realistic alternative to the abrasive-incorporating pad is a solid phase etchant which combines the etching and passivating properties of the traditional slurry without the inconvenience of mixing the slurry. Such an etchant can be used with the traditional soft polishing pad, reducing the mechanical damage which can be caused by a polymer matrix. The development of solid-phase Br-containing etchants (Section 6.5) focused on this system.

6.4 A General Model for Chemomechanical Polishing.

We have seen, from the discussions in Section 6.2, that an etching reaction on a semiconductor substrate occurs in two stages; the oxidation of the surface by the etchant and the removal of the reaction products from the substrate surface. In Section 6.3, we discussed the role of abrasive and polishing pad in the chemomechanical polishing process and concluded that their influence was critical to product removal but was not directly relevant in the oxidation of the surface. The role of the polishing pad and abrasive in product removal helps to maintain the geometry of the sample and also helps to control the selectivity of etchants such as bromine by 'masking' areas of the surface which are being etched faster than others.

In addition to these two main stages in the etching or polishing of a semiconductor substrate, there is the added complication of the diluent component e.g. water or solvent used to dilute etchants such as Br_2 or $[OCl]^-$. This component of the reaction mixture can add an additional stage to the etching or polishing process, since it may change the nature of the product material to be removed. For example, tribromide products are solvated in a methanol diluent to form secondary products which are then removed from the surface. To postulate a truly general model for the polishing process, such intermediate product 'modification' must be included. Thus, an initial framework for the model has been laid down and involves three main stages:

1. Oxidation of the semiconductor surface by the chemical etchant.

2. Hydration/solvation of the initial reaction products by the diluent component of the etchant solution.

3. Removal of these secondary products from the substrate surface, with the aid of polishing pad and abrasive (passivation).

This general framework can be applied to the three etchants we have investigated, by building upon the chemistry we discussed in Section 6.2. For example, examination of the reactions of Br_2, NaOCl and H_2O_2 on GaAs, shows that all three etchants fit into this general pattern.

6.4.1 DIBROMINE IN METHANOL

1. Dibromine oxidises the GaAs surface to form Ga and As tribromides.

2. The methanol in the etchant solution hydrates/solvates the tribromides to form secondary Ga and As products.

3. The soluble products are finally removed from the substrate surface in the etchant solution, the action of the pad and abrasive helping to passivate the remaining surface against over-vigorous etching by fresh Br_2 reagent.

Figure 6.4.1 illustrates how this pattern fits into the general model. The fate of the Ga_2Br_6 and $AsBr_3$ products in the methanol diluent has not been investigated. However, it is probable that some hydrolysis occurs in the solvent to form some Ga and As oxides and hydroxides. The remaining product is solvated by the methanol and washed away in the polish solution.

6.4.2 HYDROGEN PEROXIDE IN AMMONIA SOLUTION

1. The hydrogen peroxide solution oxidises the GaAs surface to form Ga and As oxides.

2. The NH_3 in the solution creates basic conditions in which the Ga and As oxides are more soluble.

3. The products, some of which are insoluble in the etchant solution, are removed with the aid of the polishing pad and abrasive. The surface is quite heavily passivated due to the low solubility of the reaction products, hence the slow polishing rate but high surface quality achievable with this reagent.

Figure 6.4.1 illustrates how H_2O_2, despite an etchant chemistry which differs greatly from Br_2, fits into the same general model. Although some authors[33] have suggested the complexation of Ga by NH_3, it is more likely that the NH_3 is necessary only to produce the correct pH conditions for solubility. No evidence for the production of $[Ga(NH_3)_x]^{3+}$ was provided by the authors and the chemistry for formation of such a species is not discussed.

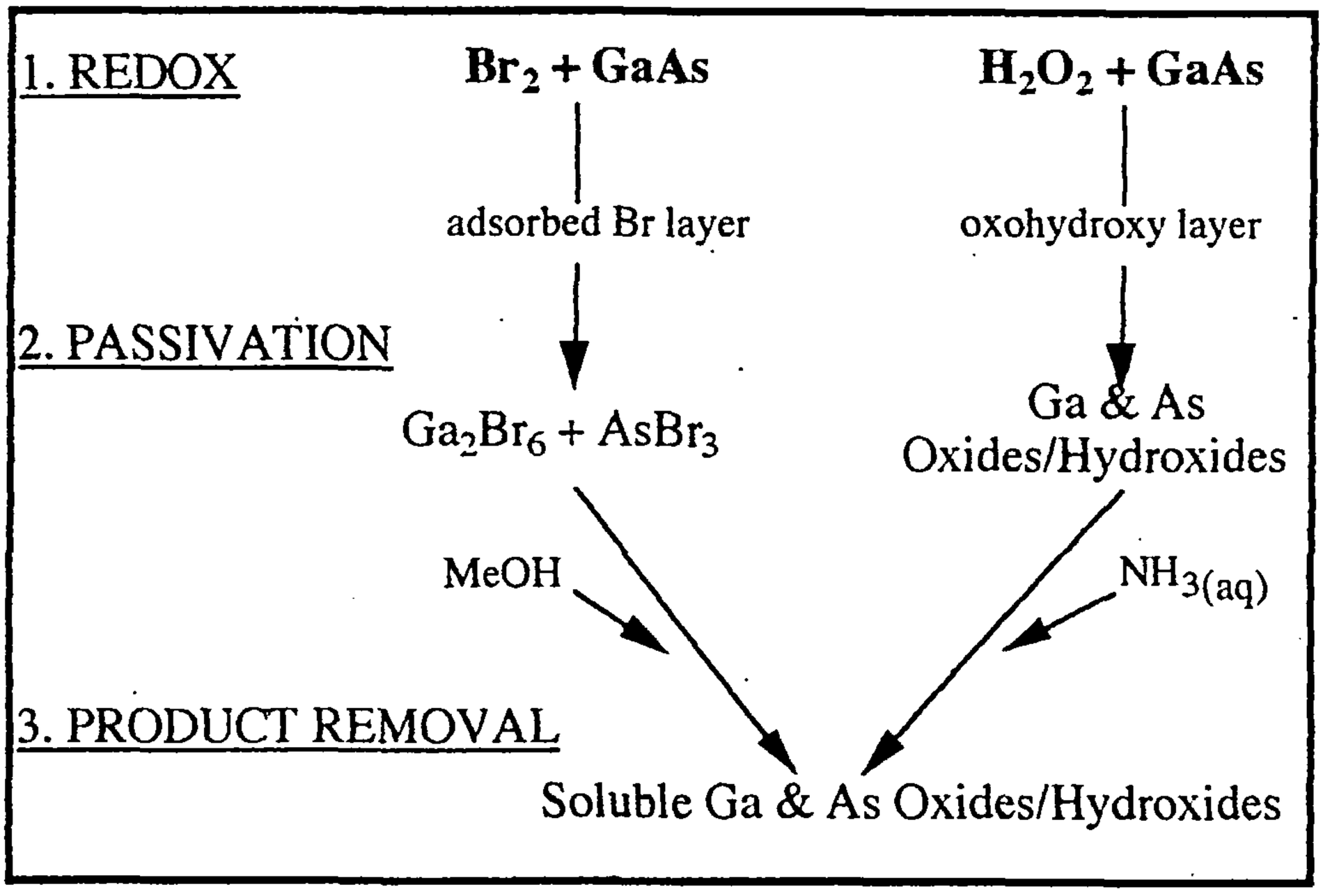

Figure 6.4.1: Schematic of the Reactions of Dibromine and Hydrogen Peroxide on GaAs.

6.4.3 SODIUM HYPOCHLORITE SOLUTION

Since the etching chemistry of NaOCl changes so dramatically with pH, it is best to consider the two extremes of pH independently:

a) Hypochlorite Solution at pH > 8

1. The GaAs surface is oxidised by $[OCl]^-$ to form Ga and As oxides.

2. The water in the hypochlorite solution hydrates the Ga and As oxides to form hydroxides which are dissolved to some extent in the basic etchant solution. At high pH, some of these products form an insoluble layer in the absence of a polishing pad or abrasive. This layer may contribute to surface reconstruction.

3. The products, some of which are insoluble in the etchant solution, are removed with the aid of the polishing pad and abrasive. Surface quality is improved by reducing pH, slowing reaction to allow easier removal of product by the pad and abrasive (Figure 6.4.2).

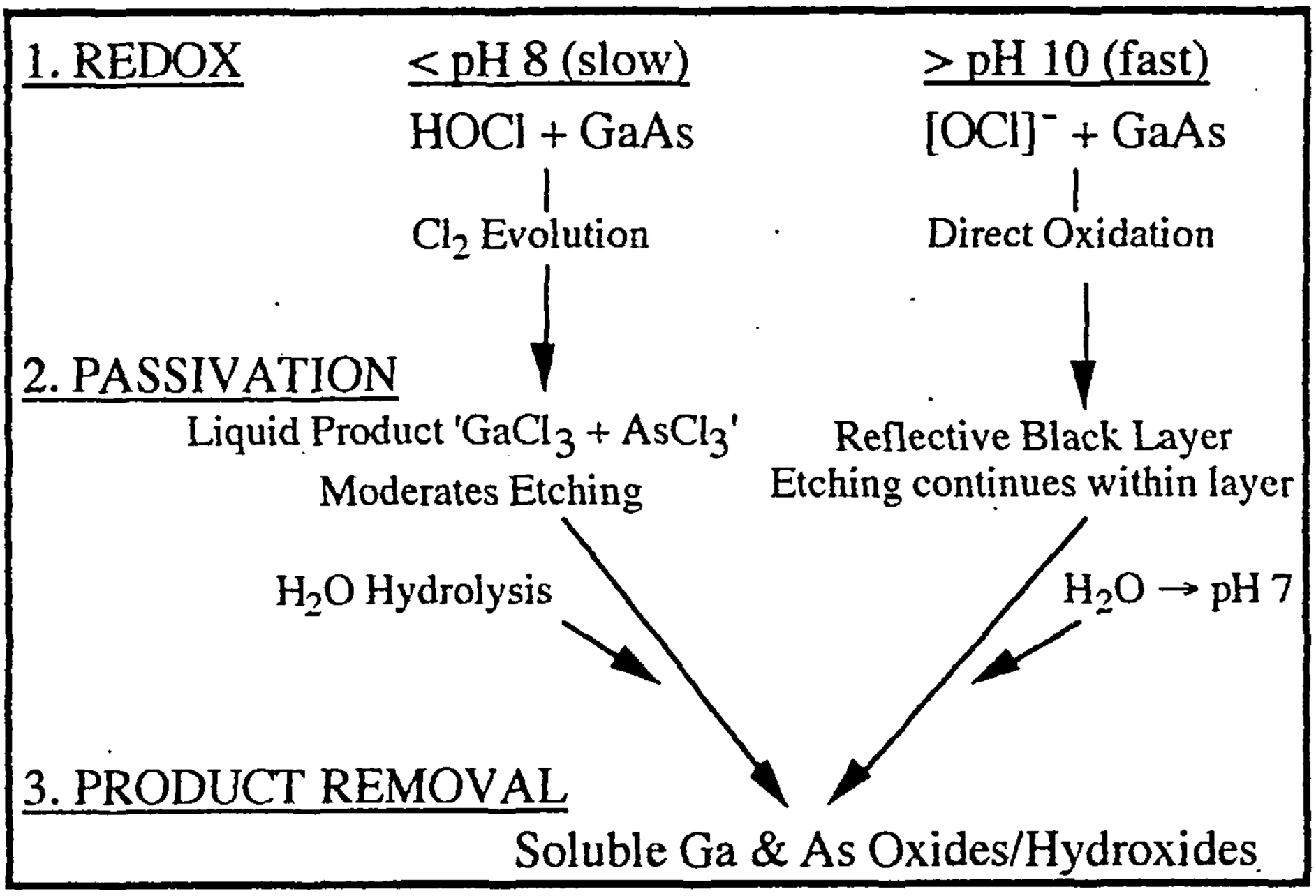

Figure 6.4.2: Schematic of the Reactions of Hypochlorite on GaAs

b) Hypochlorite Solution at pH < 8

1. Dichlorine oxidises the GaAs surface to form Ga and As trichlorides.

2. The water in the etchant solution hydrates the trichlorides to form Ga and As hydroxides.

3. The soluble products are finally removed from the substrate surface in the etchant solution with the aid of the polishing pad and any abrasive.

This rationale clearly illustrates the fact that $[OCl]^-$ solution at pH > 8 follows a model very similar to that for H_2O_2 / NH_3 and $[OCl]^-$ at pH < 8 follows a model very similar to that for Br_2 / Methanol. Hence, hypochlorite solution as an etchant forms a bridge between vigorous, halogenating etchants like Br_2 and slower, more heavily passivating etchants like H_2O_2. In fact we can view hypochlorite as a central member of the series:

X-X, O-X, O-O

where X represents a halogen. However, the chemistry of $[OCl]^-$ on GaAs is more complicated than that of Br_2 or H_2O_2. As we have already discussed, Cl_2 is a slower etchant than would be expected by comparison with Br_2, due to the passivating effect discussed in Section 4.6. Also, the product layer formed by the action of hypochlorite anion on GaAs is not as passivating as might be expected by comparison with its H_2O_2 counterpart. Despite the complex chemistry occurring at the substrate surface,

hypochlorite solution still follows the general pattern for chemomechanical polishing which has been formulated above and is illustrated in Figure 6.4.2. Sodium hypochlorite can be used as a 'variable etchant' to fill the gap between fast, vigorous etchants like dibromine and slow, highly passivating etchants like hydrogen peroxide. The easy control of reaction rate (and hence surface quality) in hypochlorite solution by pH makes the reagent ideal for this application.

However, the goal of this research was ultimately to find an etchant which met the best possible criteria of speed and surface quality for any desired material. Hence, it was useful to investigate other forms of an efficient, fast reagent like dibromine which would lead to improvements in surface quality while maintaining as much of the speed of the etchant as possible. Having established a good knowledge of etchant chemistry and chemomechanical polishing in general, this was the objective of the latter stages of the work (Section 6.5).

6.5 Design and Use of Novel Bromine Based Reagents.

From our study of the etchants most commonly used in chemomechanical polishing today, we discovered the properties which lead to a good polishing process, and how these can be applied in the design of new reagents. In this section of the work, we investigated four such properties to determine whether they could be 'designed' into a reagent with predictable chemistry.

6.5.1 Use of Physical Environment to Change the Speed of the Polishing Reaction

Etching and polishing reactions depend critically on the diffusion of fresh etchant to the substrate surface. This is the basis of the passivation theory, where the reaction is slowed by the presence of a diffusion barrier formed by insoluble product. Dibromine is a popular reagent because it is efficient (i.e. it produces a polished surface quickly) and produces a surface of acceptable quality for most applications. However, if we want to improve the surface quality, there is a need to moderate the reaction just enough to improve the passivation of the semiconductor surface while sacrificing as little speed as possible. One way to reduce the rate of the etching reaction is to limit the arrival of

dibromine at the etchant/surface interface i.e. reduce the rate of diffusion of the active etchant. This can be done by reducing the solubility of the Br_2 in the etchant solution or by increasing the size of the etchant molecule itself. In fact, using Br_2 with the ligands shown in Figure 5.1.1, the bromine complexes formed employed both of these methods to moderate the action of Br_2 on the GaAs surface. The fact that all of the resultant complexes were solid led to a reduction in solubility with reference to Br_2 in most diluents. The use of bulky organic ligand increased the size of the etchant molecules, thereby restricting their diffusion through the etchant solution to the substrate surface.

The restriction of etchant diffusion obviously depends on more than solubility and size of the complex. Such a simple model would apply only if the lability of the bromine was equal in all the complexes used. Hence, the effectiveness of these etchants was greatly dependent on the stability of the complex employed. For example, the high stock removal rate of GaAs by Br_2-dioxane in CH_2Cl_2 is an indication not only of the high solubility of the adduct in dichloromethane, but also of the ease of Br_2 removal from the adduct at the etchant/wafer interface.

There are three factors, then, which must be considered when designing such complexes to modify the action of a vigorous etchant like Br_2. These are the size of the ligand (to slow diffusion), the solubility of the complex (again to limit diffusion) and the stability of the active component within the complex. Consideration of these three factors together allows the prediction of relative mass loss results between different etchant systems. For example, given that an appropriate solvent is chosen, it might be predicted that the O-donor ligand dioxane would produce a faster etchant with dibromine than the N-donor ligands quinoline and quinuclidine, because of the weaker donor-acceptor interaction between Br_2 and O than between N and Br^+.

The other factor in operation here is, of course, the differing oxidation state of the active etching component. This will affect the nature of the chemical reaction occurring at the etchant/substrate surface. It is difficult to consider this point in isolation from the issue of chemical environment, since it is the stability of this environment which ultimately determines the oxidising ability of Br^+. It is the inherent instability of the Br^+ configuration which makes the choice of ligand so critical to the formation of a stable Br^+ organic complex. The formalism of the Br^+ notation is naive in that significant charge redistribution occurs on formation of the N-donor complex. Hence the oxidising ability of Br^+ cannot be defined with regard to this work, without consideration of the complex in which it was formed. From the results obtained, the strength of the Br^+ - N interaction required to create a stable Br^+ complex leads to a relatively gentle oxidant with respect to Br_2. Dibromine, however, forms stable complexes with many weaker donor ligands

(dioxane, methanol, crown ethers) providing a far more vigorous oxidant. The precise nature of the adsorbing species was not determined as part of this project, and will be critical to the nature of the surface remaining after the polish (Section 6.6).

6.5.2 USE OF ACID-BASE INTERACTION TO CONTROL REACTION RATE

Once an etchant has been chosen (or designed) to etch the semiconductor at a speed which roughly meets the desired criteria, it is possible to fine tune the process further *in situ*. The etching chemistry of hypochlorite solution illustrates how heavily some etchant systems may depend on pH and this may be equally applied to solid etchants if a pH dependence is designed into the complex.

The use of N-donor ligands in an etchant complex provides the perfect opportunity for control of that etchant by pH/protonation. The N-donor atom on the ligand may be easily protonated on addition of acid (Figure 5.4.1), thereby releasing the central active component and allowing easy diffusion through the etchant solution and access to the substrate surface, as shown in Equation 6.5.1:

$$\mathbf{[Bis(quinoline)Br]^{+}Br^{-} + H^{+} \rightarrow [Quinoline\text{-}H]^{+} + Br_2} \quad \text{.....(6.5.1)}$$

However, it should be noted that this method of controlling the etch rate may not be appropriate in all cases. For example, the release of Br_2 too early in an etchant solution where water is the diluent will lead to hydrolysis of the Br_2 before it reaches the semiconductor surface. This is illustrated in the polishing experiment using bis(quinuclidine) bromonium bromide in water (Section 5.4.3). The best results were achieved by spreading the solid directly onto the pad since this permitted bromine release closer to the sample surface.

The use of protonation or low pH to speed up reaction must be balanced against any advantage to be gained by the structure of the solid. If the complex structure has been designed to achieve improvements in surface geometry or selectivity, these properties will obviously be lost if the integrity of the complex is lost, as in Equation 6.5.1. For example, if a complex such as bis(quinoline) bromonium bromide is designed with bulky ligands, to encourage even etchant distribution across a surface, the structure must remain intact until it reaches the wafer surface. This is unlikely to be the case if acid is added to a random suspension of the solid etchant. More refined control of the protonation is required if the full benefit of such 'designer' ligands is to be gained.

6.5.3 MAINTENANCE OF SAMPLE GEOMETRY

During our discussions on the maintenance of sample geometry by passivation (Section 6.3) it became clear that the use of an abrasive in a suspension was critical to the production of a smooth, planar surface. In most conventional polishing reagents, the etchant is in the form of a solution and the abrasive is added to this solution to form a slurry. By using a solid etchant, it was hoped that the need for an additional abrasive could be eliminated i.e. the complex would double as etchant and abrasive, in so far as sample geometry was concerned. The soft nature of the complexes meant that any role as a stock-removing abrasive could be ruled out.

The range of complexes used met with only some success in the area of geometry maintenance. The perfect reagent for such an application would be largely insoluble in the etchant solution (i.e. form a suspension) yet would release its bromine readily at the substrate surface. None of the complexes designed as part of this work met both of these criteria. In the case of the Br_2-dioxane adduct, the only solvents which allowed easy release of the bromine for etching also readily dissolved the complex almost instantly, therefore losing any advantage of the solid etchant. The best candidates for this aspect of the polishing process were the bis(quinoline) and bis(quinuclidine) bromonium bromides. Neither of these complexes dissolved completely in any of the solvents tried, yet they did yield a slow but successful polish on GaAs. These complexes were used to 'correct' the orange peel surface produced on GaAs by a conventional Br_2/methanol polish. The biggest advantage was gained when the solid complex was spread directly on the pad and a solution facilitating release of the Br_2 was dripped on separately. This method maintained the integrity of the complex structure for as long as possible and allowed the soft solid to fulfil a passivating role at the substrate/pad interface.

6.5.4 SELECTIVITY

One complex from the range we studied clearly illustrated the possibility of selective etchant design. 18-Crown-6 is a well known molecule for the selective capture of Cd ions[92]. It would be predicted, therefore that its use in an etchant complex would lead to higher etch rates on CdTe. This was indeed found to be the case. The precise mechanism of Cd capture at the surface was not investigated. However, it is likely that an etchant selective for one component of a compound semiconductor will help to break up the surface, allowing faster dissolution in the etchant solution.

Such selectivity in an etchant might generally be undesirable, since a stoichiometric substrate surface is generally the ideal outcome of the polishing process. However, in cases where the lower solubility of one product normally leads to non-stoichiometry, such selective etchants may be employed to counteract such an effect. Hence, the ideal bromine-based reagent for CdTe would be slightly selective for Te, preventing the Te-rich surface left by conventional Br_2 and HBr etchants. Unfortunately, investigation of such a system was beyond the scope of this project. However, the work has shown that such selectivity can easily be predicted and designed into an etchant where necessary.

6.6 CONCLUSIONS AND FURTHER WORK.

6.6.1 CONCLUSIONS

This project has fulfilled its objectives in that the research has resulted in a better understanding of etching and polishing in general and of the chemistry of NaOCl, Br_2 and H_2O_2 in particular. It has been shown that the reactions of all 3 reagents follow a similar pattern and that the passivation model can be used to explain the differing surface qualities obtainable. Sodium hypochlorite solution has been investigated in particular detail, and its pH dependence has been explained in terms of the different active etchant components in the system (Cl_2 at pH < 8 and $[OCl]^-$ at pH > 8).

A General Model for Chemomechanical Polishing has been formulated which generalises the pattern of oxidation, solvation and product removal which was observed for all the reagents investigated. This model is applicable to the polishing process in general, regardless of etchant or substrate. The model was combined with the knowledge of etchant chemistry and abrasive role, gained early in the project, to design new reagents with predictable properties for the etching and polishing of GaAs and CdTe.

In summary, this research has not only established a better understanding of etching and polishing, but has shown how this understanding can be used to control and optimise the polishing process. The design of new reagents with predictable properties has also shown that chemomechanical polishing is better treated as a science rather than an art. Solutions to specific problems may be found by the application of scientific principles rather than by trial and error.

6.6.2 FURTHER WORK

Much of this research has been concerned with laying the foundations of chemical knowledge required before improvement of the polishing process could begin. Particularly in the latter stages of the project, there have been several unanswered questions which it was outwith the remit of this research to investigate.

A) SURFACE RECONSTRUCTION

There has been extensive research carried out on the adsorption of dichlorine and dibromine molecules on the GaAs surface, because of their relevance in dry-etching processes[93-95]. Much of this work has involved molecular modelling of the interaction to predict the effect of the etching reaction on the substrate surface. This type of modelling can provide essential information to the chemist about the usefulness of a reagent, since , as we have already discussed, a large degree of surface reconstruction during an etching reaction is generally undesirable. It would be useful to undertake some research into such modelling techniques for reagents like the bromine complexes designed in this project. In theory, reagents like the cyclam/Br_2 adduct, which carry the etchant directly to a given site on the substrate surface, should produce a lesser degree of surface reconstruction. Such techniques would also be useful in predicting the efficiency of etchants with 'designed-in' selectivity.

B) POLISHING PAD DESIGN

Although there was a small amount of work carried out in this project with respect to polishing pad design, only one alternative design was examined. The failure of this pad design did, in fact, tell us much about what is essential to the polishing process in terms of pad surface and availability of abrasive. There is scope for much more work, from an engineering perspective, on the mechanical operation of the pad and its combination with an abrasive or solid polishing reagent.

C) NEW REAGENTS

The new compounds synthesised and tested in this research were chosen to illustrate how predictable the etching chemistry of such reagents could be. They have proved how variable one reagent (i.e. bromine) can be if its physical and chemical environment are modified. This section of the work has obviously opened up a whole new area of etchant chemistry and there is room for much more research into new etchants, their interaction with surfaces and the products they form.

References

1. R. A. Laudise, American Institute of Physics, American Vacuum Society Series 1, Conference Proceedings No. 138, New York, 1986, 13.

2. S. M. Sze, Physics of Semiconductor Devices, 2nd Edition, J. Wiley and Sons, New York, 1981, 12.

3. D. A. Allan, J. Herniman, M. J. Gilbert, P. J. O'Sullivan, M. P. Grimshaw and A. E. Staton-Bevan, J. de Phys., **49**, 1988, 427.

4. W. L. Jones and L. F. Eastman, IEEE Trans. Electron. Devices, **33**, 1986, 712.

5. A. R. West, Solid State Chemistry and its Applications, J. Wiley and Sons, Chichester, 1987, 134.

6. D. J. Stirland and B. W. Straughan, Thin Solid Films, **31**, 1976, 139.

7. S. E. Blum, Compound Semiconductors , Volume 1, Reinhold Publishing Corporation, New York, 1962, 85.

8. J. S. Moss (Ed.), Handbook on Semiconductors, Volume 3, North Holland Publishing Co., Amsterdam, 1980, 247.

9. D. R. Lide (Ed.), Hanbook of Physics and Chemistry, 72nd Edition, CRC Press, Boston, 1991, Section 4.

10. L. Pauling, The Nature of the Chemical Bond, 3rd Edition, Cornell Univ. Press, New York, 1960, 67.

11. E. Mooser and W. B. Pearson, Acta. Cryst., **12**, 1959, 1015.

12. A. R. West, Solid State Chemistry and its Applications, J. Wiley and Sons, Chichester, 1987, 301.

13. A. R. West, Solid State Chemistry and its Applications, J. Wiley and Sons, Chichester, 1987, 237.

14. G. W. Flynn and W. J. A. Powell, The Cutting and Polishing of Electro-Optic Materials, Hilger, Bristol, 1979, 163.

15. Lord Rayleigh, Proceedings of the Optical Convention, 1905, 75.

16. B. Tuck, J. Mater. Sci., **10**, 1975, 321.

17. M. W. Geiss, N. N. Efremow and G. A. Lincoln, J. Vac. Sci. Technol. B, **4**, 1986, 315.

18. M. W. Geiss, N. N. Efremow, S. W. Pang and A. C. Anderson, J. Vac. Sci. Technol. B, **5** , 1987, 363.

19. F. Shimokawa, H. Tanaka, Y. Venishi and R. Sawada, J. Appl. Phys., **66**, 1989, 2613.

20. D. G. Lishan and E. L. Hu, Appl. Phys. Lett., **56**, 1990, 1667.

21. S. Sugata and K. Asakawa, J. Vac. Sci. Technol. B, **5** , 1987, 894.

22. E. L. Hu and R. E. Howard, J. Vac. Sci. Technol. B, **2**, 1984, 85.

23. D. E. Ibbotson, D. L. Flamm and V. M. Donnelly, J. Appl. Phys., **54**, 1983, 5974.

24. F. A. Houle, J. Vac. Sci. Technol. B, **7**, 1989, 1149.

25. F. Foulon, M. Green, F. N. Goodall and S de Unamuno, J. Appl. Phys., **71**, 1992, 2898.

26. M. R. Berman, Appl. Phys. A, **53**, 1991, 442.

27. C. Su, M. Xi, Zi-Guo Dai, M. F. Vernon and B. E. Bent, Surf. Sci., **282**, 1993, 357.

28. J. C. Patrin, Y. Z. Li, M. Chander and J. H. Weaver, Appl. Phys. Lett., **62**, 1993, 1277.

29. M. Nooney, V. Liberman, M. Xu, A. Ludviksson and R. M. Martin, Surf. Sci., **302**, 1994, 192.

30. C. S. Fuller and H. W. Allison, J. Electrochem. Soc., **109**, 1962, 880.

31. M. V. Sullivan and G. A. Kolb, J. Electrochem. Soc., **110**, 1963, 585.

32. J. C. Dyment and G. A. Rozgonyi, J. Electrochem. Soc., **118**, 1971, 1346.

33. J. J. Kelly and A. C. Reynders, Appl. Surf. Sci., **29**, 1987, 149.

34. A. Reisman and R. Rohr, J. Electrochem. Soc., **111**, 1964, 1425.

35. M. Higuchi, J. Electrochem. Soc., **136**, 1989, 2710.

36. P.F. Vengel, V. N. Tomashik and A. V. Fomin, Zh. Prikl. Khim., **65**, 1992, 751.

37. I. A. Sokolov, V. V. Kozlov and E. K. Varloshina, Poverkhnost, **6**, 1993, 75.

38. The Holy Bible, Exodus, Ch. 25 v 4.

39. J. B. A. Dumas, Ann., **32**, 1839, 101.

40. H. M. Leicester, The Historical Background of Chemistry, Dover Publications Inc., New York, 1971, 177.

41. J. W. Dobereiner, Poggendorfs Ann., **15**, 1829, 301.

42. N. N. Greenwood and A. Earnshaw, Chemistry of the Elements, Pergamon Press, Oxford, 1984, 934, 1223.

43. L. K. Blair, K. D. Parris, P. S. Hiiand C. P. Brock, J. Amer. Chem. Soc., **105**, 1983, 3649.

44. F. A. Cotton and G. Wilkinson, Advanced Inorganic Chemistry, 5th Edition, J. Wiley and Sons, New York, 1988, 550.

45. N. N. Greenwood and A. Earnshaw, Chemistry of the Elements, Pergamon Press, Oxford, 1984, 743.

46. D. R. Lide (Ed.), Hanbook of Physics and Chemistry, 72nd Edition, CRC Press, Boston, 1991, Section 8.

47. Y. Mori and N. Watanabe, J. Electrochem. Soc., **125**, 1978, 1510.

48. M. V. Sullivan and L. A. Pompliano, j. Electrochem. Soc., **108**, 1961, 60c.

49. I. Barycka and I. Zubel, J. Mater. Sci., **22**, 1987, 1299.

50. A. Mouton, C. S. Sundararaman, H. Lafontaine, S. Poulin and J. F. Currie, Jap. J. Appl. Phys., **29**, 1990, 1912.

51. L. C. Adam, I. Fábián, K. Suzuki and G. Gordon, Inorg. Chem., **31**, 1992, 3534.

52. B. S. Yiin and D. W. Margerum, Inorg. Chem., **29**, 1942.

53. B. S. Yiin and D. W. Margerum, Inorg. Chem., **29**, 2135.

54. H. Hartnagel and B. L. Weiss, J. Mater. Sci., **8**, 1973, 1061.

55. A. Khoukh, S. K. Krwezyk, R. Oliek, A. Chabli and E. Molua, J. Electrochem. Soc., **134**, 1987, 1859.

56. A. I. Vogel, A Textbook of Quantitative Inorganic Analysis, Including Elementary Instrumental Analysis, 3rd Edition, Longman, London, 1975, 295.

57. S. J. Haswell (Ed.), Atomic Absorption Spectrometry, Elesevier Science Publishers B. V., Amsterdam, 1991, 1.

58. J. H. Scofield, J. Electron. Spectrosc., **8**, 1976, 129.

59. S. G. McMeekin, M. I. Robertson, L. McGhee and J. M. Winfield, J. Mater. Chem., **2**, 1992, 367.

60. L. McGhee, S. G. McMeekin, I. Nicol, M. I. Robertson and J. M. Winfield, J. Mater. Chem., **4**, 1994, 29.

61. J. Thomson, G. Webb and J. M. Winfield, J. Chem. Soc., Chem. Commun., 1991, 23.

62. J. N. Miale and C. D. Chang, U. S. Pat., 427,791, 1984.

63. M. Tonaka and S. Ogasawara, J. Catal., **16**, 1970, 157.

64. J. Thomson, G. Webb and J. M. Winfield, J. Mol. Catal., **68**, 1991, 347.

65. M. R. Wehr, J. A. Richards and T. W. Adair, Physics of the Atom, 3rd Edition, Addison-Wesley Publishing, Massachusetts, 1980, 316.

66. D. R. Lide (Ed.), Hanbook of Physics and Chemistry, 72nd Edition, CRC Press, Boston, 1991, Section 11.

67. J. Thomson, Ph.D. Thesis, University of Glasgow, 1988.

68. G. Brauer, Handbook of Preparative Inorganic Chemistry, 2nd Edition, Volume 1, Academic Press, London, 1965, 272.

69. C. E. Sjøgren, P. Klaeboe and E. Rytter, Spectrochim. Acta, **40A**, 1984, 457.

70. I. R. Beattie, T. Gilson and P. Cocking, J. Chem. Soc. (A), 1967, 702.

71. A. Balls, A. J. Downs, N. N. Greenwood and B. P. Straughan, Trans. Far. Soc., **62**, 1966, 521.

72. I. R. Beattie and J. R. Horder, J. Chem. Soc. (A), 1969, 2655.

73. P. W. Davis and R. A. Oetjen, J. Mol. Spectrosc., **2**, 1958, 253.

74. B. Lunelli, G.Cazzoli and F. Lattanzi, J. Mol. Spectrosc., **100**, 1983, 4345.

75. P. R. Stevenson, Ph.D. Thesis, University of Glasgow, 1992.

76. N. N. Greenwood, P. G. Perkins and K. Wade, J. Chem. Soc., 1957, 4345.

77. N. N. Greenwood and A. Earnshaw, Chemistry of the Elements, Pergamon Press, Oxford, 1984, 654.

78. D. S. Boyle, J. A. Chudek, G. Hunter, D. James, M. I. Littlewood, L. McGhee, M. I. Robertson abd J. M. Winfield, J. Mater. Chem., **3**, 1993, 903.

79. D. S. Boyle and J. M. Winfield, J. Mater. Chem., **6**, 1996, 227.

80. D. H. Williams and J. Fleming, Spectroscopic Methods in Organic Chemistry, 4th Edition (Revised), McGraw-Hill Book Company, London, 1989, 40.

81. N. W. Alcock and G. B. Robertson, J. C. S. Dalton, 1975, 2483.

82. W. Shi Hua, S. J. Ajiboye, G, Haining, L. McGhee, R. M. Siddique and J. M. Winfield, J. Chem. Soc. Dalton Trans., 1995, 3837.

83. L. J. Andrews and R. M. Keefer, Molecular Complexes in Organic Chemistry, Holden-Day, London, 1964, 51.

84. O. Hassel and J. Hvoslef, Acta. Chem. Scand., **8**, 1954, 873.

85. F. A. Cotton and G. Wilkinson, Advanced Inorganic Chemistry, 5th Edition, J. Wiley and Sons, New York, 1988, 476.

86. J. L. Atwood, S. G. Bott, C. M. Means, A. W. Coleman, H. Zhang and M. T. May, Inorg. Chem.,**29**, 1990, 467.

87. L. McGhee, I. Nicol, and J. M. Winfield, J. Mater. Chem., Publication Pending.

88. A. S. Kovalenko, B. L. Druz, E. I. Gusakova and L. P. Tikhonova, Zh. Prikl. Khim., **65**, 1992, 563.

89. W. Kern, RCA Rev., **39**, 1978, 278.

90. S. L. Reidinger, D. W. Snyder, E. I. Ko and P. J. Sides, Mater. Sci. Eng. B, **B15**, 1992, L9.

91. K. Cierocki, D. Troost, L. Koenders and W. Mönch, Surf. Sci., **264**, 1992, 23.

92. C. J. Pederson, J. Amer. Chem. Soc., **89**, 1967, 7017.

93. D. Troost, H. J. Clemens, L. Koenders and W. Mönch, Surf. Sci., **286**, 1993, 97.

94. M. Balooch, D. R. Olander and W. J. Siekhaus, J. Vac. Sci. Tech. B, **4**, 1986, 794.

95. K. Balasubramanian, J. X. Tao and D. W. Liao, J. Chem. Phys., **95**, 1991, 4905.